Paleoenvironments and Taphonomy of the Middle Miocene Barstow Formation, Mojave Desert, California

by

Katharine McCarey Loughney

A dissertation submitted in partial fulfillment
of the requirements for the degree of
Doctor of Philosophy
(Earth & Environmental Sciences)
in the University of Michigan
2018

Doctoral committee:

Professor Catherine Badgley, Chair
Professor Daniel C. Fisher
Associate Professor John Kingston
Associate Professor Nathan D. Sheldon
Assistant Professor Selena Y. Smith

loughney@umich.edu
ORCID ID: 0000-0001-6752-6152

DEDICATION

To Katharine L. Loughney

ACKNOWLEDGMENTS

The work presented here was supported by funding from the Evolving Earth Foundation, the Paleontological Society, the University of Michigan Rackham Graduate School, and the University of Michigan Department of Earth and Environmental Sciences.

I would like to thank my advisor, Catherine Badgley, for all of her help and guidance throughout the course of this project. Her wealth of knowledge and skills in the field and in the lab has been a valuable resource to me and serves as a source of inspiration for this budding taphonomist. The members of the Badgley Lab have learned well from Catherine's example of generosity and intellectual rigor. Tara Smiley, Rachel Cable, Jeff Shi, and Bian Wang are friends and colleagues who have made life in graduate school a little easier.

I would also like to thank my committee members, Nathan Sheldon, Selena Smith, Dan Fisher, and John Kingston. Their support, comments, and suggestions over the course of this project have been valuable in helping me design these studies and to interpret and communicate their results. Thank you to Nathan Sheldon and Selena Smith for allowing me to use their lab space and equipment. I would also like to thank my co-authors, Catherine Badgley, Selena Smith, Michael Hren, and Janice Pappas, for providing comments and feedback on manuscripts, as well as laboratory support and training.

There are many other people who have helped me at various stages of researching and writing this dissertation. I would especially like to thank Bob Reynolds, without whom I would never have figured out how to work in the Barstow Formation. He, Mike Woodburne, Ev

Lindsay, and Don Lofgren are all Barstow veterans who have been invaluable resources, and I sincerely appreciate their dedication of time, resources, and sharing of knowledge about the stratigraphy and paleontology of the Mojave. Thank you to Rachel Thorpe and Anna Harkness for their assistance in the field and in the lab; Ethan Hyland, Katy Rico, Katherine Truong, Abigail Oakes, and Greg Harris provided training and assistance in laboratory techniques and using lab equipment. I would like to acknowledge the people and institutions that granted me access to museum collections, especially Andy Farke and Gabe Santos at the Raymond Alf Museum of Paleontology; Ian Gilbert, Jennifer Reynolds, and Melissa Russo at the San Bernadino County Museum; Pat Holroyd and Diane Erwin at the University of California Museum of Paleontology; and Judy Galkin at the American Museum of Natural History. Thank you to Carol Abraczinskas and Linda Garcia for their help and support.

The graduate students in the departments of Earth and Environmental Sciences and Ecology and Evolutionary Biology have made welcoming and supportive communities. I would like to thank Clay Tabor, Petr Yakovlev, John Fronimos, Meg Veitch, Molly Ng, and many others for their friendship over the years.

Finally, I would like to thank my parents for always encouraging me to pursue my interests and for never insisting that I follow a practical career path.

TABLE OF CONTENTS

LIST OF FIGURES

LIST OF TABLES

ABSTRACT

The fossil record of the Great Basin of western North America formed during an interval of intense tectonic activity and climate change. Geographically restricted basins formed during regional extension in the early and middle Miocene. During the Middle Miocene Climatic Optimum (MMCO) between 17 and 14 Ma, global climate warmed 2–4°C. The Barstow Formation, Mojave Desert, California, was deposited in an extensional basin and encompasses the MMCO. The sequence has a robust geochronologic framework and a well-studied mammal-fossil record, making it an ideal sequence in which to study the influence of tectonics, climate, and depositional setting on fossil preservation through time. These factors determine the observed distribution of fossils and affect reconstructions of ecological, evolutionary, biostratigraphic, and biogeographic relationships. I characterized the facies, depositional environments, and taphonomic histories of fossil localities in the Barstow Formation. I integrated and analyzed data gathered from field work, museum visits, and laboratory analyses in order to understand the influence of changing tectonic and climatic regimes on the preservation of mammal fossils.

The goals of the dissertation are introduced in Chapter 1. In Chapter 2, I characterized the major facies of the formation to understand the depositional settings and stratigraphic distribution of fossil localities. As subsidence decreased, depositional environments in the basin changed over time from alluvial fans and playa lakes to floodplains and wetlands; with this change, depositional environments became more suitable for mammal habitation and more

conducive to the preservation of vertebrate remains. In Chapter 3, I used carbon and hydrogen (D) isotopes from plant-derived biomarkers, soil organic matter, and diatoms to reconstruct environmental and hydrologic changes, and I analyzed phytolith (plant silica) assemblages to reconstruct vegetation composition and structure. Negative shifts in $\delta^{13}C$ and δD indicate that precipitation increased during the MMCO, and riparian environments formed at this time. After the MMCO, enrichment in $\delta^{13}C$ and δD values indicate decreased precipitation and changes in vegetation composition as wooded grasslands formed in the basin.

In Chapters 4 and 5, I reconstructed the taphonomic histories of fossil localities based on fossil assemblages in museum collections and the facies settings of field sites. Fossil assemblages accumulated through biological activity at long-term sites of mortality and through fluvial processes. Localities representing long-term sites of mortality formed in channel-margin settings and around waterholes, and the majority of fossil specimens were preserved in these settings. Fluvial processes concentrated fossils in channel lags and crevasse-splay deposits and preserved fewer specimens than biological accumulations. Most fossil material was from medium-size mammals (50–200 kg), as their remains were able to withstand carnivore activity, weathering, and burial better than remains of smaller and larger mammals. Mammal diversity increased through the formation, and observed turnover was high in stratigraphic intervals with localities that had high preservation potential. Inferred species ranges show turnover occurring throughout the formation. In Chapter 6, I synthesized the previous chapters and evaluated the fossil record of the Great Basin in the context of its tectonic history during the Miocene. As tectonic activity declined through the Miocene, the number of mammal genera and sediment thickness of fossiliferous formations increased. In all basins, depositional environments change with tectonics and climate. Resulting facies and depositional settings have differing potential to

preserve vertebrate remains, which determines the stratigraphic distribution of fossils and observed patterns of diversity and turnover.

CHAPTER 1

Introduction

The continental rock record forms through the interplay of tectonics and climate that operate over various spatial and temporal scales. Regional and local tectonics control rates of subsidence, accommodation, and the accumulation of sediment; climatic regime controls temperature, precipitation, weathering, and erosion (Catuneanu, 2006). The fossil record is also partly dependent on these controls, as their combined influences create the conditions under which plants and animals live, die, and are potentially buried and preserved. Plants and animals are spatially distributed over climatic and topographic gradients (Badgley et al., 2017), yet the conditions favoring fossil preservation are often localized to specific depositional settings (Behrensmeyer et al., 2000). The taxonomic composition of fossil assemblages reflects the ecology of the original ecosystem, but it can also be modified by taphonomic processes occurring in these settings. Characterizing changes in depositional environments and taphonomy reveals the patterns of preservation that determine the stratigraphic distribution of fossils with respect to tectonics and climate. The goal of stratigraphic paleobiology is to evaluate the fossil record within these contexts to enhance understanding of patterns of diversity, evolution, extinction, and biogeography through time. In addition, the potential to predict fossil occurrences based on facies distributions allows paleontologists to focus prospecting efforts and fill gaps in the record that have obscured evolutionary and biogeographic history (Patzkowsky and Holland, 2012).

The Great Basin of western North America offers a setting in which to study the role of tectonics and climate on fossil preservation through time. Widespread regional extension through the Neogene (Dickinson, 2002) created numerous geographically restricted, fault-bounded basins that record local flora and fauna. Global climate became progressively drier and cooler during the Cenozoic but was punctuated by significant warming of the Middle Miocene Climatic Optimum (MMCO; Zachos et al., 2001). Mammal diversity peaked in the Great Basin during the MMCO and the middle Miocene height of extension, and the Mojave region of southern California had the highest mammal diversity in the Great Basin from this time (Badgley et al., 2015). Understanding how these tectonic and climatic factors influenced faunal diversity requires the examination of local faunal records that formed against a backdrop of tectonic and climatic activity.

The Barstow Formation in the Mojave Desert, California, provides one of the richest continental records of middle Miocene sediments and mammalian faunas in North America, where it is one of the few continental formations to span the MMCO. The fauna of the Barstow Formation contributes substantially to the high mammal diversity in the Great Basin during the middle Miocene (Badgley et al., 2015). The large- and small-mammal faunas from the formation have been well characterized (Lindsay, 1972; Browne, 2002; Pagnac, 2005), and the mammals from the type section of the Barstow Formation are the basis for the Barstovian North American Land Mammal Age (NALMA). The lithostratigraphy has been documented and mapped in detail (Steinen, 1966; Dibblee, 1967; Woodburne et al., 1990), and the timing of deposition of the formation is constrained through radiometric dating of tuffs and magnetostratigraphy (MacFadden et al., 1990; Miller et al., 2013). The Barstow Formation offers an opportunity to

study the influence of tectonics and climate on depositional environments and fossil preservation over several million years, given the rich paleontologic record and geochronologic framework.

The goal of this dissertation is to document the depositional and environmental context for taphonomy and composition of mammal faunas of the Barstow Formation. I characterized the changes in depositional environments, facies, and vegetation through the formation in relation to tectonics and climate, and I interpreted the taphonomic histories of fossil localities in order to reconstruct the influence of facies and preservation on the fossil record. I also assessed the effects of sampling and preservation on faunal composition, richness, and turnover in the large-mammal fauna through the formation. By reconstructing local depositional environments and vegetation through time using compound-specific biomarkers, soil organic matter, and biogenic silica, I provide the depositional and climatic context for the changing faunal diversity and composition of the Barstow Formation. Developing this context is important for understanding the processes that contributed to the preservation of the Barstow fossil record and high faunal diversity from this region during the middle Miocene. The depositional history and facies of the Barstow Formation are typical of extensional basins, and fossil abundance increases through the section with decreasing tectonic influence and changing depositional environments. The pattern of fossil preservation through the formation provides a model for stratigraphic and taphonomic controls on fossil occurrences in continental extensional basins.

In Chapter 2, I present a stratigraphic and facies framework for the Barstow Formation. Through field study of the lithology and stratigraphic distribution of facies, I identified and characterized six major facies associations in the formation. A facies association encompasses suites of facies that form through processes occurring within a particular depositional environment. These facies associations represent the major environments that formed in the

Barstow Basin as it filled over time. Facies Association 1 represents channel deposits of alluvial fans that drained into playa lake deposits represented by Facies Association 2. Facies Association 3 represents the channel and proximal-floodplain deposits of meandering streams, and Facies Association 4 represents channel deposits of braided streams. Facies Associations 5 and 6 represent floodplain and wetland deposits. These depositional environments formed as rates of subsidence and accommodation changed through the tectonic evolution of the basin. Coarse clastic material was shed into the basin in alluvial fans during extension and early rapid subsidence of the basin; as rates of subsidence and sediment accumulation declined, streams and floodplains developed. With the changing depositional environments, the ability of these settings to preserve fossils changed as well, resulting in an increase in the number of fossil localities and specimens through the formation. Chapter 2 provides the depositional and stratigraphic framework on which the remaining chapters are based. This chapter has been published as Loughney and Badgley (2017).

In Chapter 3, I reconstructed the paleoenvironments of the Barstow Formation in relation to the influences of changing climate before, during, and after the MMCO. I used a combination of geochemical and micropaleontological techniques to reconstruct environmental conditions through the formation. I collected sediment samples throughout the formation for analyses of biomarkers, soil organic matter, phytoliths and diatoms. I used carbon- and hydrogen-isotopic records from normal-alkanes from biomarkers and carbon-isotopic records from soil organic matter to reconstruct hydrology, climatic, and growth conditions affecting plants at the time of deposition. I analyzed phytolith (plant silica) assemblages to reconstruct vegetation composition and structure (open-canopy grassland or closed-canopy forest) and to understand how they varied through the formation in response to changing depositional environments and climate. Diatom

assemblages provided information about moisture availability and drainage characteristics of depositional environments. Early forming environments in the Barstow Basin were dry, and moisture availability increased through the MMCO, possibly from increased precipitation during this time; palms and woody dicots grew in these humid riparian settings. After 14 Ma, climatic cooling resulted in a return to drier conditions, and increased pedogenic development indicates that seasonality of precipitation increased. Wooded grasslands formed around ephemeral wetlands during these drier and cooler conditions. Reconstructions of hydrology and vegetation through the Barstow Formation provide context for understanding the habitats that supported mammals and contributed to mammal diversity and fossil accumulation. This chapter is in preparation for submission for publication.

In Chapter 4, I evaluated the taphonomic properties of fossil assemblages from the Barstow Formation in order to reconstruct the conditions leading to their accumulation and preservation. I focused on large-mammal specimens collected from excavations and surface collections. I described detailed stratigraphic sections of 61fossil localities in the field, and I examined over 3,000 specimens in museum collections for bone-damage patterns, skeletal-element composition, and taxon body size. The majority of fossil assemblages represent accumulations at long-term sites of mortality; fluvial processes were also important factors in concentrating fossil assemblages. Fossil assemblages occurred through six taphonomic pathways as accumulations in channel-margin deposits, accumulations at waterholes, carnivore and scavenger accumulations, channel-lag concentrations, crevasse-splay deposits, and one floating carcass. The types of pathways accumulating fossils vary with facies associations through the formation, such that fossil assemblages from the channel and floodplain deposits of Facies Associations 3 and 4 accumulated only through the channel-fill pathway, whereas assemblages in the floodplain and

wetland deposits of Facies Associations 5 and 6 accumulated through multiple pathways. These taphonomic analyses are the basis for understanding the modes by which fossil assemblages formed, which can have significant effects on species richness, diversity, and size structure through the formation. This chapter is in preparation for submission for publication.

In Chapter 5, I analyzed the faunal composition and richness in relation to facies associations and taphonomic pathways. I analyzed the stratigraphic ranges of species and calculated confidence intervals on their ranges to compare observed and inferred lowest and highest occurrences and turnover through the formation. High species richness is correlated with high frequencies of localities and specimens from specific stratigraphic intervals; rich fossil localities in Facies Associations 3, 4, 5, and 6 represent major intervals of observed turnover in the formation. High preservation potential in the proximal-channel settings of Facies Association 3 captures the highest number of observed lowest occurrences of species, and this facies association has high richness. Richness declined in Facies Association 4, as mammals did not inhabit the channels represented by the amalgamated sandstone deposits that characterize this facies association. The poorly drained floodplain deposits of Facies Association 5 also had high preservation potential, and many fossil localities occur in this setting. Richness declined again in Facies Association 6, and many species have their observed highest occurrences in this facies association. Observed turnover is high in stratigraphic intervals with high frequencies of localities and specimens. In contrast, patterns of inferred turnover based on confidence intervals are gradual through the formation, demonstrating that observed turnover patterns are largely controlled by facies. Richness in facies associations with low preservation potential is therefore under-sampled and likely does not represent the number of species present the basin. By relating species richness to specimen abundance and facies setting, I showed that preservation bias is a

confounding factor in interpreting the patterns of faunal composition, richness, and turnover. This chapter is in preparation for submission for publication.

In Chapter 6, I concluded by summarizing the depositional and taphonomic history of the Barstow Basin through the MMCO from the results of the previous chapters. I also evaluated the stratigraphic and fossil records of the Barstow Formation in the wider context of the Great Basin during the Miocene. In order to assess the influences of tectonics on the stratigraphic and fossil record on a regional scale, I compared the average deformation rates from faulting in the Great Basin (McQuarrie and Wernicke, 2005) to sediment thickness of fossiliferous formations and the number of large-mammal genera in the northern and southern Great Basin over the Miocene based on data from Janis et al. (1998). Sediment thickness and number of genera show similar trends through the Miocene and do not track changes in rates of deformation. Increasing sediment thickness and number of genera correspond to declining rates of deformation, indicating that fossiliferous sequences in the Great Basin formed with waning tectonic influence. This trend of increasing fossil preservation with declining tectonic activity is similar to that observed in the Barstow Formation, where it is related to changing depositional environments through time. The timing of sediment accumulation in extensional basins determines the changes in depositional environments that influence fossil preservation. This pattern is reflected in the deposition of fossil-bearing sequences with declining deformation rates across the Great Basin.

Fossil preservation is intricately linked with the history of geologic basins and the tectonic and climatic controls that govern subsidence, deposition, hydrology, and erosion. At the basin scale, these controls determine the landscapes and environments that form and their ability to accumulate and preserve organic remains. At the regional scale, these controls affect the faunal composition and evolutionary history of taxa over millions of years. The Barstow Formation

offers an opportunity to study the history of sediment deposition and fossil accumulation through a well-characterized interval of tectonic and climatic activity. The factors underlying the diverse faunal record of the Barstow Formation are depositional, environmental, and preservational; in this dissertation, I characterized each component of the record in order to show how the geologic record and fossil record are connected.

References

Badgley, C., Smiley, T.M., and Loughney, K.M., 2015, Miocene mammal diversity of the Mojave region in the context of Great Basin mammal history, *in* Reynolds, R.E., ed., Mojave Miocene: The 2015 Desert Symposium Field Guide and Proceedings: Zzyzx, California, California State University Desert Studies Consortium, p. 34-43.

Badgley, C., Smiley, T.M., Terry, R., Davis, E.B., DeSantis, L.R.G., Fox, D.L., Hopkins, S.S.B., Jezkova, T., Matocq, M.D., Matzke, N., McGuire, J.L., Mulch, A., Riddle, B.R., Roth, V.L., Samuels, J.X., Strömberg, C.A.E., and Yanites, B.J., 2017, Biodiversity and Topographic Complexity: Modern and Geohistorical Perspectives: Trends in Ecology & Evolution, v. 32, no. 3, p. 211-226.

Behrensmeyer, A.K., Kidwell, S.M., and Gastaldo, R.A., 2000, Taphonomy and paleobiology: Paleobiology, v. 26, no. 4, p. 103-147.

Browne, I.D., 2002, Late Barstovian mammalian fauna of the Robbin's Quarry (Barstow Formation, San Bernardino County, California) [M.S. thesis]: University of California, Riverside, 111 p.

Catuneanu, O., 2006, Principles of Sequence Stratigraphy: Amsterdam, Elsevier, 375 p.

Dibblee, T.W., Jr., 1967, Areal geology of the western Mojave Desert California, Geological Survey Professional Paper 522: Washington, D.C., p. 153.

Dickinson, W.R., 2002, The Basin and Range province as a somposite extensional domain: International Geology Review, v. 44, no. 1, p. 1-38.

Janis, C.M., Scott, K.M., and Jacobs, L.L., 1998, Evolution of Tertiary Mammals of North America, Volume 1: Terrestrial Carnivores, Ungulates, and Ungulatelike Mammals: Cambridge, U.K., Cambridge University Press, p. 691.

Lindsay, E.H., 1972, Small mammal fossils from the Barstow Formation, California: University of California Publications in Geological Sciences, v. 93, p. 1-104.

Loughney, K.M., and Badgley, C., 2017, Facies, environments, and fossil preservation in the Barstow Formation, Mojave Desert, California: PALAIOS, v. 32, no. 6, p. 396-412.

MacFadden, B.J., Swisher, C.C., III, Opdyke, N.D., and Woodburne, M.O., 1990, Paleomagnetism, geochronology, and possible tectonic rotation of the middle Miocene Barstow Formation, Mojave Desert, southern California: GSA Bulletin, v. 102, no. 4, p. 478-493.

McQuarrie, N., and Wernicke, B.P., 2005, An animated tectonic reconstruction of southwestern North America since 36 Ma: Geosphere, v. 1, no. 3, p. 147-172.

Miller, D.M., Rosario, J.E., Leslie, S.R., and Vazquez, J.A., 2013, Paleogeographic insights based on new U-Pb dates for altered tuffs in the Miocene Barstow Formation, California, *in* Reynolds, R.E., ed., Raising Questions in the central Mojave Desert: The 2013 Desert Symposium Field Guide and Proceedings: Zzyzx, California, California State University Desert Studies Consortium, p. 31-38.

Pagnac, D., 2005, A systematic review of the mammalian megafauna of the middle Miocene Barstow Formation, Mojave Desert, California [Ph. D. dissertation]: University of California, Riverside, 384 p.

Patzkowsky, M.E., and Holland, S.M., 2012, Stratigraphic Paleobiology: Understanding the Distribution of Fossil Taxa in Time and Space: Chicago, University of Chicago Press, 259 p.

Steinen, R.P., 1966, Stratigraphy of the middle and upper Miocene Barstow Formation, San Bernardino County, California [M.S. thesis]: University of California, Riverside, 150 p.

Woodburne, M.O., Tedford, R.H., and Swisher, C.C., III, 1990, Lithostratigraphy, biostratigraphy, and geochronology of the Barstow Formation, Mojave Desert, southern California: GSA Bulletin, v. 102, p. 459-477.

Zachos, J.C., Pagani, M., Sloan, L.C., Thomas, E., and Billups, K., 2001, Trends, rhythms, and aberrations in global climate 65 Ma to present: Science, v. 292, p. 686-693.

CHAPTER 2

Facies, environments, and fossil preservation in the Barstow Formation, Mojave Desert, California[1]

Abstract

Continental deposits of the middle Miocene Barstow Formation formed in an extensional basin of the Mojave region. Mammalian faunas of the type section in the Mud Hills, California, are the basis for defining the Barstovian North American Land Mammal Age. Prior mapping, lithostratigraphy, geochronology, and fossil collecting have established a structural, chronostratigraphic, and biostratigraphic framework for the Barstow Formation. Here, we analyze the sedimentary facies of the lithostratigraphic sequence, infer the major depositional environments, and assess controls on fossil preservation in relation to major facies. We recognize six major facies associations that represent alluvial fans, shallow or seasonal lakes, and channels and floodplains. The transition from older, fan-dominated to younger, floodplain-dominated environments reflects changes in tectonics, accommodation, drainage, and depositional settings during the formation and filling of the basin. Fossil-mammal concentrations are common in four facies associations. Body fossils are abundant in two facies associations that represent well-drained floodplains and spring-fed wetlands. Fossil concentrations are moderately abundant in facies associations that represent floodplains and channel deposits, and fossils are rare in facies

[1] Loughney, K.M., and Badgley, C., 2017, Facies, environments, and fossil preservation in the Barstow Formation, Mojave Desert, California: PALAIOS, v. 32, no. 6, p. 396-412.

associations that represent alluvial fans and lake margins. The highest frequency of fossil localities occurs in the facies associations representing both suitable life habitats and high preservation potential for terrestrial mammals.

Introduction

The sedimentary facies that preserve the fossil record represent remnants of the ecosystem in which the organisms lived (or to which they were transported), as well as environments of preservation of organic remains and environments of deposition within a regional sedimentary system. The paleo-ecosystem—as inferred from the tectonic and depositional context, physical and chemical properties of sediments, and fossils themselves—indicates where organisms lived, died, and were ultimately buried. In a stratigraphic context, the environments of deposition indicate where and when fossils occur in the history of a sedimentary basin. Elucidating the influences of environment, preservation, and stratigraphy on the fossil record is a major goal of stratigraphic paleobiology and provides a foundation for analysis of preservation biases, diversity and abundance, and biotic change over time (Patzkowsky and Holland, 2012).

In this paper, we evaluate the facies, depositional environments, life habitats, and preservation potential for the middle Miocene Barstow Formation in the Mud Hills, located in the central Mojave Desert of southeastern California, U.S.A. (Fig. 2.1). Early Miocene (~22–18 Ma) extension in the central Mojave region created an asymmetrical basin that filled with alluvial, lacustrine, and volcaniclastic deposits of the Barstow and older formations (Fillmore and Walker, 1996). The Barstow Formation contains the type section of the Barstovian North American Land Mammal Age (Woodburne, 2004) and spans the middle Miocene Climatic Optimum (17–14 Ma), an interval of global warming that witnessed substantial changes in

mammal diversity and composition across western North America (Barnosky and Carrasco, 2002; Kohn and Fremd, 2008; Finarelli and Badgley, 2010). The goals of this study are to determine: (1) The major sedimentary facies of the Barstow Formation in the Mud Hills and their corresponding depositional environments; (2) The spatial and temporal distribution of facies in relation to sedimentary models of extensional basins; (3) The distribution of fossil localities among the major sedimentary facies; and (4) The differences among facies as habitable environments for terrestrial organisms and as settings that preserve organic remains.

Geological Background

The Mojave tectonic block is part of the Basin and Range tectonic province, where many asymmetrical basins formed during regional extension from the late Oligocene to the late Miocene (McQuarrie and Wernicke, 2005). In the central Mojave region, localized extension occurred between 24 and 18.5 Ma along the Waterman Hills detachment fault, producing 40–60 km of extended terrain (Fillmore and Walker, 1996; Glazner et al., 2002). Syn-extensional volcaniclastic breccia and alluvial deposits of the Jackhammer, Pickhandle, and Mud Hills formations were derived from uplands at the detachment breakaway zone (Fillmore and Walker, 1996) and from emerging dacite domes centered in the present-day Calico Mountains (Fig. 2.1; Singleton and Gans, 2009). The Barstow Formation unconformably overlies the Pickhandle and Mud Hills formations and was deposited during and after the late stages of extension (Ingersoll et al., 1996; Fillmore and Walker, 1996; Woodburne, 2015). The type section of the Barstow Formation lies in the Mud Hills (Fig. 2.1) north of Barstow, California (Dibblee, 1968). The sequence ranges from 19.3 to 13.3 Ma (Fig. 2.2), as determined by mammalian biostratigraphy

(Lindsay, 1972; Pagnac, 2009), magnetostratigraphy (MacFadden et al., 1990), and radioisotopic dating of tuffs (MacFadden et al., 1990; Woodburne et al., 1990; Miller et al., 2010).

The Barstow Formation crops out intermittently over approximately 5600 km^2 in the central Mojave region. The formation is best exposed in the Mud Hills, where fossiliferous outcrops have historically been the main focus of study. The formation is divided into three members (Fig. 2.2; Woodburne et al., 1990). The basal Owl Conglomerate Member consists of coarse sandstone and conglomerate; the Middle Member contains sandstone, mudstone, and marl; and the Upper Member is characterized by siltstone and marl (Dibblee, 1968; Lindsay, 1972; Woodburne et al., 1990). Locally, the Barstow Formation is overlain by Pliocene basalt flows and regionally by Quaternary alluvium (Woodburne et al., 1990). Several airfall tuffs that occur throughout the sequence serve as marker beds for correlation across covered areas and faults. Selected tuffs (Fig. 2.2) have been dated using K/Ar and Ar/Ar (MacFadden et al., 1990) and U/Pb methods (Miller et al., 2010). In the late Miocene to Pliocene, regional rotation and strike-slip faulting deformed the older deposits (Ingersoll et al., 1996; Glazner et al., 2002). In the Mud Hills, the Barstow Formation has been folded into a westward-plunging syncline, with the oldest part of the section exposed in the east and the youngest part exposed in the west.

The most abundant fossils from the Barstow Formation are skeletal remains of mammals, whereas fossils of birds, reptiles, amphibians, and fish are rare (Lofgren et al., 2014). The majority of localities producing body fossils occur in the Middle and Upper members (Lindsay, 1972; Pagnac, 2009). Invertebrate body fossils are rare in the Mud Hills, but ichnofossils are locally abundant throughout the section. Plant macrofossils occur at three localities in the Mud Hills (Reynolds, 2013; Reynolds and Schweich, 2013), and pollen (Fisk and Maloney, 2014) and phytoliths have been recovered from a few horizons, mostly in the Upper Member (Loughney

and Smith, 2015). Mammalian trackways occur throughout the formation (Alf, 1966; Lofgren et al., 2006). Fossils have been retrieved via surface collecting, quarrying, and screen washing.

Methods

We measured 23 stratigraphic sections at nine locations in the Mud Hills using a Brunton compass and Jacobs staff. We mapped the locations of stratigraphic sections using a Garmin eTrex GPS device and a 1:24,000 topographic map (USGS, 1996). These sections span approximately 1300 m, the entire thickness of the Barstow Formation exposed in the Mud Hills. We correlated our measured sections with 12 stratigraphic sections from Lindsay (1972), Woodburne et al. (1990), and MacFadden et al. (1990) to maximize lateral coverage of the Mud Hills (Figs. 2.1, S2.1). Locality information for measured sections is provided in these published sources and compiled in Table S2.1. We tied fossil localities directly into our sections when encountered in the field and recorded the GPS coordinates of these localities.

We described lithologies in detail as we measured stratigraphic sections. Facies in the Barstow Formation are typical of floodplain, lacustrine, and alluvial-fan environments, and as such, they are laterally and vertically variable. Sets of facies with similar lithological and relational characteristics can be grouped into discrete facies associations (Reading, 1978). Facies associations may be broadly distributed and represent the dominant environments at the time of deposition. We recognized major facies associations on the basis of the lateral and vertical relationships of facies sharing similar lithological, depositional, and postdepositional properties, including texture, composition, sedimentary structures, bed geometry, pedogenic features, and ichnofossil content. Environments of deposition were interpreted on the basis of known facies-

environment relationships (e.g., Reading, 1978), previous work in the Barstow Formation (e.g., Steinen, 1966; Woodburne et al., 1990), and from published studies of continental sequences.

For each facies association, we estimated sediment-accumulation rates from stratigraphic intervals of known duration and thickness, adjusted for compaction (see supplementary information for methods). For age control, we used individual paleomagnetic intervals with dated endpoints from stratigraphic sections in Woodburne et al. (1990) and MacFadden et al. (1990), using the correlation of Woodburne (1996) and updated magnetochron ages from Ogg (2013). We correlated stratigraphic sections from Steinen (1966), Dibblee (1968), and our measured sections to the age framework of MacFadden et al. (1990). We also used dated tuff units as isochrons for stratigraphic segments with known thickness and duration. We used sediment-accumulation rates of the different facies associations in evaluating sedimentary models of extensional basins and the distribution of fossil localities in relation to facies distribution.

We contrasted the preservation potential of each facies association against its suitability as habitat for terrestrial mammals. Suitable life habitats for terrestrial organisms were evaluated based on indicators of subaerial exposure and the presence of fresh water. Facies displaying evidence of prolonged exposure (e.g., root traces, insect nests, pedogenesis) were considered to represent land surfaces that supported vegetation and provided habitat for terrestrial mammals. Fossil preservation requires rapid burial and a chemical environment that stabilizes organic remains (Martin, 1999). For each facies association, preservation potential was evaluated qualitatively based on environmental setting, mode of preservation, comparison to taphonomic analyses of fossil localities reported in the literature (Eberth et al., 2007), and comparison to modern environments.

We compiled information about fossil localities from the Miocene Mammal Mapping Project database (MIOMAP, 2005), as well as from data in Alf (1970), Lindsay (1972), Woodburne et al. (1990), Lofgren et al. (2006), and Pagnac (2009). The San Bernardino County Museum (SBCM) documents 440 recorded fossil localities from the Barstow Formation (R.E. Reynolds, personal communication, 2016). We found location information for only 248 localities, based on available records from MioMap and the University of California Museum of Paleontology (UCMP), the Raymond Alf Museum (RAM), the U.S. Geological Survey, the Los Angeles County Museum, and SBCM. For this study, we evaluated 152 localities for which we could identify the facies-association context. For 64 localities, we assessed their depositional settings and facies context by direct observation; the settings of other localities were interpreted from the literature, aerial photographs and Google Earth, and topographic maps.

For these 64 localities, we present two kinds of taphonomic data that relate to the accumulation and burial of skeletal elements based on assessments of fossil material from the Barstow Formation in the collections of UCMP, RAM, and the American Museum of Natural History (AMNH). We grouped localities into depositional environments related to landscape position. For each locality and environment, we computed the mean number of skeletal elements for which weathering stage and original abrasion could be assessed.

The degree of bone weathering increases with exposure duration and daily fluctuations in temperature and moisture that occur near and at the soil surface (Behrensmeyer, 1978). Abrasion may occur through transport and reworking of material in channel settings (Behrensmeyer, 1988) or trampling of bones exposed at the surface. Weathering and abrasion can be impeded by poor soil drainage (Loughney et al., 2011), and burial can be accelerated by trampling in moist environments (Behrensmeyer and Dechant Boaz, 1980).

Results

Results include a description of the major facies associations and their lateral and vertical distribution in the Mud Hills, the distribution of fossil localities among facies associations, estimates of sediment-accumulation rates for each facies association, and taphonomic data.

Facies Associations

On the basis of field descriptions of 23 stratigraphic sections, we recognized six facies associations (FA). Table 2.1 summarizes the sedimentary characteristics of facies within each facies association and their interpretation, as elaborated below.

Facies Association 1

FA 1 is the stratigraphically lowest facies association in the Mud Hills and contains the coarsest lithologies in the Barstow Formation. The major lithological component is coarse-grained sandstone and conglomerate; finer-grained sandstones and mudstone constitute a minor component (Fig. 2.3). FA 1 is best exposed in the eastern Mud Hills on the north limb of the Barstow syncline. Here, 197 m of indurated, cliff-forming, pale olive, coarse-grained amalgamated sandstone and conglomerate are exposed (Fig. 2.4A). The conglomerate is matrix-supported and massive except for linear lenses of lithic clasts; rare trough cross-stratification and channel scours are partially defined by pebble lags. Most clasts range in length from 1-10 cm, although lenses with clasts longer than 20 cm occur throughout.

On the southern limb of the syncline, the coarse facies crops out in low hills of grayish orange, very coarse-grained, amalgamated sandstone and conglomerate with lithic clasts. Clasts are 1-20 cm in length, subangular to subrounded, and occur in discrete lenses. Trough cross-

stratification is evident where outcrops are indurated, and beds are otherwise massive except for cobble lenses. Phytoclasts (calcareous rinds precipitated around twigs and branches; Arenas-Abad et al., 2010) 2-25 cm long occur in concentrated lenses that extend laterally for up to 40 m.

The fine-grained component of FA 1 is well exposed on the north limb of the syncline as non-resistant beds sharply overlain by resistant conglomeratic sandstone (Fig. 2.4A). These fine-grained beds are 3-4 m thick and consist of cross-laminated, fine-grained sandstones interbedded with claystones. Claystone interbeds are 30-45 cm thick with moderately well-developed pedogenic structure, including root traces and well-developed slickensides. Rare phytoliths from these layers indicate the presence of grasses (Loughney and Smith, 2015). On the south limb, very fine- to medium-grained sandstone beds are bioturbated and have occasional mottles and slickensides. Indeterminate insect burrows, fine root traces, and *Celliforma* (nests and cells of bees; Genise, 2000) occur in these horizons.

On the north limb of the syncline, a layer of tufa 3 m thick occurs at the top of a thick conglomeratic sandstone. This tufa has mudcracks and undulating stromatolitic layers. On the south limb of the syncline, phytoclast lenses and stromatolites ~12 cm in diameter can be traced eastward for over 1 km. These persistent tufas mark the transition between FA 1 and FA 2.

We interpret FA 1 as deposits of bedload-dominated streams on an alluvial fan. Our interpretation follows those of Steinen (1966) and Dibblee (1968). The interbedded sandstone and siltstone represent near-channel interfluve deposits that were vegetated. The low frequency of the finer-grained facies indicates that floodplains were not extensive during this phase in Barstow deposition. Fine-grained deposits on alluvial fans typically represent mudstone plugs on the upper fan or overbank settings on the middle and distal fan (Bluck, 1967). The presence of the mudstone facies within the conglomeratic sequence indicates that interfluves were able to

form between stream channels. The composition of conglomerate clasts indicates two source areas: on the north side of the syncline, granitic and monzonitic clasts were derived from the north, possibly from the Paradise Mountain quartz-monzonite; on the south limb, the mostly andesitic and metamorphic clasts likely were derived from the Waterman Hills to the south (Dibblee, 1968; Woodburne et al., 1990; Woodburne, 2015). Throughout, volcanic clasts were likely eroded from the older Jackhammer and Pickhandle formations (Steinen 1966).

Similar thick beds of conglomerate and sandstone in the Devonian Old Red Sandstone of Scotland were interpreted by Bluck (1967) as streams traversing alluvial fans. He interpreted these streams as forming on the mid-fan, between chaotic mudflow deposits proximal to the source and incised channel deposits of the distal floodplain. In the Paleocene Beartooth Conglomerate of Wyoming and Montana, DeCelles et al. (1991) interpreted thick conglomerate and sandstone packages as deposits of laterally migrating, entrenched streams on a multi-lobe alluvial fan complex. These packages are bounded by siltstone sequences, interpreted as overbank deposits on the middle and upper fan lateral to sites of channel sedimentation.

Facies Association 2

FA 2 consists predominantly of thin beds of siltstone, claystone, and marl with sandstone and minor conglomerate (Fig. 2.3). These deposits form low hills that crop out in the eastern Mud Hills (Figs. 2.1, 2.4B) and thicken eastward (Fig. 2.5). The deposits of FA 2 include a coarse transitional facies and a fine-grained facies that is up to 250 m thick. In the eastern Mud Hills, the presence of tufa marks the transitional facies between FA 1 and 2; the fine-grained facies of FA 2 grades upward into FA 3 over approximately 10 m. East of the Mud Hills, sandstone beds

of the transitional facies are intercalated with the fine-grained facies of FA 2 over approximately 30 m.

The basal transitional facies includes sandstones and conglomerates that overlie brecciated carbonate and conglomerate probably belonging to the uppermost Pickhandle Formation. Sandstone beds are 25-35 cm thick, fine- to coarse-grained, and trough cross-stratified. Beds have incised bases and fine upwards from pebble lags to siltstone drapes with a few interbedded gravel lenses. On the south limb of the syncline, mushroom-shaped tufa mounds occur within trough cross-stratified and planar-bedded, coarse-grained, pebbly sandstone. The mounds are 10-25 cm tall, and smaller thrombolitic growths are 1-5 cm tall, covered by a thin clay drape.

The fine-grained facies of FA 2 contains thin, alternating beds of fine-grained sandstone, weakly calcareous siltstone and claystone, and marl. Beds are laminated and typically 2-10 cm thick, and thin tuff layers 1-10 cm thick also occur in this sequence. Gypsum crystals frequently weather out of the siltstone and claystone beds. A layer of small tubular phytoclasts (1.0-1.4 cm long, 0.7 cm diameter) at the top of a planar- and cross-stratified fine silty sandstone marks the beginning of this facies. Marl layers are nodular, contain oncoids and mudcracks, or have wavy parallel laminae indicating biogenic influence in their formation. Thin layers of brown-weathering, cross-stratified, fine- to medium-grained calcareous sandstone occur throughout this facies. Approximately 20 m above the phytoclast layer is a contorted stromatolite unit 30-50 cm thick within a medium- to coarse-grained sandstone bed. The stromatolites have mud drapes and mudcracks on upper surfaces. Orange oxidation stains are evident in several marls and associated claystone layers, but no root traces or burrows occur in these deposits.

We interpret FA 2 as forming at the margins of a shallow lake, representing a wet or seasonally wet playa. The transitional coarse facies represents channel deposits that drained into

the lake. Calcareous sandstone layers represent sandy mudflat deposits (Reading, 1978), and tufa and stromatolites formed along the sandy margins of the lake (Reynolds et al., 2010) during times of low sedimentation. Phytoclasts represent calcareous coatings of charophytes, which are common features in marginal lacustrine settings (Platt and Wright, 1991). The tufa mounds in the eastern Mud Hills have been interpreted as forming at the interface of alkaline lakewaters and groundwater springs (Becker et al., 2001; Cole et al., 2004). Authigenic zeolite minerals from the eastern Mud Hills formed in waters with fresh to moderate alkalinity and moderate to high salinity (Sheppard and Gude, 1969). Several layers rich in strontium and borate minerals also occur in this facies in the eastern Mud Hills and elsewhere in the Barstow Formation (Reynolds et al., 2010), although it is unresolved whether these minerals are syn-depositional or hydrothermal in origin (Dibblee, 1968).

The lake margins expanded and contracted over time, as indicated by the numerous biogenic marls and stromatolites in stratigraphically distinct horizons (Reynolds et al., 2010), but the absence of extensive or bedded evaporites indicates that this lake never completely dried out. Deposits of interbedded sandstone, siltstone, and marl in the Calico Mountains east of the Mud Hills were interpreted by Park (1995) as deposits of a shallow, saline-alkaline lake. Fluctuating water levels promoted the growth of microbial mats, but the absence of bioturbation in FA 2 indicates that conditions were unfavorable to many plants or burrowing organisms. Link and Osborne (1978) described similar deposits in the lacustrine facies of the Pliocene Ridge Basin Group, north of Los Angeles, California. There, cross-stratified sandstone, conglomerate lags, and mudstone are interbedded with sequences of laminated mudstone and sandstone containing stromatolites, oncolites, and ooids. They interpreted these deposits as forming in a lake-margin setting where shoreline sands and mudflats grade basinward into deeper lake environments.

Facies Association 3

Sandstone, minor conglomerate, siltstone, claystone, and marl constitute FA 3 (Figs. 2.3, 2.4C). FA 3 is thickest in the central part of the Mud Hills, where it overlies FA 1 (Fig. 2.5). The transition between the two facies associations is gradual over 32 m and marked by the fining and thinning of sandstone beds.

Coarse-grained facies of FA 3 include fine- to coarse-grained sandstone and conglomerate (beds 1.0-1.5 m thick). Small- to medium-scale trough cross-stratification is evident in thicker beds, and sets of planar and ripple cross-stratification 7-10 cm thick occur in thinner sandstone beds. Sandstone layers generally fine upwards and may have thin interbeds of claystone or siltstone, and parting lineations are present on the tops of some fine sandstone layers. Layers of fine- to medium-grained sandstone often have coarse sand lenses, and medium- to coarse-grained sandstone layers have conglomerate lenses of pebble- to cobble-size clasts, typically with scoured bases. Conglomerate lenses are poorly sorted with gravel-size clast lenses, 30-50 cm thick, in coarse sand matrix, typically with incised bases. Insect burrows (3-4 mm diameter) in the sandstone bodies are rare but may be well developed in brown-weathering, indurated, and irregularly shaped horizons.

The finer-grained facies of FA 3 include sandstone, siltstone, and marl. Sandstones generally fine upwards into siltstone layers that are up to 1 m thick, and sandstone beds may be interbedded with fine-grained lithologies in intervals up to 8 m thick. The finer-grained component of FA 3 includes siltstone and silty claystone, as well as interbedded siltstone, claystone, and marl. Pale olive siltstone and silty claystone layers are sometimes laminated and have common redoximorphic concentrations. Root traces 1-3 mm in diameter are common in the

mudstones, typically as dark yellowish orange redoximorphic haloes, and sometimes as carbonized remains.

Thin interbeds of claystone (0.3-1.0 cm), siltstone (1.5-2.0 cm), and brown-weathering marl (1-3 cm) are intercalated with sandstone and other fine-grained deposits. Marl layers are thin (3-5 cm) and nodular with orange mottling and are typically spaced 4-6 cm apart. Mudcracks and burrows are common in marl layers, and some layers have wavy biogenic laminae. These sequences are up to 4.5 m thick and grade upwards into silty sandstone with silt drapes, which then grades upwards into ripple-stratified, medium-grained sandstone or is sharply overlain by thin (15-20 cm thick) medium-grained sheet sandstone.

We interpret the deposits of FA 3 as several types of channel-proximal fluvial deposits. Thick trough cross-stratified sandstone and conglomeratic layers represent channel and bar deposits (Reading, 1978); sets of planar and ripple cross-stratification in fine sandstones represent channel bar deposits (Bridge, 2003) or possibly chute deposits where clay and silt drapes are common (Reading, 1978). The range of sedimentary structures from silt drapes to parting lineations indicates that flow conditions varied from standing water to upper flow regime. Laminated and rooted siltstone layers represent levee or near-channel floodplain deposits, and thin sheet sandstones occurring within these siltstones represent crevasse-splay deposits (Bridge, 2003). Lithologically and spatially variable sequences of sandstone and mudstone characterize modern channel and floodplain deposits; these sequences pass from mud-dominated backswamp to sandstone- and conglomerate-dominated channel deposits, exemplified by deposits of the lower Mississippi River Valley (Farrell, 1987). The claystone-siltstone-marl sequences represent palustrine deposits that experienced periodic, perhaps seasonal, drying. Evidence of desiccation

is common in palustrine limestones, as are iron concentrations and nodule formation, due to fluctuating water levels (Alonso-Zarza, 2003).

Facies Association 4

Stacked, multi-story sandstone packages form the majority of deposits in FA 4 (Fig. 2.3). These packages are located on the south limb of the syncline in the central part of the Mud Hills where they are approximately 240 m thick, and individual beds can be traced laterally for hundreds of meters (Fig. 2.4D). They overlie deposits of FA 3 in the central Mud Hills, and the interval marking the transition to FA 4 is 30-50 m thick. In the transition zone between FA 3 and 4, sandstone layers become thick and massive, and finer-grained deposits are thin and occur less frequently than in FA 3. To the west, boundaries of FA 4 sandstone beds are less defined and are interbedded with siltstone intervals 5-10 m thick. The western portion of FA 4 interfingers with and grades into beds of FA 6 (Fig. 2.5).

The sandstone packages that dominate FA 4 are medium- to very coarse-grained, and massive except for occasional poorly-sorted pebble lenses (~5 cm thick). Thicker conglomerate lenses also occur within this facies and contain poorly sorted lithic clasts (3-20 cm) in a coarse-grained sandstone matrix. Thin, slightly pedogenic horizons occur in the top of some sandstone beds. These horizons are 2-3 cm thick, are less resistant than bounding sandstone packages, and have faint root traces and truncated tops, but otherwise are lithologically similar to the sandstone in which they are developed. Localized, brown-weathering, irregularly shaped, well-indurated sandstone horizons occur throughout the sandstone packages, spaced roughly 1.5-m apart vertically. These horizons can be traced several meters laterally.

Lithic clast composition is mainly granitic and volcanic with rare metamorphic clasts, possibly derived from older deposits of the Jackhammer, Pickhandle, or Barstow formations (Woodburne et al., 1990). Flow directions determined from cross-stratification and channel incision indicate a northward direction of flow, and the composition of lithic clasts indicates a south-southwestern source area, likely the Waterman Hills detachment fault (Dibblee, 1968; Woodburne et al., 1990; Woodburne, 2015). The lateral extent and stacked architecture of the sandstone packages indicate that these channels were relatively unconfined, and the minor occurrence of fine-grained overbank deposits in the thickest portion of FA 4 suggests that interfluves were not well developed or were located elsewhere. The brown-weathering, indurated sandstone features represent bioturbated horizons, as burrow casts are well formed in concretions that weather out of the encasing sandstone. The weakly pedogenic and bioturbated horizons represent exposed interfluve areas or vegetated bars that were short-lived. Floodplain deposits are better developed where FA 4 interdigitates with FA 3 and FA 6.

The stacked sandstones of FA 4 roughly correspond to the Coon Canyon member of Steinen's (1966) stratigraphic scheme, and they were interpreted as coarse fanglomerate deposits by Woodburne et al. (1990). Steinen (1966) and Woodburne et al. (1990) described their respective Coon Canyon member and fanglomerate deposits as extending approximately 4 km through the central Mud Hills (Fig. 2.1); from this large-scale geometry of the unit, they interpreted it as an alluvial fan. Although we agree that FA 4 represents channel deposits of bedload-dominated streams, we interpret FA 4 as the deposits of a broad alluvial braidplain rather than those of an alluvial fan. Willis (1993) studied laterally extensive stacked sandstone bodies of the Miocene Chinji and Nagri formations of Pakistan and interpreted them as channel and downstream-accreting bar deposits in discrete braided channel belts. Individual sandstone

bodies are not deeply incised, and pedogenic alteration of the tops of sandstone beds indicate exposure during low-flow stages, much like the deposits of FA 4. Vertical accretion deposits are not significant within these sandstone packages of the Chinji and Nagri formations, although packages are vertically separated by fine-grained overbank deposits (Willis, 1993).

Facies Association 5

Lithologies in FA 5 are mudstone-dominated and have two distinctive outcrop expressions: drab brown bentonitic mudstone and gray tuffaceous mudstone (Fig. 2.3). These mudstone units differ in their color, composition, and development of pedogenic features. The transition between FA 4 and 5 is only exposed in the central Mud Hills and is marked by the Skyline Tuff, a prominent marker unit that also marks the base of the Upper Member. In the western Mud Hills, FA 5 interfingers with FA 6 (Fig. 2.5).

Yellowish-brown siltstone and clayey siltstone layers are weakly pedogenic. Ped structure ranges from fine to large blocky peds, slickensides are weakly to moderately developed, and magnesium oxide concentrations are present but rare. Horizons of concretions are present in some sections, and root traces are locally common. On weathered surfaces, this facies appears darker than unweathered exposures and has a popcorn weathering texture characteristic of bentonite (Fig. 2.4E).

Sandstone, while rare in FA 5, does occur interbedded with the fine-grained siltstones. Beds of very fine- to very coarse-grained sandstone 10-30 cm thick are bounded by pedogenic siltstone; these sandstone beds are typically bioturbated with small-scale trough cross and ripple stratification and occasional flute casts on exposed bedding planes. In the tuffaceous siltstone facies, very fine- to medium-grained sandstone beds are 5 cm to 4 m thick. These layers are

laminated to trough cross-stratified with pebble lags and abundant root casts and insect burrows, including *Spongeliomorpha* (Melchor et al., 2009) and tubes of dipteran larvae, indicating moist environmental conditions (Hasiotis, 2002).

Pale olive tuffaceous siltstone and clayey siltstone layers are interbedded with many thin tuffs and marls. Sedimentary structures and imbricated bone fragments in a few tuff layers indicate that at least some tuffs were redeposited; others may have been deposited in standing water (Sheppard and Gude, 1969). The tuffs and marls are highly bioturbated with well preserved burrows and root casts. Fine to large (0.5 mm to 1 cm) siliceous root casts are abundantly preserved throughout the tuffaceous siltstones; some horizons have fine to medium blocky ped structure, slickensides, and small carbonate nodules, but pedogenic features are generally poorly developed or absent in this facies. Where these facies occur in succession, the drab bentonitic siltstone facies grades into the gray tuffaceous siltstone facies over approximately 2-5 m.

The drab-colored siltstone horizons typically occur in association with thin (5-15 cm) and thick tuff beds (1.0-1.5 m; Fig. 2.4E). Tuff layers are structureless, plane bedded, or ripple and trough cross-stratified and may have erosional bases with rip-up clasts, indicating redeposition of some layers. Tuff layers are often bioturbated with large burrows and roots, and a large *Spongeliomorpha* burrow in a thin tuff layer indicates that water tables were locally high (Hasiotis, 2002).

Earlier workers considered deposits of the Upper Member to be primarily lacustrine in origin (Dibblee, 1968; Lindsay, 1972; Woodburne et al., 1990). Steinen (1966) mapped the drab brown siltstone lithology as the Skyline member and the gray tuffaceous siltstone lithology as the *Hemicyon* member, both interpreted to represent lacustrine environments. Although many of the

facies formed in wet or seasonally wet environments, the suite of facies in FA 5 is more representative of a poorly drained floodplain than of a lake. The pedogenic siltstones represent areas that were exposed for extended periods of time. Heavily rooted marl beds represent palustrine or floodplain pond environments, and the abundant root casts in the tuffaceous siltstone facies indicate that vegetation was widespread, although the low-chroma coloration of the tuffaceous siltstones indicates that they were poorly drained (Fanning and Fanning, 1989). In portions of the Eocene Willwood Formation in Wyoming, Kraus and Gwinn (1997) interpreted gray- and brown-colored paleosols with weakly developed features as floodplain deposits with poor or better drainage, respectively. Relatively frequent avulsions precluded the formation of well-developed pedogenic features, producing compound paleosols with indistinct horizonation. The drainage conditions of these Willwood paleosols may reflect either differences in parent material properties or landscape position. Palustrine deposits in the Jurassic Morrison Formation also consist of drab-colored mudstones and biogenic carbonate beds (Dunagan and Turner, 2004). These Morrison deposits represent a wetter environment than was present in the Barstow, as Morrison wetland facies pass vertically into lacustrine facies, but the poorly drained lithologies are very similar to those in FA 5.

Facies Association 6

Much like FA 5, FA 6 is mudstone-dominated (Fig. 2.3), and these two facies associations are widely distributed over the western Mud Hills in the upper part of the Barstow Formation (Fig. 2.5). Portions of the sandy facies of FA 6 are similar to finer portions of FA 4, and distinguishing between these facies associations is difficult where they interfinger in the central Mud Hills. The mudstone facies in FA 6 are similar to those in FA 5 but are less tuffaceous and

bentonitic, and marl layers occur more frequently. The transition between these two facies associations is gradational but rapid, occurring over approximately 5 m. The distribution of FA 5 and 6 (Fig. 2.5) indicates lateral variability across the landscape, as these facies associations occur at similar vertical positions in the Barstow sequence.

The fine-grained facies primarily consist of yellowish-gray siltstone and minor paleo olive claystone interbedded with marl (Fig. 2.4F). Siltstone layers have abundant fine to large siliceous root casts, laminations, and may have small calcareous nodules and slickensides where clay content is high. Siltstone horizons are interbedded with silty marl beds that range from 5 to 20 cm in thickness, and intervals of intercalated marls are up to 9 m thick. Thin sections of sediment samples from this facies association reveal abundant calcareous micronodules, as well as calcareous root casts and networks characteristic of pseudomicrokarst (Alonso-Zarza and Wright, 2010). Marl beds are typically stromatolitic or thrombolitic with thin, wavy, parallel laminae and are often bioturbated. Some marl layers have brecciated or nodular tops, indicating subaerial weathering or fluctuating water tables (Alonso-Zarza and Wright, 2010). Gastropod shells referable to *Lymnaia* and *Planorbula* (Taylor, 1954; Plyley et al., 2013) occur in this facies.

Sandstone facies in FA 6 are fine- to coarse-grained with pebble lags and calcareous cement; they are plane-bedded or trough cross-stratified and occasionally massive, and the tops of many sandstone beds are bioturbated. These units have sharp basal contacts and may either fine upwards into sandy siltstone or be sharply overlain by siltstone. The sandstone units thicken eastward and intergrade with FA 4 in the central Mud Hills (Fig. 2.5); there, sandstone beds ~1 m thick are typically massive and interbedded with sandy siltstone. Upsection, facies become

sandier, and siltstone and sandy siltstone are interbedded with fine- to coarse-grained sandstone. Marl layers are less abundant overall but do occur locally (Fig. 2.4F).

We interpret FA 6 as the deposits of a floodplain with well-developed wetlands or ponds. FA 6 corresponds to Steinen's Carnivore Canyon member (Steinen, 1966). The numerous heavily-rooted marls indicate that palustrine settings were more extensive than in FA 5 and that they were heavily vegetated. *Lymnaia* and *Planorbula* are aquatic gastropods that prefer standing water or low-velocity streams (Taylor, 1954). Pseudomicrokarst features, such as root casts, micro-nodules, and network-like carbonate cements, are characteristic of palustrine settings, and brecciated or nodular marl beds form in palustrine settings that experience wetting and drying cycles (Alonso-Zarza and Wright, 2010). Dunagan and Turner (2004) interpreted wetland deposits in the Jurassic Morrison Formation of Colorado as distinct from lacustrine deposits based on the abundance of pseudomicrokarst features, pedogenic alteration of carbonate layers, and root casts.

Distribution of Fossil Localities Among Facies

Approximately 450 fossil localities are recorded from the Barstow Formation (R.E. Reynolds, personal communication, 2016). The 152 fossil localities included in this study are unevenly distributed among the facies associations in the Mud Hills. More than half occur in FA 5 and 6, 25 occur FA 3 and 4, and few occur in FA 1 and 2 (Table 2.2, Fig. 2.5). The plant macrofossil localities occur in FA 3, 5, and 6. Although many trackways have been collected from the Barstow Formation, locality data exist for very few (Lofgren et al., 2006). We noted here only a handful of these localities for which we could document the facies setting with confidence. Four occur in FA 5, and two each occur in FA 2 and 3 (Table 2.2).

The uneven distribution of localities in part relates to historical prospecting efforts, which have not been equally directed among facies or lithologies in the Mud Hills (M.O. Woodburne, personal communication, 2016). Differences in areal exposure of the Barstow members may contribute to this distribution: the areal exposure of the Owl Conglomerate Member is approximately 7.3 km^2, the Middle Member is approximately 3 km^2, and the Upper Member is approximately 12 km^2. In addition to the greater areal exposure of the upper part of the formation, the more easily weathered outcrops of FA 3, 5, and 6 increase the ability of prospectors to find vertebrate fossils in those facies associations. However, the preservation potential of skeletal remains differs among facies associations, as we discuss below.

Patterns in fossil occurrence in the Mud Hills differ at broad and fine scales. The facies associations that contain the highest number of fossil localities are those representing floodplains (FA 3, 5, 6), whereas those representing mainly near-channel, channel, and lacustrine settings (FA 1, 2, 4) have significantly fewer localities (Table 2.2; $\chi^2 = 37.6$, $p < 10^{-4}$). Within each facies association, the depositional settings of individual localities are variable and represent different positions on the landscape. For the 64 vertebrate localities documented in detail, we grouped localities into six categories related to landscape position: channel and bar, proximal levee and chute, distal levee and floodplain, crevasse splay, well-drained floodplain and wetland, and poorly-drained floodplain and wetland (Table 2.3). The proportions of bones displaying incipient (0-1) and moderate to advanced (2-5) weathering stages (Behrensmeyer, 1978) and original abrasion in assemblages from each category are also shown.

The majority of the 64 localities examined at a fine scale occurs in FA 5 and 6 (73%) and represent a broad range of landscape positions. Most of the localities in FA 1, 3, and 4 represent positions close to channels, with relatively few localities occurring in distal floodplain settings

(Table 2.3). The most weathered assemblages are from localities in the crevasse splay and channel and bar categories (Table 2.3). The most abraded assemblages are from the crevasse splay, channel and bar, and distal levee and floodplain categories. The least weathered and abraded assemblages are from poorly-drained floodplain and wetland settings, and assemblages from well-drained floodplain settings also show incipient weathering stages but are more abraded than assemblages from poorly-drained settings (Table 2.3).

Bones exposed at or near the surface experience chemical and physical weathering until they are ultimately buried (Behrensmeyer, 1978), and exposure time is governed by sedimentation processes operating in distinct depositional settings (Behrensmeyer, 1988). The more diverse the landscape, the greater the range of sedimentation processes occurring. The environments of FA 1 and 4 were dominated by channel processes, and localities occur only in channel and near-channel settings. In FA 3, more localities occur in distal-channel settings, reflecting variable flow regimes and greater preservation of floodplain deposits. The landscapes of FA 5 and 6 were the most laterally variable, and localities occur in all landscape categories (Table 2.3), with most localities occurring in floodplain settings.

Although vertebrate localities are more prevalent in facies associations that dominate the Upper Member (80.7% of localities), plant macrofossils and trackways show a different distribution. The facies of the three macrofloral localities all represent floodplain settings, with important differences in landscape position. The plant locality in FA 3 (Fig. 2.3; Rainbow Loop Flora of Reynolds and Schweich, 2013) occurs in very fine, tabular sandstone and siltstone representing low-energy chute or pond deposits; the fossils are iron-oxide-stained impressions, indicating that the sediments were relatively well drained. The macrofloral remains from FA 5 and 6 occur in the drab mudstones characteristic of those facies associations (Fig. 2.4E, 2.4F),

representing seasonally ponded floodplains. Compressed palm fronds preserved in drab-colored mudstone from FA 6 indicate a high water table or poor drainage. Petrified wood reported by Alf (1970) in FA 5 reflects unusual diagenesis rather than depositional conditions. In general, rapid burial or poor drainage is required to preserve plant material in floodplain settings (Martin, 1999).

Trackways occur in FA 2, 3, 5, and 6. While the characteristics of these facies associations differ, trackways all occur on bedding planes of thin beds of marl or tuffaceous sandstone bounded by mudstones. The depositional contexts differ among these facies associations (e.g., playa margin, crevasse splay), yet they represent favorable conditions for preserving trackways, likely due to the presence of damp, well-sorted mudstone to fine sandstone as the substrate for the tracks, followed by partial desiccation and rapid burial. Substrate composition and moisture were the primary factors influencing the survival of mammal and bird tracks on the margins of Lake Manyara, Tanzania (Cohen et al., 1991). These factors varied with distance from the lake margin, with calcareous mudflats preserving tracks for longer periods than organic-rich mudflats. The likelihood of track preservation also depended on wet-dry cycles, sediment accumulation, and size of the track maker. In the Barstow Formation, the animals that left tracks (camelids, felids, amphicyonids, canids, proboscideans, equids) were present over much of the depositional history of the Barstow sequence (Pagnac, 2009), and the distribution of trackways reflects the frequency of circumstances favorable to preserving tracks.

Throughout the Barstow sequence, similar lithologies tend to preserve fossils regardless of facies association, although the incidence of fossil-bearing facies increases upwards through the formation. The settings in which fossils accumulated become more diverse through the section, reflecting the changing depositional processes and environments in the Barstow Basin.

Floodplain and wetland deposits increase upsection as a proportion of the overall facies associations, contributing to the increased occurrence of fossil localities.

Preservation potential of fossils varies among facies associations. Preservation potential is partly reflected in the number of fossil localities in each facies association (Table 2.2), but it also depends on the suitability of depositional environments as habitats for animals and plants (Table 2.4). Life habitats for terrestrial mammals are characterized by the presence of fresh water and vegetation, and these environments (e.g., floodplains) often have high preservation potential. Facies associations dominated by floodplain or near-channel deposits (FA 3, 5, 6) represent suitable habitats with high preservation potential (Table 2.4). Evidence of stable, vegetated landscapes (root casts, pedogenic features) are widespread in FA 5 and 6, which preserve the most fossil localities. In contrast, terrestrial mammals may frequent but do not inhabit river channels, and channel-dominated settings such as those of FA 1 and 4 do not typically preserve mammal material (Koster, 1987; Eberth et al., 2007). The better developed interfluve deposits in FA 4, however, increased the preservation potential of mammal fossils (Table 2.4). Playa lakes may attract terrestrial mammals seasonally when water is present, and fossil preservation can be variable in these environments. Although body fossils do not occur in FA 2, trackways are preserved (Tables 2.2, 2.4).

Sediment-Accumulation Rates

Estimates of the total thickness of the Barstow Formation range from 1040 m (Woodburne et al., 1990) to between 1200 and 1400 m (Steinen, 1966). We estimated the total thickness to be approximately 1300 m in the Mud Hills, with the Owl Conglomerate Member comprising 197 m, the Middle Member 739 m, and the Upper Member 409 m of our total measured sections. These

thickness estimates are based on composite sections measured in the eastern and western Mud Hills; a complete section cannot be documented in one location since the Barstow syncline plunges to the west. Sediments of FA 1–4 are thickest in the eastern and central Mud Hills, where sediments of FA 5 are the youngest exposures (Fig. 2.5). The full thickness of FA 5 sediments is exposed in the western Mud Hills, which is the only part of the Mud Hills where sediments of FA 6 occur. No facies association constitutes a significantly larger proportion of the total thickness of the formation than any other (*p*-values for all thicknesses > 0.006 in a two-tailed *z* test of proportion; Johnson and Bhattacharyya, 2006). The high number of fossil localities in FA 5 and 6 (Table 2.2, Fig. 2.5) is not due to the unusual thickness of these facies associations relative to the others. FA 5 is the most areally extensive of the exposed facies associations, which may contribute to its high number of vertebrate localities.

Sediment-accumulation rates vary laterally, vertically, and among facies associations (Fig. 2.6). Woodburne et al. (1990) calculated sediment-accumulation rates for a single long section measured in the Rainbow Basin area of the eastern Mud Hills (Figs. 2.5, S2.1, section 31) and highlighted differences in accumulation rates among the three members. Their sediment-accumulation rates, estimated from radiometric ages of tuff beds, ranged from 75 to 540 m/Myr. Rates were constant through the Owl Conglomerate and Middle members and decreased between the Middle and Upper members. Our estimates of sediment-accumulation rates for uncompacted thicknesses of the six facies associations, using both radiometric ages of tuff units and dated intervals from paleomagnetic stratigraphy, also show a decrease in sediment-accumulation rates above the Skyline Tuff, dated at 15.2 Ma (D.M. Miller, personal communication, 2015). Estimated average rates of sediment accumulation are 309 to 306 m/Myr (30.9 to 30.6 cm/kyr) during deposition of FA 1 and 2; average rates are lower for FA 3 (266 m/Myr; 26.6 cm/kyr) and

increase to 357 m/Myr (35.7 cm/kyr) during FA 4. Rate estimates for individual stratigraphic intervals are highly variable, especially for FA 4, where estimates range from 51 to 784 m/Myr (0.5 to 78.4 cm/kyr; Table S2.2). For the Steepside Quarry section of Woodburne et al. (1990), the estimate is 204 m/Myr (20.4 cm/kyr); this section represents a transition zone between FA 3 and 4 (Figs. 2.5, S2.1, section 30). In FA 5, the sediment-accumulation rate declines notably (Fig. 2.6); for five stratigraphic sections measured between the Skyline and *Hemicyon* Tuffs, the mean sediment-accumulate rate is 120 m/Myr (12 cm/kyr). Sediment-accumulation rates increased slightly to 149 m/Myr (14.9 cm/kyr) during deposition of FA 6, although the ages are poorly constrained for the uppermost part of the Barstow Formation.

Estimates for FA 5 and 6 and estimates based on magnetostratigraphy for FA 1 and 3 have the best agreement among stratigraphic sections, perhaps because stratigraphic sections were measured along similar transects. For some sections, there is a significant difference between age estimates based on $^{40}Ar/^{39}Ar$ of tuff beds and those based on correlation to the magnetic polarity timescale. Recent dating of the Skyline Tuff indicates that part of the correlation of the Barstow magnetostratigraphic section to the geomagnetic timescale in Woodburne (1996) may need to be revisited. We therefore emphasize that these estimates are useful in demonstrating changes in sediment-accumulation rates through time and space, but should not be considered definitive.

Discussion

The lithostratigraphic divisions of the Barstow Formation generally fine upwards through the section, a trend that is reflected in the distribution of facies associations. The coarse-grained Owl Conglomerate Member comprises FA 1 and the transitional facies of FA 2. The Middle Member includes the fine-grained facies of FA 2 as well as FA 3 and 4. The mudstone-dominated FA 5

and 6 constitute the Upper Member. The vertical and lateral distribution of facies associations results from the changes in depositional processes and environments as the basin evolved tectonically. The range of facies associations identified in the Barstow Formation corresponds to the depositional processes characteristic of a continental extensional basin (Gawthorpe and Leeder, 2000). Within this sequence, the distribution of fossil localities reflects changes in landscape and habitable environments and preservation during different stages of basin history.

Facies and Environments

The depositional environments represented by the major facies associations of the Barstow Formation include alluvial fans, confined channels, shallow lakes, and floodplain land surfaces and ponds (Table 2.1, Fig. 2.7). The absence of major unconformities (Figs. 2.2, 2.5) indicates that deposition in the basin was fairly continuous. Faulting and folding, however, have truncated parts of the section and affected outcrop exposure. Isochronous tuff units and lateral relationships (Fig. 2.5) indicate that at least two facies associations co-occurred at any one time over most of the basin history. The Miocene river systems had different source areas, as indicated by paleocurrent directions and clast composition. The oldest, alluvial-fan deposits (FA 1) were derived from sources to the north and south, and the channels of the Middle Member (FA 4) indicate a southern source area (Steinen, 1966; Woodburne et al., 1990; Woodburne, 2015). Sediment-accumulation rates were highest in the older facies associations (FA 1 and 2) and in the channel sandstones of FA 4 (Fig. 2.6). The three facies associations representing floodplains (FA 3, 5, 6) have the lowest sediment-accumulation rates. Sediment-accumulation rates among facies associations declined over time, the common trend for extensional basins (Bridge, 2003).

Distribution of facies in relation to extensional basins

Environments change during the formation and filling of extensional basins, resulting in a characteristic suite of facies (Leeder and Gawthorpe, 1987; Gawthorpe and Leeder, 2000; Bridge, 2003). The general model of structural and depositional history has three phases. (1) Initial normal faulting forms one or more depocenters. Alluvial fans derived from the footwall accumulate close to the fault scarp and prograde into the expanding basin. A shallow lake(s) develops close to the footwall; interior drainage prevails, and the lake(s) may be evaporitic in arid settings. (2) As fault displacement continues and the basin expands, streams and deltas gradually fill the lake; stream incision of both the footwall and hanging wall creates small valleys and floodplains within the basin. (3) Tilting and subsidence along the major normal faults confine an axial river to run parallel to the footwall. The axial river may achieve external drainage, and the main channel, its tributaries, and floodplains continue to fill the basin. The suite of facies associations and their distribution in the Barstow Formation conform well to this model and provide clear evidence for the changes in environments during different phases of basin evolution. Together with the fossil record, we offer a plausible history of sedimentary environments and fossil preservation through time.

Local extension began about 23 Mya, as the Central Mojave metamorphic core complex was exposed along the Waterman Hills detachment fault (Glazner et al., 2002). Deposits of the Jackhammer, Pickhandle, and Mud Hills formations were derived from the hanging wall and mylonitic footwall along the detachment fault during the period of greatest extension (Fillmore and Walker, 1996; Ingersoll et al., 1996).

Deposition of the Barstow Formation in the Mud Hills began about 19.3 Ma (Fig. 2.2). The conglomeratic sandstones of FA 1 were deposited during and following the waning stages of

extension, which ended in the Barstow area by 18.5 Ma (Glazner et al., 2002). During this time, accommodation was high, and alluvial fans depositing the sandstones and conglomerates of FA 1 spilled into the basin (Fig. 2.7A). The two vertebrate localities that occur in FA 1 are the oldest fossil localities in the Mud Hills, and their depositional settings (Table 2.3) reflect the major environments of FA 1.

FA 2 represents the westward limit of a shallow playa lake that was partly coeval with FA 1 (Fig. 2.7A). These deposits thicken from 270 m in the Mud Hills to 300 m closer to the probable depocenter, which lay southeast of the Mud Hills. The fluvial facies of FA 2 drained into this playa basin, which subsided rapidly from sediment loading after extension ceased. Deposits similar to FA 2 in the Calico Mountains have been interpreted as forming in a saline-alkaline evaporative lake (Park, 1995). In the Mud Hills, FA 2 represents the equivalent western facies and a similar depositional environment (Sheppard and Gude, 1969). Mammals and birds visited the playa margin, as indicated by trackways in FA 2, but evidence of vegetation from this setting in the Mud Hills is limited to the charophyte layer at the base of the marginal lacustrine facies. No vertebrate body fossils occur in sediments of FA 2 (Tables 2.2, 2.3). High accommodation associated with tectonic subsidence and sediment loading is reflected in the high sediment-accumulation rates during this time (Fig. 2.6).

With slowing subsidence, the floodplains of FA 3 developed. Impressions and compressions of palm, juniper, and woody dicots (Reynolds and Schweich, 2013) as well as root traces suggest that terrestrial vegetation was more extensive during this depositional phase. Evidence for terrestrial vegetation indicates that the floodplain land surfaces were relatively stable and exposed for long periods of time. The moderate frequency of vertebrate localities in FA 3 and 4 may reflect an increase in subaerial exposure and the expansion of vegetated environments as

deposition became more episodic (Fig. 2.7). Abundant plants and fresh water would have attracted terrestrial mammals, and vertebrate assemblages from these facies associations occur in channel and near-channel settings, with few assemblages occurring in distal floodplain environments (Table 2.3).

The interfingering of FA 3 and 4 implies that they were part of the same depositional regime, even as their facies-stacking patterns indicate changing accommodation or sediment supply. Amalgamated channel sandstones form during periods of low or slowly increasing accommodation or when accommodation and sediment supply are in equilibrium, and floodplain deposits are not well developed (Shanley and McCabe, 1994). The stacked sandstone units of FA 4 indicate that accommodation remained low or was in pace with sediment supply, and the increase in sediment-accumulation rates may signify a renewed episode of clastic input to the basin. The overall fining-upwards pattern of facies in extensional basins may be punctuated by coarse-grained sequences indicating episodes of increased sedimentation (Wescott, 1993), resulting from uplift of source areas and erosion at the bounding faults. Braided river systems may form in response to phases of increased erosion and sediment transport when accommodation slowly increases (Wright and Marriott, 1993), and headward incision on the footwall uplands renews clastic input to the basin (Gawthorpe and Leeder, 2000).

Accommodation remained low through the end of Barstow deposition in the Mud Hills. The low sediment-accumulation rates, abundance of root casts, and widespread pedogenic development in FA 5 and 6 indicate that land surfaces were exposed for significant periods of time. Plant communities were well established in these floodplains and spring-fed wetlands (Fig. 2.7B), and the frequency of vertebrate localities and trackways indicates high animal activity at this time. Vertebrates occur in a variety of depositional settings in FA 5 and 6 (Table 2.3). The

development of both wet and dry vegetated environments in the late phase of basin filling is related to the low rates of sediment supply, low tectonic activity, and greater landscape stability relative to earlier conditions.

Facies, environments, and fossil preservation

Continental environments differ in their suitability as life habitats and in their potential for preserving organic remains. The observed distribution of fossil localities reflects changes in environmental and preservational conditions through the deposition of the Barstow Formation. The low number of fossil localities in the lower Barstow Formation indicates that early Barstow environments were unsuitable habitats or had limited ability to preserve vertebrate remains. Later environments were more suitable life habitats and were settings that preserve vertebrate fossils (Table 2.4).

Facies associations representing active lakes or river channels would not have been suitable habitats for terrestrial mammals but would have been suitable for aquatic vertebrates. Fishes, turtles, and crocodilians are, however, notably rare or absent from the Barstow Formation (Bell and Reynolds, 2010). Crocodilians are generally rare from Miocene fossil localities outside the Great Plains, Gulf Coast, and East Coast (Markwick, 1994). The absence of aquatic vertebrates from Barstow environments suggests that they did not inhabit the Barstow Basin, since they are abundantly preserved in other Miocene continental sequences (Smith, 1981; Markwick, 1994).

The sandy to gravelly channels and alluvium of FA 1 indicate that strong currents and variable discharge events dominated these environments. Fossil localities in FA 1 only occur in channel and proximal channel settings (Table 2.3); these sediments and any vertebrate remains in them would have been subject to frequent erosion and reworking. The absence of significant

floodplain deposits may mean that bone concentrations were less likely to form in this facies association. The coarse sediment load, variable discharge, and steep gradients typical of alluvial streams are not conducive to fossil preservation, and few vertebrate fossil localities form in these settings (Koster, 1987; Eberth et al., 2007).

The playa-margin environment of FA 2 was suitable habitat insofar as it provided shallow, ponded water, but the saline-alkaline chemistry of the associated lake (Sheppard and Gude, 1969; Park, 1995), the presence of evaporites, and absence of bioturbation suggest that little plant or animal life occupied the original habitats. An arthropod fossil assemblage from concretions in sediments in the Calico Mountains indicates that wooded grassland was nearby, based on the presence of termites and thrips (Park and Downing, 2001). Although trackways from FA 2 demonstrate that mammals and birds visited the area, lake chemistry could have been an important factor in discouraging sustained vertebrate habitation at this time. Similarly, the distinct chemistry of the early Barstow lake system that contributed to the preservation of the arthropod assemblage (Park, 1995) may have prevented the preservation of vertebrate remains (Martin, 1999). The calcareous mudflats of FA 2 were, however, ideal settings for the preservation of vertebrate trackways.

The increase in frequency of fossil localities in FA 4 (Tables 2.2, 2.3) indicates that environments were more favorable for mammals or that preservation potential was higher during deposition of FA 4 (Table 2.4). Fossil localities in FA 4 occur in channel and bar, proximal levee and chute, and well-drained floodplain deposits (Table 2.3), indicating greater landscape heterogeneity than FA 1. Additionally, the high sediment-accumulation rate of FA 4 may have contributed to the burial of remains in channel-margin settings and interfluve areas. The active

channels of FA 4 would have offered suitable aquatic habitats, although no aquatic organisms are known from these deposits.

When streams and floodplains dominated the Barstow Basin, habitats became more suitable for mammals, and the incidence of mammal body-fossil preservation increased. The preservation of plant fossils and trackways also increased in the floodplain settings in FA 3, 5, and 6 (Table 2.2). The depositional settings in which localities occur in FA 3, 5, and 6 are more varied than in the other facies associations (Table 2.3), and most localities occur in distal-channel and floodplain settings. These environments represent suitable life habitats with abundant fresh water and vegetation. Floodplains are a common setting for the preservation of terrestrial fossil accumulations (Behrensmeyer, 1988; Martin, 1999) because they are habitats for plants and animals and sites of sediment deposition. Floodplain surfaces are exposed long enough to allow plants and animals to colonize the landscape and aggrade at rates variable enough to episodically bury remains on the surface. Most assemblages in the Barstow Formation occur in floodplain settings, and a high proportion of fossils in these assemblages show only incipient weathering (Table 2.3). Several localities in FA 5 and 6 occur in fossiliferous horizons that extend laterally over tens of meters. The relative stability of floodplain and wetland environments allows bones to accumulate over long periods of time, which contributes to the formation of bone concentrations (Rogers and Kidwell, 2007). Drainage is also important to the preservation of fossils, and more localities occur in poorly-drained settings in FA 5 and 6 (Table 2.3). High water tables and reducing environments contribute to fossil preservation (Martin, 1999; Loughney et al., 2011).

As environments changed in response to the extension and filling of the Barstow Basin, so too did the ability of these environments to attract animals and preserve fossils (Table 2.4). There

is limited evidence for suitable habitats existing early in the history of the Barstow Formation, and apart from mammal trackways, these early environments preserved few fossils. In contrast, later environments featured suitable habitats in a range of channel-margin and floodplain environments that preserve fossils. River channels and floodplains host vertebrate fossil concentrations that result from several different taphonomic pathways (Bown and Kraus, 1981; Badgley, 1986; Behrensmeyer, 1988; Loughney et al., 2011). The increasing frequency of fossil localities through time resulted from the deposition of facies representing high suitability both as life habitats and as preservational environments, conditions that only occurred together in FA 3, 5, and 6. We would expect a similar pattern to occur in the fossil record of other continental extensional basins, especially those of the Great Basin.

Conclusion

We examined changes in fossil preservation in relation to different depositional regimes within a continental extensional basin. The six facies associations in the Barstow Formation represent the dominant environments formed during different stages of basin filling. The distribution of these facies associations conforms to the classic depositional model of a continental extensional basin, in which alluvial fans and playa lakes develop early in the basin history, and rivers and floodplains develop during later stages (Leeder and Gawthorpe, 1987). The frequency of fossil localities increases through the section, following the different major environments that formed as the basin filled.

Environments that formed early in the subsiding Barstow Basin were alluvial fans and playa lakes that were unsuitable habitats for most mammals and preserve few vertebrate fossils (FA 1 and 2; Fig. 2.7A). Decreasing subsidence in the basin led to the development of channel and

floodplain environments (FA 3 and 4) with extensive floodplains and wetlands (FA 5 and 6) dominating during the latest stages of basin fill (Fig. 2.7B). The majority of fossil localities in the Barstow Formation are preserved in these mudstone-dominated facies associations, reflecting both the suitability of environments as habitats for mammals and favorable conditions for preservation of vertebrate remains. These conditions prevailed when subsidence and sediment-accumulation rates were low, and exposed land surfaces supported widespread vegetation and mammal communities. The pattern of fossil preservation in the Barstow Formation is similar to that in many other alluvial systems with abundant vertebrate remains and provides a useful comparison to other small continental basins.

Acknowledgments

This study was completed with support from the Evolving Earth Foundation, the Paleontological Society, University of Michigan Rackham Spring-Summer Fellowship, University of Michigan Rackham Graduate Student Research Grant, and the University of Michigan Department of Earth and Environmental Sciences Scott Turner Award. We thank Robert E. Reynolds for his help with field logistics and planning, as well as Don Lofgren, Michael Woodburne, and Everett Lindsay for help in locating fossil localities. We also thank Rachel Thorpe, Tara Smiley, and Anna Harkness for their assistance in the field, and Carol Abraczinskas for her expertise with figures. We thank Robert E. Reynolds, Raymond Rogers, and Michael Woodburne for useful comments on the manuscript.

References

Alf, R.M., 1966, Mammal trackways from the Barstow Formation, California: Bulletin of the Southern California Academy of Sciences, v. 65, p. 258–264.

Alf, R.M., 1970, A preliminary report on a Miocene flora from the Barstow Formation, Barstow, California: Bulletin of the Southern California Academy of Sciences, v. 69, p. 183–189.

Alonso-Zarza, A.M., 2003, Palaeoenvironmental significance of palustrine carbonates and calcretes in the geological record: Earth-Science Reviews, v. 60, p. 261–298.

Alonso-Zarza, A.M. and Wright, V.P., 2010, Palustrine carbonates, *in* Alonso-Zarza, A.M. and Tanner, L.H. (eds.), Developments in Sedimentology Volume 61: Carbonates in Continental Settings: Facies, Environments, and Processes: Elsevier, Amsterdam, p. 103–131.

Arenas-Abad, C., Vázquez-Urbez, M., Pardo-Tirapu, G., and Sancho-Marcén, C., 2010, Fluvial and associated carbonate deposits, *in* Alonso-Zarza, A.M. and Tanner, L.H. (eds.), Developments in Sedimentology Volume 61: Carbonates in Continental Settings: Facies, Environments, and Processes: Elsevier, Amsterdam, p. 133–175.

Badgley, C., 1986, Taphonomy of mammalian fossil remains from Siwalik rocks of Pakistan: Paleobiology, v. 12, p. 119–142.

Barnosky, A.D. and Carrasco, M.A., 2002, Effects of Oligo-Miocene global climate changes on mammalian species richness in the northwestern quarter of the USA: Evolutionary Ecology Research, v. 4, p. 811–841.

Becker, M.L., Cole, J.M., Rasbury, E.T., Pedone, V.A., Montanez, I.P., and Hanson, G.N., 2001, Cyclic variations of uranium concentrations and oxygen isotopes in tufa from the middle Miocene Barstow Formation, Mojave Desert, California: Geology, v. 29, p. 139–142.

Behrensmeyer, A.K., 1975, The taphonomy and paleoecology of Plio-Pleistocene vertebrate assemblages east of Lake Rudolf, Kenya: Bulletin of the Museum of Comparative Zoology, v. 146, p. 473–578.

Behrensmeyer, A.K., 1978, Taphonomic and ecologic information from bone weathering: Paleobiology, v. 4, p. 150–162.

Behrensmeyer, A.K. and Dechant Boaz, D.E., 1980, The recent bones of Amboseli National Park, Kenya, in relation to East African paleoecology, *in* Behrensmeyer, A.K., and Hill, A.P. (eds.), Fossils in the Making: Vertebrate Taphonomy and Paleoecology, p. 72–92.

Behrensmeyer, A.K., 1988, Vertebrate preservation in fluvial channels: Palaeogeography, Palaeoclimatology, Palaeoecology, v. 63, p. 183–199.

Bell, M.A. and Reynolds, R.E., 2010, Miocene and Late Pleistocene stickleback spines from the Mojave Desert, California, *in* Reynolds, R.E. (ed.), Overboard in the Mojave: 20 Million Years of Lakes and Wetlands: California State University Desert Studies Consortium, Fullerton, p. 162–168.

Bluck, B.J., 1967, Deposition of some Upper Old Red Sandstone conglomerates in the Clyde area: A study in the significance of bedding: Scottish Journal of Geology, v. 3, p. 139–167.

Bown, T.M. and Kraus, M.J., 1981, Vertebrate fossil-bearing paleosol units (Willwood Formation, Lower Eocene, northwest Wyoming, U.S.A.): Implications for taphonomy, biostratigraphy, and assemblage analysis: Palaeogeography, Palaeoclimatology, Palaeoecology, v. 34, p. 31–56.

Bridge, J.S., 2003, Rivers and Floodplains: Forms, Processes, and the Sedimentary Record: Blackwell Publishing, Oxford, 491 p.

Cohen, A., Lockley, M., Halfpenny, J., and Michel, A.E., 1991, Modern vertebrate track taphonomy at Lake Manyara, Tanzania: PALAIOS, v. 6, p. 371–389.

Cole, J.M., Rasbury, E.T., Montanez, I.P., Pedone, V.A., Lanzirotti, A., and Hanson, G.N., 2004, Petrographic and trace element analysis of uranium-rich tufa calcite, middle Miocene Barstow Formation, California, USA: Sedimentology, v. 51, p. 433–453.

DeCelles, P.G., Gray, M.B., Ridgway, K.D., Cole, R.B., Pivnik, D.A., Pequera, N., and Srivastava, P., 1991, Controls on synorogenic alluvial-fan architecture, Beartooth Conglomerate (Palaeocene), Wyoming and Montana: Sedimentology, v. 38, p. 567–590.

Dibblee, T.W., Jr., 1968, Geology of the Opal Mountain and Fremont Peak quadrangles, California: California Division of Mines and Geology Bulletin 188, 64 p.

Dunagan, S.P. and Turner, C.E., 2004, Regional paleohydrologic and paleoclimatic settings of wetland/lacustrine depositional systems in the Morrison Formation (Upper Jurassic), Western Interior, USA: Sedimentary Geology, v. 167, p. 269–296.

Eberth, D.A., Shannon, M., and Noland, B.G., 2007, A bonebeds database: Classification, biases, and patterns of occurrence, *in* Rogers, R.R., Eberth, D.A., and Fiorello, A.R. (eds.), Bonebeds: Genesis, Analysis, and Paleobiological Significance: University of Chicago Press, Chicago, p. 103–220.

Fanning, D.S. and Fanning, M.C.D., 1989, Gleization, *in* Soil Morphology, Genesis, and Classification: John Wiley & Sons, Ltd., New York, p. 1–16.

Farrell, K.M., 1987, Sedimentology and facies architecture of overbank deposits of the Mississippi River, False River region, Louisiana, *in* Ethridge, F.G., Flores, R.M., and Harvey, M.D. (eds.), Recent Developments in Fluvial Sedimentology, Society of Economic Paleontologists and Mineralogists Special Publication No. 39, p. 111–120.

Fillmore, R.P. and Walker, J.D., 1996, Evolution of a supradetachment extensional basin: The lower Miocene Pickhandle basin, central Mojave Desert, California, *in* Beratan, K.K. (ed.), Reconstructing the History of the Basin and Range Extension Using Sedimentology and Stratigraphy, Geological Society of America Special Paper 303: Geological Society of America, Boulder, p. 107–126.

Finarelli, J.A. and Badgley, C., 2010, Diversity dynamics of Miocene mammals in relation to the history of tectonism and climate: Proceedings of the Royal Society of London B: Biological Sciences, v. 277, p. 2721–2726.

Fisk, L.H. and Maloney, D.F., 2015, Palynology of the “Slug Bed” in the middle Miocene Barstow Formation in the Mud Hills, Mojave Desert, southern California, *in* Reynolds, R.E. (ed.), The Mojave Miocene: 15 Million Years of History: California State University Desert Studies Consortium, Fullerton, p. 130–135.

Gawthorpe, R.L. and Leeder, M.R., 2000, Tectono-sedimentary evolution of active extensional basins: Basin Research, v. 12, p. 195–218.

Genise, J.F., 2000, The ichnofamily Celliforma and allied ichnogenera: Ichnos, v. 7, p. 267–282.

Glazner, A.F., Walker, J.D., Bartley, J.M., and Fletcher, J.M., 2002, Cenozoic evolution of the Mojave block of southern California: Geological Society of America Memoir 195, p. 19–41.

Hasiotis, S.T., 2002, Continental Trace Fossils, SEPM Short Course Notes No. 51: Society for Sedimentary Geology, Tulsa, 134 p.

Ingersoll, R.V., Devaney, K.A., Geslin, J.K., Cavazza, W., Diamond, D.S., Heins, W.A., Jagiello, K.J., Marsaglia, K.M., Paylor, E.D., II, and Short, P.F., 1996, The Mud Hills, Mojave Desert, California: Structure, stratigraphy, and sedimentology of a rapidly extended terrane, *in* Beratan, K.K. (ed.), Reconstructing the History of Basin and Range Extension Using Sedimentology and Stratigraphy, Geological Society of America Special Paper 303: Geological Society of America, Boulder, p. 61–84.

Johnson, R.A. and Bhattacharyya, G.K. 2006, Statistics: Principles and Methods: John Wiley & Sons, Ltd., New York, 671 p.

Kohn, M.J. and Fremd, T.J., 2008, Miocene tectonics and climate forcing of biodiversity, western United States: Geology, v. 36, p. 783–786.

Koster, E.H., 1987, Vertebrate taphonomy applied to the analysis of ancient fluvial systems, *in* Ethridge, F.G., Flores, R.M., and Harvey, M.D. (eds.), Recent Developments in Fluvial Sedimentology, Society of Economic Paleontologists and Mineralogists Special Publication No. 39, p. 159–168.

Kraus, M.J. and Gwinn, B., 1997, Facies and facies architecture of Paleogene floodplain deposits, Willwood Formation, Bighorn Basin, Wyoming, USA: Sedimentary Geology, v. 114, p. 33–54.

Leeder, M.R. and Gawthorpe, R.L., 1987, Sedimentary models for extensional tilt-block/half-graben basins: Geological Society of London Special Publications, v. 28, p. 139–152.

Lindsay, E.H., 1972, Small mammal fossils from the Barstow Formation, California: University of California Publications in Geological Sciences, v. 93, p. 1–104.

Link, M.H. and Osborne, R.H., 1978, Lacustrine facies in the Pliocene Ridge Basin Group: Ridge Basin, California: Special Publications of the International Association of Sedimentologists, v. 2, p. 169–187.

Lofgren, D.L., Greening, J.A., Johnson, C.F., Lewis, S.J., and Torres, M.A., 2006, Fossil tracks at the Raymond Alf Museum of Paleontology and management of tracks on public lands, *in* Lucas, S.G., Spielmann, J.A., Hester, P.M., Kenworthy, J.P., and Santucci, V.L. (eds.), Fossils from Federal Lands, New Mexico Museum of Natural History and Science Bulletin 34, p. 109–118.

Lofgren, D.L., Kwon, C., Todd, J., Marquez, S., Holliday, A., Stoddard, R., and Kloess, P., 2014, Preliminary analysis of an important vertebrate-bearing horizon with abundant avian material from the Upper Member of the Barstow Formation of California, *in* Reynolds, R.E. (ed.), Not a Drop Left To Drink: California State University Desert Studies Consortium, Fullerton, p. 155–164.

Loughney, K.M., Fastovsky, D.E., and Parker, W.G., 2011, Vertebrate fossil preservation in blue paleosols from the Petrified Forest National Park, Arizona, with implications for vertebrate biostratigraphy in the Chinle Formation: PALAIOS, v. 26, p. 700–719.

Loughney, K.M. and Smith, S.Y., 2015, Phytoliths from the Barstow Formation through the middle Miocene Climatic Optimum: Preliminary results, *in* Reynolds, R.E. (ed.), The Mojave Miocene: 15 Million Years of History: California State University Desert Studies Consortium, Fullerton, p. 51–58.

MacFadden, B.J., Swisher, C.C., III, Opdyke, N.D., and Woodburne, M.O., 1990, Paleomagnetism, geochronology, and possible tectonic rotation of the middle Miocene Barstow Formation, Mojave Desert, southern California: GSA Bulletin, v. 102, p. 478–493.

Markwick, P.J., 1994, "Equability," continentality, and tertiary "climate": the crocodilian perspective: Geology, v. 22, p. 613–616.

Martin, R.E., 1999, Taphonomy: A Process Approach: Cambridge University Press, Cambridge, 508 p.

McQuarrie, N. and Wernicke, B.P., 2005, An animated tectonic reconstruction of southwestern North America since 36 Ma: Geosphere, v. 1, p. 147–172.

Melchor, R.N., Bromley, R.G., and Bedatou, E., 2009, *Spongeliomorpha* in nonmarine settings: An ichnotaxonomic approach: Earth and Environmental Science Transactions of the Royal Society of Edinburgh, v. 100, p. 429–436.

Miller, D.M., Leslie, S.R., Hillhouse, J.W., Wooden, J.L., Vazquez, J.A., and Reynolds, R.E., 2010, Reconnaissance geochronology of tuffs in the Miocene Barstow Formation: Implications for basin evolution and tectonics in the central Mojave Desert, *in* Reynolds, R.E. (ed.), Overboard in the Mojave: 20 Million Years of Lakes and Wetlands: California State University Desert Studies Consortium, Fullerton, p. 70–84.

MIOMAP: Miocene Mammal Mapping Project, 2005, http://www.ucmp.berkeley.edu/miomap/index.html. Checked April 2016.

Ogg, J.G., 2013, Magnetic polarity time scale of the Phanerozoic, *in* Ahrens, T.J. (ed.), Global Earth Physics: American Geophysical Union, Washington, D.C., p. 240–270.

Pagnac, D., 2009, Revised large mammal biostratigraphy and biochronology of the Barstow Formation (middle Miocene), California: PaleoBios, v. 29, p. 48–59.

Pagnac, D., Browne, I., and Smith, K., 2013, Stratigraphy and vertebrate paleontology of the middle Miocene Barstow Formation, San Bernardino County, California: Field Trip Guide, 73rd Annual Meeting of the Society of Vertebrate Paleontology, Los Angeles, Calif., October 23, 2013, 26 p.

Park, L.E., 1995, Geochemical and paleoenvironmental analysis of lacustrine arthropod-bearing concretions of the Barstow Formation, southern California: PALAIOS, v. 10, p. 44–57.

Park, L.E. and Downing, K.F., 2001, Paleoecology of an exceptionally preserved arthropod fauna from lake deposits of the Miocene Barstow Formation, southern California, USA: PALAIOS, v. 16, p. 175–184.

Patzkowsky, M.E. and Holland, S.M., 2012, Stratigraphic Paleobiology: Understanding the Distribution of Fossil Taxa in Time and Space: University of Chicago Press, Chicago, 259 p.

Platt, N.H. and Wright, V.P., 1991, Lacustrine carbonates: Facies models, facies distributions and hydrocarbon aspects: Special Publications of the International Association of Sedimentologists, v. 13, p. 57–74.

Plyley, A.S., Lofgren, D.L., and Farke, A.A., 2013, Nonmarine gastropods from the Temblor and Barstow formations of California, *in* Reynolds, R.E. (ed.), Raising Questions in the Central Mojave Desert: California State University Desert Studies Consortium, Fullerton, p. 68–72.

Reading, H.G., 1978, Sedimentary Environments and Facies: Elsevier, New York, 557 p.

Reynolds, R.E., Miller, D.M., Woodburne, M.O., and Albright, L.B., 2010, Extending the boundaries of the Barstow Formation in the central Mojave Desert, *in* Reynolds, R.E., and Miller, D.M. (eds.), Overboard in the Mojave: 20 Million Years of Lakes and Wetlands: California State University Desert Studies Consortium, Fullerton, p. 148–161.

Reynolds, R.E., 2013, Non-vertebrate fossils in the Miocene Barstow Formation, central Mojave Desert, California, *in* Reynolds, R.E. (ed.), Raising Questions in the Central Mojave Desert: California State University Desert Studies Consortium, Fullerton, p. 99–102.

Reynolds, R.E. and Schweich, T.A., 2013, The Rainbow Loop flora from the Mud Hills, Mojave Desert, California, *in* Reynolds, R.E. (ed.), Raising Questions in the Central Mojave Desert: California State University Desert Studies Consortium, Fullerton, p. 39–48.

Rogers, R.R., and Kidwell, S.M., 2007, A conceptual framework for the genesis and analysis of vertebrate skeletal concentrations, *in* Rogers, R.R., Eberth, D.A., and Fiorello, A.R. (eds.), Bonebeds: Genesis, Analysis, and Paleobiological Significance, University of Chicago Press, Chicago, p. 1–63.

Shanley, K.W. and McCabe, P.J., 1994, Perspectives on the sequence stratigraphy of continental strata: AAPG Bulletin, v. 78, p. 544-568.

Sheppard, R.A. and Gude, A.J., III, 1969, Diagenesis of tuffs in the Barstow Formation, Mud Hills, San Bernardino County, California: United States Geological Survey Professional Paper 634, 34 p.

Singleton, J.S. and Gans, P.B., 2008, Structural and stratigraphic evolution of the Calico Mountains: Implications for early Miocene extension and Neogene transpression in the central Mojave Desert, California: Geosphere, v. 4, p. 459–479.

Smith, G.R., 1981, Late Cenozoic freshwater fishes of North America: Annual Review of Ecology and Systematics, v. 12, p. 163–193.

Smith, R.M.H., 1993, Vertebrate taphonomy of Late Permian floodplain deposits in the southwestern Karoo Basin of South Africa: PALAIOS, v. 8, p. 45–67.

Steinen, R.P., 1966, Stratigraphy of the Middle and Upper Miocene Barstow Formation, San Bernardino County, California: Unpublished M.S. thesis, University of California, Riverside, 150 p.

Taylor, D.W., 1954, Nonmarine mollusks from Barstow Formation of southern California: U.S. Geological Survey Professional Paper 254-C, p. 67–77.

United States Geological Survey, 1996, Mud Hills, CA: United States Geological Survey, 7.5-minute series.

Wescott, W.A., 1993, Geomorphic thresholds and complex response of fluvial systems—Some implications for sequence stratigraphy: AAPG Bulletin, v. 77, p. 1208–1218.

Willis, B., 1993, Ancient river systems in the Himalayan foredeep, Chinji Village area, northern Pakistan: Sedimentary Geology, v. 88, p. 1–76.

Woodburne, M.O., Tedford, R.H., and Swisher, C.C., III, 1990, Lithostratigraphy, biostratigraphy, and geochronology of the Barstow Formation, Mojave Desert, southern California: GSA Bulletin, v. 102, p. 459–477.

Woodburne, M.O., 1996, Precision and resolution in mammalian chronostratigraphy: Principles, practices, examples: Journal of Vertebrate Paleontology, v. 16, p. 531–555.

Woodburne, M.O., 2004, Late Cretaceous and Cenozoic Mammals of North America: Biostratigraphy and Geochronology: Columbia University Press, New York, 391 p.

Woodburne, M.O., 2015, Mojave Desert Neogene tectonics and the onset of the Eastern California Shear Zone, *in* Reynolds, R.E. (ed.), Mojave Miocene: 15 Million Years of History: California State University Desert Studies Consortium, Fullerton, p. 153–199.

Wright, V.P. and Marriott, S.B., 1993, The sequence stratigraphy of fluvial depositional systems: The role of floodplain sediment storage: Sedimentary Geology, v. 86, p. 203–210.

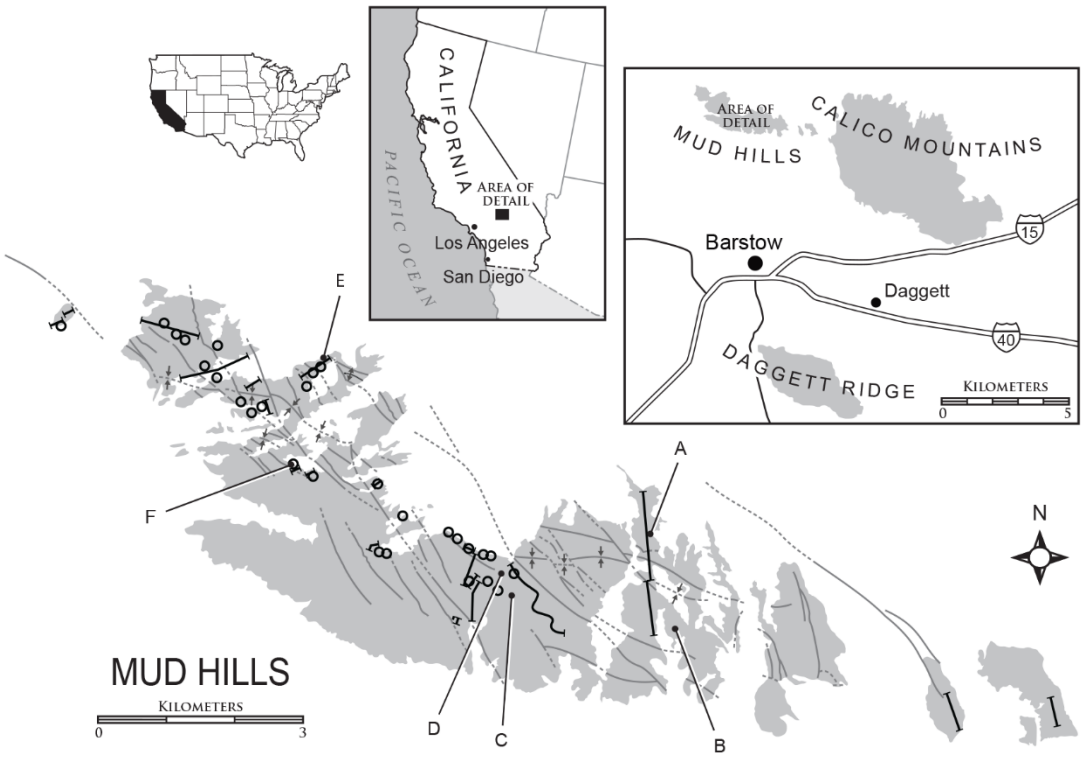

Figure 2.1. Location map of outcrop area of the Barstow Formation in the Mud Hills; gray lines = major structural features; black lines = locations of measured stratigraphic sections; circles = major fossil localities. Letters = locations of outcrop photographs in Fig. 2.4, lettering as in Fig. 2.4.

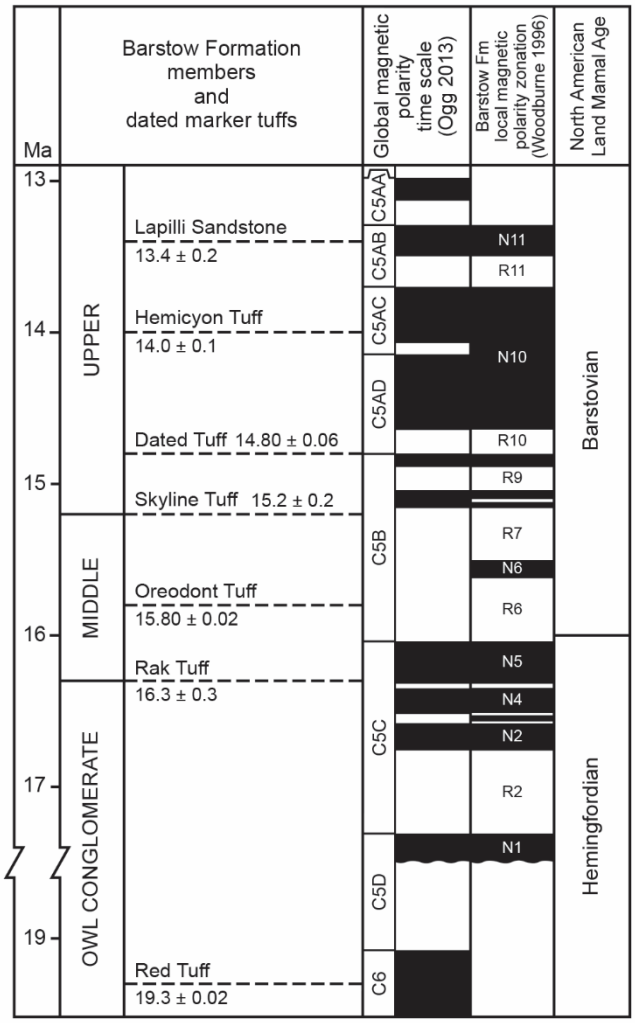

Figure 2.2. Lithostratigraphy and geochronology of the Barstow Formation in the Mud Hills. Modified from Pagnac et al. (2013).

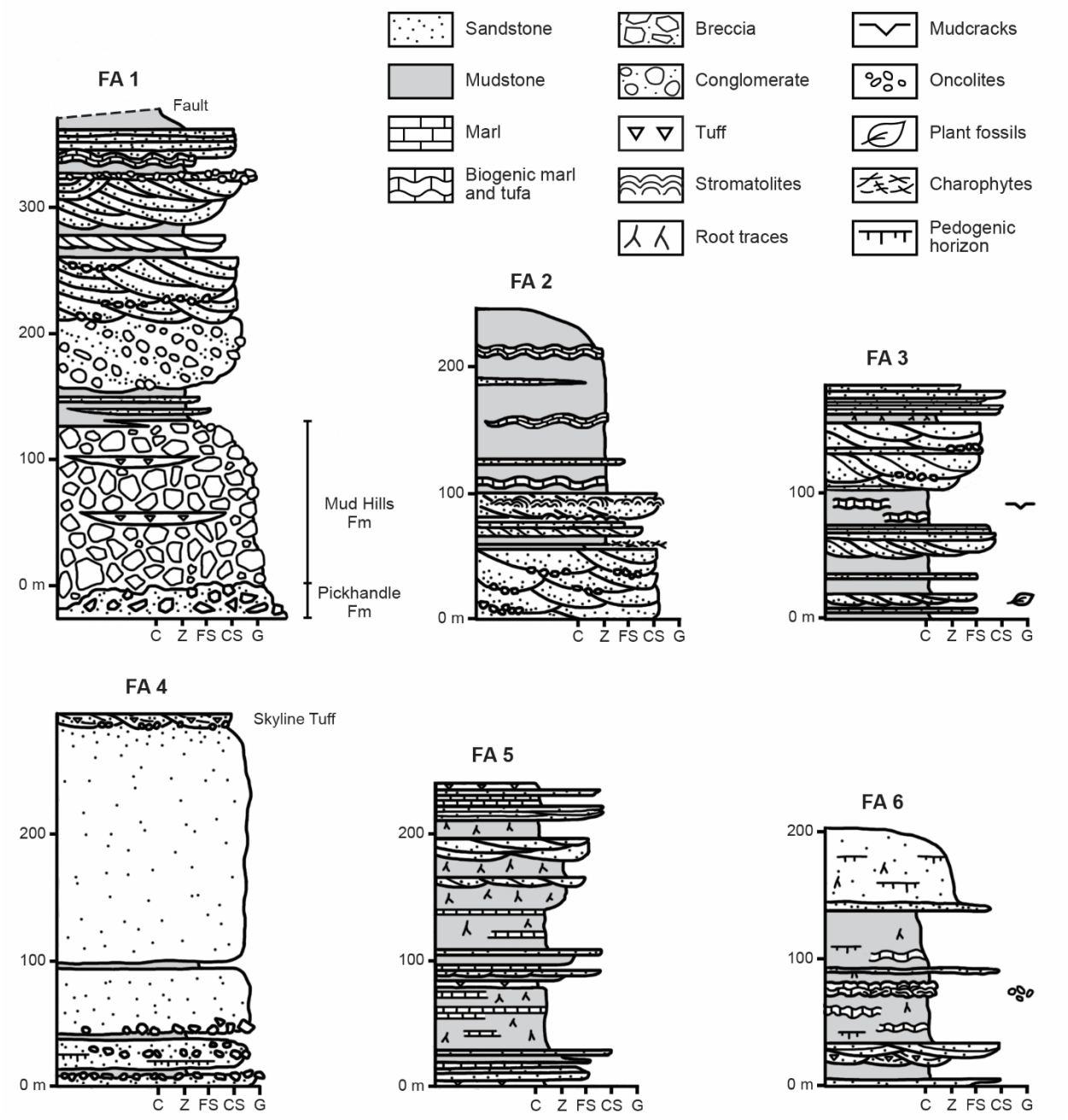

Figure 2.3. Selected stratigraphic sections exemplifying the dominant lithologies in each facies association. Grain size scale: C = clay; Z = silt; FS = fine sand; CS = coarse sand; G = gravel.

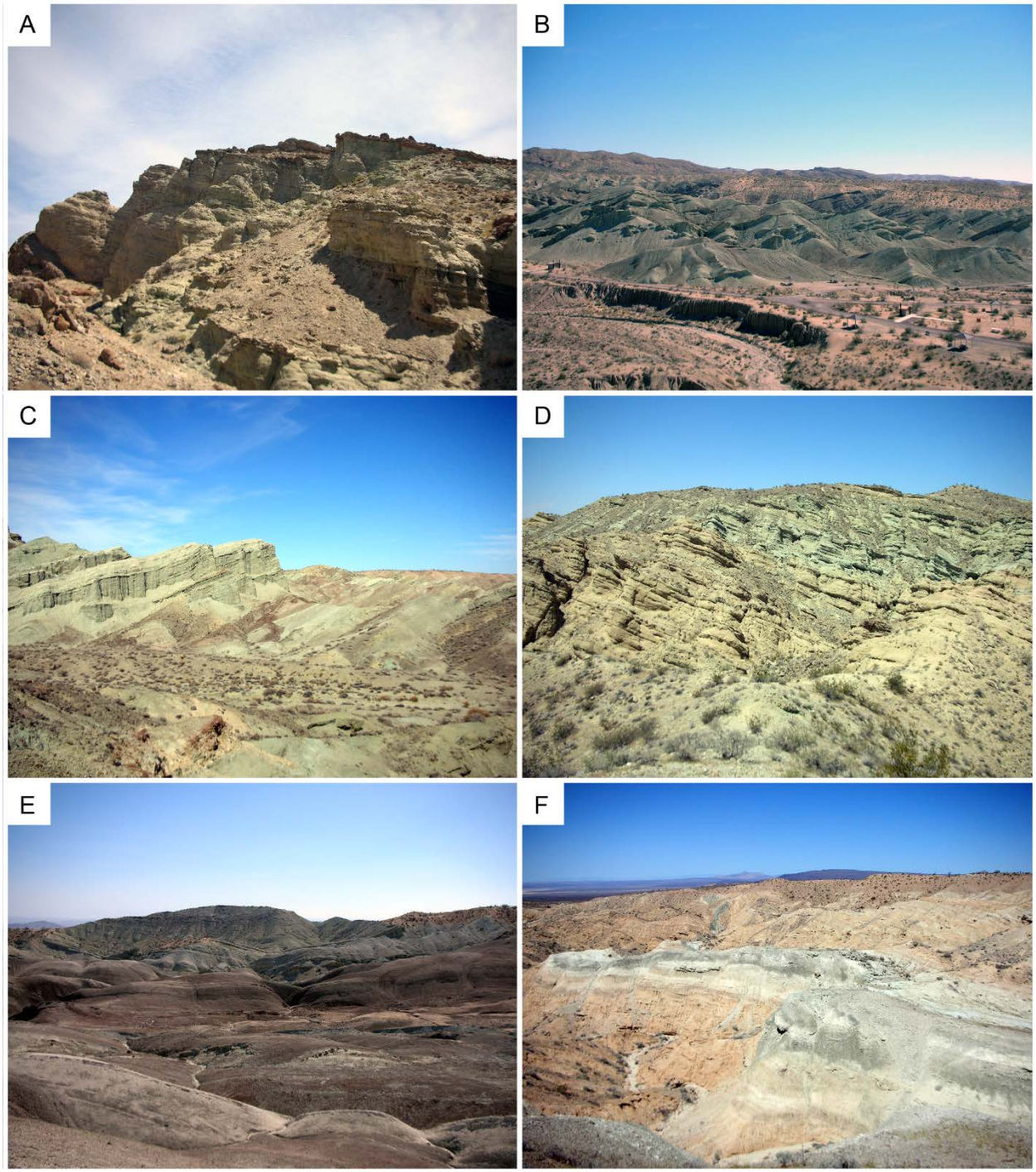

Figure 2.4. Outcrop photos of each facies association. A) FA 1. B) FA 2. C) FA 3. D) FA 4. E) FA 5. F) FA 6.

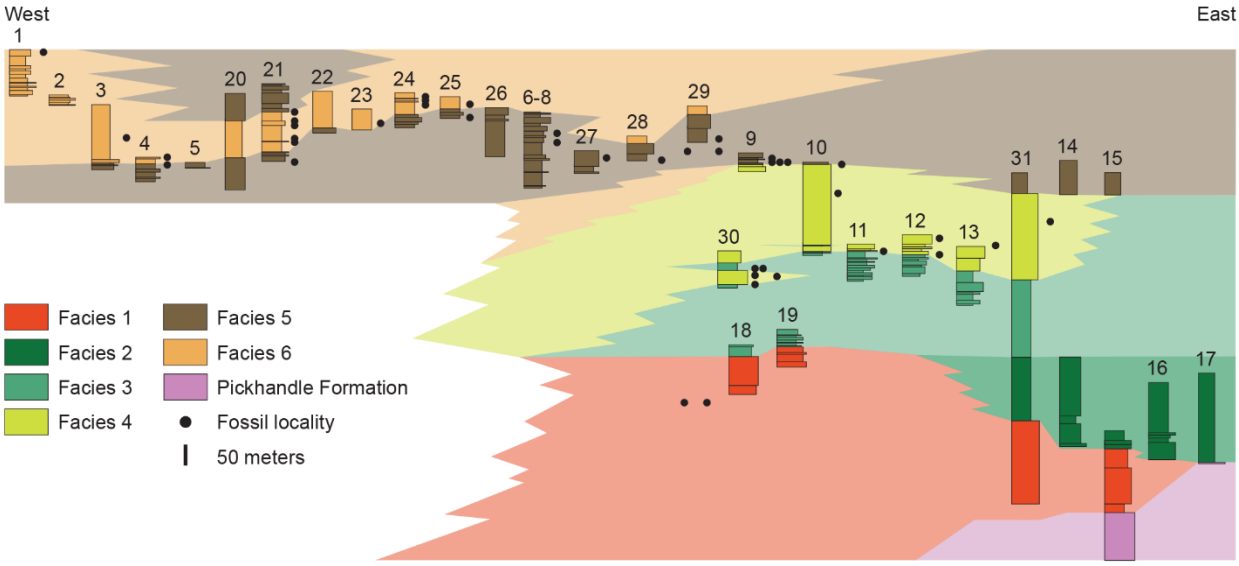

Figure 2.5. Panel diagram showing correlations of facies associations between stratigraphic sections. Sections 20, 24, 25, 27 from Lindsay (1972); sections 21, 22, 23, 26, 28, 29, 30, 31 from Woodburne et al. (1990).

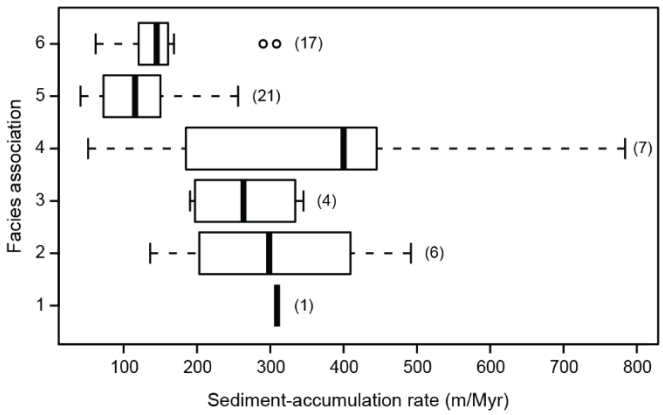

Figure 2.6. Boxplot of sediment-accumulation rates for each facies association.

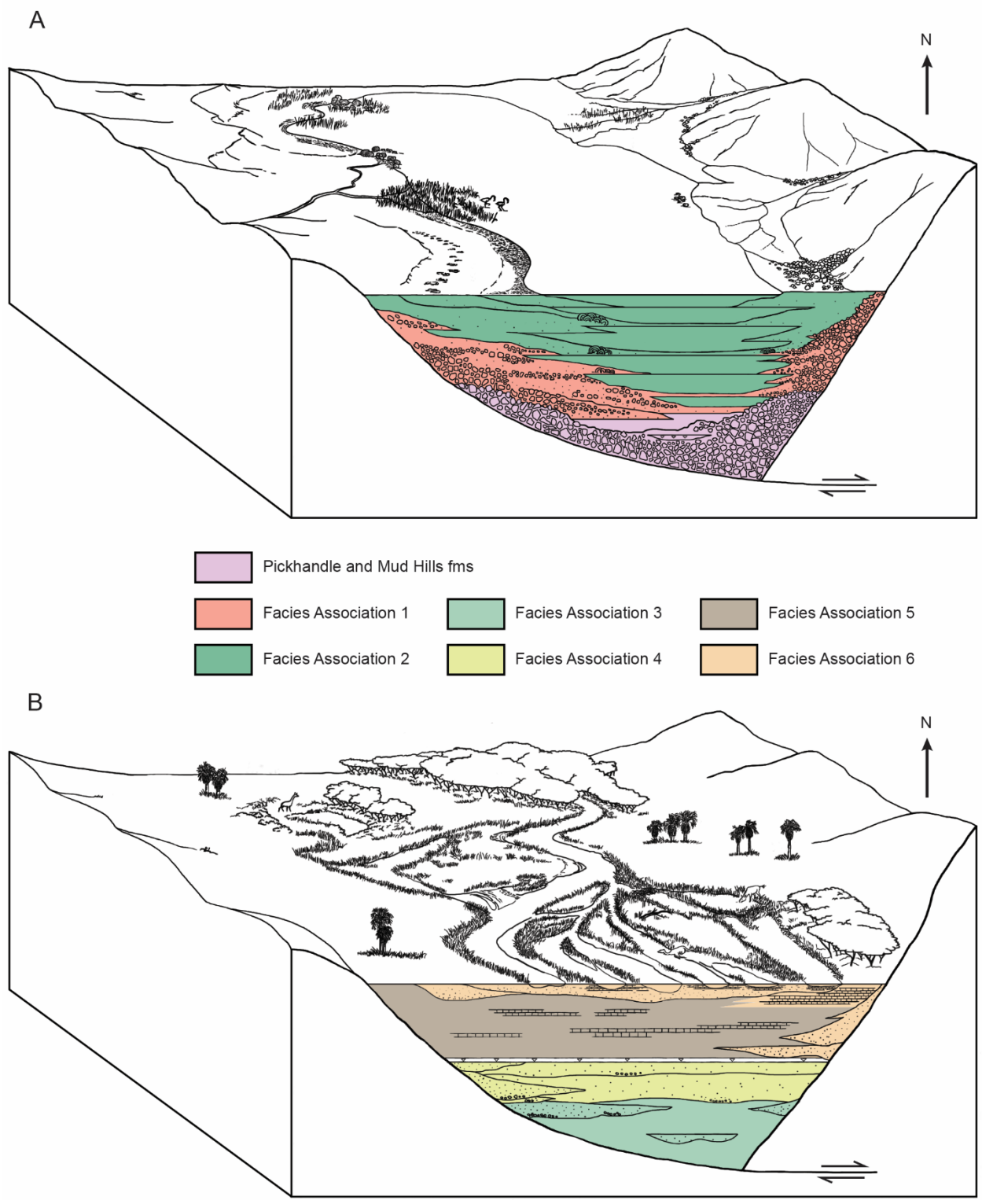

Figure 2.7. Schematic block diagrams showing environments of the Barstow Formation. Diagrams are not to scale, footwall is southwest, hanging wall is northeast. A) Environments of the early stage Barstow basin during deposition of FA 1 and 2. B) Environments of the late stage Barstow basin during deposition of FA 5 and 6.

Table 2.1. Characteristics of facies comprising each facies association (FA) with their interpretation.

FA	Dominant Lithologies	Sedimentary structures	Bed thicknesses	Spatial relationships	Interpretation
1	Amalgamated coarse sandstone and conglomerate; pale olive (10Y 6/2), grayish orange (10YR 7/4), moderate yellowish-brown (10YR 5/4), dusky yellow (5Y 6/4), or light brown (5YR 5/6)	Massive, rare trough cross-stratification, planar-oriented cobble- to boulder-sized clasts, phytoclasts	0.5 – 1.0 m	Beds are amalgamated and very thick, incised into the top of the fine-grained lithology	Channel deposits on an alluvial fan
	Interbedded very fine- to medium-grained sandstone and claystone; pale yellowish-brown (10YR 6/2), pale yellowish-green (10GY 7/2), or dark yellowish orange (10YR 6/6)	Cross-laminations, moderately developed ped structure, slickensides, root casts, burrows, phytoclasts, *Celliforma*	0.1 – 0.2 m	Localized, extend over 30 m laterally	Overbank deposits on an alluvial fan
2	Sandstone and minor conglomerate; yellowish gray (5Y 7/2)	Medium- to fine-scale trough cross-stratification, basal scours, silt/fine sand drapes	0.03 – 0.25 m	Beds fine upwards from scoured, basal lag; gradational contact with overlying fine-grained lithology	Channel deposits in basin
	Interbedded fine sandstone, siltstone, claystone, and marl; pale olive (10Y 6/2)	Stromatolites, oncolites, phytoclasts	2 – 10 cm	Laterally and vertically extensive	Marginal deposits of a shallow, restricted lake or wet playa
3	Sandstone with conglomerate lenses; yellowish gray (5Y 7/2)	Trough and ripple cross-stratification, parting lineations	1.0 – 1.5 m	Fining upwards from incised bases	Channel and levee deposits
	Siltstone and silty claystone, occasional thin sandstone; light olive gray (5Y 5/2) and pale olive (10Y 6/2)	Common root traces, rare laminations, redoximorphic concentrations	0.5 – 1.0 m	Interbedded with sandstone	Floodplain overbank deposits, crevasse splays

	Siltstone, claystone, and marl; pale olive (10Y 6/2) and yellowish gray (5Y 7/2)	Marl layers are nodular, burrows and mudcracks on upper surfaces, algal laminae	2 – 5 cm	Interbedded with siltstone-claystone-sandstone (as above), marl decreases upsection	Floodplain ponds or wetlands
4	Stacked, multi-storey sandstone; medium to coarse-grained; grayish-orange (10YR 7/4) and dusky yellow (5Y 6/4)	Massive; occasional pedogenic horizons (10YR 6/6) and bioturbated "concretions" (10YR 4/2)	1 – 2 m	Laterally extensive; grades eastward into FA 3 and westward into FA 6; locally grades upwards into FA 5	Poorly confined braidplain channel deposits in basin axis
5	Bentonitic siltstone; pale yellowish-brown (10YR 6/2), moderate yellowish-brown (10YR 5/4), or yellowish-gray (5Y 7/2)	Root casts, burrows, moderate to weak pedogenic features, slickensides	0.5 m	Grades upwards into the tuffaceous lithology	Floodplain deposits, seasonally wet or poorly drained locally
	Tuffaceous siltstone and clayey siltstone, marl, sandstone, tuff beds; yellowish-gray (5Y 7/2) to grayish-yellowish green (5Y 7/2) or pale olive (10Y 6/2)	Root casts abundant, burrows, mudcracks, *Steinichnus*	0.15 – 6.00 m	Locally overlies FA 4	Wetland or floodplain pond deposits
6	Siltstone and algal marl; yellowish-gray (5Y 7/2), pale yellowish-brown (10YR 6/2), or pale olive (10Y 6/2)	Root casts abundant, burrows, moderate to weak pedogenic features, slickensides, mudcracks	1.0 – 1.5 m	Locally overlies FA 5 and laterally interfingers with FA 4; locally grades into FA 4 and 5 over 100's of meters	Spring-fed wetland deposits

Table 2.2. Distribution of fossil localities among facies associations.

	Vertebrate localities	Plant localities	Trackways	Total localities	Percent of total
FA 1	2	0	0	2	1.3
FA 2	0	0	2	2	1.3
FA 3	15	1	2	18	11.8
FA 4	10	0	0	10	6.5
FA 5	55	1	4	60	39.5
FA 6	58	1	1	60	39.5
Total	140	3	9	152	

Table 2.3. Depositional settings and taphonomy of documented fossil localities. (A) Proportion of weathered and abraded elements in assemblages from each depositional category, (B) Numbers of documented fossil localities in each depositional category by facies association.

A) Depositional category	Number of localities	Weathering stages 0-1	Weathering stages 2-5	Bone abrasion
Channel and bar	8	108/347 (0.31)	238/347 (0.69)	175/353 (0.50)
Proximal levee and chute	16	92/109 (0.84)	17/109 (0.16)	32/122 (0.21)
Distal levee and floodplain	14	74/94 (0.79)	20/94 (0.21)	67/131 (0.51)
Crevasse splay	1	2/10 (0.20)	8/10 (0.80)	17/17 (1.0)
Poorly drained floodplain/wetland	17	103/112 (0.92)	9/112 (0.08)	32/156 (0.21)
Well drained floodplain/wetland	8	535/691 (0.77)	156/691 (0.23)	278/702 (0.40)

B) Depositional category	FA 1	FA 2	FA 3	FA 4	FA 5	FA 6
Channel and bar	1			3	2	2
Proximal levee and chute	1		4	1	5	5
Distal levee and floodplain			5		9	
Crevasse splay					1	
Poorly drained floodplain/wetland			1		10	6
Well drained floodplain/wetland				1	2	5

Table 2.4. Assessment of habitat suitability and preservation potential for each facies association. References provide examples of modern and ancient alluvial sequences that support these interpretations.

Facies Association	Depositional environment	Suitability as life habitat	Favorable preservation	Reference
1	Channel-dominated alluvial fan	Low	No	Koster, 1987; Eberth et al., 2007
2	Playa margin	Low	Yes?	Cohen et al., 1991; Behrensmeyer, 1975
3	Near-channel floodplain	High	Yes	Smith, 1993
4	River channels	Low	Yes	Martin, 1999; Behrensmeyer, 1988
5	Floodplain wetlands and land surfaces	High	Yes	Martin, 1999; Bown and Kraus, 1981
6	Floodplain wetlands and land surfaces	High	Yes	Bown and Kraus, 1981

Supplemental Information

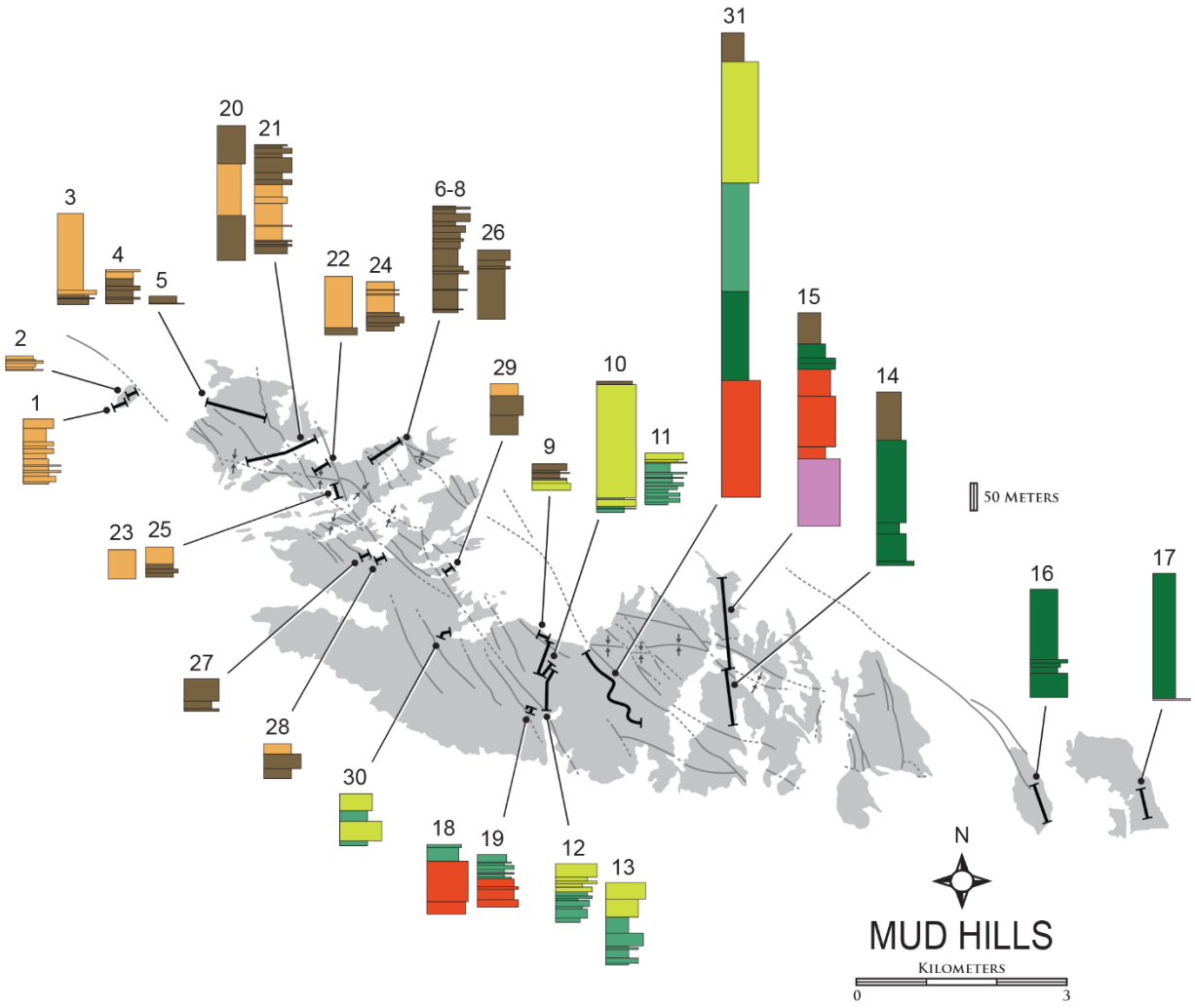

Figure S2.1. Locations of measured sections in the Mud Hills. Sections 20, 24, 25, 27 from Lindsay (1972); sections 21, 22, 23, 26, 28, 29, 30, 31 from Woodburne et al. (1990).

Table S2.1. Location of measured sections used in this study, indicating GPS coordinates of the beginning and end of each section. Coordinates are estimated for sections from Lindsay (1972), Woodburne et al. (1990), and MacFadden et al. (1990), based on locality information provided in those publications. Geographic names refer to Mud Hills quadrangle (USGS, 1996).

Section number (Fig. S1)	Reference	Section name in reference	Location	Approximate coordinates, beginning of section	Section thickness (m)
1	This paper	Truck Top Wash 1	Western Mud Hills	35.061°, -117.103°	31.5
2	This paper	Truck Top Wash 2	Western Mud Hills	35.060°, -117.103°	144
3	This paper	Falkenbach Wash 3	Western Mud Hills	35.058°, -117.087°	203
4	This paper	Falkenbach Wash 2	Western Mud Hills	35.058°, -117.085°	75.5
5	This paper	Falkenbach Wash 1	Western Mud Hills	35.058°, -117.084°	14
6	This paper	Hell Gate Basin 3	Upper Fossil Canyon	35.053°, -117.066°	78.8
7	This paper	Hell Gate Basin 2	Upper Fossil Canyon	35.053°, -117.068°	30
8	This paper	Hell Gate Basin 1	Upper Fossil Canyon	35.052°, -117.068°	135
9	This paper	Skyline	Upper Coon Canyon	35.034°, -117.052°	59
10	This paper	Cal Uranium Prospect 4	Central Mud Hills	35.029°, -117.051°	294.5
11	This paper	Cal Uranium Prospect Canyon 2	Central Mud Hills	35.028°, -117.049°	109
12	This paper	Cal Uranium Prospect Canyon 3	Central Mud Hills	35.027°, -117.048°	121.5
13	This paper	Cal Uranium Prospect Canyon 1	Central Mud Hills	35.025°, -117.048°	182
14	This paper	Owl Canyon 2	Owl Canyon	35.022°, -117.024°	384.5
15	This paper	Owl Canyon 1	Owl Canyon	35.039°, -117.025°	450
16	This paper	Copper City Road	Eastern Mud Hills	35.022°, -116.974°	244.5
17	This paper	Gypsum Basin	Eastern Mud Hills	35.021°, -116.955°	284
18	This paper	Rainy Day Canyon 1	Central Mud Hills	35.026°, -117.055°	60
19	This paper	Rainy Day Canyon 2	Central Mud Hills	35.025°, -117.052°	94
20	Lindsay (1972)	Section C, Carnivore Canyon	Western Mud Hills	35.055°, -117.082°	235
21	Woodburne et al. (1990); MacFadden et al. (1990)	Section 2, Carnivore Canyon, north limb	Western Mud Hills	35.055°, -177.075°	300
22	Woodburne et al. (1990); MacFadden et al. (1990)	Section 3a, Rodent Hill Basin, north limb	Fossil Canyon	35.051°, -117.075°	130

23	Woodburne et al. (1990); MacFadden et al. (1990)	Section 3b, Rodent Hill Basin, south limb	Fossil Canyon	35.046°, -117.076°	65
24	Lindsay (1972)	Section F, Rodent Hill Basin, north limb	Fossil Canyon	35.051°, -117.075°	104
25	Lindsay (1972)	Section G, Rodent Hill Basin, south limb	Fossil Canyon	35.047°, -117.077°	66
26	Woodburne et al. (1990); MacFadden et al. (1990)	Section 6, Hell Gate Basin, north limb	Upper Fossil Canyon	35.052°, -117.068°	186
27	Lindsay (1972)	Section I, Bird Canyon, south limb	Western Mud Hills	35.044°, -117.072°	75
28	Woodburne et al. (1990); MacFadden et al. (1990)	Section 5, Fuller's Earth Canyon, south limb	Western Mud Hills	35.042°, -117.069°	75
29	Woodburne et al. (1990); MacFadden et al. (1990)	Section 7, Hemicyon Basin, south limb	Central Mud Hills	35.039°, -117.060°	95
30	Woodburne et al. (1990); MacFadden et al. (1990)	Section 4, Steepside Quarry, south limb	Coon Canyon	35.032°, -117.060°	105
31	Woodburne et al. (1990); MacFadden et al. (1990)	Section 1, Rainbow Loop	Rainbow Basin	35.018°, -117.036°	840

Table S2.2. Measured and decompacted thicknesses and age estimates used to calculate sediment-accumulation rates for each facies association.

FA	Section number (Fig. 2.5), source	Lower meter	Upper meter	Thickness (m)	Compaction factor	Decompacted thickness (m)	Lower Age (Ma)	Upper Age (Ma)	Duration (Ma)	Sediment-accumulation rate (m/Myr)
1	Section 31, Woodburne et al. (1990)	27	186	159	0.069618	170.0693	17.31	16.76	0.55	309.22
2	Section 31, Woodburne et al. (1990)	241	357	116	0.102463	127.8857	16.58	16.32	0.26	491.87
2	Section 31, Woodburne et al. (1990)	357	440	83	0.102463	91.50443	16.32	16.04	0.28	326.80
2	Section 31, Woodburne et al. (1990)	329	357	28	0.102463	30.86896	16.35	16.32	0.03	1028.97
2	Section 31, Woodburne et al. (1990)	241	308	67	0.102463	73.86502	16.58	16.52	0.06	1231.08
2	Section 31, Woodburne et al. (1990)	308	357	49	0.102463	54.02069	16.52	16.32	0.20	270.10
2	Section 31, Woodburne et al. (1990)	308	329	21	0.102463	23.15172	16.52	16.35	0.17	136.19
3	Section 31, Woodburne et al. (1990)	5	50	45	0.088693	48.99119	16.04	15.80	0.24	204.13
3	Section 31, Woodburne et al. (1990)	357	440	83	0.088693	90.36152	16.32	16.04	0.28	322.72
3	Section 31, Woodburne et al. (1990)	440	482	42	0.088693	45.72511	16.04	15.80	0.24	190.52
3	Section 31, Woodburne et al. (1990)	482	685	203	0.088693	221.0047	15.80	15.16	0.64	345.32
4	Section 10, Loughney and Badgley	12.48	287.5	275.02	0.069213	294.055	15.80	15.20	0.60	490.09
4	Section 10, Loughney and Badgley	274.5	287.5	13	0.069213	13.89977	15.04	14.89	0.15	92.67
4	Section 10, Loughney and Badgley	186.5	287.5	101	0.069213	107.9905	15.16	14.89	0.27	399.96
4	Not figured, Loughney and Badgley	69	224.6	155.6	0.069213	166.3695	15.80	15.20	0.60	277.28
4	Section 31, Woodburne et al. (1990)	773	786	13	0.069213	13.89977	15.16	14.89	0.27	51.48
4	Section 31, Woodburne et al. (1990)	685	786	101	0.069213	107.9905	15.16	14.89	0.27	399.96

4	Section 31, Woodburne et al. (1990)	685	773	88	0.069213	94.09074	15.16	15.04	0.12	784.09
5	Section 26, Woodburne et al. (1990)	15	30	15	0.097805	16.46708	15.20	14.80	0.40	41.17
5	Section 26, Woodburne et al. (1990)	30	50	20	0.097805	21.9561	14.80	14.61	0.19	115.56
5	Section 26, Woodburne et al. (1990)	50	76	26	0.097805	28.54293	14.61	14.00	0.61	46.56
5	Section 26, Woodburne et al. (1990)	76	92	16	0.097805	17.56488	14.00	13.70	0.30	58.55
5	Section 26, Woodburne et al. (1990)	76	130	54	0.097805	59.28147	14.00	13.40	0.60	98.80
5	Section 26, Woodburne et al. (1990)	92	120	28	0.097805	30.73854	13.70	13.50	0.20	153.69
5	Section 26, Woodburne et al. (1990)	120	130	10	0.097805	10.97805	13.50	13.40	0.10	109.78
5	Section 26, Woodburne et al. (1990)	15	50	35	0.097805	38.42318	14.89	14.61	0.28	137.23
5	Section 26, Woodburne et al. (1990)	15	50	35	0.097805	38.42318	15.20	14.61	0.59	65.12
5	Section 26, Woodburne et al. (1990)	15	30	15	0.097805	16.46708	14.89	14.80	0.09	182.97
5	Sections 6-8, Loughney and Badgley	78.8	158	79.2	0.097805	86.94616	15.20	14.00	1.20	72.46
5	Sections 6-8, Loughney and Badgley	158	240	82	0.097805	90.02001	14.00	13.40	0.60	150.03
5	Section 29, Woodburne et al. (1990)	17	58	41	0.097805	45.01001	14.00	13.70	0.30	150.03
5	Section 29, Woodburne et al. (1990)	17	90	73	0.097805	80.13977	14.00	13.40	0.60	133.57
5	Section 29, Woodburne et al. (1990)	58	80	22	0.097805	24.15171	13.70	13.50	0.20	120.76
5	Section 29, Woodburne et al. (1990)	80	90	10	0.097805	10.97805	13.50	13.40	0.10	109.78
5	Section 31, Woodburne et al. (1990)	786	807	21	0.097805	23.05391	15.20	14.80	0.40	57.63
5	Section 31, Woodburne et al. (1990)	786	807	21	0.097805	23.05391	14.89	14.80	0.09	256.15

5	Section 31, Woodburne et al. (1990)	807	827	20	0.097805	21.9561	14.80	14.61	0.19	115.56
5	Section 31, Woodburne et al. (1990)	786	807	21	0.097805	23.05391	14.89	14.80	0.09	256.15
5	Section 14, Loughney and Badgley	279	310	31	0.097805	34.03196	15.20	14.80	0.40	85.08
6	Section 21, Woodburne et al. (1990)	25	83	58	0.093958	63.44956	15.50	15.04	0.46	137.93
6	Section 21, Woodburne et al. (1990)	105	190	85	0.093958	92.98643	15.20	14.00	1.20	77.49
6	Section 21, Woodburne et al. (1990)	105	140	35	0.093958	38.28853	15.20	14.61	0.59	64.90
6	Section 21, Woodburne et al. (1990)	140	190	50	0.093958	54.6979	14.61	14.00	0.61	89.67
6	Section 21, Woodburne et al. (1990)	83	140	57	0.093958	62.35561	15.04	14.61	0.43	145.01
6	Section 21, Woodburne et al. (1990)	83	120	37	0.093958	40.47645	15.04	14.80	0.24	168.65
6	Section 21, Woodburne et al. (1990)	83	105	22	0.093958	24.06708	15.04	14.89	0.15	160.45
6	Section 21, Woodburne et al. (1990)	83	275	192	0.093958	210.0399	15.04	13.70	1.34	156.75
6	Section 21, Woodburne et al. (1990)	140	275	135	0.093958	147.6843	14.61	13.70	0.91	162.29
6	Section 21, Woodburne et al. (1990)	25	275	250	0.093958	273.4895	15.50	13.70	1.80	151.94
6	Section 21, Woodburne et al. (1990)	25	140	115	0.093958	125.8052	15.50	14.61	0.89	141.35
6	Section 21, Woodburne et al. (1990)	25	300	275	0.093958	300.8385	15.50	13.50	2.00	150.42
6	Section 21, Woodburne et al. (1990)	25	190	165	0.093958	180.5031	15.50	14.00	1.50	120.34
6	Section 21, Woodburne et al. (1990)	25	105	80	0.093958	87.51664	15.50	15.20	0.30	291.72
6	Section 21, Woodburne et al. (1990)	190	275	85	0.093958	92.98643	14.00	13.70	0.30	309.95
6	Section 21, Woodburne et al. (1990)	275	300	25	0.093958	27.34895	13.70	13.50	0.20	136.74

6	Not figured, Steinen (1966)	64	131.7	67.7	0.093958	74.02814	15.20	14.00	1.20	61.70

CHAPTER 3

Paleoenvironmental reconstruction of the Barstow Formation, southeastern California, through the Middle Miocene Climatic Optimum[2]

Abstract

The Barstow Formation of southern California is a terrestrial sequence that preserves a diverse Miocene mammalian fauna. The formation spans the Middle Miocene Climatic Optimum (MMCO; 17–14 Ma) and offers the opportunity to study environmental change during the last major interval of global warming of the Cenozoic. Reconstructions of pCO_2 during the MMCO estimate 2 to 4°C of warming from CO_2 forcing. We combined isotopic analysis of carbon and hydrogen from *n*-alkanes and soil organic matter with analysis of phytoliths (plant silica) and diatoms to reconstruct vegetation composition, habitat structure, and moisture dynamics through the formation. The $\delta^{13}C$ and δD of long-carbon-chain *n*-alkanes derived from terrestrial plants and preserved in sediments of the Barstow Formation record drying through the section, punctuated by wet conditions during the peak of the MMCO. Variable isotopic results relate to changes in regional moisture between 16 and 14 Ma, driven partly by facies, vegetation composition, and climatic instability coinciding with intervals of high pCO_2. Phytolith assemblages are dominated by forest indicators during the peak of the MMCO. After 14 Ma, a shift to drier, more open-canopy habitats is represented by enrichment in $\delta^{13}C$ and δD, and grass

[2] Loughney, K.M., Hren, M.T., Smith, S.Y., and Pappas, J., Paleoenvironmental reconstruction of the Barstow Formation, southeastern California, through the Middle Miocene Climatic Optimum, in prep.

morphotypes constitute significant components of phytolith assemblages formed at this time. The establishment of dry, wooded grasslands in the Barstow Basin coincides with the end of the MMCO and the reorganization of precipitation patterns associated with cooling sea-surface temperatures in the Pacific Ocean. This record of changing vegetation composition and structure provides a basis for understanding how environments changed in southern California in response to warming climate.

Introduction

The Middle Miocene Climatic Optimum (MMCO) between 17 and 14 Ma was the last major warming interval of the Cenozoic (Zachos et al., 2001). Global temperatures were 2 to 4°C warmer than modern under moderate (350–550 ppm) atmospheric CO_2 concentrations (You et al., 2009; Knorr et al., 2011). In terrestrial ecosystems, the effects of this warming are poorly constrained due partly to regional variations in paleoenvironmental conditions, variability among proxy systems, and because the influence of climate is hard to disentangle from the influences of tectonics and other basin processes. The MMCO coincided with the height of Neogene tectonic activity in the Great Basin of western North America (McQuarrie and Wernicke, 2005), further complicating the signals of environmental change during this interval. Continental basins preserve local records of landscape evolution that integrate aspects of geomorphology and paleohydrology with faunal and floral responses to climate. Local paleoenvironmental studies add to our overall understanding of regional environmental systems and climate states of the past, and they have the ability to inform predictions of ecosystem responses to future climate.

As the Basin and Range province expanded due to regional extension, many geographically restricted basins formed throughout the western interior of North America. Some of these basins

preserve faunal and floral records of this time, including those in the Mojave tectonic block of southeastern California. Neogene mammal diversity in the Great Basin reached its peak during the MMCO (Badgley et al., 2014), with much of this peak in diversity contributed from the fossil record of the Mojave region (Badgley et al., 2015). A number of factors may have contributed to this high faunal diversity, including high speciation rates, increased topographic complexity (Badgley et al., 2014), and range shifts in response to changing climate (Badgley et al., 2015). Climate history and vegetation are important components of terrestrial ecosystem change through time, and in the Mojave region, the climatic and environmental context of this high diversity is largely unknown. Vegetation composition and paleohydrology can be reconstructed from sedimentological, paleontological, and geochemical archives to build a record of plant-growth conditions and climate states before, during, and after the MMCO. Reconstructing past environments of the Mojave region is crucial for understanding not only how they responded to climate and tectonics but also why they attracted and supported a highly diverse mammalian fauna through the Miocene.

The goals of this study are to evaluate environmental change in the Mojave region through the MMCO. We focus on the Barstow Formation in the central Mojave Desert (Fig. 3.1), a sequence of middle Miocene sediments and faunas that span the MMCO (Fig. 3.2). In the Barstow Basin, playa-dominated environments changed to floodplain-dominated environments with decreasing tectonic activity, becoming more hospitable to mammals and more conducive to fossil preservation with time (Loughney and Badgley, 2017). Vegetation changed as well, (Reynolds and Schweich, 2013; Fisk and Maloney, 2015; Loughney and Smith, 2015) and likely contributed to the high mammal richness of the Mojave region. In concert with recent investigations into the effects of basin evolution on fossil preservation in the Barstow Formation

(Loughney and Badgley, 2017), we analyzed geochemical data to constrain paleoenvironmental conditions within the Barstow Basin during the MMCO. We address four questions: 1) What were the dominant types of vegetation and habitat structure in the Barstow Formation? 2) How did vegetation composition and structure change through the deposition of the Barstow Formation? 3) Do changes in paleoenvironmental indicators correspond with changes in facies? 4) Are changes in vegetation composition, habitat structure, and moisture related to climate transitions associated with the MMCO?

Environments include the physical and biological components of landscapes that characterize local geographic settings. We differentiate between environment (as a general term for the combination of these components) and habitat structure, which we use to distinguish between open-canopy or closed-canopy settings. We reconstruct vegetation composition, structure, and paleohydrology through the MMCO using biomarkers, soil organic matter, phytoliths, and diatoms as paleoenvironmental indicators. Stable isotopes of carbon and deuterium from *n*-alkanes and soil organic matter track moisture and plant-growth conditions, phytoliths are proxies for vegetation composition and habitat structure, and diatoms are indicators of moisture and alkalinity. Combined, these indicators provide quantitative and qualitative assessment of paleoenvironments in southern California as they changed through a significant interval of global warming. This record of environmental change provides a potential basis for understanding the response of modern ecosystems to the effects of current climate change.

Geological background

The Barstow Formation crops out in the central Mojave Desert of California (Fig. 3.1) and is part of the southwestern Basin and Range. The Basin and Range physiographic province formed

through widespread extension in western North America since ~35 Ma; the most pronounced interval of tectonic activity occurred between ~25 and 10 Ma (McQuarrie and Wernicke, 2005), resulting in the formation of numerous fault-bounded basins throughout the region. Beginning in the early Miocene, the Mojave tectonic block experienced extension and detachment-style faulting associated with magmatism (Glazner et al., 2002). Extension in the central Mojave Desert proceeded from ~24 to 19 Ma, and deposits of the synextensional Pickhandle, Jackhammer, and Mud Hills formations were shed into expanding depocenters near the present-day Mud Hills and Calico Mountains (Fig. 3.1; Fillmore and Walker, 1996; Ingersoll et al., 1996). The post-extensional deposits of the Barstow Formation unconformably overlie the Pickhandle and Mud Hills formations in these areas.

The type section of the Barstow Formation occurs in the Mud Hills, where the formation is divided into the Owl Conglomerate, Middle, and Upper members (Fig. 3.2; Woodburne et al., 1990). These deposits fine upwards from the conglomerate and sandstone of the Owl Conglomerate Member to the mudstone-dominated sequences of the Upper Member. Deposition in the Mud Hills occurred between 19 and 13 Ma (Woodburne et al., 1990); the sequence is dated through biostratigraphy (Lindsay, 1972; Pagnac, 2009), magnetostratigraphy (Woodburne, 1996), and isotopic dating of prominent tuff layers (MacFadden et al., 1990; Miller et al., 2013). In the Calico Mountains (Fig. 3.1), Barstow deposits are estimated to be between 19 and 17 Ma in age, based on $^{40}Ar/^{39}Ar$ dating of intrusive dacite domes and dacite breccia of the Yermo volcanic center. Deposits of the Barstow Formation in the Calico Mountains have been designated as the Calico Member by Singleton and Gans (2008).

Depositional environments of the Barstow Formation

The lithostratigraphic members of the Barstow Formation contain numerous fine-scale facies that are grouped into facies associations that represent the dominant environments at the time of deposition. As the basin filled, depositional environments of the Barstow Formation in the Mud Hills changed through time from alluvial fans and playa lakes to floodplains and wetlands (Loughney and Badgley, 2017). In the Mud Hills, Facies Associations 1 and 2 of the Owl Conglomerate Member represent channel and near-channel deposits of alluvial fans and playa lakes, respectively (Fig. 3.2). The Calico Member is a lacustrine facies coeval to the playa facies (Facies Association 2) of the Owl Conglomerate Member in the Mud Hills and represents the deposits of a saline-alkaline playa lake in the Calico Mountains (Park, 1995). Lacustrine facies of the Owl Conglomerate and Calico members were deposited after extension had ceased, and rapid subsidence resulted in thick accumulations (>350 m) of these deposits. Facies Associations 3 and 4 in the Middle Member represent channel and floodplain deposits of meandering and braided stream systems, respectively. The mudstone-dominated deposits (Facies Associations 5 and 6) of the Upper Member represent ponded floodplains and localized wetlands (Fig. 3.2). Fossil localities occur throughout the formation, but the majority of vertebrate localities occur in the Upper Member (Pagnac, 2009; Loughney and Badgley, 2017).

Paleoenvironmental indicators

In terrestrial systems, reconstructions of vegetation composition and paleohydrology often rely on stable isotopes of organic and inorganic materials and fossils. Stable isotopes of organic matter (carbon, oxygen, deuterium), particularly those derived from vascular plants, can be used to reconstruct the environmental conditions under which the plants grew and their responses to

changing hydrology. Macro- and microfossils of plants provide evidence of moisture, taxonomy, or the functional types present on the landscape. The carbon isotopic ratio ($^{13}C/^{12}C$) of organic biomarkers preserved in soil organic matter is an indicator of dominant vegetation (i.e., photosynthetic pathway) or responses to environmental conditions (light or water stress) experienced by plants (Freeman and Pancost, 2014). Deuterium (D) in vascular plant waxes can provide a record of temperature, changes in moisture sources, and hydrology (Sachse et al., 2012).

Fossils provide direct evidence of the plants that inhabited an area. Several Miocene macrofloral assemblages from western North America provide evidence of plant paleocommunities (Axelrod, 1939; Axelrod, 1940; Renney, 1972). Plant microfossils such as pollen and phytoliths are preserved under many depositional and diagenetic conditions (Retallack, 1984), and can potentially be sampled throughout stratigraphic sequences (Strömberg, 2003; 2004). Phytoliths are taxonomically identifiable and are useful indicators for vegetation composition and habitat structure. Diatoms have specific ecological tolerances that allow them to be used to reconstruct water abundance and chemistry (Battarbee et al., 2001). When combined with stable isotope proxies, these micropaleontological indicators provide complementary records of environmental change in terrestrial sequences (Cotton et al., 2012; Hyland et al., 2013; Chen et al., 2015; Harris et al., 2017; Smiley et al., 2018).

Carbon and deuterium isotopic ratios measured in plants vary by photosynthetic pathway, functional type, and growth environment. Most trees, shrubs, and cool-season grasses fix carbon from CO_2 using the C_3 photosynthetic pathway (Sage, 2004). This pathway has a high preference for ^{12}C over ^{13}C and results in depleted $\delta^{13}C$ values in plant tissues (Farquhar et al., 1989; Koch, 1998). The fractionation between atmospheric CO_2 and plant tissues for C_3 plants is about

-19.6‰ (Passey et al., 2002), and the range of $\delta^{13}C$ values for C_3 plants is -22.0 to -35.0‰ (Farquhar et al., 1989; Koch, 1998). Some shrubs and warm-season grasses use the C_4 photosynthetic pathway, which does not discriminate against ^{13}C as strongly as the C_3 pathway (Sage, 2004). The fractionation between atmospheric CO_2 and C_4 plants is about -4.7‰ (Passey et al., 2002), and the range of $\delta^{13}C$ values for C_4 plants is -19.0 to -9.0‰ (Koch, 1998).

Enriched $\delta^{13}C$ values in purely C_3 systems may result from environmental factors. Plants experiencing light or water stress incorporate more ^{13}C into their tissues than plants growing in shaded, moist environments (Sage, 2004). Variation in the ^{13}C content of atmospheric CO_2 also causes variations in $\delta^{13}C$ values of plants. Similarly, variation in δD values may be influenced by precipitation D/H, water source, and changes in moisture and temperature (Horton and Chamberlain, 2006). Water vapor becomes D-depleted as it moves inland and towards the poles, and D depletion of precipitation from water vapors is enhanced at warmer temperatures or in regions that receive large amounts of precipitation (Sachse et al., 2012). In soils, D can be enriched due to evaporation (Sachse et al., 2012). $\delta^{13}C$ and δD measured in biomarkers reflect the environmental conditions experienced by the source plants during growth.

Biomarkers are organic, aliphatic compounds produced by bacteria and other photosynthesizing organisms (Freeman and Pancost, 2014). Because these compounds are resistant to degradation, they can be extracted from fine-grained sediments in continental and marine sections and often represent the dominant source of organic matter. *n*-Alkanes are carbon chains of varying lengths (denoted as C_n) produced in leaf-wax lipids that are common in terrestrial and aquatic plants. Fractionation of $\delta^{13}C$ between plant tissue and leaf wax ranges from 3 to 9‰ and averages about 7‰ (Chikaraishi and Naraoka, 2003; Bi et al., 2005; Vogts et al., 2009). Carbon chains in alkanes from terrestrial plant waxes are typically odd-numbered and

range from C_{25} to C_{35} (Chikaraishi and Naraoka, 2003; Freeman and Pancost, 2014). The dominant chain lengths produced by vascular plants vary as a function of vegetation type and environmental conditions. C_{27} to C_{31} are the most abundant *n*-alkanes found in leaves from woody dicots, herbs, and grasses (Vogts et al., 2009; Freeman and Pancost, 2014). Chain length does not seem to depend on phylogeny, but it may be influenced by environmental factors such as heat or moisture (Vogts et al., 2009; Bush and McInerney, 2015). *n*-Alkanes in sediment preserve the dominant vegetation inputs to the soil averaged over timescales of hundreds to thousands of years. Similarly, soil organic matter (SOM) records the ^{13}C-content of the dominant vegetation growing at the time of soil formation, with an enrichment of 1-2‰ imparted from decomposition of organic matter (Wynn, 2007).

Deuterium is incorporated into leaf waxes from environmental water. Biosynthetic fractionation between leaf water and leaf wax is ~157‰ in humid settings (Sachse et al., 2006; Feakins and Sessions, 2010); in arid environments, the net fractionation between source water and leaf wax δD is ~94‰, accounting for greater enrichment due to leaf transpiration (~+74‰; Feakins and Sessions, 2010). δD is depleted in air masses as water vapor moves inland and over coastal mountains. Groundwater averages isotopic values of waters over several seasons or years, so plant tissues may contain a mixture of groundwater sources. δD enrichment in leaf water occurs during periods of high evapotranspiration (Sachse et al., 2006). Although fractionation factors can vary widely among species and individual plants, for small catchments, average leaf wax δD values may accurately reflect source-water δD values (Feakins and Sessions, 2010).

Phytoliths are amorphous silica bodies precipitated in the cells of plants (Piperno, 2006). Phytoliths occur in many kinds of plants, and some groups produce diagnostic morphotypes. These morphotypes are identifiable to functional group (i.e., grasses, dicots) and occasionally to

specific taxa (e.g., Arecaceae, the palm family; Piperno, 2006). Identifiable morphotypes are typically classified into forest indicators (FI) and grass-silica short cells (GSSCs). GSSCs are only produced by grasses and may be distinguished on the basis of habitat preference. Open-habitat (OH) grasses are those in the Panicoideae, Arundinoideae, Chloridoideae, Micrairoideae, Aristoideae, and Danthonidoideae (combined, the PACMAD clade; Soreng et al., 2015). Closed-habitat (CH) grasses are those of the basal Bambusoideae and Erhartoideae families (Strömberg et al., 2007; Strömberg, 2011). Within the PACMAD clade, most panicoid and chloridoid grasses use the C_4 pathway, and diagnostic morphotypes produced by these groups are often used to indicate C_4 presence (Strömberg and McInerney, 2011).

Diatoms are unicellular algae that are abundant in soils and most aquatic environments and are well-preserved in sediments. Most diatoms have specific tolerances for environmental conditions such as pH, salinity, and temperature (Lowe, 1974; Battarbee et al., 2001). Because they produce complex siliceous frustules, they are typically identifiable to species or genus. Many modern genera have fossil representatives that are interpreted to have similar environmental preferences (Lohman, 1957) and are useful in paleoenvironmental reconstruction. Diatoms present in phytolith assemblages are indicators of moisture, alkalinity, and salinity in waters and soils.

Methods

Methods include description of field collection of samples, laboratory analyses, and quantification techniques for phytolith assemblages.

Sample collection

Sediment samples were collected from 19 stratigraphic sections spanning the thickness of the Barstow Formation in the Mud Hills and Calico Mountains (Fig. 3.1; Loughney and Smith, 2015; Loughney and Badgley, 2017). All members and facies associations were sampled (Figs. 3.2, 3.3). Thirty-seven samples for biomarker analysis were collected throughout the formation and at significant fossil localities; for each sample, approximately 500 g of sediment was collected for processing. Eighty-eight samples for biosilica and SOM analysis were collected at approximately 20-m stratigraphic intervals, where feasible, in fine-grained lithologies that typically preserve plant microfossils (see Loughney and Smith, 2015).

At two locations in the Upper Member of the Mud Hills (Facies Association 6), samples were collected over finer scales in order to reconstruct small-scale habitat variation. At one location, four samples were collected within 5 vertical meters to capture fine-scale temporal change in vegetation composition and structure. At one extensive fossil locality, 12 samples for biomarker, SOM, and biosilica analyses were collected along a lateral transect of ~100 m to investigate lateral variability in vegetation composition and structure. Sampling for lateral habitat variability is underutilized in paleoenvironmental studies even though modern habitats and landscapes are heterogeneous on spatial scales of tens of meters (Kingston et al., 1994; Cotton et al., 2012; Chen et al., 2015).

Biomarkers

Samples were processed at the Hren Lab at the University of Connecticut. Crushed and dried samples were extracted for 48 hours with a 2:1 dichloromethane:methanol solvent mixture. The total-lipid extracts were separated by polarity in silica-gel columns; branched and cyclic alkanes

and other unidentified compounds were separated from straight-chained and normal-alkanes via multiple rounds of urea adduction.

n-Alkane abundances for C_{25}–C_{33} were analyzed on a Thermo TRACE Ultra Gas Chromatograph, and isotopic analyses of biomarker carbon ($\delta^{13}C_{nC}$) and hydrogen (δD) composition were analyzed on a Thermo GC-Isolink connected to a Thermo Mat 253 mass spectrometer. Isotopic results are reported in standard delta-notation relative to Vienna Pee Dee Belemnite (VPDB) for $\delta^{13}C_{nC}$ values and Vienna Standard Mean Ocean Water (VSMOW) for δD values. We corrected raw $\delta^{13}C_{nC}$ values for the middle Miocene enrichment of $\delta^{13}C$ in atmospheric CO_2, using 3-Myr moving-average reconstructions from Tipple et al. (2010).

The average carbon chain length (ACL) for each sample was calculated as the weighted average of each measured chain length:

$$\mathrm{ACL} = \frac{25(C_{25}) + 27(C_{27}) + 29\,(C_{29}) + 31(C_{31}) + 33(C_{33})}{(C_{25}) + (C_{27}) + (C_{29}) + (C_{31}) + (C_{33})}.$$

The ACL metric is used to indicate the dominant chain length represented in a sediment sample that contains alkanes from a variety of sources (Freeman and Pancost, 2014). Sources with longer chain lengths, such as trees and grasses, result in higher sample ACL, and sources with shorter chain lengths, such as aquatic macrophytes (Ficken et al., 2000), result in lower sample ACL. In this way, changes in ACL over time can indicate changes in vegetation composition even when multiple inputs are averaged together (Bush and McInerney, 2013). Environmental conditions can also affect chain length in terrestrial plants, such that plants from humid environments yield shorter chain lengths, and plants from more arid environments yield longer chain lengths (Vogt's et al. 2009). Temperature also affects physiology and ACL of plant

communities, as plants growing under low mean annual temperatures have lower ACL than plants growing in regions of high mean annual temperature (Bush and McInerney, 2015). ACL can then distinguish between relative changes in moisture and temperature among samples with similar source plants.

Soil organic matter

Fifty-seven samples collected for phytolith analysis (Fig. 3.3) were prepared for isotopic analysis of soil organic matter ($\delta^{13}C_{SOM}$) in the Earth Systems Science Laboratory at the University of Michigan. Five grams of each of the bulk samples were washed in methanol and treated in 7% HCl to remove $CaCO_3$. Crushed samples were loaded into tin capsules and analyzed for weight-percent carbon on a Caltech Element Analyzer. Carbon isotopic values were measured on a Thermo Finnigan Delta Plus XL, connected to a Carlo Erba Element Analyzer via Thermo Finnigan Conflo III at the Stable Isotope Ratio Facility for Environmental Research (SIRFER) at the University of Utah. Weight-percent carbon was compared to $\delta^{13}C_{SOM}$ to identify diagenetically altered samples or samples with residual $CaCO_3$ (Fig. S3.1). Ten samples that initially yielded anomalously enriched $\delta^{13}C$ values were re-processed to ensure complete removal of $CaCO_3$ and re-analyzed at SIRFER. Results are reported in delta notation relative to Vienna Pee Dee Belemnite (VPDB) and corrected for Miocene atmospheric $\delta^{13}C$ of CO_2 using reconstructions from Tipple et al. (2010).

Biogenic silica

Samples were processed in the Earth System Science Laboratory at the University of Michigan, following procedures in Strömberg et al. (2007) for heavy-liquid (zinc bromide)

separation for 1 g of sediment. Processed samples were mounted on permanent glass slides with Cargille Meltmount (1.524 refraction index) and immersion oil (Cargille Non-Drying Immersion Oil Type A) for inspection and counting. Phytoliths were identified on immersion-oil slides which allow for rotation and 3D characterization of morphotypes. Assemblages were counted when they contained >200 well-preserved diagnostic phytoliths (Strömberg, 2003; Strömberg et al., 2007). Samples with few or no well-preserved phytoliths, and could therefore not be quantifiably counted, were analyzed qualitatively for presence of identifiable morphotypes (Table S3.1). Phytoliths were analyzed and counted on Leica DMP-1500 and Nikon LV-100 transmitted-light microscopes at 1000x. We made identifications using Strömberg (2003) and a modern reference collection of S.Y. Smith. Our morphotype terminology follows that of Strömberg (2003) and Piperno (2006). Approximately 24% of phytolith samples contained diatoms and diatom fragments. Diatoms were counted and photographed along with phytoliths and were identified using online resources (Spaulding et al., 2010). Ecological affinities of identified taxa were compiled using Lohman (1957), Lowe (1974), and Spaulding et al. (2010) and are listed in Table S3.2.

Phytolith morphotypes were classified into several categories. The forest indicators (FI) category includes those produced by palms, conifers, woody dicots, and non-grass herbaceous plants. The grass silica short-cells (GSSC) category includes all morphotypes produced exclusively by members of the Pooideae, the PACMAD clade, the Bambusoideae and basal grasses, as well as non-diagnostic GSSCs (Strömberg, 2005). For each countable assemblage, we tallied occurrences of FI morphotypes, GSSC morphotypes, aquatic morphotypes, non-diagnostic morphotypes, and phytolith morphotypes of unknown affinities (Table S3.1). Using the total sum

of FI and GSSC phytoliths in each assemblage, we calculated the proportion of FI phytoliths, GSSCs, OH grasses, and CH grasses to determine vegetation structure (Strömberg, 2005).

Useful paleoenvironmental indicators are morphotypes produced by palms, aquatic plants, and closed-habitat grasses. Sedge and palm phytoliths are moisture indicators, as sedges are common in riparian environments and indicate permanent water sources. Palms grow in warm, moist environments, requiring a permanent water source (Eiserhardt et al., 2011) and do not tolerate prolonged drought or freezing temperatures (Howard, 1992). Bambusoid and basal grasses typically inhabit humid, closed-canopy or shaded habitats (Strömberg, 2004). Phytolith morphotypes in the FI category are produced by trees, shrubs, and other herbaceous, non-grass plants (Strömberg, 2003). Because of the breadth of growth habits of plants encompassed by this category, FI morphotypes are not necessarily indicative of closed-canopy forest habitats. For this reason, and to emphasize the proportion of palm and conifer morphotypes in assemblages, we report them separately from other FI indicators.

Age model

Previous chronostratigraphic work in the Mud Hills and Calico Mountains has resulted in a robust age framework for the Barstow Formation (Woodburne et al., 1990; MacFadden et al., 1990; Singleton and Gans, 2008; Miller et al., 2013). We established stratigraphic control of samples across Barstow outcrops through correlation of measured sections in the field and from Lindsay (1972), Woodburne et al. (1990), Lindsay (1995), Abersek and Lofgren (2017), and Loughney and Badgley (2017). Using uncompacted sediment-accumulation rates for each facies association from Loughney and Badgley (2017) and published ages of dated tuffs from

Woodburne et al. (1990) and Miller et al. (2013) as tie points, we constructed an absolute age model for sediment samples (Table S3.3).

Results

Biomarker $\delta^{13}C$, δD, and ACL

Twenty-nine samples were successfully extracted and analyzed for $\delta^{13}C_{nC}$ (Table 3.1), and 27 were successfully analyzed for δD (Table 3.2). Peak abundances for nC_{27} to nC_{31} vary through the section; as such, we present abundance-weighted $nC_{27\text{-}31}$ data (Fig. 3.4) for all samples. Abundance-weighted isotope values can effectively represent the average vascular-plant-derived alkane value for an ecosystem, whereas individual nC_{29} or nC_{31} values may be subject to slightly greater effects of shifting vegetation type on individual components. Weighted $\delta^{13}C_{nC27\text{-}31}$ values range from -25.5‰ to -30.9‰ throughout the formation (Table 3.1), and $\delta D_{nC27\text{-}31}$ values range from -163.5‰ to -203.2‰ (Table 3.2). Both $\delta^{13}C_{nC27\text{-}31}$ and $\delta D_{nC27\text{-}31}$ values show an early enrichment spike between ~17.7 and 17.0 Ma, followed by a gradual trend toward more enriched values between about 16.0 and 15.5 Ma (Fig. 3.4). There is a high degree of variability among alkane isotopic values between 16.0 and 15.0 Ma, when the enrichment trend is punctuated by more depleted values in $\delta D_{nC27\text{-}31}$; $\delta^{13}C_{nC27\text{-}31}$ values vary by -4.3‰, and δD values vary by -36.1‰ through this interval. Overall, the trend in $\delta^{13}C_{nC27\text{-}31}$ is slight enrichment through the middle of the section and at the top, and δD shows a slight enrichment trend through the section.

Mean ACL of the samples ranges between 27.3 and 31.1 through the formation (Table 3.1). Chain-length maxima are at C_{27}, C_{29}, and C_{31} for most samples, consistent with terrestrial plant sources; one sample at ~12.9 Ma has a peak at C_{25} (Fig. S3.2), indicating potential contributions from aquatic sources (Chikaraishi and Naraoka, 2003) or environments with standing water. The

longest mean ACL values occur low in the section (between ~17.7 and 17.3 Ma), and the shortest mean ACL values occur just after this same time span (~17.2 Ma) and at the top of the section (~12.9 Ma; Fig. 3.4). ACL values also vary throughout the section, with the greatest variability in samples occurring between 16.5 and 15.0 Ma.

Soil organic matter $\delta^{13}C$

Soil organic matter (SOM) samples show a greater range of variation through the formation than results from *n*-alkanes. Corrected $\delta^{13}C_{SOM}$ values range from -26.6‰ to -16.2‰ (Fig. 3.4), and raw $\delta^{13}C_{SOM}$ results are listed in Table S3.4. All $\delta^{13}C_{SOM}$ values are enriched relative to $\delta^{13}C_{nC27\text{-}31}$ values due to the apparent fractionation between leaf tissue and leaf wax in *n*-alkanes. $\delta^{13}C_{SOM}$ results generally show the same trends as $\delta^{13}C_{nC27\text{-}31}$ results through the section: slightly enriched samples before 17.0 Ma and a high degree of variability between 16.5 and 15.0 Ma. A cluster of samples collected from the Upper Member shows an enrichment spike at about 13.7 Ma; these are the most enriched SOM samples from the section. These enriched $\delta^{13}C_{SOM}$ values differ from the $\delta^{13}C_{nC27\text{-}31}$ values from the same sampled horizon by almost 7‰. This offset is within the normal range of fractionation between plant tissue and *n*-alkanes (Chikaraishi and Naraoka, 2003).

Phytoliths

The majority of processed samples yielded few or no identifiable morphotypes. Ten samples were able to be quantified, and an additional 50 samples were evaluated qualitatively (Table S3.1). All members and facies associations except Facies Association 4 were sampled, yet phytoliths were identified in only 68% of samples and were only abundantly preserved in 11% of

samples. Counted assemblages were in samples from Facies Associations 3, 5, and 6. Facies Association 1 was opportunistically sampled, since dominant lithologies are coarse-grained and not conducive to preserving phytoliths. Phytoliths occurred in one of seven processed samples from Facies Association 1. Of the 15 samples processed from Facies Association 2, seven yielded identifiable phytoliths. Facies Association 3 had the most dense vertical distribution of samples of any facies association, and although phytoliths were identified in most of these samples (15 of 16 processed), they were abundant in only two samples. Facies Association 4 is dominated by coarse sandstones and was not sampled for phytoliths. For Facies Association 5, 12 of 22 processed samples yielded phytoliths, including one quantified assemblage. Facies Association 6 had the most processed samples (28), of which six samples yielded phytoliths in addition to eight counted assemblages. Nine of the counted assemblages are from the Upper Member and one is from the Middle Member in the Mud Hills (Fig. 3.2). No quantified assemblages are preserved from the Owl Conglomerate or Calico members, and samples from these members rarely yielded phytoliths.

FI morphotypes occur in all quantified assemblages and in most of the additional samples. Echinate spheres produced by palms (Fig. 3.5E) also occur throughout the section. Morphotypes referable to conifers (Fig. 3.5D) and CH grasses (Fig. 3.5J) are present in most quantified assemblages from the upper part of the formation but are not abundant. OH-grass GSSCs (Fig. 3.5) are only present in eight assemblages from the uppermost part of the formation and are otherwise extremely rare. Phytoliths from sedges (Fig. 3.5L), which are rare among all samples with diagnostic morphotypes, occur in samples from the Calico and Upper members. The results for diagnostic morphotypes from quantified assemblages are shown in Figure 3.5, and FI:GSSC and OH:CH ratios of counted assemblages are shown in Table 3.3.

The counted assemblage from the Middle Member is dominated by FI (37%) and palm (63%) morphotypes with only one OH GSSC. This assemblage had the second lowest number of phytoliths and the lowest diversity of morphotypes of any of the counted assemblages (CUP-1-12 in Table 3.3 and Fig. 3.6). Unknown phytolith morphotypes comprise 33% of the total assemblage, much higher than the 5% to 18% of unknowns in the other quantified assemblages (Table S3.1). Another sample from the Middle Member that contained abundant phytoliths but was not formally counted contained only FI morphotypes.

GSSCs are important components of well-preserved phytolith assemblages from the Upper Member. The assemblage from a sample collected directly beneath the Dated Tuff marker bed (14.8 Ma) is dominated by FI morphotypes, with 15% GSSCs (Table 3.3, Fig. 3.6). In quantified assemblages from the Upper Member, GSSCs comprise 23% to 76% of assemblages. The abundance of palm morphotypes in these assemblages varies between 2% and 47%, and morphotypes referable to conifers are consistently low, ranging from 0% to 6% (Table 3.3, Fig. 3.6). When FI morphotypes comprise >60% of the assemblage, palm morphotypes are <5%, and OH grasses are <15% of the assemblage (Fig. 3.6).

Assemblages from the four samples collected over 4.8 vertical meters (TT samples in Table 3 and Fig. 3.6) show a transition from general FI-dominated to palm-dominated composition over that span. OH GSSCs range from 11% of the assemblage in the FI-dominated sample to 37% in the palm-dominated samples. CH GSSCs are present but comprise less than 10% of GSSCs in these assemblages.

All six of the samples collected along the lateral transect (RH samples in Table 3.3 and Fig. 3.6) preserved phytoliths, but only four could be quantified. GSSCs dominate three of these assemblages (67% to 76%), and FI morphotypes dominate the fourth assemblage (77%). Palm

and conifer morphotypes are present in low abundance (<4%). Sedge phytoliths are also present but rare in each assemblage.

Diatoms

Identifiable diatoms were present in 11 phytolith samples overall, including five of the counted phytolith assemblages (Table 3.4). Fragmentary, unidentifiable diatoms were present in 21 phytolith samples; the number of fragmentary diatoms in many samples indicates that they may have been broken during transport and deposition by stream currents (Lohman, 1957). Diatoms were present in samples collected from all members of the Barstow Formation in the Mud Hills and Calico Mountains, although they occur in low abundance. Similar to the phytolith results, the abundance and diversity of diatoms increase through the section (Table 3.4). Three genera were identified in one sample from the Calico Member, one genus was present in a sample from the Owl Conglomerate Member, two genera were identified in two samples from the Middle Member, and 11 genera were present in seven samples from the Upper Member (Table 3.4).

Identified diatoms have a range of environmental affinities that agree with the environmental interpretations of the facies from which they were sampled (Table S3.2). Species of *Epithemia*, *Hantzschia*, and *Luticola* in the sample from the lacustrine facies of the Calico Member (Facies Association 2) prefer warm temperatures and have moderate to high tolerance for saline and alkaline waters (Lowe, 1974; Spaulding et al., 2010). The single genus questionably identified from Facies Association 1 (?*Frustula*) prefers freshwater, acidic to alkaline streams and lakes (Spaulding et al., 2010). Samples collected from the proximal-channel floodplain deposits of Facies Association 3 in the Middle Member contain genera (e.g., *Sellaphora*) that occur in low-

gradient streams or standing water that is neutral to alkaline. Diatoms identified from the Upper Member were all from samples collected from Facies Association 6. These genera display a range of habitat preferences, from flowing water to standing water to moist soil; among these genera, *Eunotia* and *Hantzschia* are indicative of ephemeral ponds (Tables 3.4, S3.2; Lohman, 1957; Lowe, 1974; Spaulding et al., 2010).

Discussion

Our paleoenvironmental indicators provide a fairly continuous record of environmental variability and change through the Barstow Formation. Variation among samples partly relates to sedimentological and paleohydrological variability through the basin and to changes in vegetation composition and habitat structure. Major trends in isotopic results and biosilica assemblages reflect changing climate during and after the MMCO.

Isotopic indicators

Many climatic and environmental factors can influence $\delta^{13}C$ and δD measured in plant-derived environmental indicators. Variation in $\delta^{13}C$ values may relate to changes in the ^{13}C-content of atmospheric CO_2, which is the source of ^{13}C in plant tissues, fluctuations in vegetation composition, or environmental factors affecting the growth of plants, such as water or light stress (Sage, 2004). Trends in our isotopic sample results should reflect changes in the $\delta^{13}C$ content of atmospheric CO_2, which was -0.5‰ to -1.2‰ more enriched in the middle Miocene than pre-industrial levels (Tipple et al., 2010). Additionally, the $\delta^{13}C$ content of atmospheric CO_2 increased by ~1‰ during the MMCO to a maximum value of -5.25‰ at ~15.5 Ma, followed by progressive decline between 15.0 and 10.0 Ma (Tipple et al., 2010). This enrichment in global

atmospheric $\delta^{13}C$ during the MMCO coincides with the most enriched $\delta^{13}C_{nC7\text{-}31}$ values in our data (Fig. 3.4) and contributes to the broad positive shift in our $\delta^{13}C_{nC27\text{-}31}$ data at this time.

High pCO_2 during the MMCO could also have affected the values of δD in source vegetation. Mid-Miocene pCO_2 has been estimated at ~500 ppm based on models and proxy-based reconstructions (You et al., 2009; Greenop et al., 2014), which indicate an important role for pCO_2 in climatic warming during the MMCO (Zhang et al., 2013). The effects of mass-dependent isotopic fractionation are dampened under high temperatures (Poulsen and Jeffery, 2011), which could potentially affect the values of δD in atmospheric moisture during the increased temperatures of the MMCO. Poulsen and Jeffery (2011) modeled the effect of increased atmospheric CO_2 on $\delta^{18}O$ in meteoric water; they predicted that the isotopic composition of atmospheric water vapor would be more enriched in ^{18}O and D under warm-climate scenarios. The overall enrichment of δD reaching the basin during the MMCO could mask local environmental variations in paleohydrology during deposition of the Barstow Formation; nevertheless, positive and negative changes are evident in the $\delta D_{nC27\text{-}31}$ record. Although $\delta^{13}C_{nC27\text{-}31}$, $\delta^{13}C_{SOM}$, and $\delta D_{nC27\text{-}31}$ would be expected to respond to large-scale climatic controls, the trends in isotopic indicators through the section are also influenced by environmental factors affecting the source vegetation.

Vegetation composition and structure affect the values of $\delta^{13}C$ from *n*-alkanes and SOM sampled in sediment. Although the range of $\delta^{13}C_{nC27\text{-}31}$ values (-30.0 to -24.3‰) and most $\delta^{13}C_{SOM}$ values lie within the range expected for C_3-dominated vegetation, C_4 plants were likely present and contributed to the enrichment of samples (Fig. 3.4). Thirty-one $\delta^{13}C_{SOM}$ samples were more enriched than the cutoff for pure C_3 vegetation proposed by Kohn (2010), corrected for average Miocene atmospheric $\delta^{13}C$ as -22.1‰. Decomposing organic matter can be enriched

relative to the original plant material by 1-2‰ (Koch, 1998; Wynn, 2007); taking this enrichment into account, seven SOM samples are heavier than the C_3 cutoff value. Although middle Miocene plant communities were dominated by C_3 vegetation, C_4 plants were present in low to moderate abundance in the Great Plains (Fox and Koch, 2003) and southern Rocky Mountains (Harris et al., 2017) at this time. In C_4 plants, fractionation of $\delta^{13}C$ and δD between plant tissues and *n*-alkanes is higher than in C_3 plants (Chikaraishi and Naraoka, 2003). The 4-7‰ offset between $\delta^{13}C_{nC27\text{-}31}$ and $\delta^{13}C_{SOM}$ values at ~13.7 Ma (Fig. 3.4) could be due to an increase in C_4 biomass. Phytoliths from probable C_4 grasses as well as sedges occur in samples from this interval and would have contributed to the enriched $\delta^{13}C$ values.

Some aquatic plants use the C_4 pathway or an intermediate C_3-C_4 pathway (Sage, 2004), and if present, they would impart heavier $\delta^{13}C$ values to sediments throughout the section. Relatively enriched $\delta^{13}C_{SOM}$ values from Facies Associations 3 and 5 were from interbedded claystones and marls interpreted as deposits of floodplain ponds (Loughney and Badgley, 2017). The few diatoms from samples from Facies Association 3 inhabit alkaline ponds or sluggish streams (Table 3.4; Spaulding et al., 2010). Plants growing in poorly mixed, alkaline waters often fix carbon from HCO_3 because it is more abundant than CO_2 under high pH. $\delta^{13}C$ in HCO_3 is 7 to 11‰ more enriched than $\delta^{13}C$ in CO_2, and plants growing in these waters are enriched in $\delta^{13}C$, regardless of photosynthetic pathway (Keeley and Sandquist, 1992).

Canopy cover and water stress also influence $\delta^{13}C$ in vascular plants (Sage, 2004). Kohn (2010) proposed -31.5‰ as the cutoff for $\delta^{13}C$ of plants in modern C_3 closed-canopy environments. Our $\delta^{13}C_{SOM}$ and $\delta^{13}C_{nC27\text{-}31}$ values are more enriched than this cutoff value, accounting for the ~-7‰ offset between plant tissue and plant wax (Vogts et al., 2009). These results and those from the quantified phytolith assemblages indicate the presence of relatively

open-canopy habitats throughout deposition of the Barstow Formation. We estimated the fraction of woody cover through the Barstow Formation using two approaches: the equations for $\delta^{13}C_{SOM}$ of SOM of Cerling et al. (2011) and $\delta^{13}C_{nC31}$ of *n*-alkanes of Magill et al. (2013). There is considerable offset between estimates from $\delta^{13}C_{SOM}$ and $\delta^{13}C_{nC31}$ until ~14.2 Ma, when woody cover estimates agree. All estimates based on $\delta^{13}C_{SOM}$ fall between 0.1 and 0.8 woody cover, a range encompassed by grassland (0.0-0.1), wooded grassland (0.1-0.4), and shrubland (0.4-0.8) (Cerling et al., 2011). Estimates based on $\delta^{13}C_{nC31}$ are less than SOM-based estimates, falling between 0.09 and 0.5. For both approaches, most estimates range between 0.2 and 0.6 through the formation, indicating that open-canopy settings prevailed and did not include dense forest.

Samples collected along the lateral transect in the Upper Member yield a range of $\delta^{13}C$ values that reveal heterogeneity in habitat structure and moisture. Values of $\delta^{13}C_{SOM}$ from the transect range from -20.9‰ to -16.2‰, revealing slight heterogeneity in vegetation. A 4‰ range over 100 m is not unusual in terrestrial settings. In the modern Mayumbe region of the Republic of the Congo, $\delta^{13}C$ values from SOM varied by 14‰ over transects of 40-70 m (Schwartz et al., 1996). These transects spanned the transition from savanna to forest, where a large difference in $\delta^{13}C$ values is expected due to increasing canopy cover, CO_2 recycling, and moisture (Kohn, 2010). The 4‰ variation along our transect indicates that no such change in canopy cover is captured by our samples, even though phytolith FI:GSSC ratios are as high as 78:22 (RH-16-7 in Table 3.3). The FI phytoliths from this sample may have been derived from non-arborescent woody dicots and herbaceous plants or from woody dicots living in high-light conditions.

The trend in $\delta D_{nC27-31}$ through the section shows an early enrichment before 17.0 Ma, and an enrichment after 14.0 Ma (Fig. 3.4). Through the middle of the section, $\delta D_{nC27-31}$ is relatively stable but punctuated by a negative deviation, indicating wetter conditions. Precipitation is the

main source of δD in plant tissues; D is fractionated during lipid biosynthesis, transpiration of leaf water, and evaporation of soil water (Sachse et al., 2012). D-enrichment of leaf water and soil water occurs under low humidity or at high temperatures (Smith and Freeman, 2006), and depletion occurs under cooler temperatures and with increasing amount of precipitation (Sachse et al., 2012). Global temperatures were higher during the MMCO (Zachos et al., 2001), and depleted values of $\delta D_{nC27-31}$ are unlikely to be due to cooling. Enrichment in $\delta D_{nC27-31}$ before 17.0 Ma and after 14.0 Ma may correspond to drying before and after the MMCO, and depletion of $\delta D_{nC27-31}$ between 16.0 Ma and 15.0 Ma may indicate a pronounced change in precipitation regime, especially given the probable climatic enrichment of δD in water vapor reaching the basin. Together, positive shifts in both $\delta^{13}C_{nC27-31}$ and $\delta D_{nC27-31}$ values through the Barstow Formation indicate periods of relative environmental drying, occurring at ~17.2 Ma and ~ 13.7 Ma; wet conditions are indicated by the negative shift in $\delta D_{nC27-31}$ between 16.0 and 15.0 Ma (Fig. 3.4).

Shifts in ACL toward longer lengths before 17 Ma and after 14 Ma correspond with positive shifts in $\delta^{13}C_{nC27-31}$ and $\delta D_{nC27-31}$. Increases in mean ACL may result from drier conditions or from changes in dominant *n*-alkane sources among samples. Several studies have shown that chain-length distributions in woody angiosperms are shorter (C_{27}, C_{29}) in humid, forested environments and longer (C_{31}-C_{35}) in drier, open environments (Bush and McInerney, 2013; Schwab et al., 2015). Vogts et al. (2009) showed that average chain length increased in plants sampled across a rainforest-savanna-C_4 grassland gradient. Several environmental factors combined to produce this increase in ACL, including decreasing humidity and increasing light intensity (Vogts et al., 2009). Bush and McInerney (2015) found that mean annual temperature and annual relative humidity were the most important determinants of *n*-alkane chain lengths

sampled in modern soils. Longer mean ACL before 17 Ma and after 14 Ma indicates environmental drying in agreement with the enrichment in $\delta^{13}C_{nC27-31}$ and $\delta D_{nC27-31}$ values from these intervals. Variability in mean ACL between 16 Ma and 15 Ma is likely the result of the combination of increasing temperature and moisture during the MMCO. Higher temperatures would result in longer chain lengths, but increased moisture would result in shorter chain lengths; this variability through the middle of the section may reflect the interaction of two signals with different effects on ACL.

While it is likely that the mean ACL of the Barstow samples reflects changes in moisture availability, some trends in mean ACL do not closely track the enrichment shifts shown by $\delta^{13}C_{nC27-31}$ and $\delta D_{nC27-31}$ values. Discrepancies in these environmental signals may then be due to the types of source plants contributing *n*-alkanes to the samples. Dominant chain lengths are C_{27}, C_{29}, and C_{31} for most samples (Fig. S3.2), indicative of predominantly terrestrial (nonaquatic) sources of *n*-alkanes (Chikaraishi and Naraoka, 2003) through most of the section, regardless of facies. In two samples, C_{25} is the dominant chain length (Fig. S3.2), indicating significant contribution of *n*-alkanes from aquatic macrophytes (Ficken et al., 2000). One of these samples was collected from the lacustrine facies of the Calico Member (~17.2 Ma), which had abundant aquatic vegetation at the time of deposition (Park and Downing, 2001). The low mean ACL value of this sample from the Calico Member is likely due to aquatic macrophytes in an evaporitic playa-lake setting. This short chain length explains the apparent deviation from the relatively enriched $\delta^{13}C_{nC27-31}$ and $\delta D_{nC27-31}$ values from this sample, which are consistent with drying in an evaporitic lake. Abundance of aquatic macrophytes may not, however, explain the C_{25} maximum of the other sample with low mean ACL, as this sample horizon does not show

sedimentological evidence of saturation consistent with settings preferred by aquatic macrophytes.

Similar trends in $\delta^{13}C_{nC27-31}$, $\delta^{13}C_{SOM}$, and $\delta D_{nC27-31}$ results through the section point to changes in environmental controls on plant growth through the Barstow Formation. Warm temperatures and changing atmospheric $\delta^{13}C$ of CO_2 underlie positive shifts in $\delta^{13}C_{nC27-31}$ and $\delta^{13}C_{SOM}$ and during the MMCO (Tipple et al., 2010; Poulsen and Jeffery, 2011). After climate, paleohydrology is likely the dominant control on our $\delta^{13}C_{nC27-31}$ and $\delta^{13}C_{SOM}$ results, with minor changes in vegetation composition and structure contributing to $\delta^{13}C_{SOM}$ and ACL. Positive shifts in $\delta^{13}C_{nC27-31}$, $\delta^{13}C_{SOM}$, and $\delta D_{nC27-31}$ indicate periods of drying, and negative shifts indicate wetter conditions; variability in these indicators indicate that Barstow environments experienced intervals of increasing and decreasing moisture during the peak of the MMCO. The overall trend shows initial drying before 17.0 Ma, followed by an interval of wet conditions between 16.5 and 15.0 Ma, and a return to drier conditions after 14.0 Ma.

Phytolith assemblages and Barstow flora

Phytolith assemblages reveal changes in vegetation composition and structure through time or space (Strömberg et al., 2007). OH and CH grasses are reliable indicators of open- and closed-canopy habitats, respectively (Strömberg, 2004). Morphotypes of palms and conifers are typically included in the FI category because they come from plants that may grow several meters tall and create a shaded understory. This category also includes morphotypes that are produced by non-arborescent and herbaceous plants (Strömberg, 2003), which may or may not prefer closed-canopy environments. Although palm morphotypes are typically included in the FI category, modern palms of California and northern Mexico grow in high-light conditions

(Axelrod, 1939). The modern California fan palm *Washingtonia filifera* requires permanent surface water and is shade intolerant (Howard, 1992). Modern relatives of fossil palm taxa from the middle Miocene Bopesta Formation of southern California include *Sabal uresana* and *Brahea brandegeei*, which grow along streams in arid and semi-arid regions of northern Mexico (Axelrod, 1939). Most palms occur in humid tropical to subtropical climates (>2000 mm mean annual precipitation), and palms in arid regions are dependent on permanent groundwater sources (Eiserhardt et al., 2011). The occurrence of palms in phytolith assemblages from the Barstow Formation is then more likely to indicate relatively open-canopy environments with permanent water than closed-canopy habitats. Conifers vary greatly in their shade and moisture requirements, and modern conifers in southern California and northern Mexico occur in habitats ranging from chaparral to evergreen forests (Pavek, 1994).

Few phytolith assemblages are preserved in samples from the early Barstow deposits in the Mud Hills and Calico Mountains. General forest indicators and morphotypes from palms, conifers, grasses, and sedges in samples from the lacustrine facies of the Calico Member represent a mix of lake-margin to more distal vegetation. Termites, thrips, and leafhoppers from the Calico Member provide indirect evidence of savanna-woodland vegetation before 17.0 Ma (Park and Downing, 2001). The oldest counted assemblage from the Middle Member (~15.9 Ma; CUP-1-12 in Fig. 3.6) is FI-dominated (Table 3.3 and Fig. 3.6). This locality was deposited in a near-channel floodplain setting and had abundant water to support palms; non-palm FI morphotypes probably derived from woody dicots and herbs in a riparian community. Palm and FI morphotypes are present in other samples from the same fluvial facies association, which likely hosted similar plant assemblages throughout its deposition. The counted assemblage at 14.8 Ma (OC-2-8 in Fig. 3.6) is also dominated by FI morphotypes but contains 9% conifer and

only 2% palm morphotypes; this sample is the oldest counted assemblage with OH GSSCs. The FI and conifer morphotypes in this assemblage may indicate conditions too dry to support abundant palms.

Phytolith assemblages are best preserved in the Upper Member from ~14.8 to 12.9 Ma in age. These deposits represent well-drained floodplains and spring-fed wetlands (Loughney and Badgley, 2017). OH grass morphotypes are well-represented in these assemblages and include morphotypes of panicoid and chloridoid grasses presumed to use the C_4 photosynthetic pathway (Strömberg and McInerney, 2011). In the laterally sampled transect at ~13.7 Ma, three assemblages are dominated by OH GSSCs and one is FI-dominated (RH samples in Table 3.3 and Fig. 3.6). Phytoliths from sedges are present in all of these samples. As indicated by the small range in $\delta^{13}C_{SOM}$ values from these samples, FI abundance may not signify closed-canopy habitat; CH grass phytoliths are uncommon in the FI-dominated assemblage (RH-16-7 in Fig. 3.6). Nevertheless, these assemblages show that vegetation was heterogeneous over tens of meters in a wooded grassland with low amounts of CH grasses in shadier areas. This locality represents a well-drained, spring-fed wetland environment (Loughney and Badgley, 2017) and supported wetland plants, as indicated by sedge phytoliths. Palms are sensitive to groundwater and drainage conditions (Eiserhardt et al., 2011), and the low proportion of palm morphotypes from this site may indicate that it was too wet or that water sources were seasonally variable due to fluctuations in groundwater.

The other locality in the Upper Member that was finely sampled at ~13.1 Ma shows changing vegetation over 4.8 vertical meters (TT samples in Table 3.3 and Fig. 3.6). We infer that these assemblages represent shifting vegetation composition through time. The stratigraphically lowest assemblage is FI-dominated with 7% conifer morphotypes (TT-1-15-10 in Fig. 3.6), and

successive assemblages have increasing amounts of OH GSSCs and palm morphotypes coupled with decreasing proportions of FI and conifer morphotypes. Through the 4.8 m of the vertical transect, sediments grade from marl with abundant root casts to brown siltstone with slickensides, redoximorphic concentrations and depletions, filled cracks, and mottles. These pedogenic features form from repeated wetting and drying, such as with fluctuating groundwater. The assemblage from the base of the transect represents riparian or wetland vegetation, which shifted over time to wooded grassland with abundant palms.

Grass phytoliths are rare in Barstow deposits before 14.8 Ma (Fig. 3.7), and GSSCs of OH grasses are present in four samples collected in the Owl Conglomerate, Calico, and Middle members. Grassland existed in the central Mojave region prior to 14.8 Ma, based on the arthropod fauna from the Calico Member (Park and Downing, 2001), but grass phytoliths were not well preserved in these environments. The riparian environments of the Middle Member may also have been too closed or wet to support OH grasses. Phytoliths are rare from lower Barstow deposits, and preservation bias may operate on larger scales in these facies (see below). The increasing abundance of OH GSSCs in the Upper Member indicates that open-canopy vegetation became more prevalent after 14.8 Ma. Paleosols in the Barstow Formation are also better developed and sediments are better drained after ~15.0 Ma (Loughney and Badgley, 2017), indicating drier environments than existed earlier. The composition of our phytolith assemblages is consistent with those from palm savanna or sclerophyll woodland assemblages (Strömberg, 2004) that form in warm regions receiving ~500 to 1000 mm mean annual precipitation.

The presence of wooded grasslands is supported by limited macrofloral and palynological studies from the Barstow Formation, which identified pollen from riparian and dry-adapted genera (O'Connor, 1982; Fisk and Maloney, 2015). Petrified wood and leaf impressions from

below the Skyline Tuff marker bed (~15.0 Ma; Woodburne et al., 1990) were identified by Alf (1970) as *Quercus, Juniperus,* Arecaceae, and unidentifiable shrubs. The Rainbow Loop Flora from approximately 16.4 Ma (Reynolds and Schweich, 2013) also had material referable to woody dicots and palms. Fisk and Maloney (2015) analyzed pollen from a vertebrate fossil locality in the Upper Member dated at ~14.2 Ma and found palynomorphs of *Pinus, Picea, Abies, Juglans, Populus, Salix, Ephedra, Equisetum, Juncus,* and *Carex,* in addition to Arecaceae and Poaceae pollen. They interpreted this assemblage as forming around a pond and surrounded by woodland or savanna. Another pollen assemblage collected from the Rainbow Basin (exact sampling locality unknown, but deposits in the Rainbow Basin span approximately 16.5 to 14.0 Ma) was dominated by palynomorphs of *Ephedra*, *Erigonium*, *Pinus, Quercus,* Amaranthaceae, and Asteraceae, with lower abundance of *Juglans, Platanus, Alnus, Arbutus, Typha*, and *Carya* (O'Connor, 1982). O'Connor (1982) interpreted the assemblage as a mix of lowland, shrub-dominated communities and upland, oak and pine communities growing in a summer-dry climate. The reconstructed vegetation from the macrofloral and pollen assemblages of the Barstow Formation range from wooded grassland to shrub-dominated communities, with local riparian forests. Our phytolith assemblages are consistent with these reconstructions and give additional insight into how these communities were distributed through the Barstow Formation during and following the MMCO.

Interpretation based on environmental indicators

The value of combining isotopic data with fossil indicators is the ability to integrate different kinds of environmental information. Phytolith and diatom assemblages provide qualitative assessments of vegetation and paleohydrology that can be further constrained by isotopic data.

Our phytolith and diatom assemblages provide records of paleovegetation and moisture, and the isotope results allow us to interpret the climatic conditions that influenced plant communities in the Barstow Basin during and after the MMCO. This record of hydrologic change through the MMCO provides context for understanding the response of vegetation in southern California to warming climate.

The drying trend in the isotopes between 17.7 and 17.0 Ma agrees with facies analysis, as evaporitic playa environments existed during this time in the Barstow Basin (Park and Downing, 2001; Loughney and Badgley, 2017). The highest mean ACL values in the section are from samples collected from this interval, in agreement with the enriched $\delta^{13}C_{nC27-31}$, $\delta^{13}C_{SOM}$, and $\delta D_{nC27-31}$ values. The drying trend between 17.7 and 17.0 Ma (Fig. 3.4) occurred after local extension of the Barstow Basin had ceased (Glazner et al., 2002), during a period of subsidence that resulted in the accumulation of several hundreds of meters of evaporitic lacustrine deposits in the Calico Mountains and eastern Mud Hills (Fig. 3.1). Diatoms from the Calico Member sample prefer alkaline waters, moderate salinity, and inhabit ephemeral water bodies or aerially exposed sediments (Table 3.4). Park (1995) and Park and Downing (2001) examined fossil arthropod assemblages from this facies in the Calico Mountains and found evidence for drying through the sequence. They interpreted the depositional setting as a saline-alkaline lake surrounded by savanna-woodland. FI, grass, and sedge phytoliths in samples from the Calico Member are consistent with the interpretation of Park and Downing (2001) as a vegetated lake surrounded by grassland and woodland. Palm and sedge phytoliths do not occur in the upper part of the lacustrine sequence (Fig. 3.7), where Park and Downing (2001) interpreted major reductions in lake level due to increasing aridity.

Between 16 and 15 Ma, humid conditions prevailed in the basin. Streams and floodplains formed in the basin during the MMCO, and groundwater levels were relatively high, likely due to increased precipitation. Typical fluvial environments are subject to small-scale variations in lithology and drainage (Bridge, 2003). In Facies Associations 3 and 5, channel sandstone bodies are interbedded with marls and fine-grained floodplain deposits that were well- to poorly drained (Loughney and Badgley, 2017). High or fluctuating groundwater levels are indicated by low-chroma coloration, mottling, and redoximorphic concentrations around root casts in fine-grained floodplain deposits in these facies associations. The variability in these facies relates to drainage characteristics that likely varied with precipitation regime and groundwater levels that changed with changing climate.

The phytolith and diatom records from 16.5 to 15.0 Ma are sparse but indicate relatively wet conditions. The phytolith assemblages from this interval (CUP-1-12 and OC-2-8 in Fig. 3.6) represent riparian communities of palms, woody dicots, and herbaceous plants. Such vegetation may have been representative for this time, as palm and FI morphotypes are present in other samples from Facies Association 3, but they have a discontinuous record through the Middle Member (Fig. 3.7). OH grasses were rare components of the vegetation (Fig. 3.6), and these riparian environments may have formed more closed-canopy habitats. Few diatoms were identified in samples from the Middle Member, but those present are indicators of wet conditions. *Sellaphora* was identified in a sample from this interval (CUP-1-1 in Table 3.4), and modern representatives of this genus are benthic forms that live in lakes and slow-moving streams; *Nitzschia* and *Hantzschia* (CUP-1-12 in Table 3.4) also inhabit permanent or ephemeral aquatic environments (Spaulding et al., 2010). Palms and other riparian plants may have existed near perennial water sources in the proximal-channel settings forming during this time. Shorter

ACL and depleted $\delta D_{nC27-31}$ indicate that moisture was the dominant control on paleoenvironmental proxies between 16.5 and 15.0 Ma, and changing vegetation composition and structure contributed minor variability in $\delta^{13}C_{C27-31}$ and $\delta^{13}C_{SOM}$. Data from facies, isotopes, and biosilica indicate that environments deposited between 16.5 and 15.0 Ma ranged from perennially wet to alternating wet-dry, likely in response to increased precipitation during the MMCO.

Relatively dry conditions existed in the basin after 14.0 Ma, following the end of the MMCO. At ~13.7 Ma, the positive shift in $\delta^{13}C_{nC27-31}$, $\delta D_{nC27-31}$, and $\delta^{13}C_{SOM}$, and longer ACL indicate dry conditions and increased C_4 presence in open-canopy habitats (Fig. 3.7). OH GSSCs comprise 11% to 57% of phytolith assemblages from this interval (Table 3.3), showing that vegetation composition and structure were spatially heterogeneous. These samples were from Facies Association 6, which represents well-drained floodplains and spring-fed wetlands (Loughney and Badgley, 2017). Paleosols in Facies Association 6 are well developed and have slickensides, redoximorphic concentrations and depletions, and carbonate nodules. These features form from repeated wetting and drying of soils, as with fluctuating groundwater levels or seasonally variable precipitation (Retallack, 2001), and indicate that precipitation was more seasonal and groundwater levels were lower after 14.0 Ma. Groundwater-fed wetland systems may be highly localized or spread over several kilometers but are subject to seasonal fluctuations in groundwater (Pigati et al., 2014). In modern desert wetlands of the Mojave Desert, marshes, wet meadows, and phreatophyte flats form adjacent to one another along groundwater gradients (Pigati et al., 2014). Similarly, the environments of the Upper Member must have been spatially heterogeneous, as localized wetland deposits are interbedded with well-drained paleosols in the uppermost part of the formation. Diatoms from this facies association have a variety of

environmental tolerances consistent with ephemeral wetland settings (Tables 3.4, S3.2). Diatom species from samples collected along the lateral transect in Facies Association 6 occur as attached and free-floating forms in streams, ponds, and springs. *Hantzschia* is indicative of ephemeral aquatic environments, *Aulacoseira* occurs in standing water, and *Pinnularia* occurs in subaerially exposed sediments (Lohman, 1957; Lowe, 1974). Their occurrence together in the same series of samples indicates fluctuations in water levels at these wetland sites, consistent with modern desert wetland systems (Pigati et al., 2014). The development of dry, open environments coincides with cooling of the middle Miocene climate transition (MMCT) following the end of the MMCO around 14.0 Ma.

C_4 grasses represent an increasing proportion of the vegetation growing in the drier, cooler climate of the MMCT. The presence of C_4 biomass throughout the formation is indicated by isotopic results (Figs. 3.3, 3.6), but the enrichment in $\delta^{13}C_{nC27\text{-}31}$ and $\delta^{13}C_{SOM}$ after 14 Ma indicates that C_4 plants were more prevalent in the dry, open-canopy habitats of the Upper Member. Phytolith assemblages from after 14 Ma all contain OH grass morphotypes and morphotypes produced by panicoid or chloridoid grasses (Fig. 3.6). The majority of modern panicoid and chloridoid grasses are C_4, and in the geologic record, their phytoliths are interpreted as evidence for C_4 grasses in open habitats (Strömberg, 2004). Feranec and Pagnac (2013) sampled ungulate enamel from the Barstow Formation and found that equids, camelids, and antilocaprids consumed up to 18% C_4 vegetation. Equids from the Barstow Formation consumed more C_4 material than did equids from other Californian middle Miocene formations (Feranec and Pagnac, 2017; Bowman et al., 2017). Most of the teeth sampled in this study were from localities younger than 14 Ma, where our most ^{13}C-enriched SOM samples occurred (Fig. 3.7). The seasonally dry savanna of the Barstow Basin after 14 Ma may have been important local

habitat for C_4 grasses prior to the spread of C_4 grasslands in the late Miocene. C_4 photosynthesis is an adaptation to dry and open habitats (Sage, 2004), and C_4 grasses are estimated as ~10 to 30% of Miocene grass communities in the Great Plains (Fox and Koch, 2003) and southern Rocky Mountains (Harris et al., 2017). Fox and Koch (2003) reconstructed a significant increase in C_4 biomass composition in the southern Great Plains at 14 Ma, and they linked C_4 abundance to climatic cooling after the MMCO.

Biosilica preservation

The overall dearth of biogenic silica from Barstow samples indicates that taphonomic or preservational biases affect their occurrence. Previous geochemical studies have found that surface waters in the Barstow Basin were saline and alkaline (Sheppard and Gude, 1969; Park, 1995). Silica solubility increases with pH (Becking et al., 1960), and phytoliths dissolve in pH >9 (Retallack, 1984; Piperno, 2006). The abundance of gypsum (Park, 1995) in Facies Association 2, and zeolites and smectitic clays in the Mud Hills (Sheppard and Gude, 1969) indicate high alkalinity which may have contributed to the low preservation of phytoliths and diatoms in the lower Barstow Formation. Gleyed and low-chroma mudstones of Facies Association 5 preserve abundant calcareous root casts and yield rare identifiable phytoliths or diatoms. These deposits represent poorly-drained floodplain and wetland deposits, and prolonged high, alkaline groundwater levels (Sheppard and Gude, 1969) may have contributed to the preservation of root casts (and possibly vertebrate bones) while dissolving biogenic silica. Decaying organic matter also contributes to phytolith dissolution (Piperno, 2006). Mechanical degradation could also have contributed to low phytolith and diatom preservation (Lohman, 1957). Facies Association 3 represents near-channel floodplain and channel deposits, and many

echinate spheres (Fig. 3.5E) in the counted assemblage from Facies Association 3 are rounded or abraded. Phytoliths and diatoms in Facies Association 3 may have been susceptible to transportation and reworking in these near-channel environments.

Phytoliths tend to be best preserved in sesquioxide-rich soils of low to medium alkalinity (Piperno, 2006). The best-preserved assemblages are from Facies Association 6, which is dominated by well-drained mudstones with pedogenic features (slickensides, redoximorphic depletions, root casts) that indicate low sediment-accumulation rates and relative landscape stability (Loughney and Badgley, 2017). These vegetated landscapes may have accumulated phytoliths over longer periods of time, and improved drainage reduced the chance of dissolution from alkaline groundwaters. Although additional sampling could improve biogenic silica yields, it is likely that groundwater chemistry was an important factor in limiting phytolith and diatom preservation in the Barstow Basin.

Middle Miocene vegetation and climate in southern California

Global climate models of the MMCO reconstruct 2–4°C of warming (You et al., 2009), followed by drastic cooling after 13 Ma (LaRiviere et al., 2012). Fundamental changes in the carbon cycle have been invoked to explain this global warming and subsequent cooling, including forcing from high pCO_2 (Greenop et al., 2014), enhanced volcanic activity, and organic carbon burial (Flower and Kennett, 1993). The hydrological cycle also changed through these Neogene climate states, as paleobotanical data indicate that western North America was wetter than the present day (Wolfe, 1985; Lyle et al., 2008).

Climatic conditions in the Miocene of southern California were wetter than modern, and climatic variability of the MMCO preceded the transition to the modern climate state. Modern

California climate is characterized by wet winters and dry summers (Friedman et al., 2002; Lyle et al., 2008). Water vapor reaching the modern Mojave Desert derives from the northern or central Pacific Ocean. Winter precipitation comes from air masses traveling eastward from the Pacific over the Transverse and Sierra Nevada Mountains; summer precipitation derives from the Gulf of Mexico and Gulf of California over moderate to low-lying terrain (Friedman et al., 1992).

In the Miocene, topography and wind circulation patterns were different, bringing warm, moist air to the southern Great Basin during summer months. Horton and Chamberlain (2006) proposed that the Great Basin experienced 1–3 km of downdrop during the Miocene, based on $\delta^{18}O$ and δD from authigenic calcite and smectite. Associated with this decline in elevation, they proposed that air masses delivering precipitation to the central Basin and Range arrived predominantly from the south in the Miocene (Horton and Chamberlain, 2006), consistent with the paths of modern summer-precipitation air masses.

Miocene paleofloral and pollen assemblages of southern California have been interpreted as growing under summer-wet conditions or having precipitation distributed throughout the year (Axelrod 1939; 1940; Srivastava, 1984). The Tehachapi flora from the middle Miocene Bopesta Formation includes numerous species whose extant relatives are distributed along the southern California coast, Baja California, and northern Mexico (Axelrod, 1939). Axelrod (1939) interpreted the assemblage as a mix of savanna-woodland, riparian, and chaparral-scrub communities and estimated 380–640 mm of annual precipitation distributed through the winter and summer. Pollen from the middle Miocene Monterey Formation in Santa Barbara County, California, originated from plants growing in coastal marshes and lowlands inhabited by *Salix* and *Quercus* and cooler uplands inhabited by *Pinus*, *Carya*, *Acer*, and *Ulmus* (Srivastava, 1984).

Srivastava (1984) interpreted the abundance of *Carya* and the presence of tropical taxa as indicators of a warm, summer-wet climate. Smiley et al. (2018) estimated mean annual precipitation using the CIA-K weathering index (Sheldon et al., 2002) in the middle Miocene Crowder and Cajon Valley formations at the southwestern edge of the Mojave region. Mean annual precipitation decreased from 807 ± 182 mm yr^{-1} at 17.0 Ma to 741 ± 182 mm yr^{-1} by 15.0 Ma. Sheppard and Gude (1969) published elemental composition of tuffs and one mudstone sample from the Barstow Formation. We calculated mean annual precipitation using CIA-K for this mudstone from the Rainbow Basin as 612 mm yr^{-1}. This estimate agrees well with floral-based estimates for the middle Miocene (Axelrod, 1939), although the age of the mudstone sample can only be constrained between 16.5 to 14.0 Ma.

Precipitation regimes in southern California during the middle Miocene were driven by circulation patterns in the Pacific Ocean that changed through the Neogene in response to global climate. Deep-sea isotopic records from across the Pacific Ocean show that circulation and thermocline gradients have changed since the early Miocene and experienced instability during the MMCO. Similar trends in benthic foraminiferal $\delta^{13}C$ records from drill sites in the western and eastern Pacific Ocean show that east-west, deep-ocean temperature gradients were weak or nonexistent during the peak of the MMCO (Holbourn et al., 2007). Holbourn et al. (2013) identified several deep-water warming pulses from negative shifts in benthic foraminiferal $\delta^{18}O$ and $\delta^{13}C$ from drill sites in the eastern equatorial Pacific Ocean (Fig. S3.3). From these short-lived events, they inferred high climatic variability during the MMCO. Pacific Ocean surface temperatures were also warmer than modern during the MMCO (Zhang et al., 2013), and the Pacific thermocline was deeper than modern (Matsui et al., 2017). Highly variable benthic foraminiferal $\delta^{13}C$ and $\delta^{18}O$ records during peak Miocene warming coincide with the variability

in our *n*-alkane and SOM results between 16.5 and 14.5 Ma (Fig. S3.3), indicating a relationship to circulation patterns in the Pacific Ocean.

In the modern eastern Pacific Ocean, periodic warm-water upwelling results in El Niño weather patterns and increased precipitation in western North America. Wara et al. (2005) proposed that permanent El Niño-like conditions existed during the Pliocene based on warm sea-surface temperature reconstructions, reduced east-west surface temperature gradients across the Pacific, and a deep thermocline in the eastern Pacific. Warm surface temperatures (Zhang et al., 2013), reduced east-west temperature gradients (Holbourn et al., 2013), and a deep eastern Pacific thermocline (Matsui et al., 2017) reconstructed for the middle Miocene are also consistent with El Niño-like conditions. The significant variability in the deep-ocean isotopic records indicate that, if El Niño-like conditions existed, they were intermittent through the MMCO, as deep-water warming pulses were transient (Holbourn et al., 2013). Significant changes in ocean-surface temperatures and deep-ocean gradients would affect air-circulation patterns and the timing of moist-air delivery to the southern Great Basin. Variability in our isotopic data, changes in vegetation, and groundwater fluctuations through the Barstow Formation may reflect changes in amount of precipitation or seasonality during the MMCO. If El Niño-like conditions existed through the MMCO, southern California would have experienced variation in timing and amount of precipitation in the middle Miocene.

Around 14.7 Ma, cold-water upwelling in the eastern Pacific Ocean is reflected in several positive shifts in benthic foraminiferal $\delta^{18}O$, with the most pronounced shift at ~13.8 Ma (Fig. S3.3; Holbourn et al., 2013). This positive shift slightly precedes the CM6 episode of the Monterey Excursion, a coupled positive spike in foraminiferal $\delta^{13}C$ and $\delta^{18}O$ marking a major cooling step and expansion of the East Antarctic Ice Sheet (Woodruff and Savin, 1991; Holbourn

et al., 2007). The deposition of the organic-rich sediments of the Monterey Formation along the coast of California is associated with increased productivity during upwelling and increased carbon burial (Vincent and Berger, 1985). Many paleoclimatic studies identify shifts in $\delta^{18}O$ of benthic and planktonic foraminifera at ~14.0 Ma that coincide with major expansions of Antarctic ice and upwelling in the eastern equatorial Pacific Ocean (Flower and Kennett, 1994; Holbourn et al., 2013; Zhang et al., 2013). This cooling is recognized as the onset of the MMCT and coincides with drier conditions in California and the Great Basin.

The transition to winter precipitation in California is associated with changes in ocean- and air-circulation patterns since the late Miocene (Lyle et al., 2008). By the late Miocene, the California coast was drier: precipitation estimates from the xeric scrub- to oak-savanna communities from the Mint Canyon Formation of Ventura County, California, are ~380–500 mm yr^{-1}, with most precipitation occurring during the winter (Axelrod, 1940). The Neogene pollen record from a Deep Sea Drilling Program site (Leg 63, Hole 467) off the coast of southern California shows the transition from the Miocene summer-wet climate to the modern winter-wet regime occurring in the Pliocene (Ballog and Malloy, 1981). Dinoflagellates from this drill site decrease in abundance in the late Miocene, marking a shift from warm to cool surface waters (Ballog and Malloy, 1981). Off the coast of California, surface-water temperatures decreased 3–4°C, and stratification increased through the Miocene (Bukry, 1981; Schoell et al., 1994). These floral and microfossil records document the progressive cooling and drying of coastal California through the Miocene and into the Pliocene.

Drying of the Great Basin is associated partly with the uplift of the Sierra Nevada and partly with changes in Pacific surface temperatures that drove a shift to winter precipitation in the late Miocene (Lyle et al., 2008). Feng et al. (2016) modeled a number of climate parameters

hypothesized for Neogene drying in western North America and found that an increased equator-pole surface temperature gradient best agreed with proxy records. Under this scenario, the summer subtropical high-pressure system strengthens in the eastern Pacific, driving coastal winds southward and drying the southwest. This modeled circulation pattern is similar to the modern eastern Pacific configuration that prevents moist air from reaching California during the summer (Lyle et al., 2008). Upwelling and progressive cooling of surface ocean waters during the MMCT, as well as the development of topographic barriers (e.g., the Transverse Ranges), resulted in reorganization of air-circulation pathways and drying in the Mojave region. In the Barstow Formation, low water tables and localized wetland deposits formed after approximately 14.7 Ma, coincident with the onset of MMCT cooling. Over this time in the Barstow Basin, palm savanna or sclerophyll woodlands developed around spring-fed wetlands.

The hydrologic and vegetation record of the Barstow Formation through the middle Miocene reflects the changing climate states that affected southern California. Climatic variability during the MMCO resulted in increased and variable precipitation in the Mojave region. Subsequent cooling during the MMCT resulted in drying and the spread of open-canopy habitats around ephemeral water sources. The changing vegetation composition and structure in the Barstow Formation and other formations in California through the Miocene reflect the transition from year-round to seasonal precipitation regimes that characterize modern California climate.

Conclusion

The MMCO remains an enigmatic warming interval in Neogene history despite interest in it as a potential point of reference for current climate change. Few studies have focused on reconstructing paleoenvironments from continental sequences of this time. Here, we present

paleoenvironmental proxy data that document changing environments in the Barstow Formation, an important terrestrial sequence for its diverse mammalian faunas.

Changing vegetation composition and structure in the Barstow Basin relate to changing climate and precipitation patterns through the MMCO. $\delta^{13}C$ and δD results from *n*-alkanes and soil organic matter, phytoliths, and diatoms track variations in moisture and vegetation through changing depositional environments. Our data, as well as macrofloral and palynological studies from the Barstow Formation and southern California, indicate that environments were wetter than modern and became drier through time. Dry conditions in the basin prior to 17.0 Ma correspond with the deposition of evaporitic lacustrine facies in the Mud Hills and Calico Mountains (Park, 1995; Park and Downing, 2001). With the establishment of fluvial settings between ~16.5 and 14.5 Ma, $\delta^{13}C$ and δD show that plants experienced humid and poorly to moderately drained conditions. Riparian vegetation dominated by forest indicators formed relatively closed canopies in proximal-floodplain settings during the MMCO, consistent with increased precipitation and humid climate.

By ~13.7 Ma, environments in the Barstow Basin were open and drier. Positive shifts in $\delta^{13}C$ and δD at this time resulted from drying, light-exposure, and increased C_4 presence in open-canopy habitats as global climate cooled. Wooded grasslands formed around ephemeral wetlands as precipitation became more seasonal. Our isotopic results and biosilica assemblages demonstrate drying and agree with palynological and macrofloral records from the Barstow Formation and other Miocene sequences from southern California. Together, these records of vegetation composition and structure reveal the changing climate states and precipitation regimes in California during and following the MMCO.

The combination of paleoenvironmental proxy systems is important to understanding different aspects of vegetation, moisture, and depositional setting. Different environmental indicators preserve different aspects of paleoenvironment, and multi-proxy investigations come close to capturing the scope of environmental variation that exists in terrestrial settings. Reconstructions of vegetation and climate from middle Miocene terrestrial sequences reveal regional responses to warming during the MMCO (Fox and Koch, 2003; Harris et al., 2017; Smiley et al., 2018). The record from the Barstow Formation adds to our understanding of how paleohydrology and vegetation changed in southern California during this warming interval and provides context for studying changes in faunal diversity of the Great Basin. Elucidating the link between hydrology, vegetation, and climate gives insight to the factors influencing Cenozoic mammalian ecology, diversity, and turnover through the Neogene (Janis et al., 2000). These studies not only contribute to reconstructions of regional floral and faunal change in response to past climate, they also provide a point of reference for predictions of future climate-driven ecosystem change.

Acknowledgments

This study was conducted with support from the Evolving Earth Foundation, Issaquah, WA; the University of Michigan Department of Earth & Environmental Sciences and University of Michigan Rackham Graduate School. We thank Nathan Sheldon for the use of laboratory facilities and materials, Ethan Hyland, Katherine Truong, Abigail Oakes, Gregory Harris, and Kathryn Rico for help and guidance in the lab. We also thank Rachel Thorpe, Tara Smiley, and Anna Harkness for assistance in the field and in sample processing. Thanks to Catherine Badgley for guidance, field assistance, and feedback on early drafts of the manuscript.

References

Abersek, W.F., and Lofgren, D.L., 2017, Biostratigraphy of nonmarine Miocene gastropods from the Barstow Formation of California, *in* Reynolds, R.E., ed., ECSZ Does It: Revisiting the Eastern California Shear Zone: The 2017 Desert Symposium Field Guide and Proceedings: Zzyzx, California, California State University Desert Studies Consortium, p. 229-234.

Alf, R.M., 1970, A preliminary report on a Miocene flora from the Barstow Formation, Barstow, California: Bulletin, Southern California Academy of Sciences, v. 69, no. 3–4 p. 183-189.

Axelrod, D.I., 1939, A Miocene Flora from the Western Border of the Mohave Desert, Carnegie Institution of Washington, 129 p.

Axelrod, D.I., 1940, The Mint Canyon flora of southern California; a preliminary statement: American Journal of Science, v. 238, no. 8, p. 577-585.

Badgley, C., Smiley, T.M., and Finarelli, J.A., 2014, Great Basin mammal diversity in relation to landscape history: Journal of Mammalogy, v. 95, no. 6, p. 1090-1106.

Badgley, C., Smiley, T.M., and Loughney, K.M., 2015, Miocene mammal diversity of the Mojave region in the context of Great Basin mammal history, *in* Reynolds, R.E., ed., Mojave Miocene: The 2015 Desert Symposium Field Guide and Proceedings: Zzyzx, California, California State University Desert Studies Consortium, p. 34-43.

Ballog, R.A., and Malloy, R.E., 1981, Neogene palynology from the southern California continental borderland, Site 467, Deep Sea Drilling Project Leg 63: U.S. Government Printing Office.

Battarbee, R.W., Jones, V.J., Flower, R.J., Cameron, N.G., Bennion, H., Carvalho, L., and Juggins, S., 2001, Diatoms, *in* Smol, J.P., Birks, H.J.B., and Last, W.M., eds., Tracking Environmental Change Using Lake Sediments, Volume 3: Terrestrial, Algal, and Siliceous Indicators: Dordrecht, The Netherlands, Kluwer Academic Publishers, p. 155-202.

Becking, L.G.M.B., Kaplan, I.R., and Moore, D., 1960, Limits of the Natural Environment in Terms of pH and Oxidation-Reduction Potentials: The Journal of Geology, v. 68, no. 3, p. 243-284.

Bi, X., Sheng, G., Liu, X., Li, C., and Fu, J., 2005, Molecular and carbon and hydrogen isotopic composition of n-alkanes in plant leaf waxes: Organic Geochemistry, v. 36, no. 10, p. 1405-1417.

Bridge, J.S., 2003, Rivers and Floodplains: Forms, Processes, and the Sedimentary Record: Oxford, Blackwell Publishing, 491 p.

Bukry, D., 1981, Pacific coast coccolith stratigraphy between Point Conception and Cabo Corrientes, Deep Sea Drilling Project Leg 63: U.S. Government Printing Office.

Bush, R.T., and McInerney, F.A., 2013, Leaf wax n-alkane distributions in and across modern plants: Implications for paleoecology and chemotaxonomy: Geochimica et Cosmochimica Acta, v. 117, p. 161-179.

Bush, R.T., and McInerney, F.A., 2015, Influence of temperature and C_4 abundance on *n*-alkane chain length distributions across the central USA: Organic Geochemistry, v. 79, Supplement C, p. 65-73.

Cerling, T.E., Wynn, J.G., Andanje, S.A., Bird, M.I., Korir, D.K., Levin, N.E., Mace, W., Macharia, A.N., Quade, J., and Remien, C.H., 2011, Woody cover and hominin environments in the past 6 million years: Nature, v. 476, no. 7358, p. 51-56.

Chen, S.T., Smith, S.Y., Sheldon, N.D., and Strömberg, C.A.E., 2015, Regional-scale variability in the spread of grasslands in the late Miocene: Palaeogeography, Palaeoclimatology, Palaeoecology, v. 437, no. Supplement C, p. 42-52.

Chikaraishi, Y., and Naraoka, H., 2003, Compound-specific δD–δ13C analyses of *n*-alkanes extracted from terrestrial and aquatic plants: Phytochemistry, v. 63, no. 3, p. 361-371.

Cotton, J.M., Sheldon, N.D., and Strömberg, C.A.E., 2012, High-resolution isotopic record of C_4 photosynthesis in a Miocene grassland: Palaeogeography, Palaeoclimatology, Palaeoecology, v. 337–338, p. 88-98.

Eiserhardt, W.L., Svenning, J.-C., Kissling, W.D., and Balslev, H., 2011, Geographical ecology of the palms (Arecaceae): determinants of diversity and distributions across spatial scales: Annals of Botany, v. 108, no. 8, p. 1391-1416.

Farquhar, G.D., Ehleringer, J.R., and Hubick, K.T., 1989, Carbon isotope descrimination and photosynthesis: Annual Review of Plant Physiology and Plant Molecular Biology, v. 40, p. 503-537.

Feakins, S.J., and Sessions, A.L., 2010, Controls on the D/H ratios of plant leaf waxes in an arid ecosystem: Geochimica et Cosmochimica Acta, v. 74, no. 7, p. 2128-2141.

Feranec, R.S., and Pagnac, D., 2013, Stable carbon isotope evidence for the abundance of C_4 plants in the middle Miocene of southern California: Palaeogeography, Palaeoclimatology, Palaeoecology, v. 388, p. 42-47.

Ficken, K.J., Li, B., Swain, D.L., and Eglinton, G., 2000, An *n*-alkane proxy for the sedimentary input of submerged/floating freshwater aquatic macrophytes: Organic Geochemistry, v. 31, no. 7–8, p. 745-749.

Fillmore, R.P., and Walker, J.D., 1996, Evolution of a supradetachment extensional basin: The lower Miocene Pickhandle basin, central Mojave Desert, California, *in* Beratan, K.K., ed., Reconstructing the History of Basin and Range Extension Using Sedimentology and Stratigraphy, Volume 303: Boulder, Colorado, Geological Society of America, p. 107-126.

Fisk, L.H., and Maloney, D.F., 2015, Palynology of the "Slug Bed" in the middle Miocene Barstow Formation in the Mud Hills, Mojave Desert, southern California, *in* Reynolds, R.E., ed., Mojave Miocene: The 2015 Desert Symposium Field Guide and Proceedings: Zzyzx, California, California State University Desert Studies Consortium, p. 130-135.

Flower, B.P., and Kennett, J.P., 1993, Relations between Monterey Formation deposition and middle Miocene global cooling: Naples Beach section, California: Geology, v. 21, no. 10, p. 877-880.

Flower, B.P., and Kennett, J.P., 1994, The middle Miocene climatic transition: East Antarctic ice sheet development, deep ocean circulation and global carbon cycling: Palaeogeography, Palaeoclimatology, Palaeoecology, v. 108, no. 3–4, p. 537-555.

Fox, D.L., and Koch, P.L., 2003, Tertiary history of C_4 biomass in the Great Plains, USA: Geology, v. 31, no. 9, p. 809-812.

Freeman, K.H., and Pancost, R.D., 2014, 12.15 - Biomarkers for Terrestrial Plants and Climate, *in* Turekian, H.D., and Holland, K.K., eds., Treatise on Geochemistry (Second Edition): Oxford, Elsevier, p. 395-416.

Friedman, I., Smith, G.I., Gleason, J.D., Warden, A., and Harris, J.M., 1992, Stable isotope composition of waters in southeastern California 1. Modern precipitation: Journal of Geophysical Research: Atmospheres, v. 97, no. D5, p. 5795-5812.

Friedman, I., Harris, J.M., Smith, G.I., and Johnson, C.A., 2002, Stable isotope composition of waters in the Great Basin, United States 1. Air-mass trajectories: Journal of Geophysical Research: Atmospheres, v. 107, no. D19, 4400.

Glazner, A.F., Walker, J.D., Bartley, J.M., and Fletcher, J.M., 2002, Cenozoic evolution of the Mojave block of southern California: Geological Society of America Memoirs, v. 195, p. 19-41.

Greenop, R., Foster, G.L., Wilson, P.A., and Lear, C.H., 2014, Middle Miocene climate instability associated with high-amplitude CO_2 variability: Paleoceanography, v. 29, no. 9, p. 845-853.

Harris, E.B., Strömberg, C.A.E., Sheldon, N.D., Smith, S.Y., and Vilhena, D.A., 2017, Vegetation response during the lead-up to the middle Miocene warming event in the Northern Rocky Mountains, USA: Palaeogeography, Palaeoclimatology, Palaeoecology, v. 485, no. Supplement C, p. 401-415.

Holbourn, A., Kuhnt, W., Schulz, M., Flores, J.-A., and Andersen, N., 2007, Orbitally-paced climate evolution during the middle Miocene "Monterey" carbon-isotope excursion: Earth and Planetary Science Letters, v. 261, no. 3–4, p. 534-550.

Holbourn, A., Kuhnt, W., Lyle, M., Schneider, L., Romero, O., and Andersen, N., 2013, Middle Miocene climate cooling linked to intensification of eastern equatorial Pacific upwelling: Geology.

Horton, T.W., and Chamberlain, C.P., 2006, Stable isotopic evidence for Neogene surface downdrop in the central Basin and Range Province: Geological Society of America Bulletin, v. 118, no. 3-4, p. 475-490.

Howard, J.L., 1992, Washingtonia filifera, Fire Effects Information System, U.S. Department of Agriculture, Forest Service, Rocky Mountain Research Station, Fire Sciences Laboratory.

Hyland, E.G., Sheldon, N.D., and Fan, M., 2013, Terrestrial paleoenvironmental reconstructions indicate transient peak warming during the early Eocene climatic optimum: GSA Bulletin, v. 125, no. 7-8, p. 1338-1348.

Ingersoll, R.V., Devaney, K.A., Geslin, J.K., Cavazza, W., Diamond, D.S., Heins, W.A., Jagiello, K.J., Marsaglia, K.M., Paylor, E.D., II, and Short, P.F., 1996, The Mud Hills, Mojave Desert, California: Structure, stratigraphy, and sedimentology of a rapidly extended terrane, *in* Beratan, K.K., ed., Reconstructing the History of Basin and Range Extension Using Sedimentology and Stratigraphy, Volume 303: Boulder, Colorado, Geological Society of America, p. 61-84.

Janis, C.M., Damuth, J., and Theodor, J.M., 2000, Miocene ungulates and terrestrial primary productivity: Where have all the browsers gone?: Proceedings of the National Academy of Sciences, v. 97, no. 14, p. 7899-7904.

Keeley, J.E., and Sandquist, D.R., 1992, Carbon: freshwater plants: Plant, Cell & Environment, v. 15, no. 9, p. 1021-1035.

Kingston, J.D., Marino, B.D., and Hill, A.P., 1994, Isotopic evidence for Neogene hominid paleoenvironments in the Kenya Rift Valley: Science, v. 264, no. 5161, p. 955-959.

Knorr, G., Butzin, M., Micheels, A., and Lohmann, G., 2011, A warm Miocene climate at low atmospheric CO_2 levels: Geophysical Research Letters, v. 38, no. L20701, p. 1-5.

Koch, P.L., 1998, Isotopic reconstruction of past continental environments: Annual Review of Earth and Planetary Sciences, v. 26, no. 1, p. 573-613.

Kohn, M.J., 2010, Carbon isotope compositions of terrestrial C_3 plants as indicators of (paleo)ecology and (paleo)climate: Proceedings of the National Academy of Sciences, v. 107, no. 46, p. 19691-19695.

LaRiviere, J.P., Ravelo, A.C., Crimmins, A., Dekens, P.S., Ford, H.L., Lyle, M., and Wara, M.W., 2012, Late Miocene decoupling of oceanic warmth and atmospheric carbon dioxide forcing: Nature, v. 486, no. 7401, p. 97-100.

Lindsay, E.H., 1972, Small mammal fossils from the Barstow Formation, California: University of California Publications in Geological Sciences, v. 93, p. 1-104.

Lindsay, E.H., 1995, *Copemys* and the Barstovian/Hemingfordian Boundary: Journal of Vertebrate Paleontology, v. 15, no. 2, p. 357-365.

Lohman, K.E., 1957, Cenozoic nonmarine diatoms from the Great Basin [Ph.D. dissertation]: California Institute of Technology, Pasadena, 208 p.

Loughney, K.M., and Smith, S.Y., 2015, Phytoliths from the Barstow Formation through the Middle Miocene Climatic Optimum: Preliminary results, *in* Reynolds, R.E., ed., Mojave Miocene: The 2015 Desert Symposium Field Guide and Proceedings: Zzyzx, California, California State University Desert Studies Consortium, p. 51-58.

Loughney, K.M., and Badgley, C., 2017, Facies, environments, and fossil preservation in the Barstow Formation, Mojave Desert, California: PALAIOS, v. 32, no. 6, p. 396-412.

Lowe, R.L., 1974, Environmental requirements and pollution tolerance of freshwater diatoms: United States Environmental Protection Agency, EPA-670/4-74-005 a.

Lyle, M., Barron, J., Bralower, T.J., Huber, M., Olivarez Lyle, A., Ravelo, A.C., Rea, D.K., and Wilson, P.A., 2008, Pacific Ocean and Cenozoic evolution of climate: Reviews of Geophysics, v. 46, RG2002.

MacFadden, B.J., Swisher, C.C., III, Opdyke, N.D., and Woodburne, M.O., 1990, Paleomagnetism, geochronology, and possible tectonic rotation of the middle Miocene Barstow Formation, Mojave Desert, southern California: GSA Bulletin, v. 102, no. 4, p. 478-493.

Magill, C.R., Ashley, G.M., and Freeman, K.H., 2013, Ecosystem variability and early human habitats in eastern Africa: Proceedings of the National Academy of Sciences, v. 110, no. 4, p. 1167-1174.

Matsui, H., Nishi, H., Kuroyanagi, A., Hayashi, H., Ikehara, M., and Takashima, R., 2017, Vertical thermal gradient history in the eastern equatorial Pacific during the early to middle Miocene: Implications for the equatorial thermocline development: Paleoceanography, p. 729-743.

McQuarrie, N., and Wernicke, B.P., 2005, An animated tectonic reconstruction of southwestern North America since 36 Ma: Geosphere, v. 1, no. 3, p. 147-172.

Miller, D.M., Rosario, J.E., Leslie, S.R., and Vazquez, J.A., 2013, Paleogeographic insights based on new U-Pb dates for altered tuffs in the Miocene Barstow Formation, California, *in* Reynolds, R.E., ed., Raising Questions in the central Mojave Desert: The 2013 Desert Symposium Field Guide and Proceedings: Zzyzx, California, California State University Desert Studies Consortium, p. 31-38.

O'Connor, S.K., 1982, Palynology of Barstow Formation (Miocene), Rainbow Basin, southern California: AAPG Bulletin, v. 66, no. 10, p. 1696-1697.

Pagnac, D., 2009, Revised large mammal biostratigraphy and biochronology of the Barstow Formation (Middle Miocene), California: PaleoBios, v. 29, no. 2, p. 48-59.

Park, L.E., 1995, Geochemical and paleoenvironmental analysis of lacustrine arthropod-bearing concretions of the Barstow Formation, southern California: PALAIOS, v. 10, no. 1, p. 44-57.

Park, L.E., and Downing, K.F., 2001, Paleoecology of an exceptionally preserved arthropod fauna from lake deposits of the Miocene Barstow Formation, southern California, USA: PALAIOS, v. 16, no. 2, p. 175-184.

Passey, B.H., Cerling, T.E., Perkins, M.E., Voorhies, M.R., Harris, J.M., and Tucker, S.T., 2002, Environmental change in the Great Plains: An isotopic record from fossil horses: The Journal of Geology, v. 110, no. 2, p. 123-140.

Pavek, D.S., 1994, *Pinus cembroides*, Fire Effects Information System, U.S. Department of Agriculture, Forest Service, Rocky Mountain Research Station, Fire Sciences Laboratory: http://www.fs.fed.us/database/feis (accessed May 2017).

Pigati, J.S., Rech, J.A., Quade, J., and Bright, J., 2014, Desert wetlands in the geologic record: Earth-Science Reviews, v. 132, p. 67-81.

Piperno, D.R., 2006, Phytoliths: A Comprehensive Guide for Archaeologists and Paleoecologists: Lanham, Maryland, AltaMira Press, 238 p.

Poulsen, C.J., and Jeffery, M.L., 2011, Climate change imprinting on stable isotopic compositions of high-elevation meteoric water cloaks past surface elevations of major orogens: Geology, v. 39, no. 6, p. 595-598.

Renney, K.M., 1972, The Miocene Temblor Flora of west central California [M.S. thesis]: University of California, Davis, 110 p.

Retallack, G., 1984, Completeness of the rock and fossil record: Some estimates using fossil soils: Paleobiology, v. 10, no. 1, p. 59-78.

Retallack, G.J., 2001, Soils of the Past: An Introduction to Paleopedology: Oxford, Malden, Massachussetts, Blackwell Science, 404 p.

Reynolds, R.E., and Schweich, T.A., 2013, The Rainbow Loop Flora from the Mud Hills, Mojave Desert, California, *in* Reynolds, R.E., ed., Raising Questions in the central Mojave Desert: The 2013 Desert Symposium Field Guide and Proceedings: Zzyzx, California, California State University Desert Studies Consortium, p. 39-48.

Sachse, D., Radke, J., and Gleixner, G., 2006, δD values of individual *n*-alkanes from terrestrial plants along a climatic gradient—Implications for the sedimentary biomarker record: Organic Geochemistry, v. 37, no. 4, p. 469-483.

Sachse, D., Billault, I., Bowen, G.J., Chikaraishi, Y., Dawson, T.E., Feakins, S.J., Freeman, K.H., Magill, C.R., McInerney, F.A., van der Meer, M.T.J., Polissar, P., Robins, R.J., Sachs, J.P., Schmidt, H.-L., Sessions, A.L., White, J.W.C., West, J.B., and Kahmen, A., 2012, Molecular paleohydrology: Interpreting the hydrogen-isotopic composition of lipid biomarkers from photosynthesizing organisms: Annual Review of Earth and Planetary Sciences, v. 40, no. 1, p. 221-249.

Sage, R.F., 2004, The evolution of C_4 photosynthesis: New Phytologist, v. 161, p. 341-370.

Schoell, M., Schouten, S., Sinninghe Damste, J.S., de Leeuw, J.W., and Summons, R.E., 1994, A molecular organic carbon isotope record of Miocene climate changes: Science, v. 263, no. 5150, p. 1122-1125.

Schwab, V.F., Garcin, Y., Sachse, D., Todou, G., Séné, O., Onana, J.-M., Achoundong, G., and Gleixner, G., 2015, Effect of aridity on $\delta^{13}C$ and δD values of C_3 plant- and C_4 graminoid-derived leaf wax lipids from soils along an environmental gradient in Cameroon (Western Central Africa): Organic Geochemistry, v. 78, p. 99-109.

Schwartz, D., de Foresta, H., Mariotti, A., Balesdent, J., Massimba, J.P., and Girardin, C., 1996, Present dynamics of the savanna-forest boundary in the Congolese Mayombe: a pedological, botanical and isotopic (^{13}C and ^{14}C) study: Oecologia, v. 106, no. 4, p. 516-524.

Sheldon, N.D., Retallack, G.J., and Tanaka, S., 2002, Geochemical climofunctions from North American soils and application to paleosols across the Eocene-Oligocene boundary in Oregon: The Journal of Geology, v. 110, p. 687-696.

Sheppard, R.A., and Gude, A.J., III, 1969, Diagenesis of tuffs in the Barstow Formation, Mud Hills, San Bernardino County, California: United States Geological Survey Professional Paper 634, Washington, D.C., 35 p.

Singleton, J.S., and Gans, P.B., 2008, Structural and stratigraphic evolution of the Calico Mountains: Implications for early Miocene extension and Neogene transpression in the central Mojave Desert, California: Geosphere, v. 4, no. 3, p. 459-479.

Smiley, T.M., Hyland, E.G., Cotton, J.M., and Reynolds, R.E., 2018, Evidence of early C_4 grasses, habitat heterogeneity, and faunal response during the Miocene Climatic Optimum in the Mojave Region: Palaeogeography, Palaeoclimatology, Palaeoecology, v. 490, Supplement C, p. 415-430.

Smith, F.A., and Freeman, K.H., 2006, Influence of physiology and climate on δD of leaf wax *n*-alkanes from C_3 and C_4 grasses: Geochimica et Cosmochimica Acta, v. 70, no. 5, p. 1172-1187.

Soreng, R.J., Peterson, P.M., Romaschenko, K., Davidse, G., Zuloaga, F.O., Judziewicz, E.J., Filgueiras, T.S., Davis, J.I., and Morrone, O., 2015, A worldwide phylogenetic classification of the Poaceae (Gramineae): Journal of Systematics and Evolution, v. 53, no. 2, p. 117-137.

Spaulding, S.A., Lubinski, D.J., and Potapova, M., 2010, Diatoms of the United States: http://westerndiatoms.colorado.edu (accessed November 2017).

Srivastava, S.K., 1984, Palynology of the Monterey formation (Miocene) phosphatic facies at Lions Head, Santa Maria area, California: Palynology, v. 8, no. 1, p. 33-49.

Strömberg, C.A.E., 2003, The origin and spread of grass-dominated habitats in North America during the Tertiary and how it relates to the evolution of hypsodonty in equids [Ph.D. dissertation]: University of California, Berkeley.

Strömberg, C.A.E., 2005, Decoupled taxonomic radiation and ecological expansion of open-habitat grasses in the Cenozoic of North America: Proceedings of the National Academy of Sciences of the United States of America, v. 102, no. 34, p. 11980-11984.

Strömberg, C.A.E., Werdelin, L., Friis, E.M., and Saraç, G., 2007, The spread of grass-dominated habitats in Turkey and surrounding areas during the Cenozoic: Phytolith evidence: Palaeogeography, Palaeoclimatology, Palaeoecology, v. 250, no. 1–4, p. 18-49.

Strömberg, C.A.E., 2011, Evolution of grasses and grassland ecosystems: Annual Review of Earth and Planetary Sciences, v. 39, p. 517-544.

Strömberg, C.A.E., and McInerney, F.A., 2011, The Neogene transition from C_3 to C_4 grasslands in North America: Assemblage analysis of fossil phytoliths: Paleobiology, v. 37, no. 1, p. 50-71.

Tipple, B.J., Meyers, S.R., and Pagani, M., 2010, Carbon isotope ratio of Cenozoic CO_2: A comparative evaluation of available geochemical proxies: Paleoceanography, v. 25, no. PA3202, p. 1-11.

Vincent, E., and Berger, W.H., 1985, Carbon dioxide and polar cooling in the Miocene: The Monterey hypothesis, the carbon cycle and atmospheric CO_2: Natural Variations Archean to Present, American Geophysical Union, p. 455-468.

Vogts, A., Moossen, H., Rommerskirchen, F., and Rullkötter, J., 2009, Distribution patterns and stable carbon isotopic composition of alkanes and alkan-1-ols from plant waxes of African rain forest and savanna C_3 species: Organic Geochemistry, v. 40, no. 10, p. 1037-1054.

Wara, M.W., Ravelo, A.C., and Delaney, M., L., 2005, Permanent El Niño-like conditions during the Pliocene Warm Period: Science, v. 309, p. 758-761.

Wolfe, J.A., 1985, Distribution of Major Vegetational Types During the Tertiary, *in* Sundquist, E.T., and Broecker, W.S., eds., The Carbon Cycle and Atmospheric CO_2: Natural Variations Archean to Present, Volume 32: Washington, D.C., American Geophysical Union, p. 357-375.

Woodburne, M.O., Tedford, R.H., and Swisher, C.C., III, 1990, Lithostratigraphy, biostratigraphy, and geochronology of the Barstow Formation, Mojave Desert, southern California: GSA Bulletin, v. 102, p. 459-477.

Woodburne, M.O., 1996, Precision and resolution in mammalian chronostratigraphy: Principles, practices, examples: Journal of Vertebrate Paleontology, v. 16, no. 3, p. 531-555.

Woodruff, F., and Savin, S., 1991, Mid-Miocene isotope stratigraphy in the deep sea: High-resolution correlations, paleoclimatic cycles, and sediment preservation: Paleoceanography, v. 6, no. 6, p. 755-806.

Wynn, J.G., 2007, Carbon isotope fractionation during decomposition of organic matter in soils and paleosols: Implications for paleoecological interpretations of paleosols: Palaeogeography, Palaeoclimatology, Palaeoecology, v. 251, no. 3, p. 437-448.

You, Y., Huber, M., Müller, R.D., Poulsen, C.J., and Ribbe, J., 2009, Simulation of the Middle Miocene Climatic Optimum: Geophysical Research Letters, v. 36, no. L04702, p. 1-5.

Zachos, J.C., Pagani, M., Sloan, L.C., Thomas, E., and Billups, K., 2001, Trends, rhythms, and aberrations in global climate 65 Ma to present: Science, v. 292, p. 686-693.

Zhang, Y.G., Pagani, M., Liu, Z., Bohaty, S.M., and DeConto, R., 2013, A 40-million-year history of atmospheric CO_2: Philosophical Transactions: Mathematical, Physical and Engineering Sciences, v. 371, no. 2001, p. 1-20.

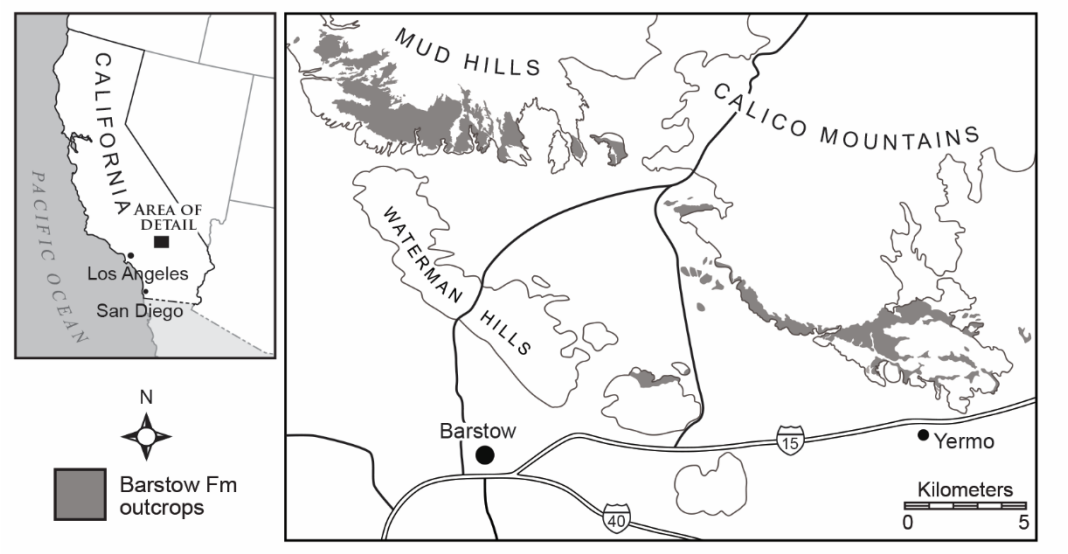

Figure 3.1. Location map of Barstow Formation outcrops in the Mud Hills and Calico Mountains, San Bernardino County, California.

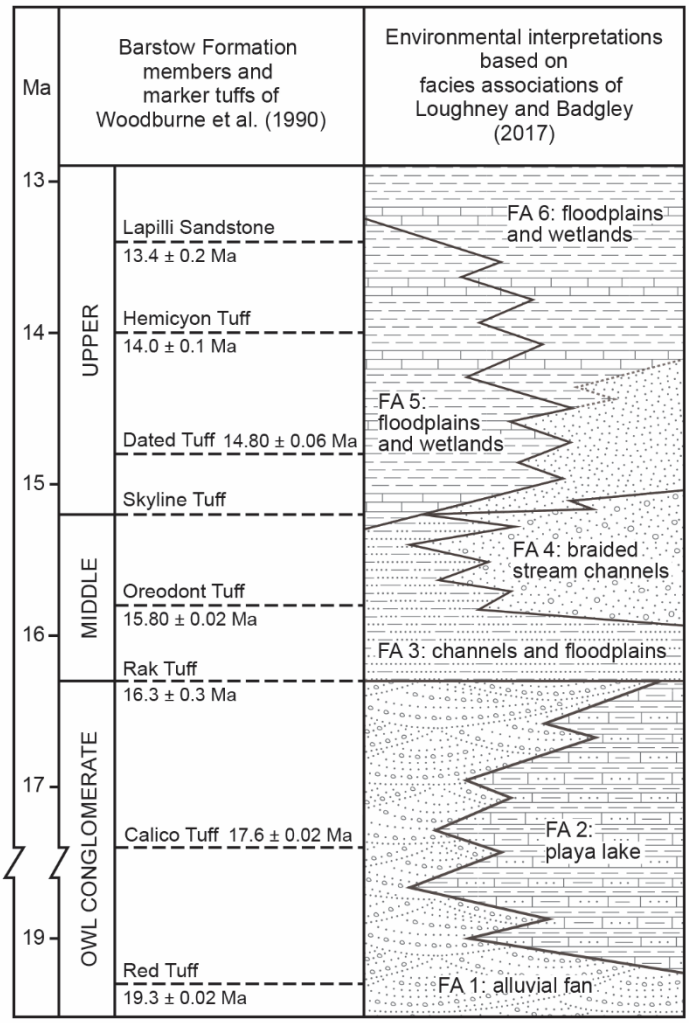

Figure 3.2. Age and dominant lithologies of the Barstow Formation with facies interpretations from Loughney and Badgley (2017). Modified from Loughney (2017).

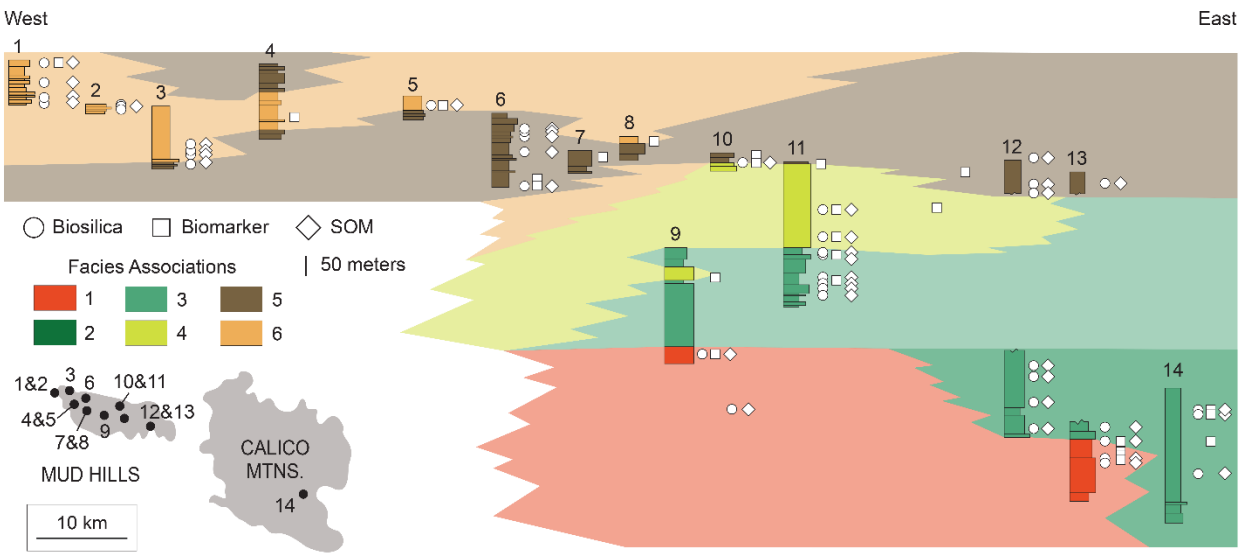

Figure 3.3. Stratigraphic and facies-association distribution of sediment samples for biomarker, soil organic matter, and biogenic silica analyses collected in the Mud Hills and Calico Mountains, San Bernardino County, California.

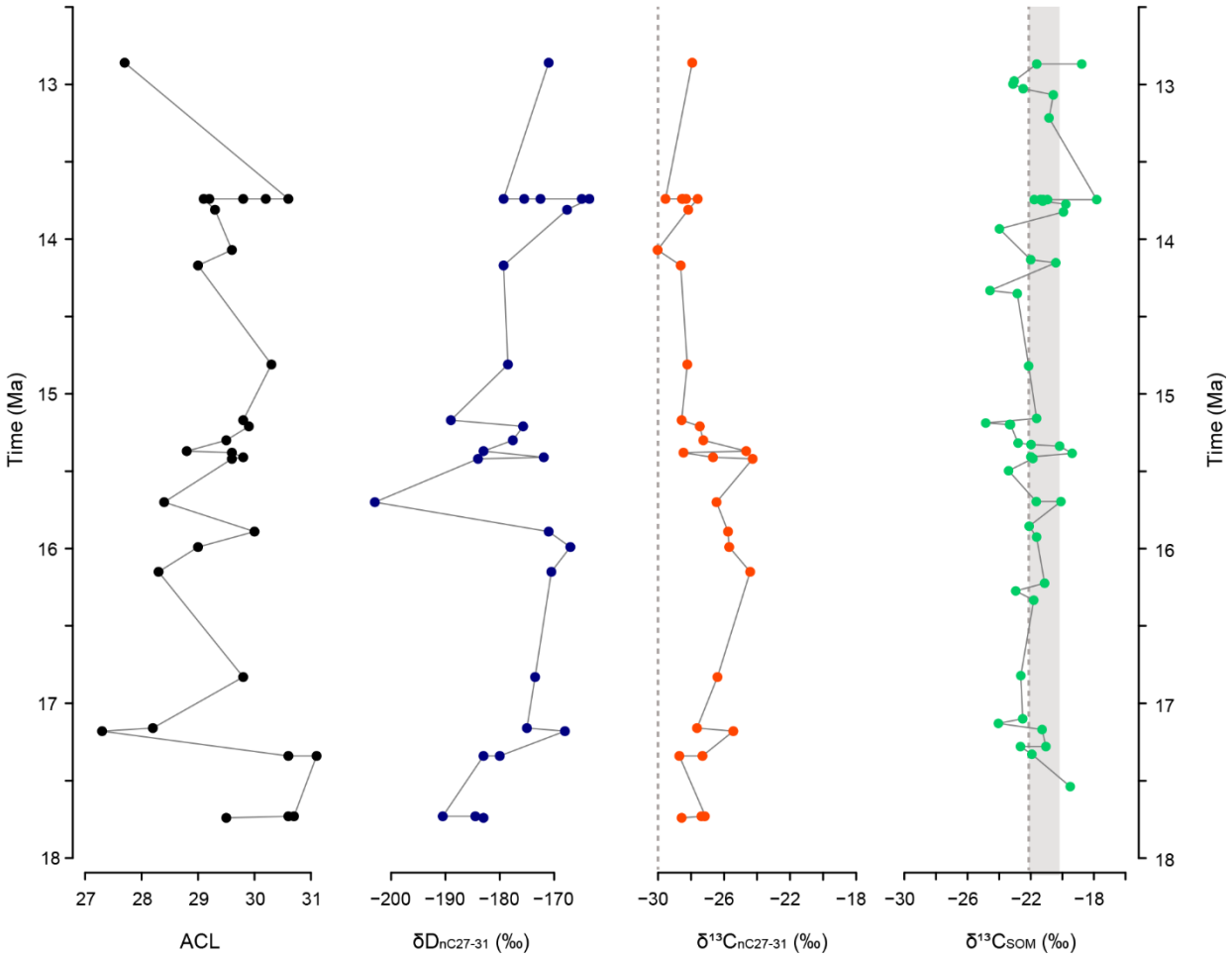

Figure 3.4. Results for average chain length (ACL), $\delta^{13}C_{alk}$ and δD for $C_{27\text{-}31}$, and $\delta^{13}C_{SOM}$. Dashed lines represent the $\delta^{13}C$ cutoff values for pure-C_3 vegetation (Kohn, 2010), adjusted for middle Miocene atmospheric CO_2. Gray shading represents range of 1-2‰ enrichment of soil organic matter derived from the pure-C_3 cutoff value possible during decomposition (Koch, 1998).

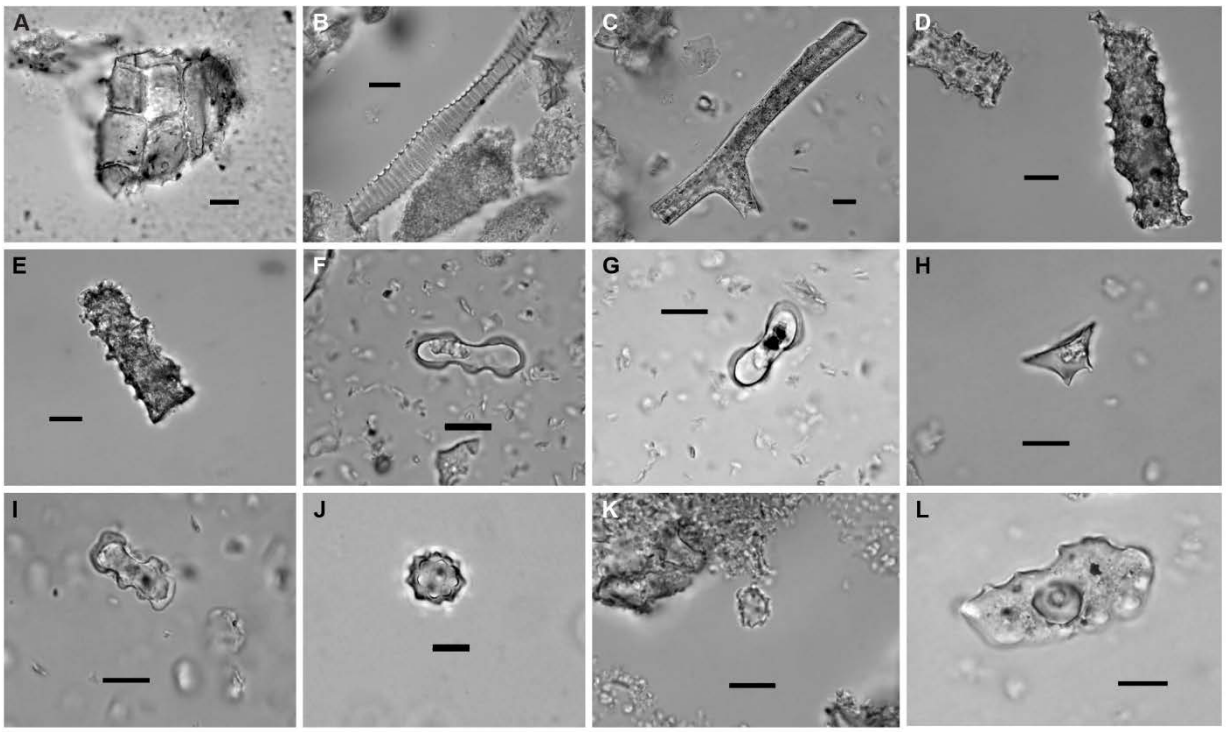

Figure 3.5. Diagnostic phytolith morphotypes identified in Barstow samples: Forest indicators (A-E), grass silica short cells (F-K), and sedges (L). (A) M-1, parenchyma cell aggregate, general FI; (B) Tra-1, helical tracheary element, general FI; (C) SclF-2, branching elongate body, non-grass plant; (D) Kn-10, *Pinus* irregular "wavy elongate," conifer; (E) Clm-2, echinate sphere, palm; (F) PO-1, polylobate, pooid; (G) BI-1, bilobate, pooid; (H) KR-1, keeled rondel, pooid; (I) CE-1, crenate, Pooideae; (J) CR4-8, cross variant, Bambusoideae; (K) CRI-2, irregular cross, Panicoideae; (L) Epi-6, epidermal plate, sedge. Scale bars = 10 μm.

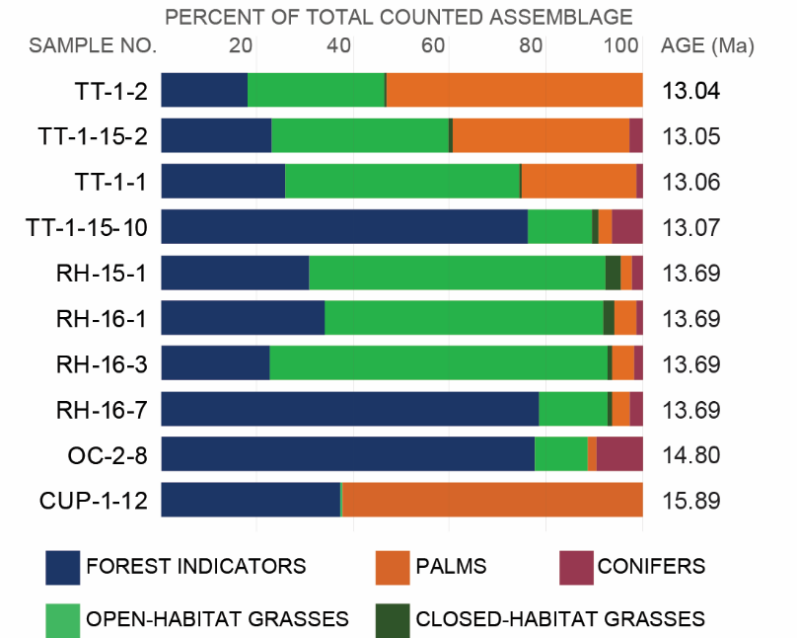

Figure 3.6. Bar charts showing percent abundance of important morphotypes in counted phytolith assemblages, by sample number and inferred age of assemblage.

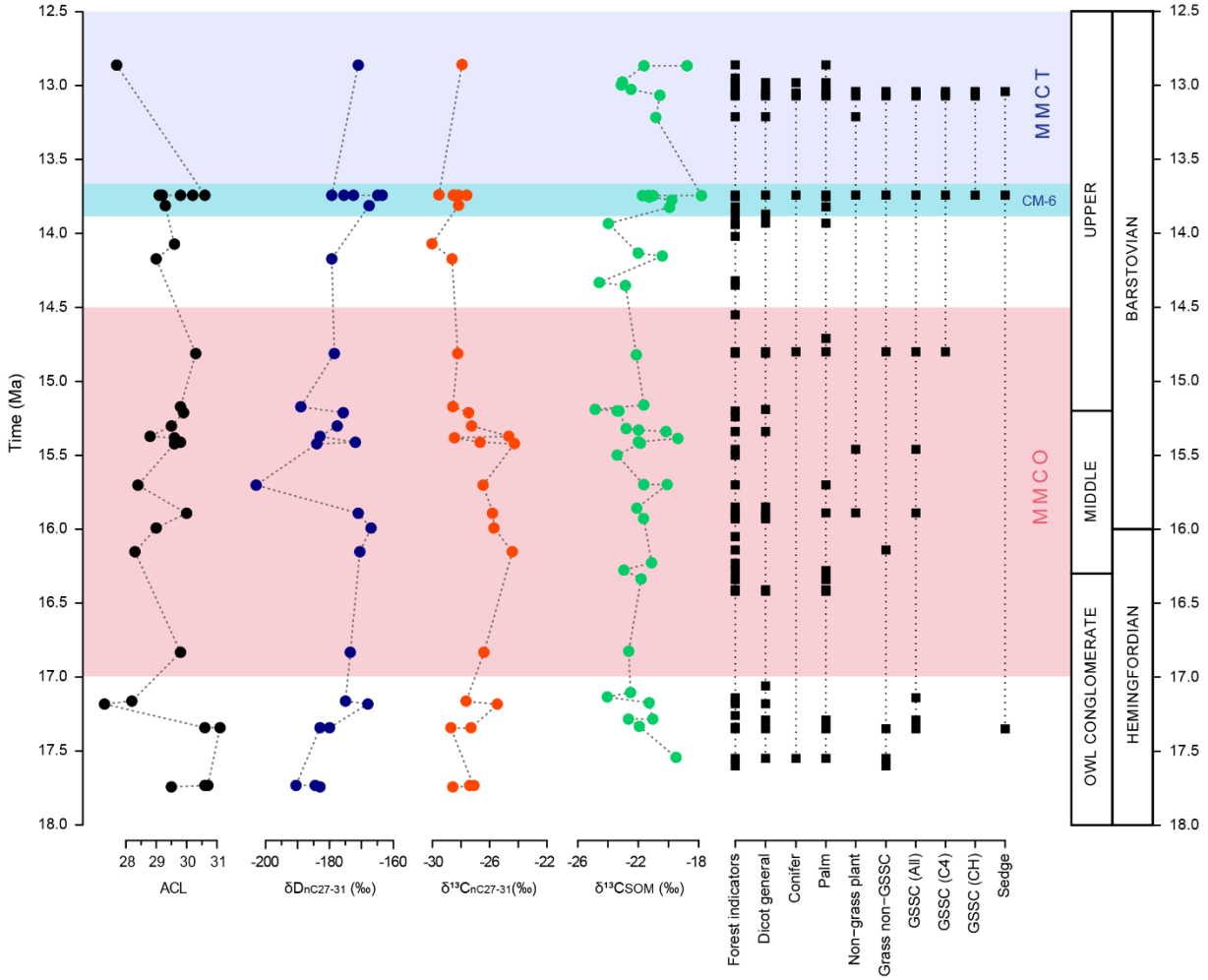

Figure 3.7. Isotopic results and observed ranges of environmentally significant phytolith morphotypes in the Barstow Formation during the Middle Miocene Climatic Optimum (MMCO), the CM-6 episode of the Monterey Excursion (Woodruff and Savin, 1991), and the middle Miocene climatic transition (MMCT).

Table 3.1. Results for biomarker $\delta^{13}C$ and average chain length (ACL), with estimated age of each sample. Means and standard deviation (σ) for odd chains C_{25} through C_{33} are given for each sample.

Sample	Age (Ma)	Mean sample $\delta^{13}C$ (‰)										ACL
		25	σ	27	σ	29	σ	31	σ	33	σ	
Margo Q	13.81	-28.5	-	-28.1	0.1	-28.8	0.1	-30.1	0.1	-29.2	0.2	29.3
Copemys Q	16.83	-26.8	1.1	-27.2	1.0	-26.9	0.9	-28.1	0.7	-27.5	0.7	29.8
COO-2-15-1	15.99	-25.4	1.1	-27.0	0.5	-26.5	0.9	-27.7	1.6	-29.2	1.1	29.0
CUP-1-15-2	15.89		-	-27.1	1.9	-27.3	1.1	-27.6	1.0	-27.8	-	28.9
CUP-1-15-3	16.15	-25.3	0.0	-25.9	0.2	-25.1	0.3	-25.9	0.5			28.3
CUP-3-1	15.70	-26.6	0.6	-27.7	1.3	-28.7	1.3	-28.7	0.5	-29.6	1.8	28.4
CUP-16-5-2	15.41	-29.8	-	-26.9	0.1	-27.4	0.1	-28.7	0.2	-27.9	0.0	29.8
Lake Bed	14.07			-28.9	0.1	-30.9	0.4	-31.6	0.0			29.6
Slugbed	14.17	-29.4	0.1	-29.2	0.2	-29.3	0.2	-30.4	0.2	-29.4	-	28.7
HG-3-1	15.42	-24.8	1.4	-25.7	0.9	-25.5	0.8	-26.5	0.6	-27.1	0.3	29.6
HG-3-3	15.37	-24.9	0.0	-25.5	0.2	-25.6	0.3	-26.6	0.6	-27.5	0.2	28.8
LB-1-15-2	17.34					-28.0	-	-28.4	-	-28.1	-	31.1
LB-1-15-3	17.18	-24.5	0.4	-24.9	0.6	-26.8	0.1	-29.1	1.6			27.3
LB-1-15-4	17.16	-28.1	-	-28.8	1.5	-28.6	0.2	-29.5	-			28.2
OC-1-15-4	17.34			-28.6	-	-30.4	-	-29.7	0.4	-30.8	-	30.6

Table 3.1. Results for mean biomarker $\delta^{13}C$ and average chain length (ACL), continued.

Sample	Age (Ma)	Mean sample $\delta^{13}C$ (‰)										ACL
		25	σ	27	σ	29	σ	31	σ	33	σ	
OC-1-15-5	17.73					-28.5	0.1	-28.0	0.0	-28.9	0.1	30.6
OC-1-15-6	17.73					-27.5	0.7	-28.2	0.6	-30.5	0.4	30.7
OC-1-15-7	17.74			-29.3	0.7	-29.4	0.6	-29.6	0.4	-29.9	-	29.5
Valley View	15.38			-29.4	0.1	-30.3	0.0	-29.2	0.0	-29.3	0.1	29.6
Saucer Butte	15.36	-28.0	0.3	-28.6	0.2	-28.1	0.1	-29.0	0	-28.2	0.1	29.5
RH-15-1	13.69	-30.0	-	-28.2	1.6	-29.0	0.2	-29.3	0.1	-30.9	1.0	30.2
RH-16-2	13.69			-28.9	0.4	-29.0	0	-29.4	0.3	-28.7	0.1	30.6
RH-16-4	13.69	-29.5	-	-28.6	0.3	-28.3	0.6	-28.2	0.5	-28.6	-	29.1
RH-16-6	13.69			-29.5	0.1	-29.9	0.2	-30.9	0.1	-28.7	0.1	29.8
RH-16-10	13.69	-29.1	-	-29.5	0.2	-28.9	0.1	-29.5	0.1	-28.5	-	29.2
SKY-1-1	14.81	-28.5	-	-28.6	0.2	-30.0	1.0	-29.3	0.0	-29.1	0.1	30.3
SKY-1-3	15.17	-30.3	-	-29.1	0.9	-29.4	0.5	-30.2	0.9	-30.5	0.4	29.8
SKY-16-2	15.21	-26.9	-	-28.5	-	-28.4	0.1	-29.0	0.3	-28.1	-	29.9
TT-2-15-1	12.86	-27.7	2.2	-27.6	0.8	-30.0	0.2	-29.9	0.4	-31.3	-	27.3

Table 3.2. Results of biomarker δD, with estimated age of each sample. Means and standard deviation (σ) for odd chains C_{25} through C_{33} are given for each sample.

Sample	Age (Ma)	Mean sample δD (‰)									
		25	σ	27	σ	29	σ	31	σ	33	σ
Margo Q	13.81	-163.5	9.2	-169.5	0.7	-169.0	1.4	-164.5	0.7		
Copemys Q	16.83	-182.5	2.9	-173.4	1.6	-171.9	1.1	-173.9	5.7	-160.4	2.7
COO-2-15-1	15.99	-185.8	2.3	-169.0	1.4	-168.4	2.4	-162.6	2.8	-161.0	0.7
CUP-1-15-2	15.89	-154.4	-	162.9	5.8	-172	4.2	-174.4	2.3		
CUP-1-15-3	16.15	-171.9	7.6	-169.3	2.5	-170.7	0.3	-172.7	2.7	-148.2	0.6
CUP-3-1	15.70	-207.6	0.3	-212.8	0.2	-197.8	3.3	-196.7	2.6	-190.3	1.3
CUP-16-5-2	15.41	-171.0	-	-175.0	-	-179.0	-	-132.0	-		
Lake Bed	14.07										
Slugbed	14.17	-178.0	-	-174.0	-	-180.0	-	-186.0	-		
HG-3-1	15.42	-194.1	0.1	-179.0	1.7	-182.8	1.3	-187.1	0.8	-164.7	3.5
HG-3-3	15.37	-189.2	0.3	-181.2	0.7	-178.6	5.2	-188.0	6.4	-172.2	2.5
LB-1-15-2	17.34					-177.1	0.3	-181.5	4.8	-158.5	0.8
LB-1-15-3	17.18	-151.6	5.7	-160.3	1.3	-171.7	1.4	-182.4	-	-161.3	-
LB-1-15-4	17.16	-183.9	4.0	-170.6	0.7	-172.5	0.1	-181.7	0.3	-154.9	0.2
OC-1-15-4	17.34			-175.2	-	-173.9	-	-187.1	-	-171.9	-

Table 3.2. Results of biomarker δD, continued.

Sample	Age (Ma)	Mean sample δD (‰)									
		25	σ	27	σ	29	σ	31	σ	33	σ
OC-1-15-5	17.73	-175.3	20.9	-180.7	0.4	-186.1	2.8	-193.1	0.4	-180.7	2.1
OC-1-15-6	17.73	-141.4	8.1	-172.2	3.7	-178.6	0.1	-187.1	0.1	-156.3	21.8
OC-1-15-7	17.74			-171.1	7.1	-176.9	1.9	-187.2	0.6	-166.1	1.3
Valley View	15.38										
Saucer Butte	15.36	-172.0	-	-163.0	-	-170.0	-	-193.0	-		
RH-15-1	13.69	-174.3	7.6	-163.2	1.6	-172.5	0.2	-179.5	0.3	-166.9	4.2
RH-16-2	13.69	-153.0	-	-167.0	-	-168.0	-	-150.0	-		
RH-16-4	13.69	-166.0	-	-170.0	-	-189.0	-	-172.0	-		
RH-16-6	13.69	-175.0	-	-160.0	-	-173.0	-	-176.0	-		
RH-16-10	13.69	-167.0	-	-170.0	-	-164.0	-	-135.0	-		
SKY-1-1	14.81	-172.4	4.9	-164.1	0.1	-169.4	3.1	-186.4	3.7	-166.4	1.5
SKY-1-3	15.17	-179.6	7.4	-186.4	0.9	-190.4	2.0	-188.7	0.5	-164.9	1.4
SKY-16-2	15.21	-161.0	-	-175.0	-	-182.0	-	-186.0	-		
TT-2-15-1	12.86	-120.2	29.9	-177.7	2.9	-143.9	11.3	-149.2	-		

Table 3.3. Totals for quantified phytolith assemblages, showing counts of palm, conifer (CONI), total forest indicator (FI), grass silica short cells (GSSC), open-habitat (OH), and closed-habitat (CH) morphotypes. FI total = sum of palm, conifer, and other diagnostic FI phytoliths.

Assemblage	Total	Palm total	CONI total	FI total	GSSC total	FI:GSSC	OH total	CH total	OH:CH	Member	Age (Ma)
TT-1-2	422	198	0	264	157	63:37	107	2	98:2	Upper	13.04
TT-1-15-2	586	152	11	258	328	44:56	150	5	97:3	Upper	13.05
TT-1-1	694	128	8	272	422	39:61	256	1	99.6:0.04	Upper	13.06
TT-1-15-10	329	8	19	244	85	74:26	37	4	90:10	Upper	13.07
RH-15-1	440	9	9	134	304	31:69	234	13	95:5	Upper	13.69
RH-16-1	502	18	7	167	334	33:67	240	10	96:4	Upper	13.69
RH-16-3	736	28	12	174	558	24:76	422	4	99:1	Upper	13.69
RH-16-7	394	12	11	303	90	78:22	51	4	93:7	Upper	13.69
OC-2-8	271	5	25	229	42	85:15	28	0	100:0	Upper	14.80
CUP-1-12	294	184	0	293	1	99.7:0.3	1	0	100:0	Middle	15.89

Table 3.4. Diatoms identified in phytolith samples from the Barstow Formation by member, inferred age, and facies association (FA), with environmental interpretations of sample locality based on diatom assemblage.

Sample number	Age (Ma)	Member	FA	Taxa	Environmental interpretation
LB-1-9	17.55	Calico	2	*Epithemia adnata*, *Hantzschia amphioxys*, *Luticola mutica*	Alkaline, saline to freshwater ephemeral lake
COO-1-15-2	16.83	Owl Conglomerate	1	?*Frustulia* sp.	Acidic to alkaline, freshwater stream
CUP-1-1	16.41	Middle	3	*Sellaphora bacilloides*	Alkaline, freshwater pond or slow-moving stream
CUP-1-12	15.89	Middle	3	*Nitzschia* sp. or *Hantzschia* sp.	Alkaline to neutral, brackish to freshwater pond, stream, or ephemeral aquatic habitats and soil
RH-15-1	13.69	Upper	6	*Hantzschia amphioxys*, *Fragilaria nevadensis*	Alkaline, freshwater ephemeral aquatic habitats and soil
RH-16-1	13.69	Upper	6	*Pinnularia brebissonii* species complex	Alkaline to neutral, freshwater pond
RH-16-3	13.69	Upper	6	*Anomoeneis* sp., *Eunotia* cf. *arcuoides*, *Nitzschia recta*, *Pinnularia brebissonii* species complex	Neutral, freshwater pond, possiby ephemeral
RH-16-7	13.69	Upper	6	*Aulacoseira granulata*, *Fragilaria nevadensis*, *Navicula* sp.	Alkaline, neutral to freshwater pond or spring
TT-1-1	13.06	Upper	6	*Hantzschia amphioxys*, *Caloneis bacillum*, *Cymbopleura* sp., *Eucocconeis laevis*	Alkaline to neutral, freshwater pond or spring
TT-1-2	13.04	Upper	6	*Nitzschia* sp. (large form)	Alkaline to neutral pond
TT-2-3	12.97	Upper	6	*Fragilaria nevadensis*	Alkaline, freshwater pond, spring, or stream

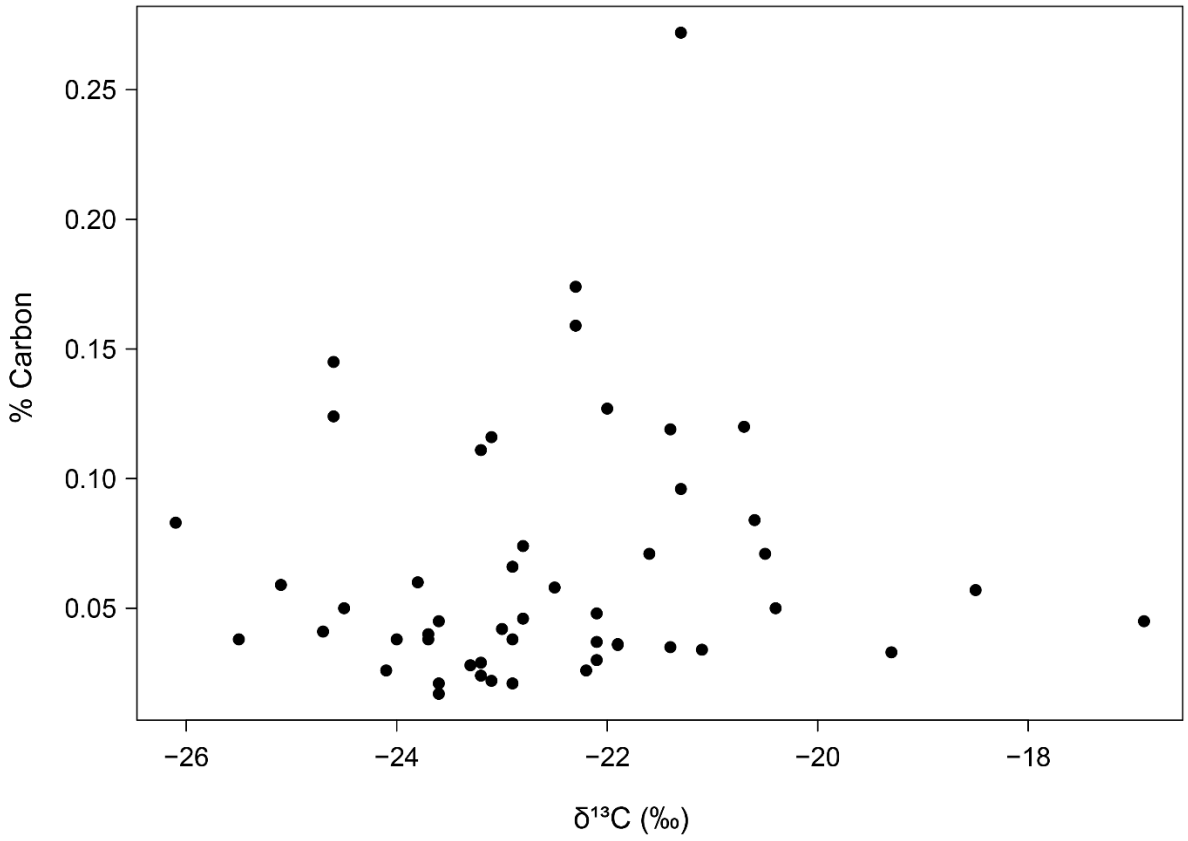

Figure S3.1. Plot of weight-percent carbon against $\delta^{13}C$ of soil organic matter for 49 samples from the Barstow Formation. Weight-percent carbon and raw $\delta^{13}C_{SOM}$ values are listed in Table S3.4.

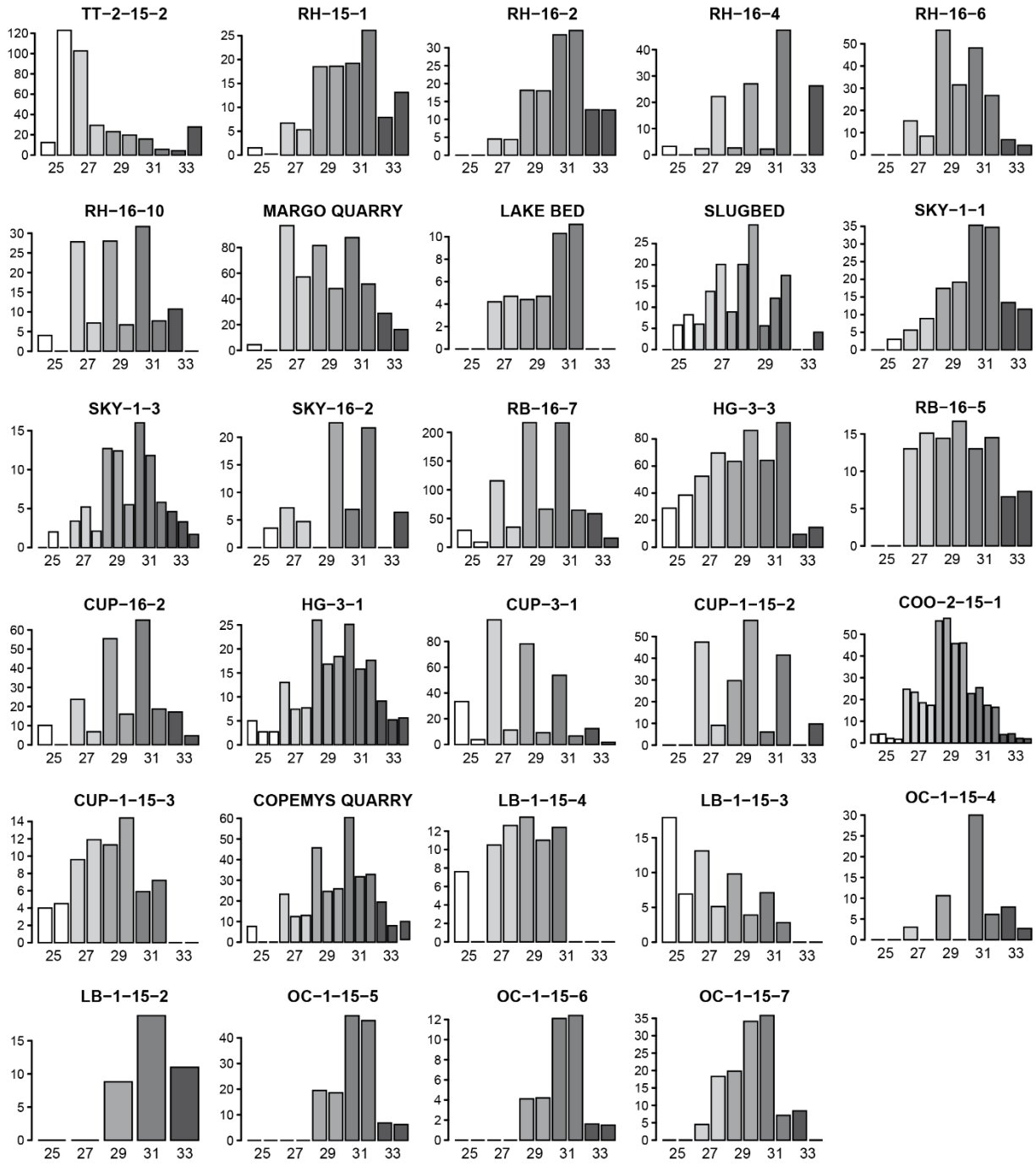

Figure S3.2. Carbon-chain length abundances for C_{25} through C_{33} of 29 *n*-alkane samples.

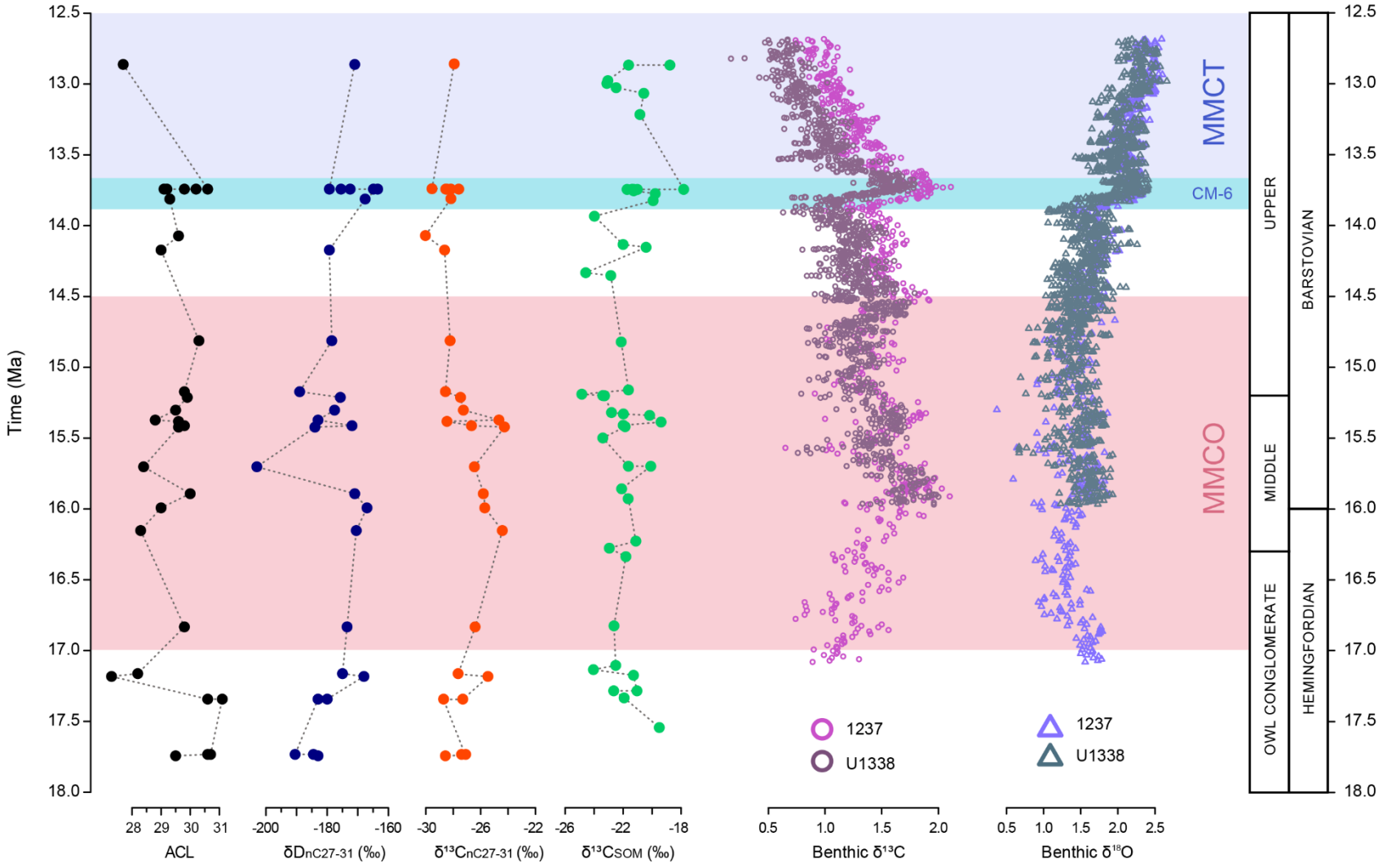

Figure S3.3. Isotopic results from the Barstow Formation and Pacific Ocean during the middle Miocene. Results for average chain length (ACL), $\delta^{13}C_{alk}$ and δD for $C_{27\text{-}31}$, and $\delta^{13}C_{SOM}$ from the Barstow Formation compared to $\delta^{13}C$ and $\delta^{18}O$ from Pacific Ocean benthic foraminifera from Holbourn et al. (2007) and Holbourn et al. (2013).

Table S3.1. Results of phytolith samples from the Barstow Formation. Counted assemblages noted with asterisks, and total number of morphotypes is given for the assemblage. Terminology follows Stromberg (2003). AQ = aquatic plant morphotypes; CONI = conifer; FI = forest indicator; GSSC = grass silica short cell; CH = closed habitat; POOID-D = Pooid, diagnostic; POOID-ND = Pooid, nondiagnostic; PACMAD = Panicoideae, Arundinoideae, Chloridoideae, Micrairoideae, Aristoideae, Danthonioideae; OTHG = other grass GSSC; Grass-D = grass, diagnostic; ND + OTH = non-diagnostic and other morphotypes; UNKN = unknown morphotypes; p = present; vab = very abundant. After Stromberg (2005).

Sample	Age	Non-GSSC				GSSC						ND + OTH (%)	UNKN	Total
		AQ (%)	Palm (%)	CONI (%)	Other FI (%)	CH (%)	POOID-D	POOID-ND	PACMAD	OTHG	Grass-D			
TT-2-7	12.86		p		p									
TT-2-6	12.86		p				p							
TT-2-4	12.95				p									
TT-2-1	12.98		p	p	p							p		
TT-2-2	12.99				p									
TT-1-2*	13.04	0.19	36.94	0	11.75	0.37	11.57	2.24	5.97	6.72	0.75	15.11	8.4	536
TT-1-15-2*	13.05	0	17.21	1.25	10.76	0.57	7.13	1.93	7.93	19.59	0	20.72	12.91	883
TT-1-1*	13.06	0	13.78	0.86	14.64	0.11	12.16	6.78	8.61	17.76	0.65	25.3	11.09	929
TT-1-15-10*	13.07	0	1.27	3.01	34.34	0.63	3.16	0.316	2.37	6.96	0.16	32.44	15.35	632
TT-1-15-9	13.21				p							p		
RH-15-1*	13.69	0.34	1.54	1.54	19.86	2.23	19.35	3.25	17.47	9.76	0.86	19.18	4.62	584
RH-16-1*	13.69	0.15	2.71	1.05	21.35	1.5	18.2	5.26	11.43	12.63	0.75	16.54	8.42	665
RH-16-3*	13.69	0.41	2.86	1.22	13.67	0.41	22.65	5.61	14.8	13.47	1.02	15.71	8.16	890
RH-16-5	13.69				p									
RH-16-7*	13.69	0.14	1.67	1.53	42.2	0.56	4.32	0.97	1.81	4.74	8.08	26.18	7.8	718
RH-16-9	13.69		p	p	p							p		
OC-2-9	13.75		p		p									
HG-1-4	13.82		p		p									
OC-1-7	13.87				p									
HG-16-7	13.94		p		p									
HG-1-3	13.94				p									
FW-3-10	14.02				p?									
FW-3-7	14.32				p?									
HG-1-1	14.35				p?									
OC-1-6	14.55				p									
FE-16-10	14.71		p											
OC-2-8*	14.8	0	1.21	6.05	48.18	0	2.42	3.87	0.48	3.39	1.21	15.01	18.16	413
FE-16-1	14.81				p									
FW-3-2	15.19				p									

OC-2-7	15.2				p									
FW-3-1	15.24				p									
OC-2-6	15.34				vab									
OC-2-4	15.46				p		p					p		
OC-2-3	15.5				p									
CUP-3-2	15.7		p		p									
OC-2-1	15.7		p		p									
CUP-1-14	15.85				p									
CUP-1-13	15.86													
CUP-1-12*	15.89	0	45.65	0	14.89	0	0.25	0	0	0	0	2.48	36.72	403
CUP-1-11	15.91				p									
CUP-1-9	15.93											p		
CUP-1-8	15.94											p		
Steepside	15.99											p		
CUP-1-7	16.05				p?							p		
CUP-1-6	16.14				p						p			
CUP-1-5	16.23				p?									
CUP-1-4-2	16.28		p		p									
CUP-1-4-1	16.34		p		p							p		
CUP-1-1	16.41		p		p									
CUP-1-21B	16.42		p		p							p		
OC-1-5	17.06				p									
OC-1-4	17.14				p		p					p		
LB-1-6	17.16				p									
LB-1-5	17.18				p									
LB-1-2	17.26				p							p		
OC-1-3	17.29		p		p		p					p		
OC-1-2	17.34				p									
LB-1-1	17.35	p	p		p		p			p	p	p		
LB-1-9	17.55		p	p	p						p			
LB-1-8	17.6				p						p			

Table S3.2. Ecological tolerances and affinities of diatom taxa identified and phytolith samples from the Barstow Formation. Compiled from Lohman (1957), Lowe (1974), and Spaulding et al. (2010).

Taxon	Habit tolerances	Ecology	Preferred environment
Anomoeoneis sp.	pH: 7 to >8.5 Brackish to freshwater (no salt) Eutrophic to oligotrophic	Epipelic, periphytic Rheophilic to indifferent	
Aulacoseira granulata	pH: 7 to 8.5 Freshwater (some salt) Eutrophic	Planktonic	Ponds and lakes
Caloneis bacillum	pH: 7 to 8.5 Brackish to freshwater (some salt)	Benthic, periphytic	Streams and springs
Cymbopleura cf. *heinii*	Freshwater	Benthic, epipelic	Ponds and lakes
Epithemia adnata	pH: 7 to >8.5 Freshwater (some salt)	Epiphytic, periphytic, Rheophilic to limnophilic	Streams, ponds, and lakes
Eucocconeis laevis	pH: ~7 Freshwater Oligotrophic	Benthic, epipelic	Ponds and lakes
Eunotia cf. *arcuoides*	pH: 5.5 to ~7 Freshwater (no salt to some salt) Eutrophic to oligotrophic	Periphytic, limnobiontic to aerophilic	Lakes, ponds, and soil
Fragilaria nevadensis	pH: 7 to 8.5 Freshwater (no salt to some salt) Eutrophic to mesotrophic	Periphytic, epilithic, planktonic, Limnobiontic to indifferent	Streams, lakes, ponds, and springs
?Frustulia	Freshwater (no salt to some salt)	Benthic, periphytic	Streams, lakes, and bogs
Hantzschia amphioxys	pH: 7 to 8.5 Freshwater (some salt)	Periphytic, aerophilic	Ephemeral pools, moist soil
Hippodonta cf. *coxiae*	Freshwater (some salt)	Benthic	Ponds and lakes
Luticola mutica	pH: 6.5 to 8.5 Freshwater (no salt to some salt) Eutrophic to mesotrophic	Periphytic, aerophilic	Streams, springs, and moist soil
Navicula sp.	pH: <5.5 to 8.5 Freshwater (some salt)	Periphytic, rheophilic to aerophilic	Streams, springs, ponds, and lakes
Nitzschia recta	pH: >7 Freshwater (some salt)	Epipelic	
Nitzschia, large form	pH: 7 to >8.5 Freshwater (some salt)	Periphytic, rheophilic, crenophilic, or limnophilic	Streams, springs, ponds, and lakes
Nitzschia or *Hantzschia*	pH: >7 Freshwater (some salt)		Streams, ponds, lakes, or soil
Pinnularia borealis	pH: ~7 Freshwater (some salt) Eutrophic	Periphytic, aerophilic	Streams, ponds, lakes, and soil
Pinnularia brebissonii	pH: <7 to >7 Freshwater	Benthic	Ponds, lakes, and marshes
Sellaphora bacilloides	pH: ~7 Freshwater	Benthic	Ponds, lakes, and low-gradient streams

Table S3.3. Age model of phytolith, biomarker, and soil organic matter (SOM) samples collected from the Barstow Formation. Sediment-accumulation rates are from Loughney and Badgley (2017). Asterisks denote dated units that serve as tie points for age estimates.

Sample number	Locality Name	Composite stratigraphic level (m)	Sample type	Rate m/Myr	Age preferred (Ma)	Age estimate (Ma)	Age reference
TT-2-6	Truck Top Quarry	1129.9	phytolith	154.1	12.86	12.864	
TT-2-7	Truck Top Quarry	1129.9	phytolith	154.1	12.86	12.864	
TT-2-15-1	Truck Top Wash 2	1129.9	biomarker	154.1	12.86	12.864	
TT-2-5	Truck Top Wash	1069.9	phytolith	148.66	12.94	12.541	
TT-2-4	Truck Top Wash	1063.4	phytolith	148.66	12.95	12.876	
TT-2-3	Truck Top Wash	1049.2	phytolith	148.66	12.97	12.850	
TT-2-1	Truck Top Wash	1020.9	phytolith	148.66	12.98	12.910	
TT-2-2	Truck Top Wash	1002.9	phytolith	148.66	12.99	12.992	
TT-1-15-11	Truck Top Wash 1	999.4	phytolith	148.66	13.02	13.015	
TT-1-15-8	Truck Top Wash	998.9	phytolith	148.66	13.02	13.019	
TT-1-2	Truck Top Wash	995.4	phytolith	148.66	13.04	13.042	
TT-1-15-1	Truck Top Wash 1	994.5	biomarker	148.66	13.05	13.048	
TT-1-15-2	Truck Top Wash 1	994.5	phytolith	148.66	13.05	13.048	
TT-1-15-3	Truck Top Wash 1	994.5	phytolith	148.66	13.05	13.048	
TT-1-15-4	Truck Top Wash 1	994.5	phytolith	148.66	13.05	13.048	
TT-1-15-5	Truck Top Wash	994.5	phytolith	148.66	13.05	13.048	
TT-1-15-6	Truck Top Wash	994.5	phytolith	148.66	13.05	13.048	
TT-1-15-7	Truck Top Wash	994.5	phytolith	148.66	13.05	13.048	
TT-1-1	Truck Top Wash	993.4	phytolith	148.66	13.06	13.055	
TT-1-15-10	Truck Top Wash 1	990.7	phytolith	148.66	13.07	13.074	
TT-1-15-9	Truck Top Wash 1	981.7	phytolith	148.66	13.21	13.211	
FW-3B-2	Falkenbach Wash	953.5	phytolith	148.66	13.26	13.327	
FW-3B-1	Falkenbach Wash	948.0	phytolith	148.66	13.3	13.299	

*Lapilli Sandstone	Hell Gate Basin	933.0			*13.4	*13.4	MacFadden et al. (1990)
HG-1-7	Hell Gate Basin	900.0	phytolith	111.24	13.696	13.697	
RH-16-1	Rodent Hill	898.0	phytolith	148.66	13.697	13.679	
RH-16-10	Rodent Hill	898.0	biomarker	148.66	13.697	13.679	
RH-16-2	Rodent Hill	898.0	biomarker	148.66	13.697	13.679	
RH-16-3	Rodent Hill	898.0	phytolith	148.66	13.697	13.679	
RH-16-4	Rodent Hill	898.0	biomarker	148.66	13.697	13.679	
RH-16-5	Rodent Hill	898.0	phytolith	148.66	13.697	13.679	
RH-16-6	Rodent Hill	898.0	biomarker	148.66	13.697	13.679	
RH-16-7	Rodent Hill	898.0	phytolith	148.66	13.697	13.679	
RH-16-8	Rodent Hill	898.0	biomarker	148.66	13.697	13.679	
RH-16-9	Rodent Hill	898.0	phytolith	148.66	13.697	13.679	
RH-15-1	Rodent Hill	898.0	phytolith	148.66	13.697	13.679	
RH-15-1	Rodent Hill	898.0	biomarker	148.66	13.697	13.679	
OC-2-9	Owl Canyon	895.5	phytolith	119.85	13.72	13.717	
HG-1-6	Hell Gate Basin	881.0	phytolith	119.85	13.77	13.766	
CARN-16-4	Margo Quarry	875.0	biomarker	119.85	13.81	13.816	
HG-1-4	Hell Gate Basin	873.0	phytolith	109.51	13.82	13.817	
OC-1-7	Owl Canyon	867.5	phytolith	85.08	13.87	13.866	
HG-16-7	Sunnyside	860.0	phytolith	111.24	13.94	13.937	
HG-16-8	Sunnyside Quarry	860.0	fossils	111.24	13.94	13.937	
HG-1-3	Hell Gate Basin	860.0	phytolith	111.24	13.94	13.937	
*Hemicyon Tuff		853.0			*14	*14	MacFadden et al. (1990)
Hemicyon Tuff	Hell Gate Basin	853.0			14	14.000	
FW-3-11	Falkenbach Wash	851.5	phytolith	148.66	14.01	14.010	
FW-3-10	Falkenbach Wash	850.5	phytolith	148.66	14.02	14.017	
FW-1-15-2	Falkenbach Wash Quarry 1	850.0	biomarker	119.85	14.03	14.025	
FW-3-15-4	Falkenbach Wash 3	846.0	biomarker	119.85	14.06	14.058	
FE-16-7	Lake Bed	843.9	biomarker	148.66	14.07	14.067	
HG-1-2	Hell Gate Basin	839.0	phytolith	111.24	14.12	14.126	
FW-3-9	Falkenbach Wash	839.0	phytolith	111.24	14.12	14.126	
FW-3-8	Falkenbach Wash	834.0	som	148.66	14.13	14.128	
FE-16-9	Slugbed	828.3	biomarker	148.66	14.17	14.166	
FW-3-5	Falkenbach Wash	809.5	phytolith	148.66	14.3	14.293	

FW-3-7	Falkenbach Wash	811.8	phytolith	128.53	14.32	14.321	
FW-3-6	Falkenbach Wash	810.0	phytolith	128.53	14.33	14.335	
HG-1-1	Hell Gate Basin	818.0	phytolith	100.97	14.35	14.347	
OC-1-6	Owl Canyon	825.5	phytolith	85.08	14.55	14.548	
FE-16-10	Fuller's Earth Canyon	813.0	phytolith	148.66	14.71	14.706	
FW-3-4	Falkenbach Wash	800.5	phytolith	148.66	14.79	14.790	
*Dated Tuff		799.0			*14.8	*14.8	MacFadden et al. (1990)
OC-2-8	Owl Canyon	799.0	phytolith	85.08	14.8	14.800	
SKY-1-1	Skyline 1	798.1	biomarker	85.08	14.81	14.809	
SKY-1-2	Skyline 1	798.1	phytolith	85.08	14.81	14.809	
FE-16-1	V98004	798	phytolith	148.66	14.813	14.807	
FE-16-5	V98004	798.0	phytolith	148.66	14.813	14.807	
FW-2-3	Falkenbach Wash	776.5	phytolith	119.85	15.15	15.146	
SKY-1-5	Skyline 1	775.9	biomarker	119.85	15.15	15.146	
SKY-1-4	Skyline 1	774.4	phytolith	119.85	15.16	15.163	
SKY-1-3	Skyline 1	773.9	biomarker	119.85	15.17	15.167	
FW-3-3	Falkenbach Wash	773.5	phytolith	119.85	15.17	15.171	
FW-3-2	Falkenbach Wash	771.5	phytolith	119.85	15.19	15.187	
*Skyline Tuff		770.0			*15.2	*15.2	D.M. Miller, written commun., April, 2016
OC-2-7	Owl Canyon	770.0	phytolith	72.5	15.2	15.200	
FW-1-1	Falkenbach Wash	769.8	phytolith	119.85	15.2	15.202	
FW-2-2	Falkenbach Wash	769.7	phytolith	119.85	15.2	15.203	
SKY-16-2	Skyline Quarry	768.0	biomarker	327.57	15.21	15.206	
FW-3-1	Falkenbach Wash	764.8	phytolith	119.85	15.24	15.243	
RB-16-7	Saucer Butte	740.0	biomarker	204.13	15.3	15.347	
FW-2-15-3	Falkenbach Wash 2	755.5	phytolith	119.85	15.32	15.321	
FW-2-15-4	Falkenbach Wash 2	755.5	biomarker	119.85	15.32	15.321	
FW-2-15-2	Falkenbach Wash 2	755.0	phytolith	119.85	15.32	15.325	
FW-2-15-1	Falkenbach Wash 2	751.5	phytolith	119.85	15.33	15.354	
OC-2-6	Owl Canyon	731.0	phytolith	286.19	15.34	15.336	

HG-3-4	Hell Gate Basin	715.7	phytolith	100.97	15.37	15.360	
HG-3-3	Hell Gate Basin	715.3	biomarker	100.97	15.37	15.364	
RB-16-5-1	Valley View Quarry	710.0	biomarker	327.57	15.38	15.383	
RB-16-5-2	Valley View Quarry	710.0	SOM	327.57	15.38	15.383	
OC-2-5	Owl Canyon	694.0	phytolith	327.57	15.387	15.432	
CUP-16-5-1	V94179	700	SOM	327.57	15.41	15.414	
CUP-16-5-2	V94179	700.0	biomarker	327.57	15.41	15.414	
HG-3-1	Hell Gate Basin	696.1	biomarker	111.24	15.42	15.419	
HG-3-2	Hell Gate Basin	696.1	phytolith	111.24	15.42	15.419	
OC-2-4	Owl Canyon	637.0	phytolith	580.83	15.46	15.429	
OC-2-3	Owl Canyon	610.5	phytolith	580.83	15.5	15.473	
OC-2-1	Owl Canyon	524.0	phytolith	580.83	15.7	15.622	
CUP-3-1	Camp Quarry	523.5	biomarker	286.19	15.7	15.704	
CUP-3-2	Camp Quarry	523.5	phytolith	286.19	15.7	15.704	
CUP-1-14	Cal-Uranium Prospect Canyon	482.0	phytolith	286.19	15.85	15.849	
CUP-1-13	Cal-Uranium Prospect Canyon	480.2	phytolith	286.19	15.86	15.855	
CUP-1-12	Cal-Uranium Prospect Canyon	469.0	phytolith	286.19	15.89	15.894	
CUP-1-15-2	Cal Uranium Prospect Canyon 1	469.0	biomarker	286.19	15.89	15.894	
CUP-1-11	Cal-Uranium Prospect Canyon	468.0	phytolith	286.19	15.91	15.898	
CUP-1-9	Cal-Uranium Prospect Canyon	459.0	phytolith	286.19	15.93	15.929	
CUP-1-8	Cal-Uranium	457.0	phytolith	286.19	15.936	15.936	

	Prospect Canyon						
Steepside Q	Steepside Q	456.0	phytolith	204.13	15.99	15.996	
Steepside Q	Steepside Q	456.0	biomarker	204.13	15.99	15.996	
CUP-1-7	Cal-Uranium Prospect Canyon	425.5	phytolith	286.19	16.05	16.046	
RV6402	Barstow Site 21	402.34	locality	286.19	16.13	16.128	
CUP-1-6	Cal-Uranium Prospect Canyon	399.0	phytolith	286.19	16.14	16.139	
CUP-1-15-3	Cal Uranium Prospect Canyon 1	394.5	biomarker	286.19	16.15	16.155	
CUP-1-18		390.5	som	286.19	16.17	16.169	
CUP-1-5	Cal-Uranium Prospect Canyon	373.0	phytolith	286.19	16.23	16.230	
CUP-1-5 alt	Cal-Uranium Prospect Canyon	373.0	phytolith	286.19	16.23	16.230	
CUP-1-4-2	Cal-Uranium Prospect Canyon	360.0	phytolith	286.19	16.28	16.275	
*Rak Tuff		198.0		286.19	16.3	17.199	
CUP-1-4-1	Cal-Uranium Prospect Canyon	340.5	phytolith	286.19	16.34	16.343	
CUP-1-1	Cal-Uranium Prospect Canyon	320.5	phytolith	286.19	16.41	16.413	
CUP-1-15-1	Cal Uranium Prospect Canyon 1	316.0	biomarker	286.19	16.42	16.429	
CUP-1-21B	Rainbow Flora locality	316.0	phytolith	286.19	16.42	16.429	
Copemys Q	Copemys Quarry	266.5	phytolith	309.22	16.83	16.828	
Copemys Q	Copemys Quarry	266.5	biomarker	309.22	16.83	16.828	
*Dacite breccia		-175.0			*17	*17	Singleton and Gans (2008)
LB-1-7	Little Borate	-174.0	phytolith	534.69	17.02	17.002	

LB-1-11	Little Borate	-170.5	phytolith	534.69	17.02	17.005	
LB-1-10	Little Borate	-192.0	phytolith	534.69	17.05	17.032	
OC-1-5	Owl Canyon	146.0	phytolith	306.24	17.06	17.058	
RDQ-2	Red Division Quarry	180.0	biomarker	309.22	17.11	17.108	
RDQ-1	Red Division Quarry	168.0	phytolith	309.22	17.11	17.147	
OC-1-4	Owl Canyon	120.5	phytolith	306.24	17.14	17.143	
LB-1-15-4	Little Borate	-252.0	biomarker	534.69	17.16	17.160	
LB-1-6	Little Borate	-252.0	phytolith	534.69	17.16	17.160	
RDQ-3	Red Division Quarry	163.0	phytolith	309.22	17.16	17.163	
RDQ-4	Red Division Quarry	163.0	biomarker	309.22	17.16	17.163	
LB-1-15-3	Little Borate	-262.0	biomarker	534.69	17.18	17.178	
LB-1-5	Little Borate	-262.0	phytolith	534.69	17.18	17.178	
LB-1-4	Little Borate	-282.5	phytolith	534.69	17.22	17.217	
LB-1-3	Little Borate	-295.5	phytolith	534.69	17.24	17.225	
LB-1-2	Little Borate	-306.5	phytolith	534.69	17.26	17.261	
OC-1-15-1	Owl Canyon 1	69.0	phytolith	309.22	17.29	17.291	
OC-1-15-2	Owl Canyon 1	69.0	phytolith	309.22	17.29	17.291	
OC-1-15-3	Owl Canyon 1	68.0	biomarker	309.22	17.29	17.294	
OC-1-3	Owl Canyon	69.0	phytolith	309.22	17.29	17.291	
OC-1-15-4	Owl Canyon 1	54.0	biomarker	309.22	17.34	17.339	
OC-1-2	Owl Canyon	54.0	phytolith	309.22	17.34	17.341	
OC-1-1 B	Owl Canyon	53.5	phytolith	309.22	17.34	17.341	
LB-1-15-2	Little Borate	-352.0	biomarker	534.69	17.34	17.347	
LB-1-1	Little Borate	-352.0	phytolith	534.69	17.35	17.347	
LB-1-15-1	Little Borate	-463.5	phytolith	534.69	17.55	17.555	

LB-1-9	Little Borate	-463.5	phytolith	534.69	17.55	17.555	
LB-1-8	Little Borate	-488.0	phytolith	534.69	17.6	17.599	
*Calico tuff	Little Borate	-487.5			*17.6	*17.6	Miller et al. (2013)
OC-1-15-5	Owl Canyon 1	-67.5	biomarker	309.22	17.73	17.731	
OC-1-15-6	Owl Canyon 1	-67.5	biomarker	309.22	17.73	17.731	
OC-1-15-7	Owl Canyon 1	-69.0	biomarker	309.22	17.74	17.738	

Table S3.4. Raw carbon isotope results from soil organic matter, weight percent carbon, estimated age of sample, and reconstructed atmospheric $\delta^{13}C$ from Tipple et al. (2010). Reprocessed samples are indicated by number of runs, suspect samples not included in results are in gray.

Sample No.	Member	Age (Ma)	$\delta^{13}C_{VPDB}$ (‰)	Weight % C	$\delta^{13}C_{atm}$ (‰)
TT-2-6	Upper	12.86	-19.34	0.03	-5.93
TT-2-7	Upper	12.86	-22.19	0.03	-5.93
TT-2-3	Upper	12.97	-23.64	0.02	-5.91
TT-2-2	Upper	12.99	-23.63	0.05	-5.91
TT-1-15-11	Upper	13.02	-23.07	0.02	-5.91
TT-1-1	Upper	13.06	-21.16	0.03	-5.91
TT-1-15-9	Upper	13.21	-21.44	0.04	-5.90
RH-15-1 run 1	Upper	13.69	-18.52	0.06	-5.80
RH-15-1 run 2	Upper	13.69	-16.85	0.04	-5.80
RH-16-1	Upper	13.69	-21.92	0.04	-5.80
RH-16-3	Upper	13.69	-22.07	0.04	-5.80
RH-16-7	Upper	13.69	-22.08	0.05	-5.80
RH-16-5	Upper	13.69	-21.64	0.07	-5.80
RH-16-9	Upper	13.69	-22.48	0.06	-5.80
OC-2-9	Upper	13.72	-21.95	0.13	-5.79
HG-1-6 run 1	Upper	13.77	-18.18	0.19	-5.79
HG-1-6 run 2	Upper	13.77	-20.49	0.07	-5.79
HG-1-4	Upper	13.82	-20.66	0.12	-5.77
OC-1-7 run 1	Upper	13.87	-2.63	0.36	-5.76
OC-1-7 run 2	Upper	13.87	-1.99	0.32	-5.76
HG-16-7	Upper	13.94	-24.74	0.04	-5.74
HG-1-3 run 1	Upper	13.94	-3.46	0.43	-5.73
HG-1-3 run 2	Upper	13.94	-2.59	0.56	-5.73
FW-3-9	Upper	14.12	-22.84	0.05	-5.66
FW-3-8	Upper	14.13	-21.26	0.09	-5.65
FW-3-6	Upper	14.33	-25.53	0.04	-5.55
HG-1-1	Upper	14.35	-23.82	0.06	-5.53
OC-1-6 run 1	Upper	14.55	-4.34	0.49	-5.44
OC-1-6 run 2	Upper	14.55	-1.73	0.52	-5.44
OC-2-8 run 1	Upper	14.80	-14.44	0.17	-5.33
OC-2-8 run 2	Upper	14.80	-9.78	0.44	-5.33
FE-16-5	Upper	14.81	-23.34	0.02	-5.29
SKY-1-4	Upper	15.16	-22.86	0.02	-5.27
FW-3-2	Upper	15.19	-26.08	0.08	-5.27
OC-2-7	Upper	15.20	-24.57	0.14	-5.27
FW-1-1	Upper	15.20	-24.51	0.05	-5.27
FW-2-15-3	Middle	15.32	-24.03	0.04	-5.27
FW-2-15-1	Middle	15.33	-23.22	0.11	-5.26
OC-2-6	Middle	15.34	-21.41	0.12	-5.26
RB-16-5 run 1	Middle	15.38	-12.92	0.28	-5.26
RB-16-5 run 2	Middle	15.38	-9.08	0.43	-5.26

Table S3.4. Raw soil organic matter results, continued.

Sample No.	Member	Age (Ma)	$\delta^{13}C_{VPDB}$ (‰)	Weight % C	$\delta^{13}C_{atm}$ (‰)
OC-2-5	Middle	15.39	-20.62	0.08	-5.26
CUP-16-5-1	Middle	15.41	-23.23	0.03	-5.26
HG-3-2	Middle	15.42	-23.09	0.12	-5.27
OC-2-3	Middle	15.50	-24.65	0.12	-5.25
OC-2-1	Middle	15.70	-22.89	0.07	-5.26
CUP-3-2	Middle	15.70	-21.33	0.27	-5.26
CUP-1-13	Middle	15.86	-23.34	0.03	-5.26
CUP-1-9	Middle	15.93	-22.84	0.07	-5.29
CUP-1-6	Middle	16.14	-27.74	0.33	-5.32
CUP-1-18 run 1	Middle	16.17	-8.75	0.42	-5.32
CUP-1-18 run 2	Middle	16.17	-18.38	0.15	-5.32
CUP-1-5	Middle	16.23	-22.29	0.17	-5.33
CUP-1-4-2	Middle	16.28	-24.13	0.03	-5.32
CUP-1-4-1	Middle	16.34	-22.97	0.04	-5.34
COO-1-15-2	Owl Congl.	16.83	-23.73	0.04	-5.40
RDQ-1	Owl Congl.	17.11	-23.57	0.02	-5.44
OC-1-4	Owl Congl.	17.14	-25.11	0.06	-5.44
LB-1-6 run 1	Calico	17.16	0.54	3.15	-5.44
LB-1-6 run 2	Calico	17.16	1.28	3.34	-5.44
LB-1-5	Calico	17.18	-22.34	0.16	-5.44
OC-1-15-1	Owl Congl.	17.29	-25.26	0.07	-5.49
OC-1-15-2	Owl Congl.	17.29	-23.66	0.04	-5.49
OC-1-3	Owl Congl.	17.29	-22.05	0.03	-5.59
OC-1-1B	Owl Congl.	17.34	-22.92	0.04	-5.51
LB-1-9 run 1	Calico	17.55	-2.92	5.53	-5.61
LB-1-9 run 2	Calico	17.55	-20.39	0.05	-5.61

CHAPTER 4

Taphonomy of mammals from the Barstow Formation in the Mud Hills, California, Part I: Taphonomic pathways and depositional environments[3]

Abstract

The pathways through which fossils accumulate determine the quality of preservation, the type of material preserved, and the taxonomic composition of the assemblage. Taphonomic histories of fossil assemblages may then affect patterns of specimen abundance and taxonomic diversity and are expected to differ among depositional settings. The Barstow Formation in the Mojave region of California preserves a diverse middle Miocene mammalian faunal assemblage. The formation was deposited in an extensional basin, and six major facies associations represent the dominant environments that formed through the evolution of the basin as tectonic influences subsided. Depositional environments changed over time from early-forming playa- and alluvial-fan-dominated environments to forested floodplain environments, to wooded grassland and spring-fed wetlands. Both the number of vertebrate fossil localities and mammal diversity increase upsection with changing paleoenvironments.

The taphonomic histories of large-mammal assemblages change through the formation in relation to changes in depositional environments. Taphonomic histories of fossil assemblages can be interpreted through evaluation of taphonomic features of specimens in the assemblage;

[3] Loughney, K.M., and Badgley, C., Taphonomy of mammals from the Barstow Formation in the Mud Hills, California, in prep.

combined with field-based observations of the lithological characteristics of the fossil locality, the depositional setting and agent of fossil accumulation can be interpreted. I documented the lithological characteristics and facies settings of 61 vertebrate localities in the field, and I examined skeletal material for taphonomic indicators from 78 fossil localities in museum collections. I evaluated taphonomic features of specimens in museum collections, including weathering stage and bone damage patterns, to interpret mode of accumulation and to reconstruct skeletal-element composition of fossil assemblages. The depositional settings of the 62 fossil localities examined in the field include channel and bar deposits (12.5%), proximal-channel settings (26.5%), distal-channel settings (21.8%), well-drained floodplains (12.5%), and poorly drained floodplains (26.5%). For 47 localities with both field- and collections-based observations, I interpreted the taphonomic pathways through which bones accumulated, recognizing channel fill, waterhole, carnivore and scavenger accumulations, channel lag, crevasse splay, and floating carcass as distinct pathways. The majority of localities accumulated at long-term mortality sites in channel fills and around waterholes (78.7%), with fewer concentrations forming exclusively from fluvial processes in channel lags (4.3%) and crevasse splays (4.3%) or through carnivore or scavenger activity (10.6%). Taphonomic pathways are more diverse in facies of the upper part of the formation than in facies from lower in the section. Facies associations that preserve a greater range of depositional settings preserve more vertebrate taxa and more assemblages with complex taphonomic pathways. Taphonomic histories of fossil localities change with depositional environment and directly affect the preservation quality, skeletal-element composition, and quantity of material preserved.

Introduction

Bone accumulations in terrestrial settings can accrue under a variety of circumstances that are dependent on processes occurring at the land surface. Processes may be biological or geological in nature and may take place over the span of minutes to thousands of years (Behrensmeyer, 1975). By evaluating the physical features of bones in a fossil assemblage and the depositional setting of the site of accumulation, ancient processes and agents of bone accumulation can be interpreted. The wide scope of taphonomic processes that contribute to the accumulation of fossils may have implications for a range of paleontologic investigations, from systematics to paleoecology.

The Barstow Formation in southeastern California preserves a well-studied mammalian fauna. The type fauna of the Barstovian North American Land Mammal Age (NALMA) is documented from the type section of the Barstow Formation in the Mud Hills (Fig. 4.1) near Barstow, California. Large- and small-mammal biochronologies have been established for the formation (Lindsay, 1972; Woodburne et al., 1990; Pagnac, 2009). Most work on the mammal faunas of the formation has been systematic, and few studies have focused on assemblages from individual fossil localities (Browne, 2002). Facies analysis (Chapter 2) and paleoenvironmental reconstructions (Chapter 3) provide new contexts for studying the taphonomy of the Barstow Formation. Fossil localities are unevenly distributed through the major facies of the formation, indicating some relationship between environment and taphonomy. As paleoenvironments changed through time in response to tectonics and climate (Loughney and Badgley, 2017), I expect taphonomic processes to have changed as well.

In this chapter, I describe the taphonomy of the large-mammal (>1 kg) faunas of the Barstow Formation. I focused on large mammals because the majority of specimens from the formation

are of large mammals, they have been more consistently collected throughout the formation than small mammals, and taphonomic features are easier to evaluate on large-mammal material. I examined fossil specimens collected throughout the formation to evaluate the relationship of taphonomic processes to major facies associations and their distribution through the formation. This chapter addresses three questions: 1) What are the major taphonomic pathways through which large-mammal fossils accumulated? 2) How do taphonomic pathways differ in terms of taphonomic features of fossil assemblages? 3) Do taphonomic pathways vary by facies association?

Here, I analyze the physical features and skeletal-element composition of fossil assemblages from the Barstow Formation. Taphonomic processes can also affect the faunal composition and representation of taxonomic groups in the fossil record. Barstow faunas went through several transitions over the depositional history of the formation (Pagnac, 2009). Taphonomic analyses of fossil assemblages from the formation are important to understanding how preservational processes change with depositional environments, as well as tectonics and climate. The taphonomy and analysis of diversity and turnover in the large-mammal fauna are the focus of Chapter 5.

Geological Background

The Barstow Formation crops out in the central Mojave Desert in the Mud Hills and Calico Mountains near Barstow, California (Fig. 4.1). Early Miocene extension in the Mojave region was associated with widespread extension throughout the Basin and Range physiographic province (McQuarrie and Wernicke, 2005). Detachment-style faulting throughout the Mojave region caused the exhumation of metamorphic core complexes and the creation of fault-block

basins (Dokka, 1989). The Jackhammer, Pickhandle, and Mud Hills formations were deposited during the most active period of extension in the central Mojave region during the early Miocene and are now exposed in the Mud Hills and Calico Mountains (Fig. 4.1). The Barstow Formation was deposited after active extension had ended, and it unconformably overlies the Pickhandle and Mud Hills formations in these areas (Ingersoll et al., 1996; Glazner et al., 2002).

The Barstow Formation is divided into three lithostratigraphic members in the Mud Hills (Fig. 4.2): the Owl Conglomerate, Middle, and Upper members (Woodburne et al., 1990). The Calico Member was named for Barstow deposits in the Calico Mountains by Singleton and Gans (2008) and is coeval with the Owl Conglomerate Member. The Barstow Formation has been dated through biostratigraphy (Woodburne et al., 1990; Pagnac, 2009), magnetostratigraphy (MacFadden et al., 1990; Woodburne, 1996), and isotopic dating of airfall tuffs (Woodburne et al., 1990; Miller et al., 2010; Miller et al., 2013). In the Mud Hills, the formation extends from ~19 to 13 Ma and from 19 to 17 Ma in the Calico Mountains (Woodburne et al., 1990; Singleton and Gans, 2008).

Six major facies associations (FA) in the Barstow Formation in the Mud Hills record the dominant environments and landscapes that formed during deposition of the formation (Loughney and Badgley, 2017; Chapter 2). Environments changed from closed-drainage playa lake settings to open-drainage fluvial and floodplain settings in response to changes in accommodation and subsidence. Facies associations 1 and 2 represent environments that formed early in the basin history when rates of subsidence and rates of sediment accumulation were high. FA 1 represents channels and interfluves of alluvial fans that drained into playa lake deposits of FA 2. As rates of subsidence decreased, meandering streams were established, and FA 3 represents the channel and proximal floodplain deposits of these environments. Deposits of

FA 3 grade into those of FA 4, which are stacked sandstone bodies that represent channel deposits of braided streams. FA 5 and FA 6 are both mudstone-dominated and formed when rates of sediment accumulation and subsidence were low. Deposits in these facies associations represent interfingering poorly drained and well-drained floodplain deposits and spring-fed wetlands (Loughney and Badgley, 2017).

Barstow fauna and fossil localities

Fossils from the Barstow Formation have been described and collected since the early 20th century (Merriam, 1919; Woodburne et al., 1990). Important early collections were made by the University of California Museum of Paleontology (UCMP) and the American Museum of Natural History. The American Museum parties under Childs Frick (F:AM) established numerous fossil localities throughout the Mud Hills, and some of the largest and most productive localities are Frick-era quarries. Collectors from the University of California, Riverside, the San Bernardino County Museum in San Bernardino, California, and the Webb Schools in Claremont, California, began making collections from the formation in the 1960's (Pagnac et al., 2013). The San Bernardino County Museum (SBCM) and the Webb Schools (RAM) continue to add to their collections from the Barstow Formation.

The mammal fauna of the Barstow Formation is characteristic for North America during the Miocene. The most abundant herbivorous groups are represented by eight species of equids, seven species of camelids, and six species of antilocaprids. Other ungulates that occur in low abundance or in restricted intervals include three species of oreodonts, three species of tayassuids, two species of palaeomerycids, two genera of proboscideans, and one species of rhinoceros. The carnivore fauna is dominated by canids, and 13 species are recognized in the

formation. Other important carnivores that range through the formation are three species of amphicyonids, three species of mustelids, two species of felids, one species of ursid and one species of procyonid (Pagnac et al., 2013). Many small mammal species are also recognized from the formation, including numerous species of heteromyids and cricetids, sciurids, and insectivores (Lindsay, 1972).

Fossils occur throughout the formation in the Mud Hills, although they are relatively rare in the Owl Conglomerate Member. Few large-mammal fossils occur in FA 1, and only vague stratigraphic information exists for localities in this interval (Woodburne et al., 1990). Red Division Quarry (F:AM) is the most important quarry from this interval and is the stratigraphically lowest locality included in this study. Only mammal trackways are known from FA 2, and no fossils from this facies association were included in my taphonomic analyses. Many more fossil localities occur in FA 3 and FA 4, including several important localities that have produced hundreds of specimens. Steepside, Camp, and Deep Quarries (F:AM) in FA 3 and Valley View and Skyline Quarries (F:AM) and RAM V94179 in FA 4 are among the prominent localities of the Middle Member. The majority of fossil localities occur in FA 5 and FA 6 (Loughney and Badgley, 2017). New Year and *Hemicyon* Quarries (F:AM) and Robbins Quarry (SBCM) are productive localities in FA 5. RAM V98004, Rodent Hill (UCMP), and UCMP V3849 are important localities in FA 6.

Taphonomic pathways and indicators

The taphonomic processes that affect the ultimate preservation of fossils are diagenetic and biostratinomic. Diagenesis includes the alteration and replacement of organic matter after burial, and bones and teeth may also be subject to physical deformation or breakage from compaction of

sediment as well as from localized folding and faulting (Fernández-Jalvo and Andrews, 2016). Biostratinomy focuses on the processes affecting animal and plant remains following the death of the individual until deposition and final burial. The remains of organisms may be deposited through a variety of biostratinomic or taphonomic pathways (Fig. 4.3) that disperse or concentrate remains at the surface. Often, agents and processes of dispersal and concentration act on vertebrate remains at different times before final burial, and most pathways represent combinations of processes. Although distinct taphonomic pathways can be recognized based on physical characteristics of fossil assemblages (Table 4.1), concentrations of fossils typically accumulate through a variety of pathways due to the types of processes operating within an ecosystem over time. Biological activity, physical processes, and duration of accumulation are the main factors that determine taphonomic pathway (Behrensmeyer, 1991).

Agents of accumulation in terrestrial systems are typically either biological or physical. Biological taphonomic agents can concentrate or disperse remains. The behavior and life habits of animals determine where they live, and consequently, where they die. Life events such as spawning, migration, and nesting concentrate individuals, and mortality during these activities results in concentrated monospecific assemblages (Rogers and Kidwell, 2007). Environmental stressors such as drought may also cause animals to congregate near water and food sources, resulting in multispecific assemblages (Behrensmeyer, 1975). Biological agents of bone dispersal and accumulation include predators, bone collectors, and scavengers. Bone collectors and scavengers modify bone assemblages by collecting individual elements or by disarticulating and dispersing remains from a mortality site, respectively (Rogers and Kidwell, 2007).

Physical agents that disperse or concentrate animal remains are hydraulic and sedimentologic. Water and wind move skeletal elements to varying degrees and partly control

the skeletal-element composition of transported assemblages. Size, shape, and density of elements determine their susceptibility to transport from fluid flows, and easily transported elements (e.g., scapulae and vertebrae) are typically winnowed from assemblages (Voorhies, 1969). Sediment budgets affect the concentration of bones and teeth at a locality or within a depositional sequence. High rates of sediment supply relative to rates of bone input will result in fossil occurrences that are sporadic within sediment packages; low rates of sediment supply and deposition relative to rates of bone input result in concentrations of fossils (Kidwell, 1986). Sedimentation rates must be high enough to bury remains and prevent destruction at the surface, yet low enough not to overwhelm bone input (Behrensmeyer, 1988).

The duration of accumulation at a locality can affect many aspects of the assemblage, including the number of individuals, the elements present, the concentration of individuals or skeletal elements, and the spatial extent of the locality. Long-term sites of mortality are places where animals live, interact, and die over long periods of time. Fossil assemblages resulting from the gradual or attritional accumulation of bones are time-averaged over the duration of accumulation, and many individuals and species may be represented in the assemblage (Rogers and Kidwell, 2007). The spatial extent of the bone-bearing horizons may be extensive or concentrated, and remains of individuals and elements are typically dispersed. Assemblages that accumulate over short periods of time may be spatially constrained and preserve few individuals or species. Mass mortality events can result in the deaths of few or hundreds of individuals and occur over minutes to weeks (Rogers and Kidwell, 2007).

Methods and Analyses

Field descriptions

I visited 61 fossil localities in the Mud Hills over three field seasons. Sites were selected based on the amount of material in museum collections, facies-association setting, ability to locate in the field, and historical importance or number of references by other workers. Localities that are representative for their facies-association settings were visited in FA 1 (Owl Conglomerate Member), FA 3 and FA 4 (Middle Member), and FA 5 and FA 6 (Upper Member) in the Mud Hills. Because the majority of large-mammal fossil localities are in the Upper Member, these 61 localities are unevenly distributed among lithostratigraphic members or facies associations.

Localities were located using aerial photographs, topographic maps, Google Earth, and field maps and notes from museum archives. Coordinates of localities were measured with a Garmin eTrex and hand-held GPS unit. The stratigraphic position of each locality encountered in the field was measured into stratigraphic sections using a Jacobs staff and Brunton compass. Most localities in the Barstow Formation have been collected by numerous institutions and many have multiple names and institution numbers. I assigned a University of Michigan locality number (MMR) to each locality.

I made detailed stratigraphic and sedimentologic descriptions of each of 61 fossil localities (Appendix 1), including lithologic descriptions, vertical and lateral extent of the locality, and number of bone layers. The number of bone layers was documented from positions of *in situ* bones and teeth; at localities without *in situ* elements, I estimated at least one source layer and more than one if the locality had multiple excavation scars. This approach may underestimate the actual number of bone layers, as fossils were likely deposited in multiple layers, particularly for

some taphonomic pathways. I made surface collections of bone and tooth fragments at these localities where appropriate.

Taphonomic data from museum collections

I visited museum collections at four institutions with significant amounts of fossil material from the Barstow Formation: the American Museum of Natural History (AMNH), University of California Museum of Paleontology (UCMP), Raymond Alf Museum of Paleontology (RAM), and the San Bernardino County Museum (SBCM). I examined 3,285 specimens of bones, teeth, and fossil fragments of mammals from 78 vertebrate localities to document taphonomic features useful for interpreting taphonomic pathways. These features include breakage patterns, abrasion, rounding, tooth marks, and number of punctures (Fig. 4.4). I recorded the completeness of all specimens and categorized each as whole, partial, or fragmentary. Whole specimens were 90% to 100% complete, partial elements were 40% to 90% complete, and fragmentary specimens were less than 40% complete. I also measured length, width, and height of all specimens.

Inferring taphonomic pathways

In order to interpret taphonomic pathways from fossil assemblages, certain criteria must be established to differentiate among pathways. These criteria are based on field observations of the fossil locality and taphonomic features of the fossil assemblage (Table 4.2). Ideally, the positions of *in situ* bones would be noted in the field at the time of excavation; however, this information was not available for most of the localities examined here. Instead, I used the taphonomic features of bones, the skeletal-element composition of collected assemblages, and the field observations of localities to interpret the depositional conditions associated with fossil

accumulation. Combining lithological descriptions from the field and evaluations of taphonomic features from fossil assemblages is a robust means of interpreting taphonomic pathways (Behrensmeyer, 1991), even when these data are collected separately.

The depositional setting of fossil localities can be interpreted from lithological characteristics at the locality (Table 4.2), including the grain size and composition, bed thickness and geometry, sedimentary structures, and presence of root casts or ichnofossils. The vertical and lateral extent of bone layers can be used to infer the duration of accumulation and whether the agent of accumulation concentrated or dispersed remains at the locality. At long-term sites of mortality, bones are typically dispersed, reflecting the addition of material over time and the scattering of remains from trampling or scavenging; many bone layers may result from the time-averaged accumulation of material. Fluvial processes may concentrate fossil material in discrete layers and sort elements by size or density (Behrensmeyer, 1988), and predators or scavengers typically concentrate remains at den sites (Rogers and Kidwell, 2007). The physical features of bones (Fig. 4.4) in the assemblage can be used to infer processes and agents acting on bones at the surface. Weathering stage can indicate the duration of exposure before burial (Behrensmeyer, 1978), element completeness and damage patterns such as abrasion, tooth marks, and breaks are evidence of trampling or scavenging and predation (Fernández-Jalvo and Andrews, 2016). The articulation and association of material, skeletal-element composition of the assemblage, and hydraulic equivalence are indicators of transport or sorting of elements (Table 4.2). Assemblages accumulating through fluvial processes have low amounts or no associated material, and less dense, easily winnowed elements such as vertebrae and ribs are typically missing (Voorhies, 1969; Behrensmeyer, 1975). Hydraulic equivalence compares sediment matrix at the locality and

the elements in the fossil assemblage to test whether they could have been transported at the same time (Badgley, 1986a).

The combinations of these criteria can indicate the agent or mode of accumulation of fossil assemblages (Table 4.1). Sites of long-term mortality accumulate time-averaged assemblages. The channel-fill taphonomic pathway accumulates material in proximal-channel deposits; these assemblages show little or no evidence of transport or prolonged exposure of material before burial. Waterhole assemblages are preserved in floodplain deposits and are similar to channel-fill assemblages but may show a greater range of weathering stages and bone damage, reflecting lower rates of burial and prolonged exposure at the surface. Natural-trap assemblages are characterized by high numbers of articulated and complete skeletons and the preservation of upright orientations of individuals that indicates miring (Weigelt, 1989; Rogers and Kidwell, 2007). Assemblages accumulating through fluvial processes are preserved in channel deposits or proximal-floodplain deposits and include channel-lag, crevasse-splay, and floating carcass pathways. Channel-lag and crevasse-splay assemblages comprise unassociated material that is typically abraded, rounded, and missing easily winnowed elements. Floating carcasses are preserved in channel deposits but are distinct in being articulated partial or complete skeletons. Carnivore and scavenger collections typically include partial and fragmentary material that show breakage patterns consistent with carnivore damage (tooth marks, punctures). Catastrophic death assemblages are typically distinguished from other taphonomic pathways by monotaxic composition, a range of ages of individuals in the assemblage, and a high degree of articulation or association of elements (Voorhies, 1969; Martin, 1999). These assemblages may be preserved in a range of sedimentary deposits, from channel sandstones to tuff layers.

Analyses

For each locality, I calculated the hydraulic equivalence of specimens in the assemblage. Fossil specimens may be considered sedimentary particles that can be transported in sedimentary environments. Fossil clasts are often larger than the sediment particles in the bone layer, and hydraulic equivalence compares settling velocities of fossils and their encasing sediment matrix to estimate if they could have been transported and deposited by the same flow velocities (Badgley, 1986a). Hydraulically equivalent fossil specimens and sediment could have been transported and deposited together, whereas non-hydraulically equivalent specimens and sediment have no shared transport history. Hydraulic equivalence, however, is not evidence of transport, which must be based on features of the fossil assemblage (Badgley, 1986a).

Hydraulic equivalence is determined by calculating the diameter of a quartz sphere (d_q) with equivalent density to a bone or tooth (Behrensmeyer, 1975; Badgley, 1986a):

$$d_q = (\rho_b - 1) \times \frac{d_b}{1.65},$$

where ρ_b is bone density, which varies depending on the amount of cancellous and compact bone in an element, and d_b is the nominal diameter of bone, calculated from the volume (v_b) of a specimen:

$$d_b = \sqrt[3]{1.91 \times v_b}.$$

I calculated v_b using the dimensions of specimens measured in museum collections and the measured densities of bone and teeth in Badgley (1982) to calculate nominal bone diameters and the equivalent densities of quartz spheres.

For each taphonomic pathway, I determined the skeletal-element composition. The relative frequencies of skeletal elements present in an assemblage can be compared to the skeletal-element composition of the average whole mammal (Badgley, 1986a). The average whole mammal contains approximately 210 bones, grouped into morphologically functional and taphonomically similar categories (i.e., vertebrae, podials, long bones). The differences in composition between the assemblages from each pathway can be assessed by comparing them to the average whole mammal composition. Frequencies of over- and under-represented skeletal elements indicate the types of processes acting on fossil assemblages, especially those that winnow or concentrate specific elements.

Principal components analysis (PCA) and cluster analyses were run on counts of skeletal elements from 44 localities with field and collections observations. PCA was run on standardized counts of 2,609 specimens in 24 categories of skeletal elements; localities from which fewer than three specimens were counted were excluded from the analysis. Cluster analysis was run on standardized counts of 2,546 specimens in 22 categories from 43 localities. The “shaft” and “skeleton” categories were excluded from the cluster analysis. Dissimilarity distances between samples were computed using the Bray-Curtis method, which is based on the percent shared abundance of objects between samples (Legendre and Legendre, 2012). Clustering was performed with the Ward’s minimum variance method, an agglomerative method that clusters pairs of objects in the order that minimizes the total sum of squared distances between all object clusters and cluster centroids. This method emphasizes similarity between objects and produces

tightly clustered groups (Legendre and Legendre, 2012). All analyses were performed in R using the “vegan” (Oksanen et al., 2017) and “cluster” (Maechler et al., 2017) packages.

Results

For 47 localities, I had both field descriptions of the locality and evaluations of museum collections (Table 4.3). These localities are distributed throughout fossiliferous facies associations of the Barstow Formation (Table 4.4). Stratigraphic sections for each locality are in Appendix 1. From field and museum observations, I identified six taphonomic pathways: channel fill, waterhole, carnivore and scavenger accumulations, channel lag, crevasse splay, and floating carcass (Table 4.3). These pathways can be grouped into two broad categories of fossil accumulations: those representing long-term sites of mortality and those forming through fluvial processes. The assemblages from channel-fill, waterhole, and carnivore or scavenger pathways accumulated at long-term mortality sites; assemblages from channel-lag, crevasse-splay, and floating carcass pathways accumulated predominantly through fluvial processes.

Long-term sites of mortality

Bones accumulating at sites of repeated mortality are attritional assemblages that are subject to a variety of biostratinomic processes (Rogers and Kidwell, 2007). Assemblages in these settings are typically time averaged, representing the input of bones over 10^1 to 10^4 yr (Behrensmeyer, 1982). Channel-fill, waterhole, and carnivore and scavenger pathways are distinguished based on taphonomic criteria and assessment of the depositional settings, although there is often overlap among pathways.

Channel fill

The channel-fill pathway includes assemblages from 25 localities forming in abandoned-channel and channel-margin settings in FA 3, FA 4, FA 5, and FA 6. Localities belonging to this pathway have multiple fossil-bearing horizons and are typically spatially extensive. Fossil-bearing horizons at these localities are mudstone and fine to medium sandstone and may fine upwards from a basal coarse sandstone or pebble conglomerate (see Appendix 1 for individual localities).

Ten fossil localities in FA 3 occur in siltstone or sandy siltstone layers that either grade up from or sharply overlie sandstone or conglomerate. The tops of the fossil-bearing sequences are typically truncated by thick sandstone beds. Siltstone layers may have thin clay and thin marl beds (2-3 cm) with oncolites and root casts, and root casts are typically common throughout these sequences. The lateral extent of these localities ranges from 5 to 20 m.

In FA 4, six localities occur in structureless to cross-stratified medium sandstone to siltstone layers. The fine-grained fossiliferous horizons grade upwards from coarse or medium sandstone, and their upper boundaries are truncated by overlying sandstone beds. One locality, Valley View Quarry, is developed in claystone interbedded with thin marl beds and is capped by a 40-cm-thick marl layer. Many of these localities are defined by large quarry scars that are laterally traceable up to ~40 m.

In FA 5, six localities occur in tuffaceous siltstone and sandy siltstone horizons with numerous fine to medium root casts throughout. At New Year Quarry and MMR-049, cross-stratified tuffaceous fine sandstone grades into siltstone interbedded with thin, bioturbated and brecciated marl layers (10-20 cm). Within this sequence, *in situ* bones were observed in three horizons; this sequence is sharply overlain by coarse sandstone. New Year Quarry and MMR-

049 are developed in the same fossil-bearing horizon and are laterally continuous over 60 m. MMR-029 and MMR-051 occur in tuffaceous fine sandstone and siltstone deposits similar to those at New Year Quarry; these localities are developed along a horizon that is continuous over 50 m. At Robbins Quarry, tuffaceous siltstone is interbedded with sandy siltstone and thin-bedded sandstone layers (20-25 cm) with rip-up clasts. *In situ* bones were observed at five intervals in the quarry, which is approximately 6 m wide. Easter Quarry occurs within clayey siltstone with interbedded marls and numerous root casts that sharply overlies thick, trough cross-stratified sandstone. This quarry is approximately 3.5 m wide, and other localities occur at this horizon over approximately 40 m.

Fossil localities in FA 6 occur in medium sandstone or siltstone. At UCMP V6449, fine sandstone with ripple cross-stratification grades up to siltstone and claystone with slickensides, pore linings, and root casts; the claystone layer is overlain by fine silty sandstone and marl. The quarry extends laterally for ~4 m. The fossil-bearing horizons of RAM V98004 extend over ~12 m of interbedded fine sandstone and siltstone capped by ~30 cm of siltstone (Lofgren et al., 2014) with large blocky ped structure and carbonate nodules. This locality is ~3 m wide and bounded by thick, structureless fine sandstone. SBCM 1.130.421 is in a thick (2 m) sequence of medium sandstone that has internal scours filled with lenses of coarse sand- to gravel-sized clasts and clay drapes. The quarry is approximately 1 m wide.

As many as five bone layers were identified in these localities, but the number of bone layers was sometimes difficult to estimate; for all localities, multiple bone layers were inferred, given the episodic deposition of sediment in channel fills. Localities representing channel fills were typically laterally continuous for 10’s of meters. There was no hydraulic equivalence between elements in the fossil assemblage and the sediment at these localities. Of the 1,385 specimens I

examined from museum and surface collections from these localities, the majority were isolated elements (62.5%), 431 (31.1%) were associated, and 88 (6.4%) were articulated (Table 4.3). Weathering stages of bones ranged from incipient to moderate (1 to 3; Behrensmeyer, 1978), although few bones were more weathered than stage 1. Approximately one third of bones from these assemblages were broken and abraded, and tooth marks were identified on 14.3% of elements (Table 4.3). Forty-eight specimens (3.5%) were from juveniles.

These localities all represent deposits forming in channel fills and channel margins. The specific depositional settings of these localities vary slightly by facies association, related to the types of streams that were present on the landscape at the time of deposition. FA 3 represents channel and proximal-channel deposits of meandering streams (Loughney and Badgley, 2017; Chapter 2). Localities in FA 3 formed in the fine-grained fills of abandoned channels and at channel margins. Abandoned channels form when stream segments avulse to new positions on the floodplain, and fine-grained channel fills develop when channels are suddenly abandoned (Bridge, 2003). Although I cannot reconstruct the distribution of bone horizons, the fine-grained sediment and the occurrence of root casts throughout these deposits indicate that these channels were filled gradually over time (Behrensmeyer, 1988), and multiple bone layers likely occur at these sites. Several specimens from localities in FA 3 were deformed from compaction in soft sediment; such deformation typically occurs soon after burial (Fernández-Jalvo and Andrews, 2016), and is particularly common in moist sediment (Behrensmeyer, 1975).

The amalgamated sandstone beds of FA 4 represent channel and bar deposits of braided streams (Loughney and Badgley, 2017; Chapter 2). Fossil localities occur in the fine-grained sandstone and mudstone deposits that are interbedded with the sandstone bodies. These fine-grained deposits also represent channel fills, but their depositional settings are not as uniform as

those in FA 3. These localities developed in intermittently active channels on the braidplain that were gradually filled or overtaken by downstream-accreting bars (Bridge, 2003). At Valley View Quarry, channel filling was gradual, as indicated by the rooted marl layer that represents a pond developed within an inactive channel. The greater complexity of this channel system relative to that of FA 3 is indicated by the lateral extent of bone-bearing horizons and the variable lithologies of fill deposits.

In FA 5 and FA 6, localities of the channel-fill pathway also developed in different types of channel settings. In FA 5, channel systems were small-scale, and localities formed in abandoned channels that were filled gradually, allowing the establishment of vegetation and the formation of ponds. In FA 6, channel systems were larger and sandier than in FA 5, and localities forming at channel margins were filled more quickly. Pedogenic development or marls at the tops of these localities indicate that sedimentation rates decreased at these sites through time.

Assemblages in channel-fill settings are typically attritional and represent the site of mortality with little or no transport (Behrensmeyer, 1988). Almost one third of material from these assemblages was associated, indicating that remains were not transported to the sites of deposition. Elements are disassociated from one another during transport by fluvial processes (Badgley, 1986b; Behrensmeyer, 1991). The combination of cranial and axial material also indicates that these assemblages were not sorted by currents, as these elements have different susceptibility to transport (Voorhies, 1969). Breakage and abrasion of specimens occurred from trampling or from carnivore and scavenger activity at the site of mortality.

Waterhole

I referred assemblages from four sites in FA 5 and eight sites in FA 6 to the waterhole taphonomic pathway. These 12 localities occurred in fine-grained sequences and were developed in siltstone and claystone with interbedded marls. Marls at these localities were thicker (10 to 90 cm) and more closely spaced than those in channel-fill settings and typically had abundant fine to medium root casts. In FA 5, localities were typically developed in 3 to 15 m of interbedded siltstone and marl with low-chroma coloration. Root casts were abundant through these sequences, and pedogenic features were absent or were poorly developed. These localities extended 5 to 40 m laterally. In FA 6, localities were also developed in sequences of siltstone and marl; marl beds at some localities had nodular or brecciated upper surfaces. Carbonate nodules, ped structure, and clay linings were typically present and weakly to moderately developed. One prominent locality, Rodent Hill, extends laterally over approximately 100 m. Gastropod shells referable to *Lymnaea* and *Planorbula* (Abersek and Lofgren, 2017) were locally abundant at sites in FA 5 and FA 6.

Waterhole localities were laterally continuous for 10's of meters, and at least two bone layers were documented or estimated at these sites. I documented taphonomic features from 1,094 specimens belonging to this pathway. None were hydraulically equivalent with sediment at the site of deposition. Elements were complete, partial, and fragmentary (Fig. 4.5); isolated elements comprised the majority the assemblage (93.5%), nine elements were articulated (0.8%), and 62 were associated (5.7%). Weathering stages of bones ranged from 1 to 3, and most were in preliminary stages of weathering (0 to advanced 1). Fewer than 20% of elements had original breakage, and 32.4% were abraded. Trample and tooth marks were present on 42.2% of elements, and 13 elements (1.2%) belonged to juveniles.

These localities represent floodplain and spring-fed wetland deposits with variable drainage (Loughney and Badgley, 2017; Chapter 2). The low-chroma coloration and prominence of thin, rooted marl horizons in FA 5 localities indicate that they were poorly drained. The slightly better pedogenic development and brecciated marls at waterhole localities in FA 6 indicate that these sites experienced periodic drying.

Assemblages accumulating in waterhole settings are attritional and time-averaged. The lateral and vertical extent of these localities, as well as the wealth of material collected, indicates that these settings were relatively stable landscape features accumulating material over long periods of time, perhaps hundreds to thousands of years. The occurrence of tooth and trample marks in these assemblages was high compared to other pathways, and assemblages in this pathway category had low amounts of articulated or associated material compared to other long-term mortality sites. Original breakage was relatively low among assemblages in this pathway, and most specimens were partial or complete, and almost one third of specimens were abraded. Breakage and abrasion of specimens occurred from carnivore and scavenger activity as well as from trampling, which contributes to the disassociation and scattering of elements (Hill, 1979). Many of the complete specimens from these localities were small elements that may have escaped breakage from trampling. Few specimens showed evidence of corrosion, which occurs when bones are submerged in standing water for prolonged periods, during digestion in carnivore guts, or from roots growing around bones (Fernández-Jalvo and Andrews, 2016).

Carnivore and scavenger accumulations

Five localities in FA 5 and FA 6 represent carnivore and scavenger accumulations. These localities were united primarily through the taphonomic features of the assemblages and

represent a variety of depositional settings. Lithologically, these localities were similar to the waterhole localities. Four localities occur in drab-colored mudstone with thin, interbedded marls. Fine to large root traces were locally present, and pedogenic features were absent or were weakly developed. One F:AM locality in FA 5 (Saucer Butte Quarry) was developed in reddish brown sandy siltstone and claystone that is sharply overlain by fine gray sandstone.

Fossils at these localities were all spatially concentrated over <20 m^2. Elements in the assemblage were not hydraulically equivalent with sediment, and the 194 specimens from assemblages in this category were predominantly fragmentary and partial (Fig. 4.5). Four partial skeletons from Saucer Butte Quarry comprised the articulated portion of the overall assemblage (40.2%), and 55 elements were associated (28.4%). Assemblages from these localities were characterized by breakage patterns consistent with carnivore damage (66.2%; Fig. 4.4), and the proportion of elements showing rounding, polishing, and other modification was greater than for other pathways (Table 4.3). Weathering stages of bones were incipient to moderate (1 to advanced 2), and identifiable elements of juveniles were 2.6% of specimens.

I distinguished carnivore and scavenger accumulations from channel-fill and waterhole assemblages on the basis of the patterns of breakage and fragmentation of specimens. Lithological characteristics of the localities were not distinctly different from surrounding deposits, making it hard to interpret whether a den structure originally existed. The physical features of specimens, however, are consistent with carnivore damage and are similar to features of assemblages in modern carnivore dens. Four of the five localities had assemblages that were highly fragmented, with damage consistent with chewing and breakage by carnivores. Tooth marks and punctures were common in these assemblages, and the proportion of rounded, polished, and corroded material was high compared to other pathways (Table 4.3). Many bone

fragments from the five localities in this category had conchoidal breakage or were diamond-shaped shaft fragments that are characteristic of processing by carnivores (Fernández-Jalvo and Andrews, 2016). Rounding, polishing, and corrosion of bones and bone fragments can also result from licking and digestion by carnivores (Fernández-Jalvo and Andrews, 2016). The taxonomic composition of these assemblages included material from small- to large-bodied herbivores and carnivores. Modern carnivores often prey on smaller carnivores or are even cannibalistic (Vaughan et al., 2015), and modern carnivore dens often contain a combination of material from both herbivores and carnivores (Brain, 1980). In addition to material from larger animals, one locality produced abundant leporid and rodent material that was evident at the surface. This locality could represent a small carnivore latrine. Many modern carnivores that prey on rodents and small mammals habitually use latrines, where bones can be deposited over long periods of time in scat or regurgitate (Rogers and Kidwell, 2007).

The assemblage from Saucer Butte Quarry was very different from the other four carnivore assemblages, and it may represent a unique scenario of accumulation. Saucer Butte Quarry represents a well-drained floodplain setting from which four partial camel skeletons were collected by F:AM parties. These skeletons were still in jackets, allowing observation of the degree of articulation, disassociation, and orientation of elements, but precluding close examination of the elements themselves. Weathering stages of these specimens were incipient. Thoracic and lumbar vertebrae were articulated, often with ribs, complete pelves, and scapulae articulated or associated. If limb bones were present, femora were articulated and humeri were disarticulated but associated. These articulated partial skeletons represent a different taphonomic history from the fragmentary specimens of the other carnivore and scavenger accumulations. Rather than a den or latrine where carnivores or scavengers collected material, Saucer Butte

Quarry may represent a kill site or a scavenged assemblage from which elements were removed. Predators and scavengers feeding on a carcass typically focus on soft tissues and leave patterns of damage to particular parts of the carcass. In modern African communities, carnivores typically consume much of the carcass, but are most likely to leave the skull and horns, vertebrae, ribs, pelves, and long bones; other parts of the carcass may be carried away from the kill site by carnivores or scavengers (Behrensmeyer, 1975). Carcasses are typically processed and disarticulated quickly after death, and remains that are not eaten can persist for extended periods of time (Hill, 1980), allowing carcasses to be gradually buried. Elements that remain articulated may be protected by skin or held together by ligaments, which, in dry environments, may remain intact for months or years after death of the individual (Behrensmeyer, 1975; Hill, 1979). That the axial elements of these skeletons remained articulated may not be unusual, especially if the environment was warm and dry.

Fluvial accumulations

Fossil assemblages that accumulate predominantly through fluvial processes are typically composed of disassociated allochthonous material from multiple individuals (Badgley, 1986b). Elements in these assemblages tend to have distinctive shapes, sizes, or densities that affect their hydraulic equivalence and therefore their potential for winnowing and dispersal in currents (Voorhies, 1969; Behrensmeyer, 1975). Assemblages may represent considerable time averaging of elements that may have been in the fluvial system for up to 10^4 yr (Behrensmeyer, 1982).

Channel lag

Two localities were identified as channel-lag accumulations, Red Division Quarry in FA 1 and RAM V200047 in FA 6. The lithologies at these localities are fine to coarse massive sandstone with pebble clasts. At Red Division Quarry, coarse sandstone fines upward to fine sandstone and silty fine sandstone, truncated at the top by a lenticular bed of fine sandstone. Slickensides, mottling, and clay-filled root traces are well-developed in the silty fine sandstone (Appendix 1). *Celliforma* cells (bee nests; Genise, 2000) and tufa deposits occur at the base of the quarry. RAM V200047 is also developed in coarse to medium sandstone with pebble- and cobble-sized lithic clasts. The coarse sandstone grades upwards to faintly cross-stratified, fine sandstone and sandy siltstone with manganese concentrations (Appendix 1).

Fourteen specimens were observed from channel-lag assemblages, five from Red Division Quarry and nine from RAM V200047. These specimens included long bones, podials, and several cranial and girdle elements. All specimens were disassociated, partial, or fragmentary (Fig. 4.5) save for one complete tarsal. Both localities were spatially constrained (2 to 4 m lateral extent); no fossils were found *in situ*, and I estimated one bone layer for each locality. These assemblages had a high proportion of broken (50%) and abraded (75%) specimens that were hydraulically equivalent with the sediment matrix (Table 4.3). Weathering stages were incipient to moderate (1 to 2).

Red Division Quarry and RAM V200047 represent channel-margin or channel-bar deposits where bones accumulated during waning flow. Elongate and small, dense elements or fragments characterize these assemblages. Channel lags are the coarse bedload particles that move through traction transport or saltation (Bridge, 2003). Fossils that are hydraulically equivalent to inorganic bedload particles can be incorporated into channel lags. Elements with low

susceptibility to transport are typically found in channel-lag deposits and include long bones, girdle elements, and cranial elements (Voorhies, 1969). Abrasion of bones occurs when sediment particles move past the surface of the bone (Fernández-Jalvo and Andrews, 2016). Bones may enter the stream channel from existing assemblages at channel margins that have been scavenged or trampled. Bones can also be trampled in dry stream beds, where they are ground against sediment grains. Breakage does not occur from fluvial transport (Behrensmeyer, 1991), and breakage of elements in the assemblages was likely due to trampling and predation or scavenging prior to entrainment.

Crevasse splay

I identified two localities as crevasse splays, Starlight Quarry and MMR-043, both in FA 5. Starlight Quarry occurs in fine sandstone with ripple cross-stratification and coarse sand-sized clasts. The sandstone is 30 cm thick and sharply overlies siltstone with fine to medium root casts. Impressions of palm fronds occur in the fine sandstone bed. MMR-043 is in a brown-weathering coarse-sandstone to pebble-conglomerate layer, 25 cm thick, with ripple cross-stratification and lithic clasts 1-5 cm long. This locality was discovered in the field, and *in situ* specimens were counted over 150 m^2 of the exposed sandstone bed. The fossil-bearing sandstone layer has a sharp contact with underlying interbedded sandy siltstone and marl.

Sixty specimens were examined from Starlight Quarry and MMR-043. Elements in the assemblages include teeth, shafts of long bones, girdle and axial elements, and podials. Several specimens were unidentifiable fragments. Most specimens were partial or fragmentary (Fig. 4.5), and only three were associated. The lateral extent of these localities varies from 3 to 30 m. The vertical extent of MMR-043 was restricted to the primary sandstone bed. Almost half of all

specimens were broken, abraded, or rounded, and all were hydraulically equivalent with the sediment matrix of the bone layer (Table 4.3). Weathering stages were incipient to moderate (1 to 3).

The assemblages from Starlight Quarry and MMR-043 were deposited in crevasse-splay events on the proximal floodplain peripheral to the active channel. The thin, sheetlike geometry of the sandstone beds within thicker mudstone deposits is typical of crevasse splay units. Crevasse splays are deposited during episodes of high discharge and flow velocities when channels are at bankfull levels (Bridge, 2003). Clasts entrained in the flow or moving along the bed are deposited when water overtops or erodes through the bank. Flow velocities quickly dissipate and rapidly lose competence, and a range of clast sizes is deposited in crevasse channels and distal-splay margins.

The assemblage is attritional and time averaged in that specimens were added to the channel system at different times and may have been reworked from previously deposited floodplain sediments (Behrensmeyer, 1988). At least one completely rounded bone pebble was present at Starlight Quarry, representing the incorporation of heavily reworked material into the assemblage. Specimens accumulating through fluvial processes have low probabilities of association and likely each derive from different individuals (Badgley, 1986b). The high proportion of broken and abraded specimens indicates complex taphonomic histories. Breakage occurred from trampling and carnivore activity, and abrasion and rounding of specimens occurred during trampling or transport in the channel. The elements in these assemblages display a mixture of transportability. Ribs, vertebrae, and scapulae are thin or uniquely shaped with low density, making them the most susceptible elements to winnowing (Voorhies, 1969; Behrensmeyer, 1975). Teeth and long bones are not easily transported but are often found in

channel deposits (Behrensmeyer, 1991). High flow velocities producing splay events move a range of materials, from denser bedload particles (e.g., teeth) to lighter entrained particles (e.g., vertebrae).

Floating carcass

The floating carcass pathway was represented by one nearly complete, articulated camel skeleton (RAM 7648) collected from RAM V200047, which also produced a channel-lag assemblage. RAM 7648 was recovered from coarse to medium sandstone with pebble- to cobble-sized clasts; the elements were hydraulically equivalent with the sediment at this locality.

The skeleton was articulated at the time of collection and was nearly complete, missing the skull, mandible, and several distal forelimb elements (Lofgren and Anand, 2010). A total of 125 elements were present, and most of the skeleton is on display in its jacket, allowing assessment of its posture. Very few elements showed original breakage or abrasion, and weathering stage for all elements was incipient (1 to advanced 1).

The depositional setting of RAM V200047 is a channel margin or bar that also accumulated a lag assemblage of bones in addition to the nearly complete skeleton. Animals drowning during river crossings are not unusual in modern environments, providing a potential mode for the preservation of whole or partial skeletons (Behrensmeyer, 1975). Transport of drowned individuals can occur by either “bloat and float” or as carcasses held together by connective tissues (Martin, 1999). A bloated carcass could be deposited with a lag accumulation if flow velocities drop rapidly, but the carcass might be too buoyant to settle with individual elements moving as bedload. The missing forelimb elements were lost from recent weathering (Lofgren and Anand, 2010), but the skull and mandibles may have been separated before burial. The neck

of RAM 7648 curves under the body, and if present, the head should have been buried and preserved. Other parts of decaying bodies, such as the shoulder girdle and caudal vertebrae, typically detach before the head (Hill, 1979). These elements are present in RAM 7648, and the specimen does not show evidence of scavenging, indicating that it was buried quickly. The head may have been removed during the early stages of decay or by recent weathering. RAM 7648 was deposited with the lag component of RAM V200047 as flow velocities in the channel subsided.

Fossil assemblages

The composition of fossil assemblages can vary among taphonomic pathways and depositional settings. The skeletal-element composition of an assemblage depends on the agents or processes that accumulate or disperse fossil material at the surface. The duration of accumulation and exposure also affects the skeletal-element composition and abundance of material preserved in the assemblage.

Skeletal-element composition

Skeletal-element composition for each taphonomic pathway differed from the composition of the average whole mammal (Fig. 4.6; Table 4.5). The channel-fill pathway had more cranial material and distal podial elements than the average whole mammal; waterhole assemblages were dominated by isolated teeth and distal podial elements. The skeletal-element composition of the carnivore and scavenger pathway was similar to the average whole mammal in having more vertebrae and ribs than other pathways, but it preserved few teeth or limb elements. The channel-lag assemblages were predominantly composed of limb elements and podials, and the

crevasse-splay assemblages were dominated by isolated teeth and limb elements. The floating carcass did not differ significantly from the average whole mammal, except that cranial material was absent (Fig. 4.6). In a Tukey HSD test of all pathway compositions against the average whole mammal composition, all were significantly different ($p < 0.05$; Table 4.6) except the carnivore and scavenger and floating carcass pathways.

Cluster analysis

Clustering is a useful method for visualizing similarities in counts data. The clusters of skeletal-elements in assemblages across 43 localities from the Barstow Formation resulted in three primary clusters (Fig. 4.7) based on abundance and shape of elements. Shape is an important physical property that affects the behavior and survival of skeletal elements in different environments. Clusters based on shape illustrate which elements are most susceptible to environmental sorting. Additionally, the grouping of elements shows which elements typically occur together in assemblages. Together with skeletal-element composition, these analyses are helpful in showing the underlying properties of fossil assemblages that reflect taphonomic pathways.

The three main clusters of elements grouped together primarily by abundance, with group C representing the most common elements across all assemblages, and groups A and B representing rarer elements present at a few localities (Fig. 4.7). Within group C, two main subclusters group elements by shape. The grouping of these different elements suggests that they have similar behavior as physical particles in depositional settings, or they are affected by the same physical processes across assemblages and taphonomic pathways. As this group encompasses the most common elements across assemblages, these elements are preserved at

long-term sites of mortality and accumulate through fluvial processes. Teeth and distal podial elements are small, compact, and durable; these features contribute to their preservation and abundance in fossil assemblages. The movement of skeletal elements in streams is linked to their size, shape, and density (Badgley, 1986a). Elements with irregular shapes are winnowed by currents, and long bones move more slowly as bedload; the sorting of elements by shape and density accounts for the skeletal-element composition of fluvial accumulations (Voorhies, 1969; Behrensmeyer, 1975). The elements in group C represent the most common and abundant elements present in fossil assemblages from the Barstow Formation. The similar shapes and physical properties of these elements contribute to their preservation across depositional settings.

The clustering of cranial elements and proximal limb bones in cluster A is partly based on abundance and partly represents the association of these elements in certain assemblages. Cranial elements (aside from teeth) and proximal limb bones were not as common in fossil assemblages as the elements in cluster C. These elements were, however, more common in channel-fill assemblages (i.e., Steepside Quarry, RAM V94179, Deep Quarry), which produced multiple skulls, maxillae, and dentaries, as well as long bones. Because cranial elements and proximal limb bones are not abundant across all assemblages in the formation, favorable preservation conditions result in the occurrence of cranial elements and proximal limb bones in channel-fill assemblages. The grouping of these elements in cluster A (Fig. 4.7) reflects their common occurrence in the same assemblages.

Cluster B (Fig. 4.7) includes the rarest elements across all assemblages. Ribs and fibulae were the rarest elements in museum collections, due to the low preservation potential of these elements. Ribs are thin elements that are easily broken and scattered by trampling, destroyed by carnivores, or removed from assemblages by winnowing in stream channels (Voorhies, 1969).

Fibulae and pelves are also easily destroyed or winnowed. Radioulnae are included in cluster B, whereas radii and ulnae are part of cluster C (Fig. 4.7). This distinction results from the abundance of disarticulated ungulate radii and ulnae in Barstow assemblages; articulated radioulnae of ungulates were fairly rare elements among assemblages, accounting for their inclusion in this cluster. The elements in cluster B typically occurred in channel-fill assemblages, which had higher overall potential to preserve rare elements.

Principal components analysis of fossil localities

Specimen abundance (axis 1, 0.49) and skeletal-element composition (axis 2, 0.11) determine the distribution of fossil localities on the first two PC axes (Fig. 4.8A; Table 4.7). A cluster of localities with high abundance of specimens reflects the assemblages from channel-fill and waterhole pathways (Fig. 4.8A). There is a large amount of overlap between the assemblages of channel-fill and waterhole pathways, as these pathways account for the majority of assemblages, and these localities produce the majority of specimens. The channel-fill and waterhole pathways are distinguished mostly by differences in skeletal-element composition of assemblages, as illustrated by their distribution along PC 2 and by the loadings for specific elements. The presence of cranial elements and proximal limb bones separates many of the channel-fill assemblages from assemblages in the waterhole and other pathways. The waterhole pathway assemblages are characterized more by distal limb and podial elements, which were the most common elements across assemblages (Fig. 4.7). Assemblages of the other taphonomic pathways are clustered together to the right on PC 1 and are determined by smaller specimen counts, rarer elements, and more fragmentary material.

Depositional settings of fossil assemblages show more differentiation among localities and the assemblages preserved there (Fig. 4.8B). The channel-fill pathway divides into assemblages accumulating in abandoned channels and proximal-channel settings; these settings preserve many specimens and most of the occurrences of cranial elements and proximal limb bones. The waterhole category encompasses localities formed in wetland environments, and waterhole assemblages are divided between wetland settings that were perennially wet or intermittently wet. Localities formed in perennially wet wetland environments significantly overlap with proximal-channel and abandoned channel settings, showing the similarity in skeletal-element composition among these depositional environments. Assemblages from intermittent wetland settings overlap somewhat with assemblages from channel-margin and well-drained floodplain environments, due to similarities in skeletal-element composition of assemblages from these depositional environments.

Discussion

Although relatively few fossil localities were included in this assessment of taphonomic pathways (47 of >400 documented localities in the Mud Hills), these pathways are representative for the modes of fossil accumulation in the Barstow Formation. The majority of fossils examined were deposited in channel-fill and waterhole settings, which represent long-term sites of mortality. The types of bone modification in these assemblages indicate that bones were subjected to a variety of taphonomic processes that concentrated or dispersed bones in these environments. Taphonomic histories of specimens from long-term mortality sites are complex, resulting from the accumulation of skeletal material over long periods of time. Fewer specimens accumulated through purely fluvial processes, although these assemblages also have complex

taphonomic histories of transport, deposition, and burial. Pathways representing long-term sites of mortality and fluvial processes share many characteristics of assemblages and depositional settings.

Long-term sites of mortality

The wealth of material from localities representing channel-fill and waterhole pathways reflects the time-averaged, attritional accumulation of bones on the land surface. These sites represent the depositional environments that were inhabited by the mammals of the Barstow Formation. At long-term sites of mortality, a greater range of skeletal elements is present than in assemblages accumulating through fluvial processes (Table 4.3, Fig. 4.6). The majority of skeletal elements in channel-fill and waterhole settings did not move far from the site of mortality, given the combination of elements with different susceptibility to transport in streams (e.g., long bones, podials, cranial elements; Voorhies, 1969). Time-averaged, autochthonous assemblages such as these accumulate material from many individuals and many taxa over time. In channel-fill and waterhole pathways, skeletal-element compositions were more similar to one another than to the carnivore and scavenger pathway (Fig. 4.6, Table 4.6), but there is a high degree of overlap in the types of taphonomic features documented among assemblages.

Differences in skeletal-element composition between channel-fill and waterhole pathways indicate aspects of the duration of accumulation and biostratinomic processes. Although there is significant overlap in the composition of these pathways (Fig. 4.8A), the channel-fill pathway assemblages are dominated by cranial elements and limb bones, whereas the waterhole-pathway assemblages are dominated by isolated teeth and distal podial elements (Fig. 4.6). The greater abundance of cranial elements and long bones, as well as the greater abundance of articulated

and associated material at channel-fill localities than at waterhole localities (Table 4.3), indicates that remains were buried more quickly in channel-fill settings. Some fluvial sorting of material may have occurred at the channel-fill localities, as easily winnowed elements (i.e., vertebrae, ribs) are uncommon in these assemblages. These elements may also have been destroyed or removed by carnivores.

The low abundance of articulated and associated material from waterhole settings indicates that remains stayed at the surface, subject to scavenging, scattering, and trampling, for longer periods of time before burial. The pronounced abundance of teeth and podial elements over all other elements reflects the greater duration of accumulation. The composition of an assemblage changes over time as a result of the taphonomic agents acting at the surface. Limb bones and ribs are easily broken and fragmented during trampling or predation, whereas teeth, podials, and phalanges resist degradation and destruction from carnivores and scavengers (Behrensmeyer and Dechant Boaz, 1980). The abundance of isolated teeth and phalanges (particularly of equids) represents the extreme sorting of the remains of many individuals over long periods of time (months to hundreds of years). Although weathering stages of elements in this pathway range from incipient to advanced (1 to 3; Table 4.3), most elements display incipient stages of weathering; either these bones were buried quickly or the most weathered remains were destroyed prior to burial. Heavily weathered bone is brittle and is easily broken (Behrensmeyer, 1978). Small elements such as podials and teeth are easily buried in mud from trampling (Behrensmeyer and Dechant Boaz, 1980), perhaps contributing to the abundance of this material in waterhole assemblages.

The carnivore and scavenger pathway more closely resembles the skeletal-element composition of the average whole mammal (Table 4.5). This similarity is due to the preservation

of partial skeletons at Saucer Butte Quarry, which increased representation of vertebrae and ribs in the assemblages. Selective sorting of remains also influences the distribution of skeletal elements in this category. Predators and scavengers often remove limbs and sometimes carry them great distances (Behrensmeyer, 1975; Hill, 1980), perhaps accounting for the under-representation of distal elements in these assemblages (Fig. 4.6). Fewer specimens and a less diverse range of elements separate the carnivore and scavenger assemblages from channel-fill and waterhole assemblages (Fig. 4.8A). The abundance of fragmentation, breakage patterns, and bone modification of the assemblages further distinguishes the carnivore and scavenger pathway from the channel-fill and waterhole pathways. Tooth marks, however, were also abundant in the waterhole pathway assemblages. Both herbivores and carnivores tend to congregate around water sources, increasing interactions and predation (Behrensmeyer, 1975). Predation and scavenging likely occurred in many environments, but taphonomic features indicative of these interactions are diluted by the amount of material accumulating through other attritional processes. The abundance and concentration of material showing bone modification and breakage patterns consistent with carnivore damage is distinct in the carnivore and scavenger assemblages compared to other pathways.

Fluvial accumulations

Fossil assemblages resulting from fluvial processes have a broad range of taphonomic characteristics and preservation modes, from articulated skeletons to isolated fragments (Behrensmeyer, 1988). In this regard, they share taphonomic patterns with the carnivore and scavenger assemblages (Fig. 4.8A), but they are not fragmented to the same degree. Fluvial accumulation pathways have distinct distributions of elements and features (Table 4.3, Fig.

4.8A). Relatively little fossil material from these pathways is represented in museum collections from the Barstow Formation. Most fossil material from the formation accumulated at long-term sites of mortality rather than through fluvial processes, and fossil material may not have been as well preserved in these depositional settings.

Aside from the floating carcass pathway, all pathways accumulating primarily due to fluvial processes were significantly different than the average whole mammal (Fig. 4.6, Table 4.5). Skeletal elements in both the channel-lag and crevasse-splay pathways are highly sorted, but the crevasse-splay assemblages have more elements, especially those that are susceptible to fluvial winnowing from an average whole mammal. The overall distribution of skeletal elements is very similar between the channel-lag and crevasse-splay pathways, and these pathways are not significantly different from one another ($p > 0.1$; Table 4.7); both assemblages have a large number of limb bones, podials, and metapodials represented (Fig. 4.6). The higher number of specimens from the crevasse-splay localities rounds out the distribution of elements in this pathway compared to the small sample of elements represented in the channel-lag assemblages. Many of these specimens are elements (vertebrae, ribs, girdle elements) that are typically winnowed from skeletal remains in fluvial settings. The processes that produce splays contribute to the mixing of elements with different susceptibility to transport. The skeletal-element composition of the two crevasse-splay localities included here differ somewhat, as one includes more limb bone fragments and the other has more axial material. The skeletal-element composition of assemblages in crevasse-splay deposits should be highly variable from assemblage to assemblage. This variability would depend on the sinuosity of the stream, the geometry of the fluvial channel, the size of the splay, and where the splay is sampled along its distributary. Elements should sort by density along the splay, such that more easily transported

elements would be carried further by waning flows and deposited at the distal margins of the splay.

Assemblages from the channel-lag pathway are the most distinct from the composition of the average whole mammal (Fig. 4.6, Table 4.5), and the most abundant elements in an average mammal skeleton are missing from the channel-lag assemblages. It is surprising that teeth are absent from the channel-lag assemblages, as teeth are small, durable components common in lag deposits (Behrensmeyer, 1991). The geometry of the stream bed could affect where elements of different densities come to rest during waning flow. Similar to the sorting expected in crevasse-splay deposits, stream beds or bar forms should accumulate elements of different sizes and densities during different stages of flow. Dense elements such as teeth may concentrate in the thalweg of channels (true lag deposits), whereas lighter elements or carcasses may get stranded on emergent bars as flow subsides. The overall paucity of specimens attributed to the channel-lag pathway is another possible factor contributing to the absence of teeth and other small elements such as phalanges that might be expected in lag deposits. Collecting bias may affect the distribution of skeletal elements in the channel-lag pathway. Fragmentary or unidentifiable material is often not collected, and specimens representing channel-lag assemblages may be under-represented in museum collections.

Depositional settings of fossil assemblages

The depositional settings in which bones accumulate affect the preservation potential of fossils and the completeness and quality of preservation of the fossil assemblage. Some taphonomic pathways are related to specific environments of deposition, whereas other pathways are related to processes and agents that operate across the landscape and across environments of

deposition. Fossil assemblages show important variation within taphonomic pathways when their depositional environments are compared.

Loughney and Badgley (2017) divided the depositional settings of 64 fossil localities in the Barstow Formation into six categories based on paleolandscape position. There were broad differences in weathering stages and abrasion among depositional categories, related to sedimentary processes and duration of accumulation in these settings. These categories reflect the variation in depositional settings and drainage characteristics of localities more directly than do the taphonomic pathways. Depositional categories also indicate how fossil assemblages are affected by landscape position (Fig. 4.8B).

For the 47 localities evaluated here, I grouped their depositional settings into seven categories: abandoned channel, channel and channel margin, proximal channel, poorly drained floodplain, well-drained floodplain, perennial wetland, and intermittent wetland. The primary effect of coding fossil localities by depositional category is to reveal the variation in assemblages from the major taphonomic pathways: the channel-fill pathway separates into abandoned-channel and proximal-channel localities, and the waterhole pathway separates into perennial and intermittent wetland localities.

There remains a lot of overlap among fossil assemblages when coded for depositional setting, but differences within taphonomic pathways are more pronounced (Fig. 4.8B). The largest differences in skeletal-element composition and abundance among depositional settings are due to drainage and proximity to the channel. Localities deposited in or near channel margins have similar assemblages to localities deposited in perennially wet wetlands. Assemblages from abandoned-channel and perennial-wetland deposits have more cranial material than other localities. Localities in proximal-channel settings and intermittent wetlands account for most of

the axial and appendicular material (Fig. 4.8B). Channel-margin and poorly drained wetland settings preserve the least amount of fossil material, and few localities examined here occur in these settings. Material from these localities is also more fragmentary than material from other depositional settings.

Localities in poorly drained settings have more cranial and limb elements than localities in better drained settings, and poorly drained environments also tend be closer to channels. Depositional settings close to active channels, such as abandoned channels, are common sites for fossil preservation. The sporadic input of sediment to abandoned channels keeps pace with bone input, burying bones before they are destroyed by surface processes (Behrensmeyer, 1988). Perennially wet environments have variable potential to preserve bones, often relating to pH and abundance of organic matter (Martin, 1999). Wet and vegetated environments attract animals, and skeletal remains concentrate in low-lying areas (Behrensmeyer, 1991; Therrien and Fastovsky, 2000). If sedimentation rates are high due to flooding or proximity to channels, bones are preserved in these settings. Bones in moist, soft sediments can also be buried by trampling (Behrensmeyer and Dechant Boaz, 1980). Connective tissues degrade more easily in wet environments, contributing to disarticulation (Hill, 1979), and disassociated or isolated elements may be more common in wetland settings.

In the well-drained environments of the Barstow Formation, assemblages experienced more sorting by physical and biological agents. Intermittent wetlands and well-drained floodplain settings have more isolated teeth and distal podial elements. Alternating wet-dry cycles contribute to bone weathering and destruction at the surface (Behrensmeyer, 1978), and weathered bones are more easily broken (Behrensmeyer, 1991). In intermittent wetland settings, wet-dry cycles could affect the taphonomic features of bone assemblages. During wet phases,

animals congregate around the water source, submerged carcasses disarticulate, and bones are buried by trampling or flooding; during dry phases, exposed bones crack and flake, and dry bones are scattered and broken by trampling. Sedimentation rates may have been low in intermittent wetland environments far from active channels, and bones at the surface may be subject to sorting from scavenging and trampling and scattering over long periods of time. Teeth and distal podial elements are durable and resist trampling more easily than more fragile bones, resulting in greater proportions of these elements in dry and intermittently dry settings.

There is a range of preservation and abundance of material across localities in all depositional categories. All depositional categories have localities that produce mostly fragmentary material as well as localities that produce complete or articulated material. Fossil assemblages preserved in channel and channel-margin and poorly drained floodplain environments are on the whole more fragmentary and preserve fewer types of elements than other environments. Abundance of material also varies greatly among localities within depositional categories.

The relationships between depositional environment and taphonomic pathways are intuitive. Abandoned channels, proximal channels, wetlands, and floodplains are all typical settings for long-term sites of mortality. Most fossil localities from the Barstow Formation formed in these environments, and assemblages accumulated through the channel-fill and waterhole taphonomic pathways. These pathways accumulated attritional, time-averaged assemblages, and the different depositional and taphonomic conditions in each environment preserved different parts of these assemblages. Proximal-channel, wetland, and floodplain settings overlap with channel and channel-margin environments where fluvial processes also concentrated fossil material.

Assemblages in these environments were more fragmentary than assemblages in the other settings.

Characteristics of fossil assemblages vary over the landscape with transitions in depositional environment. Systematic variation in taphonomic assemblages among facies has been identified in many formations, including the Cretaceous Two Medicine and Judith River formations in Montana (Rogers and Kidwell, 2000), the Eocene Willwood Formation of Wyoming (Bown and J. Kraus, 1981), and the Miocene Siwalik sequence of Pakistan (Badgley, 1986a). In the Barstow Formation, taphonomic patterns are related to broad changes in depositional environment with the evolution of the basin. Individual localities were subject to local variation in sedimentation rate, vegetation cover, and drainage. These controls vary among and within depositional settings and determine preservation potential and quality of fossil assemblages. As local environments and landscapes change over time, the taphonomic characteristics of fossil assemblages should vary with depositional environments that change in response to tectonics and climate.

Distribution of taphonomic pathways among facies associations

Taphonomic pathways are unevenly distributed among the facies associations of the Barstow Formation (Table 4.4), and their distribution follows changes in depositional environments. Localities in FA 1, FA 3, and FA 4 have assemblages that accumulated only through channel-fill and channel-lag pathways. Localities in FA 5 and FA 6 have assemblages that formed through all taphonomic pathways. The deposition of the facies associations relates to the change in environments as subsidence in the basin decreased, sediment-accumulation rates decreased, and accommodation declined (Loughney and Badgley, 2017). During the evolution of the basin, moisture patterns and vegetation were affected by climate change associated with the Middle

Miocene Climatic Optimum (Loughney et al., in prep; Chapter 3). Against the backdrop of changing environments in the basin, taphonomic patterns changed as well (Fig. 4.9).

The majority of channel-fill localities occur in FA 3 and FA 4. The dominance of this pathway in these facies associations is directly related to the fluvial deposits that characterize FA 3 and FA 4. The depositional settings of individual localities differ somewhat among FA 1, FA 3, and FA 4 and are related to the types of streams that existed in the Barstow Basin at the time of deposition. FA 1 is dominated by coarse sandstones and conglomerates representing stream channels and bars of alluvial fans, sequences of sandstone and mudstone in FA 3 represent channel and proximal-channel floodplain deposits of meandering streams, and the amalgamated sandstone beds of FA 4 represent channel and bar deposits of braided streams (Loughney and Badgley, 2017; Chapter 2). These environments were present in the Barstow Basin during the early and middle parts of its history. Long-term sites of mortality were at channel margins and abandoned channels, and fluvial processes sorted, winnowed, and reworked bones in these channel systems.

As sedimentation and subsidence slowed (Chapter 2) and the climate became drier and cooler (Chapter 3), environments and landscapes in the Barstow Formation changed (Fig. 4.9). Deposits representing channels, poorly drained floodplains, and perennial wetlands in FA 5 interfinger with the deposits of FA 6, which represent channels, well-drained floodplains, and intermittent wetlands. Animals continued to frequent channel margins and continued to be preserved in those settings, but the landscape and depositional environments were more heterogeneous. Channel margins continued to be long-term sites of mortality, and wetland environments represented additional habitats that attracted mammals over long periods of time. As the climate cooled and became drier, animals congregated near sources of water, and carnivore and scavenger activity

was concentrated in these areas. Lower rates of sediment accumulation in these facies associations (Fig. 4.9; Chapter 2) allowed bones to accumulate over longer periods of time, resulting in more time-averaged assemblages than those in FA 3 or FA 4.

The behaviors of animals and processes of fossil accumulation were not substantially different between the middle part of the Barstow Formation and the upper part of the formation. More heterogeneous landscapes in the upper part of the formation created many more opportunities for fossil preservation under varying local depositional conditions. More diverse taphonomic pathways are detectable in the fossil assemblages from FA 5 and FA 6 because landscapes were able to capture greater variation of biological activities and physical processes than in FA 1, FA 3, or FA 4. Landscape plays an important role in determining the distribution of plants and animals, depositional settings, and taphonomic processes.

Conclusion

The taphonomic history of a fossil locality encompasses aspects of landscape, depositional setting, physical surface processes, and biological agents. The means by which fossils accumulate on the landscape often are influenced by the behavior of animals and the physical processes operating in the depositional setting. Animals congregate near food and water sources, determining which environments their remains are deposited in and the taxonomic composition of the assemblage. Fluvial processes winnow or concentrate specific elements, and local sedimentation rates and cycles vary among depositional environments, affecting burial of remains and duration of accumulation. These factors combine in different ways on different parts of the landscape, such that some depositional environments accumulate and bury bones rapidly

(e.g., abandoned channels) and others are places where bones are exposed to scattering and destruction at the surface (e.g., well-drained floodplain).

Heterogeneous landscapes increase the chances of preserving fossils by increasing the number of microhabitats available to accumulate and bury remains. In the Barstow Formation, early forming environments were fairly homogeneous across the basin, and the sedimentological processes were as well. Channels of alluvial fans in FA 1 had some ability to preserve vertebrate fossils, and the playa lakes of FA 2 were not conducive to the preservation of bone. (Lake margins were, however, excellent for preserving animal trackways). Fluvial environments of FA 3 and FA 4 created more opportunities for fossil preservation in abandoned channels and in proximal-floodplain settings. Animals lived in these habitats, and local sedimentation rates were high enough to bury bones regularly. The stable, longer-lived floodplain and wetland environments of FA 5 and FA 6 formed landscapes that were more diverse in terms of sedimentary environments and vegetation than had existed earlier in the basin. The spatial distribution of depositional environments and taphonomic processes created many potential locations for bones to accumulate. Lower sedimentation rates in the basin during this time allowed environments to accumulate large amounts of attritional material around permanent or intermittent water sources.

The change in environments in the Barstow Formation from alluvial fans and playa lakes to streams and floodplains over time reflect the climate and the tectonic evolution of the basin. With this change in depositional environments, preservation potential increased, local landscapes became more heterogeneous, and taphonomic processes became more diverse. A wide range of depositional settings and taphonomic processes led to the preservation of a wider range of plants and animals and more detailed records of paleoecosystems. Different depositional settings and

taphonomic pathways preserve different aspects of faunal assemblages, including skeletal-element and taxonomic composition, which may reflect predictable patterns of preservation across fossil-bearing sequences. Understanding how taphonomy changes through a formation is crucial for studying the composition and ecology of the fauna and flora and the patterns of turnover that are the basis for reconstructions of biostratigraphy, biogeography, and evolution.

Acknowledgments

Thank you to Bob Reynolds, Mike Woodburne, Don Lofgren, and Ev Lindsay for providing help and resources for accessing and locating fossil localities in the field. I also appreciate the help and assistance of Rachel Thorpe, Catherine Badgley, Tara Smiley, and Anna Harkness in the field. Thank you to Pat Holroyd and Diane Erwin at UCMP, Andy Farke and Gabe Santos at RAM, Ian Gilbert and Melissa Russo at SBCM, and Judy Galkin at AMNH for granting access to museum collections and providing resources during my visits. Thank you to Catherine Badgley for guidance throughout the course of this study.

References

Abersek, W.F., and Lofgren, D.L., 2017, Biostratigraphy of nonmarine Miocene gastropods from the Barstow Formation of California, *in* Reynolds, R.E., ed., ECSZ Does It: Revisiting the Eastern California Shear Zone: The 2017 Desert Symposium Field Guide and Proceedings: Zzyzx, California, California State University Desert Studies Consortium, p. 229-234.

Badgley, C., 1982, Community reconstruction of a Siwalik mammalian assemblage [Ph.D. dissertation]: Yale University, 364 p.

Badgley, C., 1986a, Taphonomy of mammalian fossil remains from Siwalik rocks of Pakistan: Paleobiology, v. 12, no. 2, p. 119-142.

Badgley, C., 1986b, Counting individuals in mammalian fossil assemblages from fluvial environments: PALAIOS, v. 1, no. 3, p. 328-338.

Behrensmeyer, A.K., 1975, The taphonomy and paleoecology of Plio-Pleistocene vertebrate assemblages east of Lake Rudolf, Kenya: Bulletin of the Museum of Comparative Zoology, v. 146, no. 10, p. 473-578.

Behrensmeyer, A.K., 1978, Taphonomic and ecologic information from bone weathering: Paleobiology, v. 4, p. 150-162.

Behrensmeyer, A.K., and Dechant Boaz, D.E., 1980, The recent bones of Amboseli Park, Kenya, in relation to East African paleoecology, *in* Behrensmeyer, A.K., and Hill, A.P., eds., Fossils in the Making: Vertebrate Taphonomy and Paleoecology: Chicago, University of Chicago Press, p. 72-92.

Behrensmeyer, A.K., 1982, Time resolution in fluvial vertebrate assemblages: Paleobiology, v. 8, no. 3, p. 211-227.

Behrensmeyer, A.K., 1988, Vertebrate preservation in fluvial channels: Palaeogeography, Palaeoclimatology, Palaeoecology, v. 63, no. 1–3, p. 183-199.

Behrensmeyer, A.K., 1991, Terrestrial vertebrate accumulations, *in* Allison, P.A., and Briggs, D.E.G., eds., Taphonomy: Releasing the Data Locked in the Fossil Record, Volume 9: New York, Plenum Press, p. 291-335.

Bown, T.M., and J. Kraus, M., 1981, Vertebrate fossil-bearing paleosol units (Willwood Formation, Lower Eocene, Northwest Wyoming, U.S.A.): Implications for taphonomy, biostratigraphy, and assemblage analysis: Palaeogeography, Palaeoclimatology, Palaeoecology, v. 34, no. Supplement C, p. 31-56.

Brain, C.K., 1980, Some criteria for the recognition of bone-collecting agencies in African caves, *in* Behrensmeyer, A.K., and Hill, A.P., eds., Fossils in the Making: Vertebrate Taphonomy and Paleoecology: Chicago, University of Chicago Press, p. 107-130.

Bridge, J.S., 2003, Rivers and Floodplains: Forms, Processes, and the Sedimentary Record: Oxford, Blackwell Publishing, 491 p.

Browne, I.D., 2002, Late Barstovian mammalian fauna of the Robbin's Quarry (Barstow Formation, San Bernardino County, California) [M.S. thesis]: University of California, Riverside, 111 p.

Dokka, R.K., 1989, The Mojave Extensional Belt of southern California: Tectonics, v. 8, no. 2, p. 363-390.

Fernández-Jalvo, Y., and Andrews, P., 2016, Atlas of Taphonomic Identifications: 1001+ Images of Fossil and Recent Mammal Bone Modification: Dordrecht, Springer, Vertebrate Paleobiology and Paleoanthropology Series.

Genise, J.F., 2000, The ichnofamily Celliformidae for Celliforma and allied ichnogenera: Ichnos, v. 7, no. 4, p. 267-282.

Glazner, A.F., Walker, J.D., Bartley, J.M., and Fletcher, J.M., 2002, Cenozoic evolution of the Mojave block of southern California: Geological Society of America Memoirs, v. 195, p. 19-41.

Hill, A., 1979, Disarticulation and scattering of mammal skeletons: Paleobiology, v. 5, no. 3, p. 261-274.

Hill, A.P., 1980, Early postmortem damage to the remains of some contemporary East African mammals, *in* Behrensmeyer, A.K., and Hill, A.P., eds., Fossils in the Making: Vertebrate Taphonomy and Paleoecology: Chicago, University of Chicago Press, p. 131-152.

Ingersoll, R.V., Devaney, K.A., Geslin, J.K., Cavazza, W., Diamond, D.S., Heins, W.A., Jagiello, K.J., Marsaglia, K.M., Paylor, E.D., II, and Short, P.F., 1996, The Mud Hills, Mojave Desert, California: Structure, stratigraphy, and sedimentology of a rapidly extended terrane, *in* Beratan, K.K., ed., Reconstructing the History of Basin and Range Extension Using Sedimentology and Stratigraphy, Volume 303: Boulder, Colorado, Geological Society of America, p. 61-84.

Kidwell, S.M., 1986, Models for fossil concentrations: Paleobiologic implications: Paleobiology, v. 12, no. 1, p. 6-24.

Legendre, P., and Legendre, L., 2012, Developments in Environmental Modelling: Amsterdam, Elsevier, 968 p.

Lindsay, E.H., 1972, Small mammal fossils from the Barstow Formation, California: University of California Publications in Geological Sciences, v. 93, p. 1-104.

Lofgren, D.L., and Anand, R.S., 2010, 75 years of fieldwork in the Barstow Formation by the Raymond Alf Museum of Paleontology, *in* Reynolds, R.E., and Miller, D.M., eds., Overboard in the Mojave: 20 Million Years of Lakes and Wetlands: The 2010 Desert Symposium Abstracts and Proceedings: Zzyzx, California, California State University Desert Studies Consortium, p. 169-176.

Lofgren, D.L., Kwon, C., Todd, J., Marquez, S., Holliday, A., Stoddard, R., and Kloess, P., 2014, Preliminary analysis of an important vertebrate-bearing horizon with abundant avian material from the Upper Member of the Barstow Formation of California, *in* Reynolds, R.E., ed., Not a Drop Left To Drink: The 2014 Desert Symposium Field Guide and Proceedings: Zzyzx, California, California State University Desert Studies Consortium, p. 155-164.

Loughney, K.M., and Badgley, C., 2017, Facies, environments, and fossil preservation in the Barstow Formation, Mojave Desert, California: PALAIOS, v. 32, no. 6, p. 396-412.

MacFadden, B.J., Swisher, C.C., III, Opdyke, N.D., and Woodburne, M.O., 1990, Paleomagnetism, geochronology, and possible tectonic rotation of the middle Miocene Barstow Formation, Mojave Desert, southern California: GSA Bulletin, v. 102, no. 4, p. 478-493.

Maechler, M., Rousseeuw, P., Struyf, A., Hubert, M., and Hornik, K., 2017, Cluster: Cluster Analysis Basics and Extensions.

Martin, R.E., 1999, Taphonomy: A Process Approach: Cambridge, U.K., Cambridge University Press, 508 p.

McQuarrie, N., and Wernicke, B.P., 2005, An animated tectonic reconstruction of southwestern North America since 36 Ma: Geosphere, v. 1, no. 3, p. 147-172.

Merriam, J.C., 1919, Tertiary mammalian faunas of the Mohave Desert: University of California Publications Bulletin of the Department of Geological Sciences, v. 11, no. 5, p. 437-585.

Miller, D.M., Leslie, S.R., Hillhouse, J.W., Wooden, J.L., Vazquez, J.A., and Reynolds, R.E., 2010, Reconnaissance geochronology of tuffs in the Miocene Barstow Formation: Implications for basin evolution and tectonics in the central Mojave Desert, *in* Reynolds, R.E., ed., 2010 Desert Symposium: California State University Desert Studies Center, Zzyzx, California, California State University Desert Studies Consortium, p. 70-84.

Miller, D.M., Rosario, J.E., Leslie, S.R., and Vazquez, J.A., 2013, Paleogeographic insights based on new U-Pb dates for altered tuffs in the Miocene Barstow Formation, California, *in* Reynolds, R.E., ed., Raising Questions in the central Mojave Desert: The 2013 Desert Symposium Field Guide and Proceedings: Zzyzx, California, California State University Desert Studies Consortium, p. 31-38.

Oksanen, J.F., Blanchet, G., Friendly, M., Kindt, R., Legendre, P., McGlinn, D., Minchin, P.R., O'Hara, R.B., Simpson, G.L., Solymos, P., Stevens, M.H.H., Szoecs, E., and Wagner, H., 2017, Vegan: Community Ecology Package.

Pagnac, D., 2009, Revised large mammal biostratigraphy and biochronology of the Barstow Formation (Middle Miocene), California: PaleoBios, v. 29, no. 2, p. 48-59.

Pagnac, D., Browne, I., and Smith, K., 2013, Stratigraphy and vertebrate paleontology of the middle Miocene Barstow Formation, San Bernardino County, California, *in* Proceedings 73rd Annual Meeting of the Society of Vertebrate Paleontology, Los Angeles, California, 29 October 2013, p. 1-26.

Rogers, R.R., and Kidwell, S.M., 2000, Associations of vertebrate skeletal concentrations and discontinuity surfaces in terrestrial and shallow marine records: A test in the Cretaceous of Montana: The Journal of Geology, v. 108, no. 2, p. 131-154.

Rogers, R.R., and Kidwell, S.M., 2007, A conceptual framework for the genesis and analysis of vertebrate skeletal concentrations, *in* Rogers, R.R., Eberth, D.A., and Fiorello, A.R., eds., Bonebeds: Genesis, Analysis, and Paleobiological Significance: Chicago, University of Chicago Press, p. 1-63.

Singleton, J.S., and Gans, P.B., 2008, Structural and stratigraphic evolution of the Calico Mountains: Implications for early Miocene extension and Neogene transpression in the central Mojave Desert, California: Geosphere, v. 4, no. 3, p. 459-479.

Therrien, F., and Fastovsky, D.E., 2000, Paleoenvironments of early theropods, Chinle Formation (Late Triassic), Petrified Forest National Park, Arizona: PALAIOS, v. 15, p. 194-211.

Vaughan, T.A., Ryan, J.M., and Czaplewski, N.J., 2015, Mammalogy: Burlington, Massachussetts, Jones & Bartlett Learning, 755 p.

Voorhies, M.R., 1969, Taphonomy and population dynamics of an early Pliocene vertebrate fauna, Knox County, Nebraska: University of Wyoming Contributions to Geology Special Papers, v. 1, p. 1-69.

Weigelt, J., 1989, Recent Vertebrate Carcasses and their Paleobiological Implications: Chicago, University of Chicago Press, 188 p.

Woodburne, M.O., Tedford, R.H., and Swisher, C.C., III, 1990, Lithostratigraphy, biostratigraphy, and geochronology of the Barstow Formation, Mojave Desert, southern California: GSA Bulletin, v. 102, p. 459-477.

Woodburne, M.O., 1996, Precision and resolution in mammalian chronostratigraphy: Principles, practices, examples: Journal of Vertebrate Paleontology, v. 16, no. 3, p. 531-555.

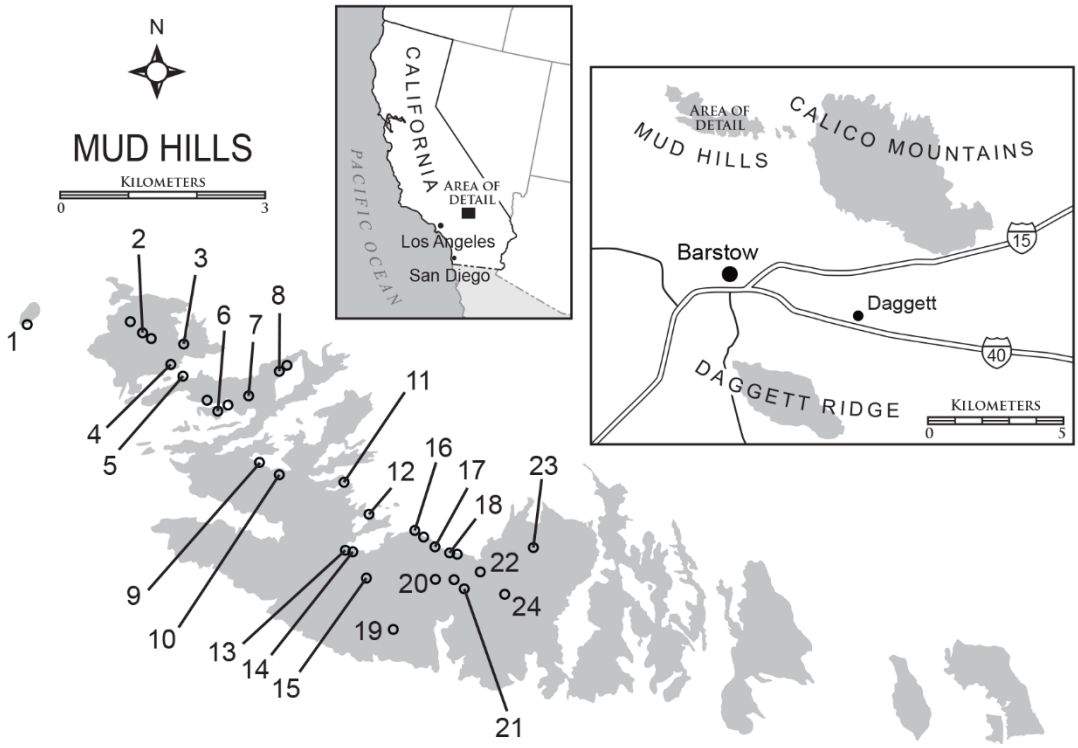

Figure 4.1. Location map of the Barstow Formation in the Mud Hills, California, with locations of fossil localities shown in Figure 4.2. Modified from Loughney and Badgley (2017). 1 = 1.130.421; 2 = MMR-029, MMR-051, MMR-043; 3 = Margo Quarry; 4 = UCMP V6448; 5 = UCMP V6447; 6 = Rodent Hill Basin; 7 = Leader Quarry, Sunnyside Quarry; 8 = Robbins Quarry, Hidden Hollow Quarry; 9 = Lake Bed, RAM V200047; 10 = RAM V98004, Slugbed; 11= *Hemicyon* Quarry; 12 = Easter Quarry; 13 = Steepside Quarry, Sunset Quarry; 14 = Oreodont Quarry, Turbon Quarry; 15 = Rak Quarry; 16 = Hailstone Quarry; 17 = May Day Quarry, New Year Quarry, MMR-049; 18 = Skyline Quarry, Starlight Quarry; 19 = Red Division Quarry; 20 = Deep Quarry; 21 = Camp Quarry; 22 = Valley View Quarry; 23 = Saucer Butte Quarry; 24 = Sunder Ridge.

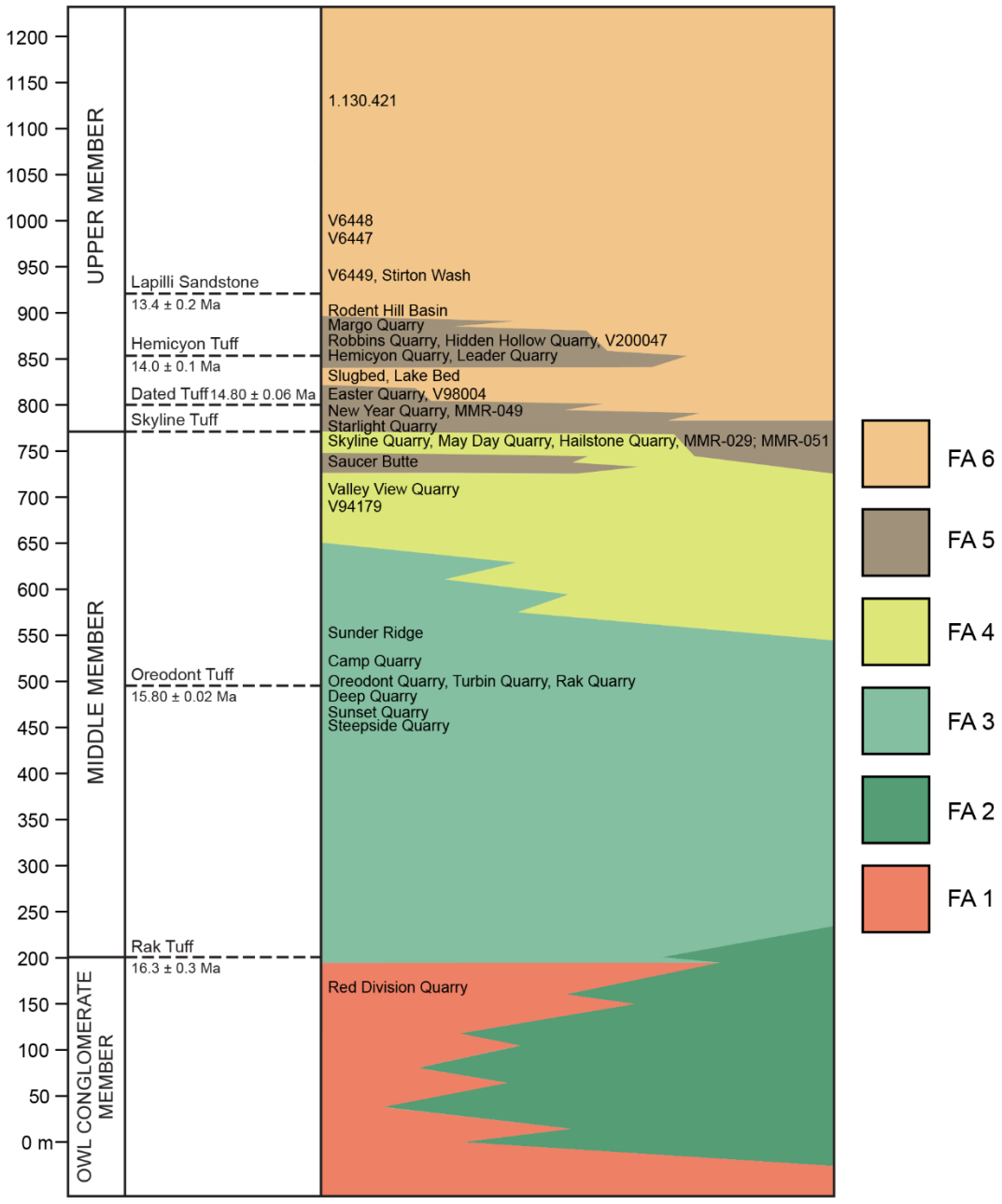

Figure 4.2. Stratigraphy of the Barstow Formation showing showing dated tuff units (MacFadden et al., 1990), relationships of facies associations, and stratigraphic positions of fossil localities in Figure 4.1.

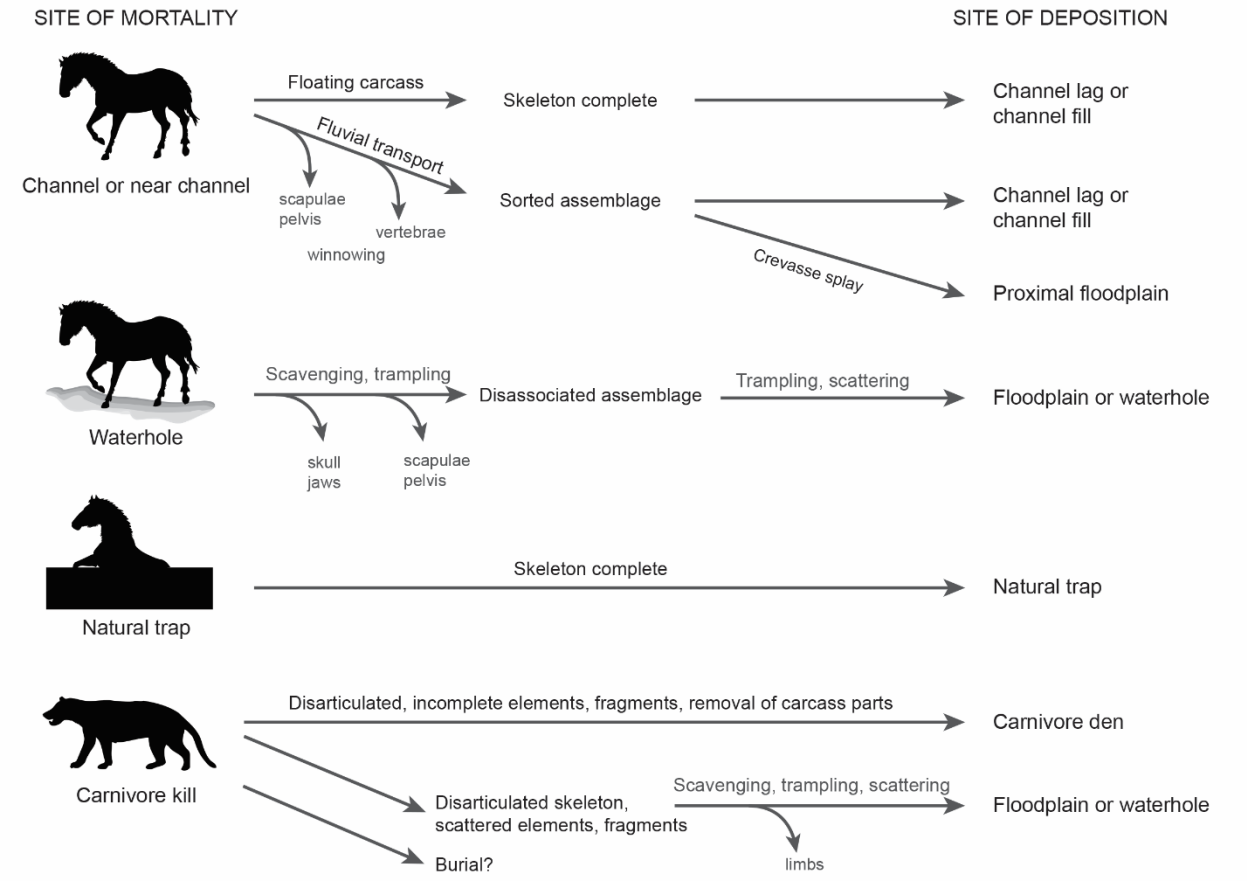

Figure 4.3. Schematic diagram of hypothetical taphonomic pathways through which fossil assemblages may accumulate, showing how composition of assemblages may be affected by taphonomic processes.

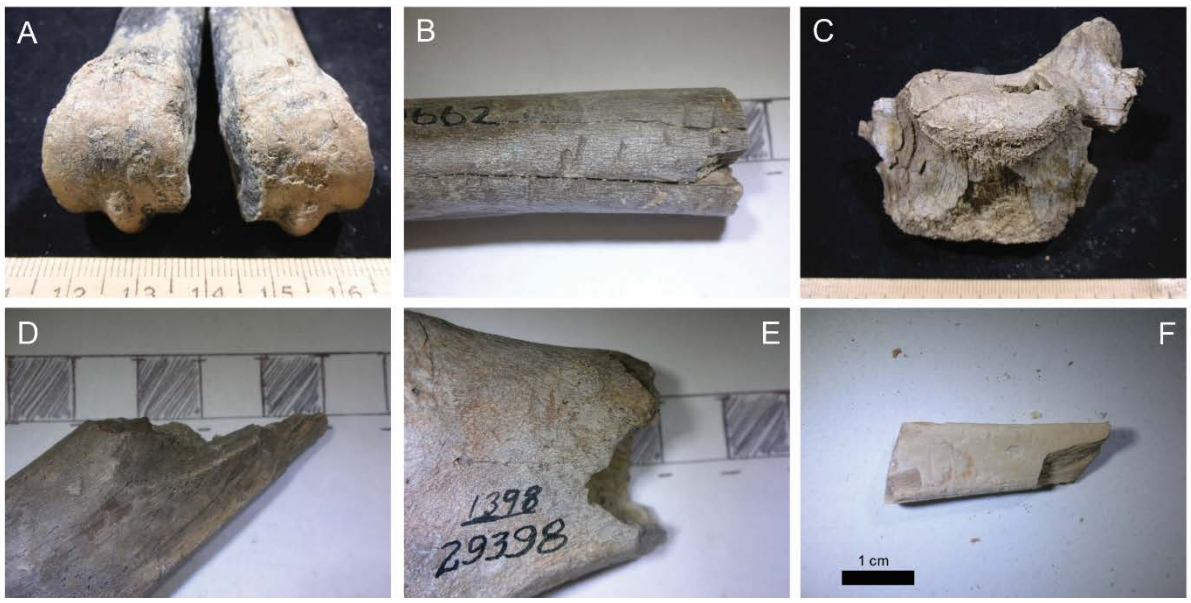

Figure 4.4. Examples of taphonomic features of fossils. A) Pitting and abrasion from impacts with sediment grains; B) Trample marks; C) Abrasion and weathering; D) Breakage; E) Damage from chewing by carnivores; F) Tooth marks.

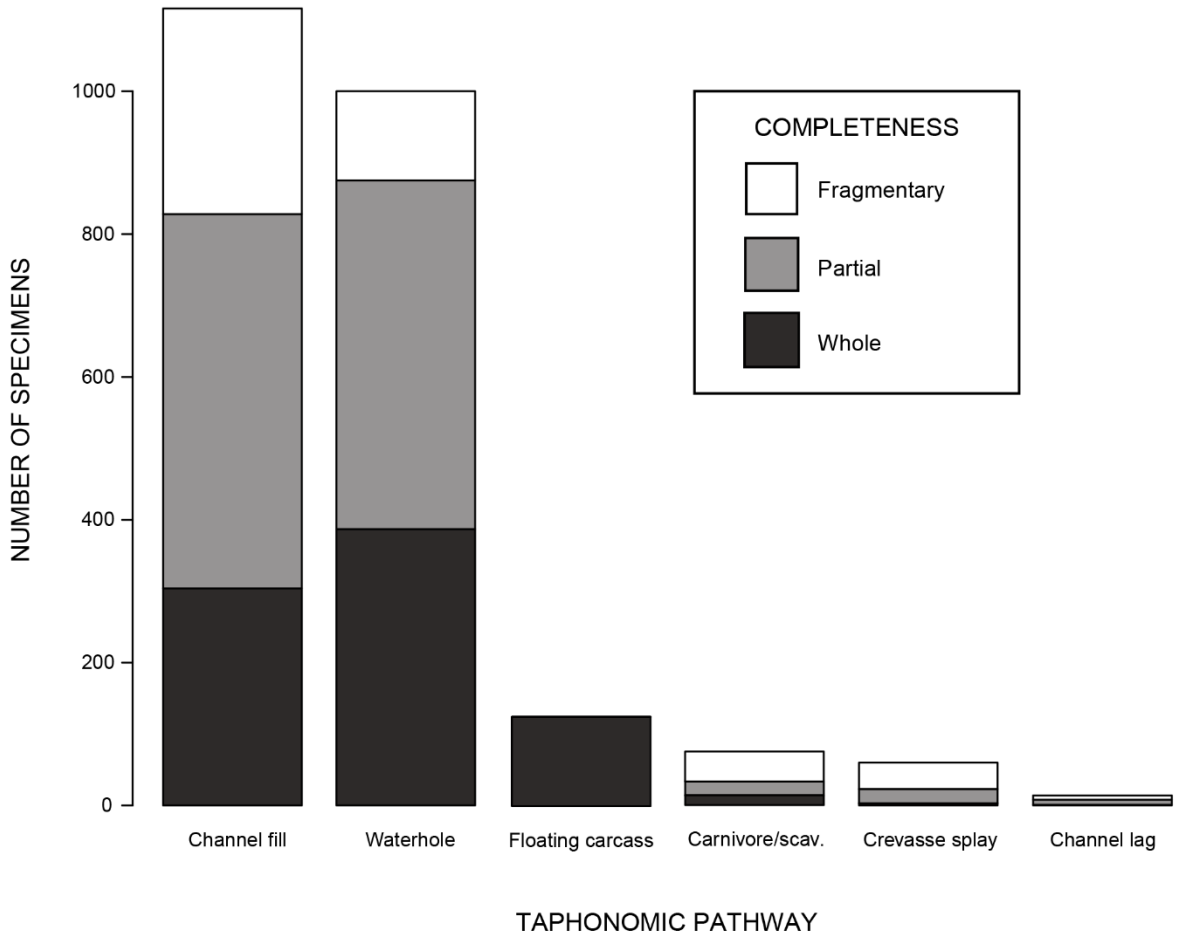

Figure 4.5. Element completeness by taphonomic pathway.

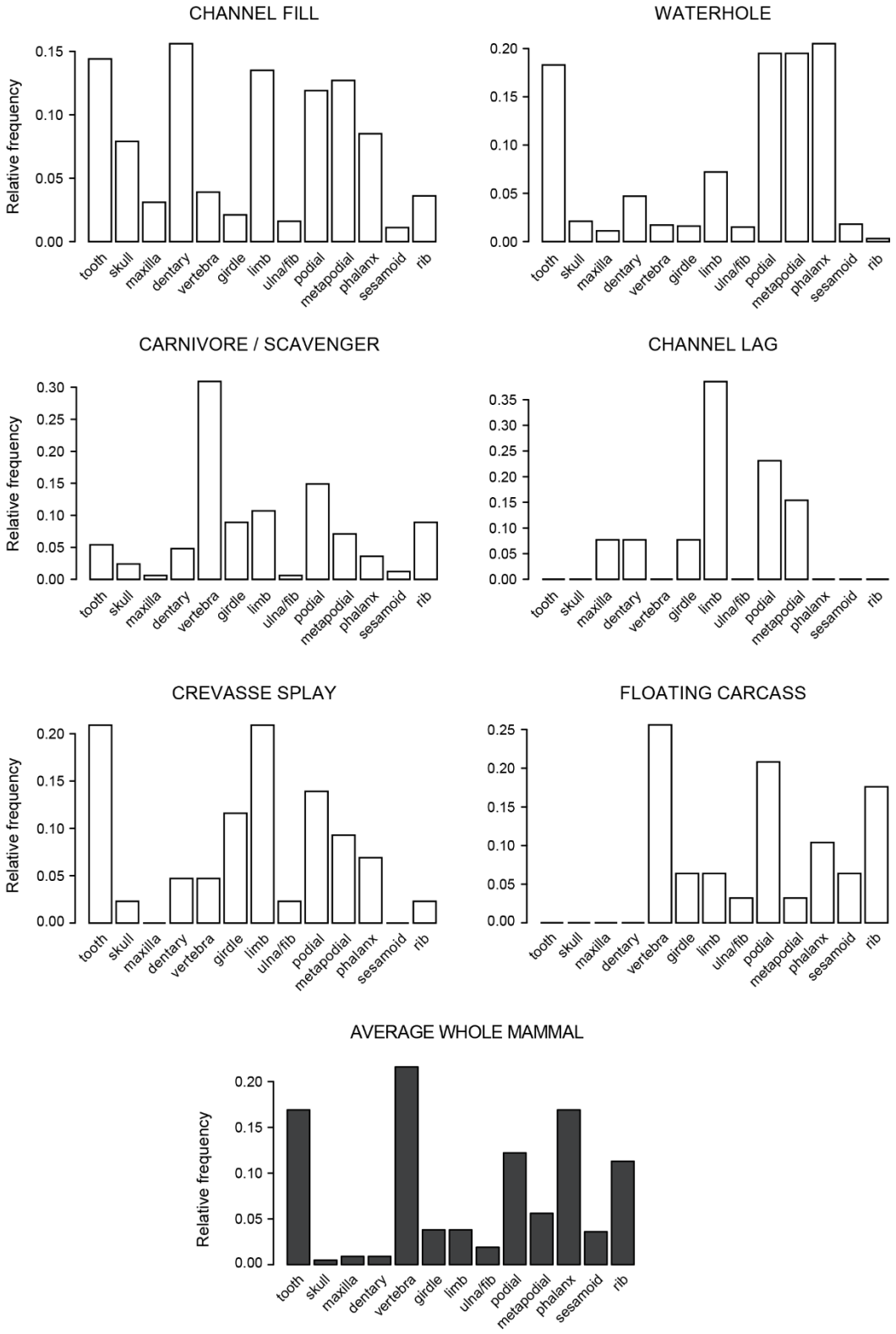

Figure 4.6. Skeletal-element composition of taphonomic pathways compared against skeletal-element composition of an average whole mammal with 213 elements.

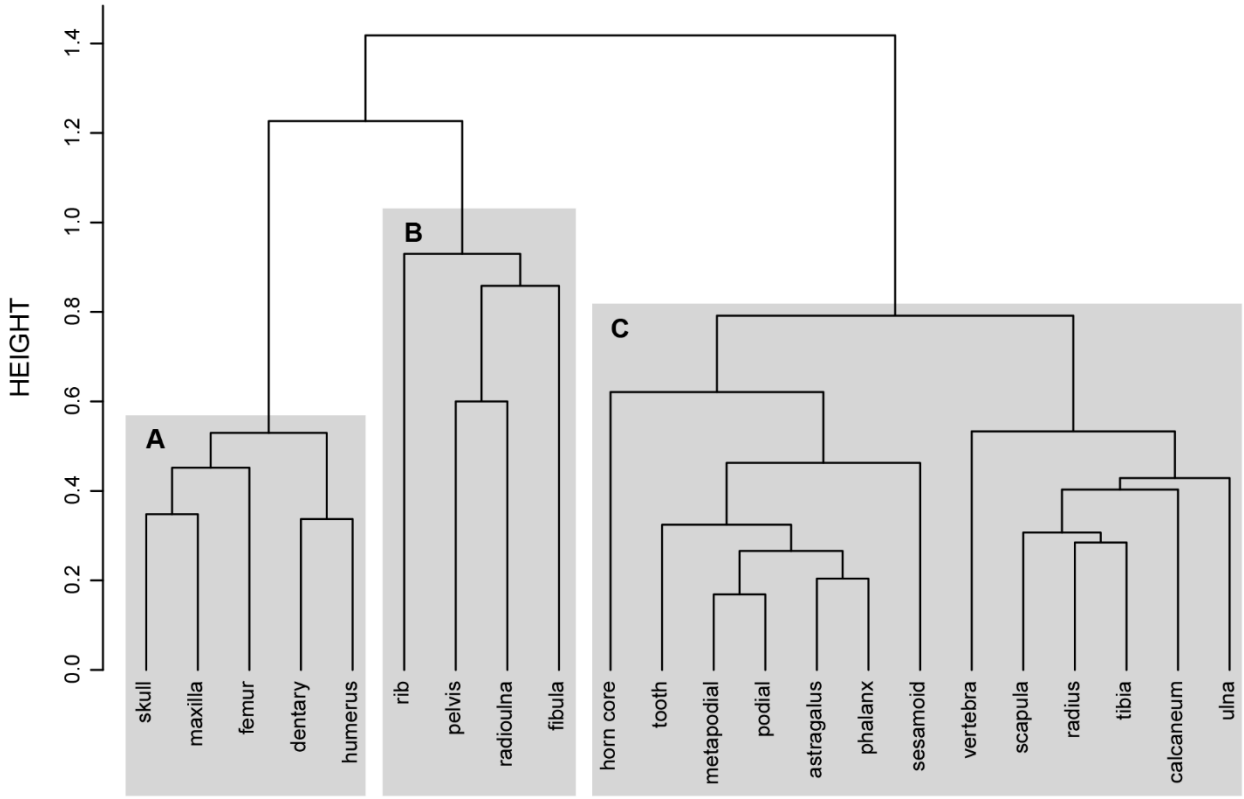

Figure 4.7. Cluster diagram of skeletal element assemblages from 43 fossil localities.

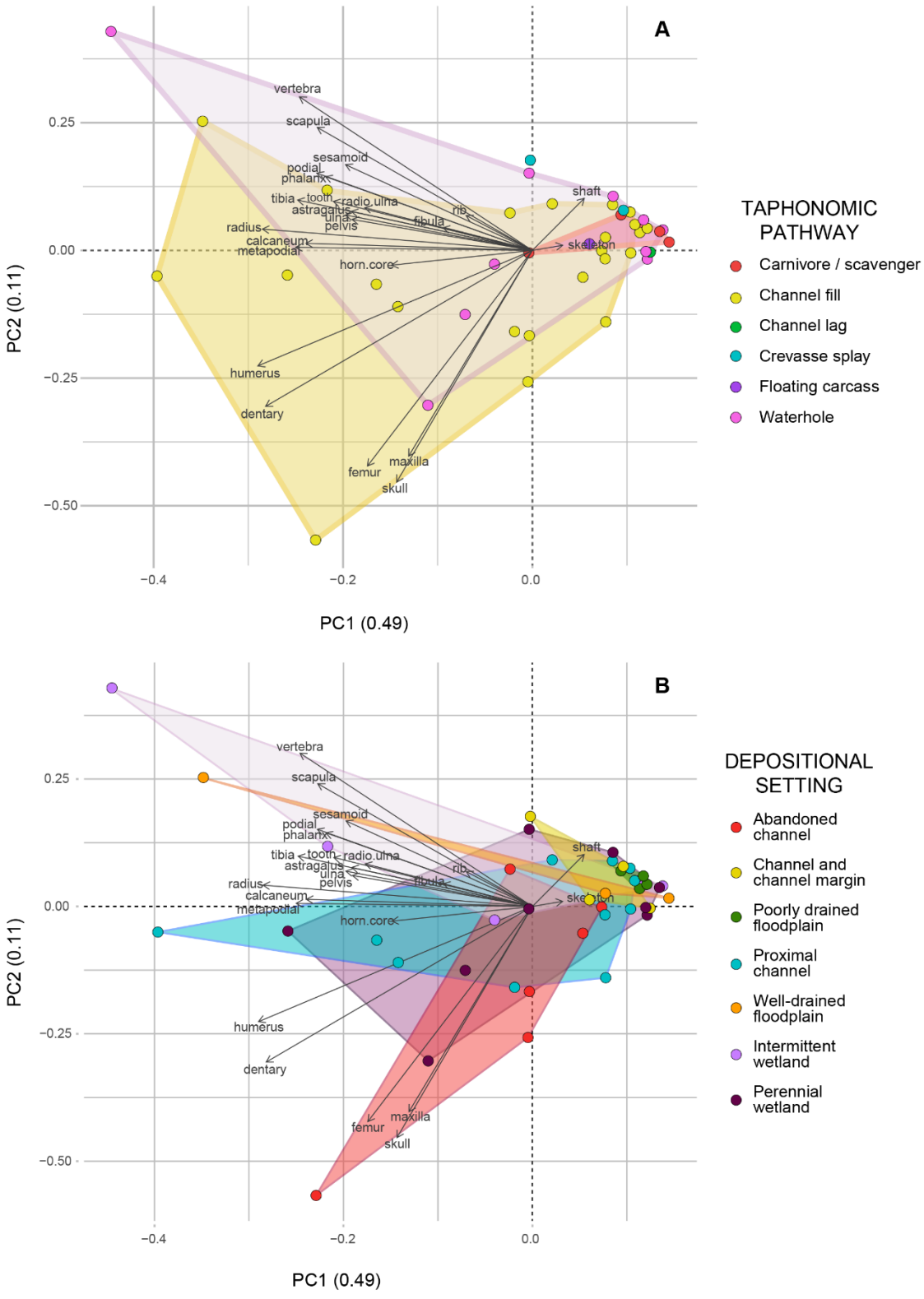

Figure 4.8. Principal components analysis (PCA) of skeletal elements from 43 fossil localities coded by A) taphonomic pathway and B) depositional setting.

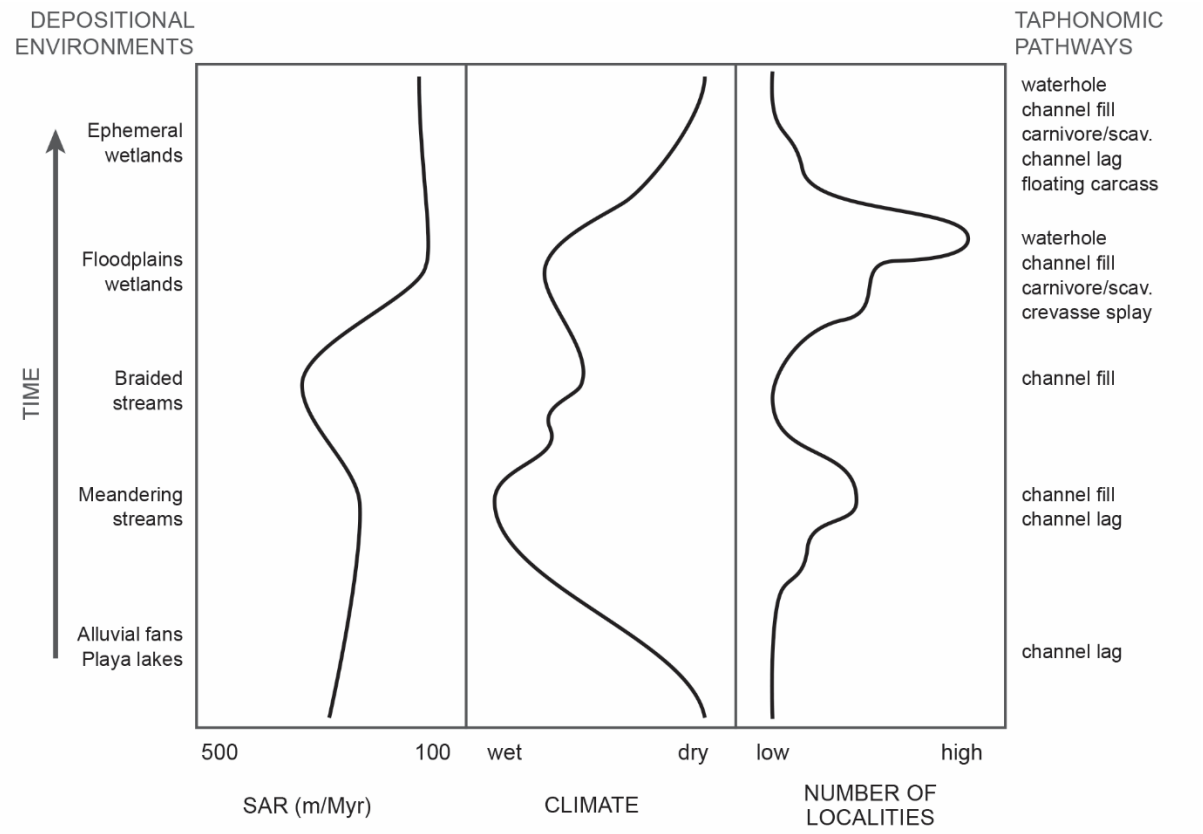

Figure 4.9. Schematic representation of depositional environments and taphonomic pathways of the Barstow Formation, showing changes in sediment-accumulation rate (SAR), climate, and number of fossil localities through time.

Table 4.1. Taphonomic characteristics of fossil assemblages accumulating through hypothetical taphonomic pathways for terrestrial vertebrate faunas. HE = hydraulic equivalence; WS = weathering stage.

Taphonomic pathway		No. bone layers	No. individuals	No. taxa	Articulation/ Association	Skel. elem. comp.[1]	HE	WS	Bone damage
Fluvial accumulation	Channel lag	Few	Many	Many	No	1b, 4, 5	Equivalent	1+	Abrasion, rounding, polish
	Crevasse splay	One to few	Many	Many	No	1b, 5	Equivalent	1-3+	Abrasion, rounding, polish
	Floating carcass	One	One	One	Yes	6	No	1	Breakage, abrasion
Long-term mortality site	Channel fill	Few to many	Many	Many	Yes and no	1-5	Yes, no	1+	Abrasion, breakage
	Waterhole	Few to many	Many	Many	Yes and no	1-5	No	1-3+	Trampling, abrasion, corrosion, tooth marks, chewing
	Natural trap	Few to many	Many	One to many	Yes	1-5, 6	No	1	Breakage, tooth marks
Carnivore/scavenger collection		One to few	Many	Few to many	No	1-5	No	1-3+	Tooth marks, breakage, punctures, chewing, trampling, corrosion
Catastrophic death assemblage		One	Many	One to few	Yes	6	Yes, no	1+	Breakage, abrasion

[1]Skeletal element numbering: 1a = skull, mandibles; 1b = isolated teeth, 2 = vertebrae, 3 = scapula, pelvis; 4 = long bones; 5 = podial elements; 6 = skeleton.

Table 4.2. Criteria for determining taphonomic pathways based on characteristics of fossil localities (in the field) and fossil assemblages (from museum collections).

Criteria	Assessment	Determination
Facies and depositional setting	Lithological characteristics of fossil locality	Field observation
Spatial extent of bone layers	Number, lateral and vertical extent of bone layers	Field observation
Skeletal-element composition	Abundance and types of skeletal elements present in fossil assemblage	Museum collections
Hydraulic equivalence of skeletal elements	Density of skeletal elements compared to sediment matrix at fossil locality	Field observation, calculations
Weathering stage	Weathering stages of material in fossil assemblage	Museum collections
Completeness of elements	Proportion of complete, partial, fragmentary material in fossil assemblage	Museum collections
Bone-damage patterns	Frequency of breaks, abrasion, trample marks, tooth marks, punctures	Museum collections
Articulation and association	Abundance and type of articulated or associated elements in fossil assemblage	Museum collections

Table 4.3. Characteristics of fossil assemblages from recognized taphonomic pathways in the Barstow Formation. Number of specimens is listed in each column. For breakage, abrasion, rounding, polish, corrosion, and tooth marks, the number of specimens exhibiting that taphonomic feature is given relative to the total number of specimens assessed for that feature. The percentage of these counts is in parentheses. Number of taxa includes the lowest possible taxonomic identifications for specimens; number of genera is in parentheses. TNS = total number of specimens documented in each pathway. ANS = average number of specimens per locality; total number of specimens divided by number of localities ± one standard deviation. WS = weathering stage. HE = hydraulic equivalence. Skeletal element composition shows the range of skeletal elements present in each pathway; numbering scheme: 1a = skull, mandibles; 1b = teeth, 2 = vertebrae, 3 = scapula, pelvis; 4 = long bones, 5 = podial elements, 6 = articulated skeleton.

Taph. pathway	No. locs	No. bone layers	TNS	ANS	No. taxa	Artic. (%)	Assoc. (%)	Skel. elem. comp.
Channel lag	2	1+	14	7 ± 3	4 (0)	0	0	1a, 1b, 3, 4, 5
Crevasse splay	2	2 to 5	60	30 ± 10	7 (2)	0	3 (5)	1a, 1b, 4, 5
Channel fill	25	1 to 5	1385	55 ± 72	39 (30)	88 (6.4)	431 (31.1)	1a, 1b, 2, 3, 4, 5
Floating carcass	1	1	125	125	1 (1)	125 (100)	0	6
Waterhole	12	1 to 3	1085	90 ± 223	34 (28)	9 (0.8)	62 (5.7)	1a, 1b, 2, 3, 4, 5
Carnivore/scavenger	5	1 to 2	194	38 ± 39	9 (6)	78 (40.2)	55 (28.4)	1a, 1b, 2, 3, 4, 5, 6

Table 4.3. Continued.

Taph. pathway	Breakage (%)	Abrasion (%)	Rounding (%)	Polish (%)	Corrosion (%)	Tooth marks (%)	WS	HE
Channel lag	7/14 (50)	9/12 (75.0)	0	0	0	3/14 (21.4)	1 to 2	Yes, no
Crevasse splay	30/60 (50)	28/60 (46.7)	20/44 (45.5)	3/47 (6.4)	0	3/60 (5.0)	1 to 3	Yes
Channel fill	327/1165 (28.1)	381/1165 (32.7)	74/1165 (6.4)	39/1165 (3.3)	21/1165 (1.8)	167/1165 (14.3)	1 to 3	No
Floating carcass	2/125 (1.6)	3/125 (2.4)	0	0	0	0	1 to adv. 1	Yes
Waterhole	165/947 (17.4)	307/947 (32.4)	50/947 (5.3)	84/947 (8.9)	35/947 (3.7)	400/947 (42.2)	1 to 3	No
Carnivore/scavenger	45/68 (66.2)	21/55 (38.2)	9/58 (15.5)	16/44 (36.4)	15/51 (29.4)	18/46 (39.1)	1 to adv. 2	No

Table 4.4. Distribution and number of taphonomic pathways by facies association (FA).

	FA 1	FA 3	FA 4	FA 5	FA 6
Channel fill		10	6	6	3
Waterhole				4	8
Carnivore/scavenger				3	2
Channel lag	1				1
Crevasse splay				2	
Floating carcass					1

Table 4.5. Analysis of variance (ANOVA) summary table for skeletal-element composition of the six taphonomic pathways compared to the skeletal-element composition of the average whole mammal.

	Degrees of freedom	Sum of squares	Mean of squares	F value	P (>F)
Skeletal-element composition	6	137.36	22.893	21.22	5.27×10^{-15}
Residuals	84	90.63	1.079		

Coefficients	Estimate	Standard error	t value	p-value
Whole mammal	2.4033	0.2881	8.343	1.25×10^{-12}
Carnivore and scavenger	-0.3558	0.4074	-0.873	0.38493
Channel fill	1.8610	0.4074	4.568	1.67×10^{-5}
Channel lag	-1.9144	0.4074	-4.699	1.01×10^{-5}
Crevasse splay	-1.2021	0.4074	-2.951	0.00411
Floating carcass	-0.6820	0.4074	-1.674	0.09786
Waterhole	1.2478	0.4074	3.063	0.00295

Table 4.6. Results of Tukey method for comparison of means for skeletal-element compositions of taphonomic pathways. CI = confidence interval.

Comparison	Difference of means	95% CI, lower limit	95% CI, upper limit	p-value
Carnivore – Whole mammal	-0.35583	-1.58659	0.874929	0.975554
Channel fill – Whole mammal	1.860989	0.630227	3.091751	0.000327
Channel lag – Whole mammal	-1.91439	-3.14515	-0.68362	0.000199
Crevasse splay – Whole mammal	-1.20215	-2.43291	0.028616	0.060061
Floating carcass – Whole mammal	-0.68198	-1.91274	0.548786	0.635041
Waterhole – Whole mammal	1.24779	0.017028	2.478552	0.044732
Channel fill – Carnivore	2.216822	0.98606	3.447583	1.04×10^{-5}
Channel lag – Carnivore	-1.55855	-2.78932	-0.32779	0.004511
Crevasse splay – Carnivore	-0.84631	-2.07707	0.384449	0.375572
Floating carcass – Carnivore	-0.32614	-1.5569	0.904619	0.984316
Waterhole – Carnivore	1.603623	0.372861	2.834385	0.003118
Channel lag – Channel fill	-3.77538	-5.00614	-2.54461	0.000000
Crevasse splay – Channel fill	-3.06313	-4.2939	-1.83237	0.000000
Floating carcass – Channel fill	-2.54296	-3.77373	-1.3122	3.00×10^{-7}
Waterhole – Channel fill	-0.6132	-1.84396	0.617563	0.741009
Crevasse splay – Channel lag	0.712241	-0.51852	1.943003	0.586130
Floating carcass – Channel lag	1.232411	0.001649	2.463172	0.049468
Waterhole – Channel lag	3.162176	1.931415	4.392938	0.000000
Floating carcass – Crevasse splay	0.52017	-0.71059	1.750932	0.860588
Waterhole – Crevasse splay	2.449936	1.219174	3.680697	9.00×10^{-7}
Waterhole – Floating carcass	1.929766	0.699004	3.160528	0.000173

Table 4.7. Results of principal components analysis (PCA) on skeletal-element counts from 43 fossil localities in the Mud Hills.

Principal Component	Square root of eigenvalue	Proportion of variance	Cumulative proportion
1	0.8653	0.4888	0.4888
2	0.4014	0.1052	0.5940
3	0.3294	0.0708	0.6648
4	0.2996	0.0586	0.7234
5	0.2788	0.0508	0.7742

CHAPTER 5

Taphonomy of mammals from the Barstow Formation of the Mud Hills, California, Part II: Faunal analysis[4]

Introduction

The Miocene fossil record of the Mojave Desert contains an important component of Cenozoic mammal diversity in western North America. In the Great Basin, mammal diversity peaked during the middle Miocene, and much of this diversity is known from the fossil record of the Mojave region (Badgley et al., 2015). The Barstow Formation in particular contributes to this high diversity and is well known for its mammal fauna, for which the Barstovian North American Land Mammal Age is named (Tedford et al., 2004). The Barstow Formation was deposited during the height of tectonic activity in the Basin and Range (Dickinson, 2002) and spans the Middle Miocene Climatic Optimum (MMCO), the last major warming interval of the Cenozoic (Zachos et al., 2001). The Barstow Formation provides one of the best continental records of middle Miocene sediments and faunas in North America. This record is excellent for investigating the influence of tectonics and climate on mammalian diversity. The tectonic and topographic fragmentation of the region may have resulted in increased rates of speciation in isolated basins, whereas the geographic ranges of mammals may have shifted in response to

[4] Loughney, K.M., and Badgley, C., Faunal analysis of large mammals from the Barstow Formation, Mojave Desert, California, in prep.

climate change (Badgley et al., 2014). To test these scenarios, faunal assemblages must have well-resolved stratigraphic and environmental contexts.

Environments in the Barstow Basin changed through the MMCO in response to changing tectonic influences. As depositional environments changed from alluvial fans and playa lakes to streams and floodplains over time, habitats became more hospitable to mammals and better able to preserve vertebrate material (Loughney and Badgley, 2017). In addition, the changing depositional conditions influenced the taphonomic pathways through which fossils accumulated, contributing to different patterns of fossil preservation through the formation (Chapter 4). The Hemingfordian-Barstovian transition in mammal faunas of the Barstow Formation has been analyzed by previous workers (e.g., Woodburne et al., 1990; Pagnac, 2009), and the most significant turnover in the large-mammal fauna of the formation occurs during the MMCO (Pagnac, 2005a). This transition coincides with major changes in facies and environments.

In Chapter 4, I evaluated the influence of facies and depositional environments on fossil accumulation and taphonomic properties of fossil assemblages. Taphonomic assemblages are related to the environments of fossil accumulation and preservation, which vary by facies association. Faunal composition of fossil assemblages is influenced by taphonomic processes, and if taphonomic assemblages of individual localities are linked to the facies setting and environment of deposition, faunal assemblages may also vary by facies association. In this chapter, I examine the role of facies changes and depositional environment on faunal composition and turnover through the formation. I address four main questions: 1) How do faunal diversity and composition differ among facies associations? 2) How does taxon-body size affect preservation potential and faunal composition of fossil assemblages? 3) How does faunal turnover relate to changes in facies? 4) How do sampling and fossil specimens of localities affect

turnover through the formation? Faunal analysis of the Barstow Formation is the companion to the facies and taphonomic analyses in previous chapters. Together, these evaluations of faunal composition and diversity elucidate the timing of major faunal transitions in the Barstow Formation in relation to climatic and tectonic change in the Mojave region during the middle Miocene.

Geological background

The Barstow Formation was deposited in an extensional basin in the central Mojave Desert, southeastern California, between ~19 and 13 Ma (Fig. 5.1). The formation unconformably overlies early Miocene volcaniclastic breccia and lacustrine deposits of the Pickhandle and Mud Hills formations (Ingersoll et al., 1996; Glazner et al., 2002). In the type section in the Mud Hills, the Barstow Formation is divided into three members: the Owl Conglomerate, Middle, and Upper members (Fig. 5.2; Woodburne et al., 1990). Magnetostratigraphy and isotopic dating of prominent tuff layers provide a robust age framework for the formation (MacFadden et al., 1990).

Loughney and Badgley (2017) identified six facies associations (FA) in the type Barstow Formation of the Mud Hills, and their stratigraphic distribution is shown in Fig. 5.2. In the lowest part of the formation, roughly corresponding to the Owl Conglomerate Member, coarse sandstones and conglomerates grade laterally into thinly bedded claystone and siltstones. FA 1 represents fluvial deposits of alluvial fans that drained into playa lakes, represented by deposits of FA 2. FA 3 overlies FA 1 and FA 2 and represents channel and proximal floodplain deposits of meandering streams. FA 3 is overlain by FA 4, which represents braided channels and interfluves. A prominent tuff layer, the Skyline Tuff, rests on top of deposits of FA 4 and marks

the boundary between the Middle and Upper members (Woodburne et al., 1990). Above the Skyline Tuff, FA 5 is mudstone-dominated and represents poorly and well-drained floodplains and ponds. Deposits of FA 6 are also mudstone-dominated and represent well-drained floodplains and wetlands. FA 5 interfingers with FA 6 in the upper part of the formation (Fig. 5.2).

The Barstow fauna and biostratigraphy

Since the early 20th century, paleontologists from several institutions have collected in the Mud Hills near Barstow, California (Fig. 5.1). Fossils from the "Fossiliferous Tuff member" (Upper Member of the Barstow Formation in the Mud Hills; Baker, 1911) were first described in detail by Merriam (1919). Collectors from the University of California Museum of Paleontology (UCMP) visited the Barstow Formation from the early 1920's to late 1930's. During the late 1920's through late 1930's, collecting parties under the guidance of Childs Frick from the AMNH made significant collections of fossil-mammal material from numerous fossil localities in the Mud Hills. Collecting intensity diminished somewhat through the middle part of the 20th century but resumed in the late 1960's, as paleontologists from the University of California, Riverside; the San Bernardino County Museum in San Bernardino, California; and the Webb Schools in Claremont, California, made collections from the formation. The San Bernardino County Museum and the Webb Schools Raymond Alf Museum of Paleontology (RAM) continue to add to their collections from the Barstow Formation (Pagnac et al., 2013).

The Barstow Formation spans the late Hemingfordian and Barstovian NALMAs (Fig. 5.2; Woodburne et al., 1990; Tedford et al., 2004). Fauna from the type section of the Barstow Formation in the Mud Hills forms the basis of the Barstovian NALMA, and the Barstovian is

further divided into large- and small-mammal biochrons. Pagnac (2009) revised the base of the Barstovian NALMA as the first appearance of the ursid *Plithocyon* at Steepside Quarry in the lower Middle Member (at approximately 16 Ma; Fig. 5.2). Pagnac (2009) also redefined early (Ba1) and late (Ba2) biochrons of the Barstovian, as well as interval zones based on stratigraphic ranges of specific large mammals in the Mud Hills. In describing the small-mammal fauna of the formation, Lindsay (1972) erected a small-mammal biochronology based on the local ranges of heteromyid and cricetid rodents. Lindsay (1995) later extended the base of these ranges into Hemingfordian portions of the formation in the Owl Conglomerate Member.

The large-mammal fauna (>1 kg) of the Barstow Formation (Table 5.1), known from surface collection and excavation, is typical of middle Miocene North American faunas. Pagnac (2005a) reviewed the systematics of the large-mammal fauna from the Green Hills, Second, and Barstow divisions and named new genera and synonymized taxa lacking published diagnoses. I follow the taxonomic revisions and faunal lists of Pagnac (2005a). Eight species of equids, seven species of camelids, and six species of antilocaprids constitute the dominant herbivore groups in the assemblage. Three oreodont species, three tayassuids, and two palaeomerycids occur in limited stratigraphic intervals. Two proboscidean families, Gomphotheriidae and Mammutidae, are represented. Rhinocerotid material occurs throughout the formation and has been referred to *Aphelops megalodus, Peraceras hessei,* and *Teloceras* sp. by various workers. Pagnac (2005a) considered all rhinocerotid material from the Barstow Formation to belong to *Aphelops* sp. indet.

The carnivore assemblage is dominated by canids (Table 5.1), with 11 species of borophagines, one species of hesperocyonine, and one canine species (Wang, 1994; Wang et al., 1999). Amphicyonids are the largest carnivores and include *Amphicyon ingens, Amphicyon* sp., and *Cynelos sinapius* (Woodburne et al., 1990; Pagnac, 2005a). Hunt (1998) reported

Ischyrocyon from the Upper Member of the formation, but Pagnac (2005a) could not definitively differentiate this material from *Amphicyon*. Two felids from the formation include the long-ranging *Pseudaelurus intrepidus* and *Nimravides marshi* (Browne and Reynolds, 2015), which is known only from Robbins Quarry in the Barstow Division (Pagnac, 2005). Three mustelids and one procyonid are known from fragmentary material, and one ursid species, *Plithocyon barstowensis*, is recognized from a few localities in the Green Hills and Barstow divisions (Frick, 1926; Pagnac, 2005a).

Barstow faunal divisions

Fossil-collecting parties from the American Museum of Natural History (AMNH) recognized five informal faunal divisions in the Mud Hills. These divisions were partly biostratigraphic and partly lithostratigraphic and were based on changes in large-mammal faunal composition and the major facies of the formation (Pagnac, 2005a). The Red, Rak, Green Hills, Second, and Barstow divisions are still used as distinct local faunas of the Barstow Formation (Fig. 5.2; Tedford et al., 2004). Their stratigraphic distribution, although approximated, was determined by Woodburne et al. (1990) and Pagnac (2009) based on the stratigraphic positions of important fossil localities.

Fossils occur throughout the Barstow Formation in the Mud Hills, although the frequency of fossil localities increases upwards through the formation. The informal faunal units roughly correspond to the major facies associations, such that the Red Division encompasses outcrops of FA 1, in the lowermost Barstow Formation in the Mud Hills. Localities in the Rak Division occur above outcrops of FA 1 in a distinctive, fine-grained facies in the lower part of FA 3. This facies is characterized by thin beds of siltstone and sandstone with abundant gypsum; it is transitional between FA 2 and FA 3 and represents marginal lacustrine deposits of a playa lake.

The Green Hills Division includes the remaining deposits of FA 3 and lower deposits of FA 4. The Second Division spans the upper extent of FA 4 and its transition into FA 5 above the Skyline Tuff. The Barstow Division includes the majority of deposits of FA 5 and FA 6, beginning at the stratigraphic level of New Year Quarry and extending to the top of the formation in the Mud Hills (Fig. 5.2).

Few fossil localities occur in the lower part of the Barstow Formation, and the faunas of the Hemingfordian-age Red and Rak divisions have fewer species than later faunal units. All information about the faunal composition of FA 1 and the Red Division comes from the Red Division Quarry (Tedford et al., 2004). Fossils are more abundant in the Rak Division. In museum collections and literature, the provenance of fossil material from the Red and Rak divisions is typically given as the faunal unit, and most material is not attributed to specific localities. Most of the fossil material from the formation comes from Barstovian-age localities in the Green Hills, Second, and Barstow divisions. Many more localities occur in these faunal units than occur in the Hemingfordian units, and thousands of specimens have been collected from these localities. Steepside, Camp, and Deep Quarries (in FA 3) are rich localities in the Green Hills Division, and Valley View Quarry, Skyline Quarry, and RAM V94179 (in FA 4) are the most productive localities of the Second Division. The majority of fossil localities occur in the Barstow Division, which encompasses most localities in FA 5 and all localities in FA 6. In addition to New Year Quarry, Robbins and *Hemicyon* Quarries are productive localities in FA 5, and RAM V98004, Rodent Hill, and Slugbed are rich localities in FA 6 (Woodburne et al., 1990; Pagnac, 2005a; personal observation).

Methods

In order to analyze mammal diversity and faunal change in relation to facies and taphonomic pathways in the Barstow Formation, I compiled taxon occurrence and abundance data and combined them with stratigraphic and facies analyses of fossil localities. These data are the basis for calculating faunal diversity among facies associations, analyzing the stratigraphic ranges of taxa in relation to facies association and environmental changes, and calculating faunal turnover through the formation. Estimates of taxon-body size and the skeletal-element compositions of families are the basis for analyzing differential preservation among taxa.

I visited the University of California, Berkeley (UCMP), Raymond Alf Museum of Paleontology (RAM), the American Museum of Natural History (AMNH), and the San Bernardino County Museum (SBCM) to examine fossil collections from the Barstow Formation. I examined 3,285 specimens from 78 localities and documented taphonomic features of fossil material as described in Chapter 4. I documented the stratigraphic position and facies associations of 61 localities based on field observations, specimen-label information, published literature, aerial photos, and Google Earth, as described in Chapters 2 and 4. For some specimens and localities, I could not determine the stratigraphic position or facies setting. When this was the case, I excluded these specimens and localities from analyses based on facies settings, but I included these specimens and localities in faunal analyses if the faunal unit was known. For Red Division Quarry, I relied on published taxon occurrences from Woodburne et al. (1990) and Tedford et al. (2004). I examined some material from the Rak Division in museum collections and also relied on published sources to complete the faunal list from this faunal unit. Woodburne et al. (1990), Tedford et al. (2004), and Pagnac et al. (2013) listed taxa present in each faunal unit but did not indicate the number of specimens; for localities in the Red and Rak divisions, I

only include taxon presence-absence information, and I excluded these localities from analyses based on abundance data.

Specimens were identified to the lowest taxonomic level possible. In many cases, confident identification below the family level was not possible, especially for non-diagnostic and fragmentary material. I relied on literature sources for taxonomic identifications of Barstow fauna. Pagnac (2005a) provided the most recent comprehensive review of Barstovian large mammals from the Barstow Formation. He did not examine late Hemingfordian material from the formation, and many of these taxon identifications are tenuous and in need of revision. I follow the taxonomic identifications of Wang (1994) and Wang et al. (1999) for canids, and Pagnac (2005a), Pagnac (2005b), Pagnac (2006) for other species- and genus-level assignments. I followed McKenna and Bell (1997) and Janis et al. (1998) for subfamily and higher classification.

In addition to material examined in collections, I gathered presence-absence and abundance information for taxa and localities using literature sources, MioMap (Carrasco et al., 2005), and the UCMP and AMNH online databases. Together with my observations, I compiled presence-absence data for taxa from 111 localities and abundance data for taxa from 147 localities. Presence-absence information is used to determine species ranges and to calculate confidence intervals on species ranges and turnover. Taxon-abundance data are necessary for calculating diversity and evenness, which are based on the proportions of taxa within a sample.

I used presence-absence data to construct stratigraphic ranges (Fig. 5.3) of large mammals in the Barstow Formation. For each species, I calculated 80% confidence intervals on its reconstructed stratigraphic range in the formation. Inferred stratigraphic ranges based on confidence intervals are not subject to preservation or sampling biases that may affect observed

ranges, and they provide alternate estimates on species ranges. The confidence interval (R_E) represents the stratigraphic range over which a taxon likely occurs at a given confidence level, based on the observed range (R_O) and the number of sampled horizons (Marshall, 1997):

$$R_E = R_O[(1 - C)^{-\frac{1}{H-1}} - 1], \quad (1)$$

where C is the selected confidence level and H is the number of stratigraphic horizons in which the taxon occurs. I also calculated the unbiased point estimate of the lowest and highest occurrence of each taxon (Marshall, 2010):

$$PE = \frac{R_O}{(H-1)}. \quad (2)$$

The unbiased point estimate (PE) of the lowest and highest occurrences is based on the average length of the gaps between horizons in which the taxon occurs. The lower and upper point estimates for a taxon represent the likely "true" horizons of lowest and highest occurrences, respectively.

I used presence-absence data to calculate species richness of localities and turnover, and I used abundance data, when available, to calculate diversity and evenness among faunal units and facies associations. Richness is the number of taxa present in a sample, and turnover measures changes in richness among time bins or stratigraphic intervals. Diversity is similar to richness but measures the relative abundance of taxa within a sample (Lyons and Smith, 2010). Evenness is a measure of the proportions of taxa in a sample and demonstrates whether taxa are represented in similar frequencies or if the sample is dominated by individuals of a particular taxon.

Some of these metrics rely on the number of individuals in a sample, which can be calculated in different ways for fossil assemblages of different taphonomic histories (Badgley, 1986a; Behrensmeyer, 1991). As most of the assemblages in the Barstow Formation represent accumulations that were time-averaged over months to hundreds of years, it is likely that remains of many individuals are represented at each locality. Most fossil assemblages accumulated through biological activity at long-term sites of mortality or through fluvial processes (Chapter 4). The remains of individuals accumulating at long-term mortality sites are typically spatially concentrated and have relatively high probabilities of association compared to elements accumulating through fluvial processes (Behrensmeyer, 1991). Fluvial processes winnow and sort skeletal elements by size, shape, and density, and the resulting accumulations are based more on the physical properties of elements than on original association (Behrensmeyer, 1975). The appropriate estimate of the number of individuals represented in fossil assemblages should then differ based on the depositional context, taphonomic history, and probability of element association (Badgley, 1986b). For localities interpreted as long-term mortality sites, I estimated the minimum number of individuals (MNI). MNI estimates the smallest number of individuals that could account for the skeletal elements of each taxon and is typically based on the number of a limiting skeletal element (i.e., left dentaries). For localities with assemblages accumulating through fluvial processes, I used the total number of specimens (TNS) to represent the number of individuals.

To compare species abundance among facies associations and faunal units, I calculated diversity using the Simpson index (*D*). This metric represents the probability of sampling two individuals of the same species in a sample, drawn at random (Lyons and Smith, 2010). By comparing diversity among facies associations and faunal units, I assess relative differences in

faunal composition in relation to changes in depositional environment and time. In diverse assemblages, taxa occur in relatively even proportions, whereas in assemblages with low diversity, common taxa comprise a greater proportion of the assemblage than rare taxa. The Simpson index places greater weight on rare taxa than other diversity measures (e.g., Hurlbert's Probability of Intraspecific Encounter; Lyons and Smith, 2010). I used this method because taxon abundance varies greatly among localities in the Barstow Formation, and rare taxa are often represented by few individuals in the formation. *D* is the sum of the squared proportion (*p*) of each species (*i*) in a sample (Lyons and Smith, 2010):

$$D = \sum p_i^2 \, . \tag{3}$$

Because *D* increases with increasing diversity, I report it as 1 – *D*.

Evenness measures the proportion of taxa within a sample and is based on abundance and species richness. This metric shows how the relative abundance of taxa is distributed in a sample and whether the faunal community is dominated by a few common taxa or whether taxa occur in equal abundance. In samples with uneven distributions, taxa are represented by very different numbers of individuals, whereas in samples with even distributions, taxa occur at similar frequencies. I used Pielou's *J* (Pielou, 1966) to measure evenness,

$$J = \frac{-\sum_i^S p_i \ln p_i}{\ln S}, \tag{4}$$

where *p* is the proportion of the *i*th species in the sample, and *S* is the number of species in the sample. In a sample with a perfectly even distribution of species, $J = 1$, and the value decreases with increasingly uneven proportions of species (Lyons and Smith, 2010).

Turnover measures the number of taxa added or lost between successive samples (Foote and Miller, 2007). I counted the numbers of localities, specimens, and the lowest and highest occurrences of species in 10-m stratigraphic bins. In the Barstow Formation, many localities occur in the same stratigraphic horizons, and I chose 10-m bins to emphasize differences among fossil-bearing and depauperate horizons. To calculate turnover between 10-m bins, I counted the number of distinct, identifiable taxa from all localities at each stratigraphic level. I included presence data for each distinct species or genus from each stratigraphic level, as well as for families that were present but not represented by identified species or genera (e.g., Equidae indet.). I used the equation for species richness for a stratigraphic or faunal unit from Foote and Miller (2007),

$$S_t = S_{t-1} + N_{LO} - N_{HO} . \quad (5)$$

Richness at a particular stratigraphic level (S_t) equals the richness of the previous level (S_{t-1}), plus the number of lowest occurrences in S_t (N_{LO}), minus the number of highest occurrences (N_{HO}) in S_{t-1} (Foote and Miller, 2007). Turnover at a stratigraphic level (T_t) is the absolute difference between richness at that level and richness at the previous level:

$$T_t = |S_t - S_{t-1}| . \quad (6)$$

I calculated turnover for observed and inferred stratigraphic ranges of species, based on point estimates and 80% confidence intervals. By comparing observed and inferred turnover, I compare stratigraphic intervals with low and high observed turnover to facies changes and intervals with low and high inferred turnover.

Body mass is an important component of the faunal composition of an assemblage, and it affects taphonomic processes acting on mammal remains (Behrensmeyer and Dechant Boaz, 1980; Badgley, 1986b). Differences in body-mass composition among assemblages can indicate differing influence of preservation (e.g., absence of small-bodied species). In addition, biological and physical taphonomic processes have different effects on skeletal elements of different sizes, potentially controlling their representation in fossil assemblages. To evaluate differences in body mass for large mammals (>1 kg, including small mustelids and leporids) between faunal units, I compiled reconstructions of body mass for extinct genera and species using estimates in Voorhies (1969), White (1988), Scott (1990), Van Valkenburgh (1990), Baskin (1998), Honey et al. (1998), Janis and Manning (1998b), Munthe (1998), Pagnac (2005a), Sorkin (2006), Figueirido et al. (2010), and Wang (2016). When these sources only gave extant species as size references, I used body-mass averages of referenced extant species in Silva and Downing (1995). Body-mass estimates for Barstow mammals are listed in Table S5.1. Mammals of the Barstow Formation encompass a wide range of body sizes, with many small- and medium-size species. In order to represent the breadth of this range, as well as to emphasize differences among smaller and larger species, I grouped taxa into six body-size categories: micro (<1 kg), small (1-10 kg), small-medium (10-50 kg), medium (50-200 kg), large (200-900 kg), and mega (>900 kg). I included mammals in the micro category with the large-mammal fauna in order to capture the

full range of body sizes of non-rodent mammals in the Barstow Formation. I grouped skeletal elements into six size categories corresponding to mammal body-mass ranges.

Results

Through my visits to museum collections, I examined fossils from 78 localities. I collected abundance and presence-absence data from literature and online resources for an additional 70 localities, for a total of 5,168 specimens from 148 localities. The distribution of specimens among localities is important to understanding the patterns of richness, diversity, and turnover in relation to facies associations of the Barstow Formation.

Taxon abundance

Specimen abundance varied greatly among fossil localities. Of the 148 localities included in my analyses from both museum collections and online sources, 59 had 10 or more specimens, 24 had over 50 specimens, and 15 had over 100 specimens. The 15 richest localities occur in FA 3, FA 4, FA 5, and FA 6. Localities with records of fewer than 10 specimens occur in all facies associations. The majority of specimens documented from museum collections were from localities in FA 6 (1,108), in FA 3 (664), then FA 4 (517), and FA 5 (449). Most of this material consists of unassociated, isolated skeletal elements and teeth, although several partial skeletons have been collected from localities in these facies associations. Most material identified to species level is from localities in FA 3, followed by FA 5, FA 6, and FA 4.

Based on data from museum collections, the majority of fossil material from the Barstow Formation is from equids, followed by camelids and antilocaprids (Fig. 5.4). Among herbivores, equids and camelids accounted for 55% of the specimens I observed in museum collections. All

other families represented 10% or less of the faunal assemblage. Equid and camelid material occurs in all facies associations that preserve vertebrate fossils and mostly consists of isolated distal limb elements or teeth. Isolated and fragmentary equid and camelid material occurs in many localities, especially in FA 5 and FA 6, where it often forms much of the collected material. Most of this material consists of unidentifiable fragments and partial elements that cannot be identified to species, but identifiable cranial elements and partial skeletons occur at several localities. The eight equid species from the formation differ in their stratigraphic distribution, but most are well sampled through their ranges (Fig. 5.3). Apart from *Parapliohippus*, which is restricted to FA 1, *Archaeohippus* occurs at the fewest number of localities, and *Scaphohippus sumani* has the longest range in the formation. The seven camelid species vary more in the number of occurrences than equid species. Two species, *Paramiolabis tenuis* and *Miolabis fissidens*, are known from single occurrences, and *Michenia* occurs at three localities; in contrast, *Aepycamelus* and *Protolabis* are well sampled through FA 3, FA 4, FA 5, and FA 6.

Antilocaprids comprise the third most common herbivore group in fossil assemblages, and they are mostly represented by partial horn cores from FA 3, FA 4, FA 5, and FA 6. The stratigraphic ranges of antilocaprids vary by genus: *Merycodus* is present at many localities throughout the formation, whereas most other antilocaprid genera have restricted distributions (Fig. 5.3). *Merriamoceros* occurs at two localities in FA 3, and *Ramoceros* only occurs in the transition between FA 4 and FA 5 that characterizes part of the Second Division (the *Ramoceros brevicornis/Megahippus mckennai* Interval Zone of Pagnac, 2009).

Oreodonts occur in most localities in FA 3 and have very limited occurrences from localities in FA 5. At least three genera occur in the formation and each is represented by different

amounts of material. *Merychyus* is rare and poorly represented in FA 1 and FA 3. *Brachycrus* is known from several skulls and jaws from several localities in FA 3, in stark contrast to *Mediochoerus*, which is represented by isolated elements at a few localities in FA 5.

Palaeomerycids, tayassuids, and proboscideans are represented by the fewest specimens in the Barstow Formation (Fig. 5.4). The two palaeomerycid genera are restricted to localities in FA 3. Tayassuid material is only present at 10 localities in FA 3, FA 4, FA 5, and FA 6. Of the three tayassuid genera in the formation, *Dyseohyus* is known from the most localities, occurring in FA 3, FA 5, and FA 6; *Hesperhys* occurs at a few localities in FA 3 and FA 4, and *Cynorca* only occurs in FA 4. Proboscidean material only occurs in FA 5 and FA 6, mostly as isolated teeth. A partial skull of *Zygolophodon* is known from the Barstow Division in the Mud Hills (Lofgren and Anand, 2011), but I did not see this material or visit the locality where it was collected.

Carnivore material is much less abundant than herbivore material throughout the formation (Fig. 5.4). The majority of carnivore material is from canids and amphicyonids. Canids range throughout the formation and are known from all facies associations except FA 1. Most identified canid material consists of skulls and dentaries, which are very abundant at localities in FA 3. The smallest canid, *Cynarctoides*, is known from one specimen from FA 4, and the relatively large *Aelurodon* (40 kg; Table S5.1) occurs at many localities and is represented by the most material. A few species smaller than 15 kg are also well represented by fossil material and have nearly as many occurrences as *Aelurodon*. Amphicyonids and felids are the common large-bodied carnivores. *Amphicyon* is long-ranging and occurs at many localities in FA 3, FA 4, and FA 5, whereas *Pliocyon* and *Cynelos* are restricted to FA 3. *Pseudaelurus* is the most common felid and is known from modest amounts of material from many localities in FA 3, FA 4, FA 5, and FA 6. In contrast, the felid *Nimravides* is known from one locality in FA 5. The ursid

Plithocyon has a fairly long temporal range but is a rare component of the assemblages in which it occurs and is absent from localities in FA 4. Small-carnivore material was rare in museum collections. Procyonids and mustelids occur at several localities throughout the formation and have relatively long stratigraphic ranges (Fig. 5.3).

Skeletal-element composition of families

The skeletal-element composition of assemblages in museum collections varies substantially among large-mammal families in the Barstow Formation (Fig. 5.5). Equids are represented mostly by isolated teeth, podials, and metapodials, with relatively little cranial and other postcranial material. Camelid material is overwhelmingly dominated by podials, particularly calcanea and astragalae, with phalanges and limb elements the next most common elements. Most antilocaprid material in museum collections are horn cores; phalanges, dentaries, teeth, and distal limb elements were fairly well represented. Similarly, palaeomerycids are mostly represented by cranial material, especially dentaries and horn cores. After tayassuid material, palaeomerycid material is the rarest herbivore material in museum collections. In contrast to the other herbivore families, oreodonts are mostly represented by skulls and dentaries and by scarce postcrania (Fig. 5.5). Leporids and castorids, as well as proboscideans, were mostly represented by isolated teeth with little identifiable postcrania.

The skeletal-element composition of carnivoran families differs from those of the herbivores and from one another (Fig. 5.5). Most canid material in museum collections is dentaries or partial crania. For amphicyonids, ribs, metapodials, and dentaries are most abundant, which causes this family to most closely resemble the composition of the average whole mammal. This resemblance is largely due to a partial skeleton of *Amphicyon ingens* from Valley View Quarry

that includes vertebrae and ribs. Felid material is mostly limb elements, and rare ursid material is dominated by skulls and dentaries. Mustelid and procyonid material includes dentaries and teeth.

Body-size distributions

There are large differences in the amount of fossil material in each body-size category (Fig. 5.6). Most of the fossil material (63%) in museum collections is from species in the medium-size body-mass category (50-200 kg). This category includes most of the equids and camelids, as well as the larger carnivores. Material in the small- to medium-size category (10-50 kg) was the next most abundant, with almost a quarter of the material as the medium-size category. The large-size category (200-900 kg) and small-size category (1-10 kg) were represented by similar amounts of material. Of taxa in the large body-size category (200-900 kg), most material was distal limb elements of *Aepycamelus* or amphicyonid dentaries; rhinocerotids were represented by articulated limbs, which was unusual for most taxa in the formation. Both the smallest (<1 kg) and the largest (>900 kg) body-size categories were represented by very little material (Fig. 5.6), represented by isolated teeth and few other elements. Leporid material was mainly isolated teeth and a few postcrania. The small mustelid *Miomustela* was represented by a single dentary (Lofgren et al., 2016). Proboscidean material was also mostly isolated teeth and two weathered bone fragments.

The distribution of body masses also varies among faunal units. The range of body sizes is similar among faunal units in that species occur in small (<50 kg), medium (50-200 kg), and large (>200 kg) size categories in all faunal units except the Red Division, which does not include mammals in the large body-size category (Fig. 5.7). The average body mass of taxa is 84 kg in the Red Division, 235 kg in the Rak Division, 121 kg in the Green Hills Division, 114 kg in

the Second Division, and 214 kg in the Barstow Division. The Barstow Division encompasses the greatest range of body masses, including the smallest non-rodent mammal (*Miomustela*) as well as the largest mammals (*Gomphotherium*, *Zygolophodon*) known from the Barstow Formation. Mammals less than 50 kg comprise a greater proportion of the assemblages in the Green Hills (0.44), Second (0.45), and Barstow (0.58) divisions than in the Red (0.25) or Rak (0.27) divisions. The median body mass for species decreases through successive faunal units (Fig. 5.7). Nearly half the species occurring in the Rak, Green Hills, and Second divisions are medium-sized species with body masses between 50-200 kg, and they comprise a greater proportion of the Red Division fauna (0.75) and lower proportion of the Barstow Division fauna (0.28). Large-bodied species over 200 kg constitute low proportions of the Barstow fauna, and only three to five large species occur in any faunal unit.

Diversity among facies associations and faunal units

Facies associations and faunal units show slightly different patterns of species richness, diversity, and evenness through the formation (Table 5.2). Richness among facies associations increases substantially between FA 1 and FA 3, then fluctuates between FA 3 and FA 6. Among faunal units, species richness is highest in the Green Hills and Barstow divisions and lowest in the Red and Rak divisions. In the Second Division, 32 species occur, but if range-through species are included, the number of species potentially present in this faunal unit is 36.

Because abundance data were unavailable for the Red Division Quarry, FA 1 and the Red Division were excluded from analysis of diversity and evenness. Values of Simpson's *D* do not vary substantially among facies associations or faunal units. *D* is highest for FA 3 and FA 6 and slightly lower for FA 4 and FA 5. The Rak and Green Hills divisions have the highest diversity,

and the Barstow division has the lowest value of *D*. Evenness is highest in FA 4, similar in FA 5 and FA 6, and lowest in FA 3. Among faunal units, the Rak Division has the highest evenness; the Green Hills Division has the lowest evenness, and the Second and Barstow divisions have similar evenness (Table 5.2). The overall low species abundance based on MNI resulted in most species occurring in low proportions within assemblages for each facies association and faunal unit. These low proportions across assemblages contributed to the low values of *D*, even for facies associations and faunal units with high species richness.

Faunal turnover

The stratigraphic distribution of observed lowest and highest occurrences in the formation is strongly correlated with the number of specimens (r = 0.82) and the number of localities (r = 0.85) in stratigraphic bins (Fig. 5.8). Horizons with many localities produce more specimens, and more taxa are recognized in these rich assemblages. Observed lowest and highest occurrences cluster in intervals from which many taxa are identified. Thus, preservation and sampling are important influences on the observed pattern of turnover in the formation. There are several intervals of turnover in the Barstow Formation based on observed species ranges: a large spike at about 500 m and several pulses high in the section between 800 and 1000 m (Fig. 5.9). These turnover episodes correspond to horizons with large numbers of observed lowest and highest occurrences of species.

Species observed lowest occurrences (OLO) cluster near the base of the section in FA 3 and decrease upwards through the formation. Observed highest occurrences (OHO) are distributed throughout the formation; they cluster stratigraphically in FA 4 and at the top of the section in FA 6 (Fig. 5.9). The highest number of OLOs occurs in 10-m bins that contain rich fossil

localities and include Steepside Quarry in FA 3, and Skyline and Valley View quarries in FA 4. The highest number of OHOs occurs near the top of the section where several localities occur in FA 6. Observed turnover is highest at the level of Steepside Quarry, reflecting the OLOs of 11 species and the OHOs of two species, and at Red Division Quarry, which has low specimen counts but nearly complete turnover of species. Two intervals of increased observed turnover occur in the middle and upper parts of the formation as well. At the level of Skyline, May Day, and Hailstone quarries, six species have OLOs and two have OHOs. Six species have OHOs at ~900 to 950 m, and above this level, observed turnover varies as one to three species have OHOs at successive horizons through the top of the section (Fig. 5.9). Inferred lowest occurrences (ILO), based on point estimates and confidence intervals, are distributed throughout the middle and lower portion of the section; inferred highest occurrences (IHO) are distributed over the upper ~400 m of the section, with a small cluster at ~550 m (Fig. 5.10). The pattern of turnover based on the inferred stratigraphic ranges is nearly constant throughout the section. The largest spike in inferred turnover occurs between 450 and 500 m, similar to the largest spike in observed turnover. Inferred turnover also increases the upper part of the formation, and there is slight offset between turnover based on point estimates and confidence intervals.

Discussion

Localities that produce abundant fossil material (>100 specimens) occur in all facies associations included in these analyses except FA 1. The productive facies associations represent vegetated environments near water sources that attracted and supported mammals, and depositional settings within these facies associations were conducive to preserving vertebrate

remains. Changes in diversity, evenness, and turnover through the section partly reflect the number of localities and change in preservation potential among major facies associations.

Taxon abundance and distribution

Fossils of herbivores are overall more abundant than those of carnivores, which is typical in terrestrial ecosystems and reflects energetics required to sustain mammals in terrestrial food webs (Vaughan et al., 2015). The abundance of equid and camelid material in Barstow assemblages may in part reflect the original abundance of these groups but is also determined by preservation potential. As many as six equid species and five camelid species co-occur in the formation at one time (Fig. 5.3), and as many as four species of each co-occur at some localities. Equids and camelids comprise large proportions of taxa from many Miocene localities in North America (Honey et al., 1998; MacFadden, 1998), so their abundance in the Barstow Formation is not unusual. Not only were these families diverse in the middle Miocene, their behavior could have contributed to the high proportion of material in the formation. Modern equids and camelids are gregarious, and if Miocene species were as well (Voorhies, 1969; Pagnac, 2005a), they could have accounted for more individuals at these localities than solitary species, and therefore result in a greater proportion of fossil material.

Preservation bias may also contribute to the abundance of equid and camelid fossil material. Preservation bias for particular body sizes has been documented in studies of modern and fossil assemblages. In modern live-dead surveys of mammals in Amboseli National Park, Kenya, mammals with body masses greater than 100 kg are well represented in the death assemblage compared to mammals under 100 kg (Behrensmeyer and Dechant Boaz, 1980). Most equid and camelid species in the Barstow Formation had inferred body masses of 100 to 200 kg (Table

S5.1), similar to body masses of well-represented species in Amboseli death assemblages. In addition to the possible preservation bias for medium-size mammals (50-200 kg), skeletal-element composition indicates that taphonomic processes may favor the representation of equid and camelid material in fossil assemblages. Most equid and camelid material consists of isolated teeth and podial elements (Fig. 5.5). Equid molars and phalanges are compact, durable elements that are easily preserved under most burial conditions (see Chapter 4). Similarly, camelid podials, phalanges, and metapodials are rather large, durable elements that may also have increased ability to survive surface processes and burial.

Oreodonts in the Barstow Formation were similar in size to contemporaneous equids and camelids, yet they are known from much less fossil material. The preservation bias for medium-size mammals may not have been as strong for oreodont postcrania, as oreodonts have more digits and less robust podial elements than equids and camelids. The paucity of postcranial material, however, is likely the result of collection bias. The Frick crews that collected most oreodont material selected for cranial material, accounting for the skewed distribution of skeletal-element composition toward cranial elements (Fig. 5.5). Oreodont material is present at most localities in FA 3 but is very rare in localities in FA 5 and FA 6. By the middle Miocene, oreodonts were declining in abundance and diversity in North America (Lander, 1998), and their occurrence in the Barstow Formation represents some of the youngest occurrences of this family in western North America (Pagnac, 2005a). Oreodonts may have been regular components of ecosystems represented in FA 3, but in later-forming environments, they had become rare in the Barstow Basin.

Canid abundance patterns differ with body size (Fig. 5.4). The 13 canid species known from the formation range in size from 4 to over 40 kg (Table S5.1). Small-bodied mammals under 15

kg are typically rarer components of death assemblages (Behrensmeyer and Dechant Boaz, 1980) and fossil assemblages (Badgley, 1986b) than mammals greater than 15 kg. Canid material occurs throughout the formation, yet most canid species have long or variable gaps between occurrences; gaps in species ranges may be partly related to the low abundance of identifiable material at many localities. Postcranial material of smaller carnivores is either not preserved as frequently or is not identifiable to genus or species. The skeletal-element composition of canids shows a combination of cranial and postcranial material (Fig. 5.5). Where identifiable specimens occur, several canid species are typically present at the same locality, and a range of body sizes is often represented. The greatest number of canid species co-occur at localities in FA 3, FA 4, and FA 5. High preservation potential in these depositional settings and the accumulation of material over long periods of time likely contributed to the range of species and body sizes present. The ecology of these extinct canids is not well understood. It is therefore difficult to interpret behavior or niche preference from the co-occurrence of species, or whether these factors contributed to their preservation or stratigraphic occurrence. The larger *Aelurodon* and *Protepicyon* may have been solitary hunters in mosaic habitats. The smaller canids from Barstow may have filled niches occupied by modern mustelids and procyonids, based on their small size and inferred solitary lifestyle (Munthe, 1998).

Mustelids and procyonids, too, are small taxa (<10 kg) that are not abundant in the Barstow Formation (Fig. 5.4). Although mustelid and procyonid material is relatively rare, members of these families generally have long stratigraphic ranges through the section (Fig. 5.3). As carnivores in size categories under 50 kg, mustelids and canids may have been subject to preservation bias against small mammals. Additionally, postcranial material, if preserved, is difficult to identify to the family or genus level, which affects the reconstructed ranges of these

taxa. Postcranial material in museum collections is often assigned to “Carnivora indet.” if it cannot be assigned based on diagnostic characters or size. Postcrania of many small canids and mustelids may be relegated to this diagnosis.

Large carnivores are present at many localities through the formation (Fig. 5.3). Amphicyonid material is nearly as abundant as canid material (Fig. 5.4), but most is not identifiable to species. Amphicyonids may be differentiated from other carnivores based on large size if other diagnostic material is not available. Large carnivores in the Barstow Formation are mostly represented by postcranial material, in contrast to small carnivores, which are mostly known from cranial material (Fig. 5.5). Partial skeletons of *Amphicyon* and *Pseudaelurus* contribute to this distribution of skeletal elements, but postcranial material is more likely to be referred to these genera based on size. Most postcranial material from large amphicyonids is referred to *Amphicyon*; similarly, most felid material is referred to *Pseudaelurus* because it is the most common felid. The relatively long stratigraphic ranges of large carnivores may be influenced by the assignment of material to these genera based on size rather than diagnostic anatomical characteristics.

All taxa in the Barstow Formation are subject to sampling and preservation bias, but originally rare taxa are especially susceptible to these controls on occurrence. Many of these taxa are only known from rich, well-sampled intervals in FA 3 and FA 5 (Fig. 5.8). Palaeomerycids and tayassuids are the ungulate families represented by the least amount of fossil material in museum collections (Fig. 5.4). Members of these groups may have originally been rare components of the Barstow fauna or may have preferred uncommon environments. Most fossil assemblages in FA 3 and FA 5 are time-averaged accumulations in abandoned-channel and wetland settings that had high preservation potential (Chapter 4). As taxon richness generally

increases with time averaging, rare taxa are more likely to be captured in such assemblages (Martin, 1999). The preservation potential of these taxa may then be higher in these settings than in other facies in the formation. Because the different facies associations represent different depositional environments, it is hard to disentangle the influences of preservation from original behavior or habitat preferences of taxa.

Taxa with short stratigraphic ranges may be subject to all three of these factors. Most taxa with limited stratigraphic ranges occur in FA 3, in which many productive localities occur. These taxa, including the palaeomerycids, the oreodont *Brachycrus*, and the antilocaprid *Merriamoceros*, are well sampled in this interval, and the confidence intervals on their ranges are short or match their observed ranges (Fig. 5.3). These taxa may only have occurred in the Barstow Basin during the deposition of the floodplain environments of FA 3. Palaeomerycids are interpreted as browsers that lived in small groups in forested environments (Janis and Manning, 1998b), and *Brachycrus* has been interpreted as a tapir-analogue based on skull morphology (Pagnac, 2005a). Modern antilocaprids live in the open grassland habitats of western North America. Although fossil members of this group are typically associated with open environments, a few extinct genera may have been solitary browsers in closed habitats (Janis and Manning, 1998a).

Body mass and preservation

Medium-sized mammals, particularly mammals between 100-200 kg, are represented by more fossil material in the Barstow Formation than taxa of smaller and larger size (Fig. 5.6). Preservation bias in favor of medium-size mammals may contribute to the abundance of this material. In live-dead surveys of large mammals from Amboseli, representation of mammals in

the surface bone assemblage declined with decreasing body size compared to the live assemblage (Behrensmeyer and Dechant Boaz, 1980). For species weighing 100 kg or greater, bone counts accurately represented the live assemblage. Large herbivore and carnivore species (≥15 kg) were nearly all represented in the Amboseli bone assemblage, whereas small herbivore and carnivore species (≤15 kg) comprised only 60% and 21% of the bone assemblage, respectively (Behrensmeyer and Dechant Boaz, 1980).

A number of factors, including predation and weathering, contribute to the under-representation of smaller skeletal elements (Behrensmeyer et al., 1979). Bones of smaller animals are more likely to be destroyed by predators or scavengers during feeding, especially by bone crushers, than bones of larger animals (Marean et al., 1992). A few carnivores (e.g., *Aelurodon*, *Protepicyon*) present in the Barstow Formation had adaptations for bone crushing and may have been osteophagous (Wang et al., 1999). These carnivores would have been possible agents of preferential destruction of remains of mammals under ~200 kg. Vertebrae, ribs, and girdle elements for mammals under 200 kg are under-represented relative to the average whole mammal (Fig. 5.5). These skeletal elements are targeted by extant bone crushers because they are less dense than compact elements, such as podials and teeth, which typically escape destruction (Marean et al., 1992). This preference may also account for the skeletal-element distribution of equid and camelid material, which is dominated by podial elements and teeth and mostly lacks axial material (Fig. 5.5). Even if they were not habitually osteophagous, all carnivores of the Barstow Formation would have been likely to modify the skeletal-element composition of the death assemblage, either by preferentially removing elements to dens or by destroying bones of small animals, as they do in modern ecosystems (Behrensmeyer and Dechant Boaz, 1980).

Surface processes also affect the size distribution of taxa in death assemblages. Bones of small animals are more likely to be broken and fragmented from trampling than bones of larger animals (Behrensmeyer et al., 1979). Weathering processes differentially affect elements of different sizes, as small elements have greater surface area compared to volume than large elements and weather more quickly (Behrensmeyer, 1978). Weathering stages of specimens from the Barstow Formation were skewed across body-size categories (Table 5.3), with a greater proportion of specimens in the larger size categories showing advanced stages of weathering (3 to 5). Specimens in smaller body-size categories mostly showed incipient to moderate weathering stages (0 to 2), indicating that they were buried quickly or destroyed at the surface. Small-sized elements are easier to bury than large elements, which reduces exposure to surface processes; small-sized elements, such as postcranial elements of taxa under 50 kg, that were not quickly buried may have been destroyed by predators, scavengers, or surface weathering processes and were not preserved in localities in the Barstow Formation. Highly weathered elements of larger animals, although not common, better withstood these processes than smaller elements and are represented in greater numbers in fossil assemblages (Table 5.3).

Depositional environment and agent of accumulation were also important factors in determining the distribution of body-size categories. Across all taphonomic pathways, medium-size mammals (50-200 kg) were well represented (Fig. 5.11). The channel-fill and waterhole pathways captured a greater range of body sizes than the other pathways. These taphonomic pathways represent sites of long-term mortality that accumulated attritional assemblages over months to hundreds of years; such assemblages typically capture most of the faunal community without substantial bias (Martin, 1999). These settings represent habitats where mammals congregated and have high preservation potential due to high local rates of sediment

accumulation and burial (Chapter 4), increasing the representation of all body-size categories. In contrast, the material from assemblages accumulating through the carnivore and scavenger pathway represented body sizes under 200 kg, and assemblages accumulating through fluvial processes encompassed body sizes from 10 to 200 kg. Carnivores and scavengers in the Barstow Formation ranged in size from less than 10 kg to over 500 kg, and the possible size selection of prey allows for a wide range of body sizes. Material in the carnivore and scavenger pathway is dominated by medium-sized herbivores and also includes more material from smaller-sized herbivores than most other pathways (Fig. 5.11). This distribution may reflect the selection of prey by large and small predators. If the 16 carnivores under 50 kg in the Barstow Formation selected prey in the same size range, it could account for the greater amount of material from herbivores under 50 kg. The smaller range of body sizes represented in the channel-lag and crevasse-splay taphonomic pathways results from the winnowing of material by fluvial processes. Winnowing during fluvial transport naturally separates elements of different sizes and densities, and so material from mammals in the smallest and the largest size categories would be under-represented in the assemblages accumulating through fluvial processes. Most material in assemblages accumulating in these pathways was fragmentary and abraded and could not be assigned to a body-size category.

Stratigraphic ranges of taxa

Many species occurrences are concentrated in a few stratigraphic intervals (Fig. 5.3). Major gaps in species occurrences occur below about 430 m and in the interval between 550 and 700 m. The interval below 430 m corresponds to FA 1 and the transitional facies of FA 3, in which few localities occur (Fig. 5.8). FA 1 represents channel and bar deposits of alluvial fans that

preserved little vertebrate material (Loughney and Badgley, 2017). The transitional facies of FA 3 begins at approximately 200 m and extends to approximately 430 m (Woodburne et al., 1990). I found little locality information for fossil material from this interval (the Rak Division), and most specimen labels refer to generalized horizons or locations. Fossil material is not abundant in this facies, which represents the transition between the playa-lake environments of FA 2 and floodplain environments of FA 3. Since the playa-lake environments of FA 2 do not preserve vertebrate body fossils, unfavorable preservation conditions or unsuitable habitats of these playa environments (Chapter 2) account for the low preservation of fossils in the lower portion of FA 3.

With the change of environments to proximal floodplain and channel settings represented by most of FA 3, habitats became more attractive to mammals and fossil preservation increased (Chapters 2 and 3). Fossil localities in FA 3 formed in abandoned channels and channel margins and greatly increased the potential of fossil preservation over settings in FA 1 and the transitional facies of FA 3. As FA 3 changed to channel and bar deposits of FA 4, fossil localities again became scarce. Although fossils do occur within these channel deposits, the two localities that produce the most fossil material in FA 4 occur in deposits that represent interfluves or periodically inactive channel environments that accumulated fossils over tens to hundreds of years. Wetland deposits of FA 5 and FA 6 also represent environments with high preservation potential, and many species are preserved in these settings. Species with occurrence gaps through FA 4 again appear at localities in FA 5 (Fig. 5.3), perhaps attracted by perennially ponded wetlands. Many localities in FA 6 represent intermittent wetlands that would have been places where animals congregated as climate cooled and the basin became drier (Chapter 3).

The stratigraphic ranges of individual species are influenced by habitat, preservation and sampling, as well as regional species abundance and longevity. In Amboseli, bones of the most abundant herbivores were found in all habitats surveyed regardless of habitat preference, whereas bones of herbivores with strong habitat preferences were predominantly found in those habitats (Behrensmeyer and Dechant Boaz, 1980). Equids and camelids have a long stratigraphic record in the formation, and along with the antilocaprids, they are the only families represented in all faunal divisions and all fossiliferous facies associations (Fig. 5.3). These families are represented by abundant material throughout the formation. Species with restricted stratigraphic ranges or those known from few specimens may have been rarer components of faunal communities or were only briefly present in the basin. Among carnivores, the felid *Pseudaelurus* and the mustelid *Plionictis* have the longest ranges, even though they are represented by less than one tenth the amount of material as the abundant herbivore families.

The gaps in species ranges coincide with stratigraphic intervals representing specific environments or environments with low preservation potential. Both long-ranging species and species with restricted ranges give indications of the changing habitats and preservation potential through the formation. For example, *Aepycamelus* is one of the longest-ranging taxa in the Barstow Formation (Fig. 5.3) and is identified from localities in FA 3, FA 4, FA 5, and FA 6. *Aepycamelus* was a giraffe-sized, canopy-level browser (Honey et al., 1998), and its regular occurrence through the formation may be a strong indication of wooded habitats. Trees were not likely to have been abundant in the channel settings of FA 4, where there is a long gap in the range of *Aepycamelus*. The other conspicuous gap in the range of *Aepycamelus* occurs in FA 6, representing a time of drying in the basin when habitats became more open.

Apart from taxa with single occurrences, the palaeomerycid *Rakomeryx*, the antilocaprid *Merriamoceros*, and the oreodont *Brachycrus* have the most restricted ranges (Fig. 5.3). These taxa only occur in FA 3 and may be the species with the strongest environmental preferences for riparian habitats. The small canid *Euoplocyon* and the amphicyonid *Pliocyon* may also have preferred wooded habitats (Hunt, 1998), as they, too, are restricted to FA 3. *Euoplocyon* only occurs at Steepside Quarry and may be a rare species or was under-sampled elsewhere. Environments represented by deposits of FA 3 were proximal-channel floodplains and likely supported abundant riparian vegetation under humid conditions, as indicated by the abundant palm morphotypes in the counted phytolith assemblage from this facies association (Chapter 3). These environments may have been unique in the history of the Barstow Formation, and taxa preferring these environments may have left the Barstow Basin by the time environments changed to those represented by FA 4. Palaeomerycids and oreodonts were widespread in the Great Basin and Great Plains of North America in the middle Miocene, and most species disappeared in the Great Basin by the latest Barstovian (Janis et al., 1998). Cooling climate and the spread of increasingly open habitats in the Barstow Basin may have encouraged these species to leave the area once environments began to change (Chapter 3).

Four species only occur at localities in FA 5. These species include two camels, the oreodont *Mediochoerus*, and the felid *Nimravides*; these genera are known from relatively little material from a handful of localities. Deposits of FA 5 represent floodplain environments, some of which were perennially ponded; few plant fossils are known from FA 5, but abundant root casts in these deposits show that these wet environments were vegetated. *Nimravides* has been interpreted as a semi-arboreal ambush predator (Browne and Reynolds, 2015) and the browsing ungulates would have preferred habitats with broad-leaved plants. Environments of FA 5 were coeval with the

wooded grasslands and wetlands of FA 6 (Chapter 3). Only two taxa are restricted to FA 6, the small mustelid *Miomustela* and the castorid *Monosaulax*. *Monosaulax* occurs at localities representing ponds or wetlands, indicating a strong preference for these environments, much like modern beavers. *Miomustela* is represented by one specimen. The locality from which this specimen was collected, RAM V98004, also preserves abundant avian material, and preservation conditions were especially favorable for preserving small and rare taxa.

Diversity and turnover in the Barstow Formation

Diversity and species richness vary substantially through the formation with changes in facies. Prominent spikes in richness and observed turnover are correlated with very high specimen abundance at seven intervals in the formation. Instances of lowest and highest occurrences are influenced by the high specimen counts from localities in these intervals (Figs. 5.8, 5.9). The high number of specimens in certain intervals of the formation is related to the depositional settings of fossil localities and the facies associations in which they occur. These factors influence the trends in diversity, turnover, and observed lowest and highest occurrences. Inferred lowest and highest occurrences, based on point estimates and confidence intervals of species' stratigraphic ranges, differ somewhat from observed occurrences and help to separate patterns in species turnover from sampling effects (Fig. 5.10).

The significant increase in richness between FA 1 and FA 3 is the result of changes in sampling and preservation between these facies associations. The fossil record from one locality (Red Division Quarry) determines the species richness of FA 1 (Fig. 5.8), which has lower preservation potential than the other facies associations (Chapter 2). This single locality occurs within the coarse-grained channel and channel-margin deposits that characterize FA 1.

Additionally, the channel-lag assemblage from Red Division Quarry had limited potential to capture the range of diversity of the time, as specimens from fluvial accumulations typically have low taxonomic resolution (Chapter 4). Of the four species that occur at Red Division Quarry, three only occur at this locality, resulting in the near-complete apparent replacement of species between FA 1 and FA 3 and a small spike in observed turnover (*Merychyus* sp. survives into FA 3 and is present elsewhere in the Great Basin until the Hemphillian [Janis et al., 1998]). Inferred turnover based on confidence intervals differs from the observed pattern (Fig. 5.10). Inferred lowest occurrences (ILO) are distributed over the upper portion of FA 1 and lower portion of FA 3, and are not clustered at the level of Red Division Quarry. Rather than representing the near-complete replacement of species that only occur at Red Division Quarry, the small increase in inferred turnover between 150 and 200 m (Fig. 5.10) results from the number of ILOs of species with observed lowest occurrences (OLO) higher in the section.

The transition between FA 1 and FA 3 represents a substantial change in environments from alluvial fans and playa lakes to streams and floodplains. Fossil preservation increased with the change in facies, and many species have OLOs in FA 3 (Fig. 5.9). In the transitional facies between FA 1 and FA 3, sampling and preservation are low and few localities occur in these deposits (Fig. 5.8). Richness in FA 3 does not substantially increase over that of FA 1 until the establishment of channel and floodplain deposits. In this interval of FA 3, the number of fossil localities increases, as do the number of specimens and taxonomic richness, which contribute to high *D* (Table 5.2). Favorable preservation conditions at these localities may explain why FA 3 sustains high *D* and richness among fewer localities than in the other facies associations. Relatively low evenness in FA 3 results from a greater difference among the proportions of common and rare taxa in fossil assemblages, as MNI ranges between one and 90 (68% are five or

fewer). If these proportions reflect the original abundance of species, localities forming in FA 3 may have been able to capture both common and rare components of the ecosystem. With the large number of specimens from this interval, 30 new species occur in FA 3, 11 of them at Steepside Quarry, which produces a large spike in OLOs at ~450 m. Species with OLOs in this interval were likely present in the basin but not sampled until the likelihood of preservation increased. Many species with OLOs between ~440 to 460 m have confidence intervals that extend several tens of meters below their first occurrence (Fig. 5.3). The ILOs of species are dispersed throughout the stratigraphic extent of FA 3 (Fig. 5.10), further indicating that OLOs are strongly influenced by sampling and preservation. If species with ILOs in this interval were present in the basin, their presence was not recorded until depositional environments were conducive to fossil preservation, resulting in the clustering of OLOs in discrete stratigraphic intervals.

Fewer localities occur in FA 4 than in FA 3, but large specimen counts from some of these localities accompany a modest increase in observed lowest and highest occurrences (OHO). Mammals did not inhabit the channel settings represented by FA 4, contributing to lower overall specimen abundance (Chapter 2). Preservation in the amalgamated sandstones of FA 4 is lower than in the proximal-floodplain deposits of FA 3, and localities are separated by longer stratigraphic intervals. Species richness and *D* decrease in FA 4 (Table 5.2), and many species have gaps in their ranges through FA 4 (Fig. 5.3) because few mammals were present in these settings and fossil preservation was lower. High evenness in FA 4 is likely a product of lower preservation and sampling through this facies association. Most species occur in low abundance, as MNI ranges between one and 13 (77% of MNI are five or fewer); thus, these species comprise similar, low proportions of fossil assemblages. OLOs increase at the stratigraphic levels of two

rich localities (Valley View and Skyline quarries), as these intervals reflect the higher preservation potential of these horizons relative to the majority of deposits in FA 4. ILOs are not concentrated at the same stratigraphic horizons (Fig. 5.10) but are distributed throughout FA 4. Spikes in observed turnover at the levels of Valley View and Skyline quarries correspond with high specimen numbers and taxon richness (Fig. 5.9).

The abrupt change in facies above the Skyline Tuff, as well as radiometric dates from tuff layers, indicates the presence of a hiatus at the level of the Skyline Tuff or just above it. The Skyline Tuff has been dated at 15.2 Ma (D. Miller, written communication), and the Dated Tuff, which is 18 m above the Skyline Tuff, is dated at 14.8 Ma (MacFadden et al., 1990). Sediment-accumulation rates decrease from 357 m/Myr in FA 4 to 120 m/Myr in FA 5 above the Skyline Tuff (Loughney and Badgley, 2017). A substantial condensed interval should affect the stratigraphic occurrences of lowest and highest occurrences, especially if there is a significant hiatus. Lowest and highest occurrences are expected to cluster at hiatal surfaces and increase in number with duration of the hiatus (Holland, 1995). The spike in OLOs occurs at the level of Skyline Quarry, just below the Skyline Tuff, and a small increase in ILOs occurs just below this interval. The major facies transition, and many OHOs, are expected at the level of Skyline Quarry if it is also disconformable. Instead, only two OHOs are recorded at this level (Fig. 5.9), within a cluster of OHOs near the top of FA 4. Fossil assemblages at hiatal surfaces are typically concentrated through extensive reworking of older deposits (Rogers and Kidwell, 2000). Fossil material from this horizon has moderate abrasion, but damage overall is not severe, and the material does not indicate evidence of extensive reworking. Rather, the increase in OLOs below the hiatus is more characteristic of the concentration of lowest occurrences in a horizon where preservation conditions are enhanced (Holland, 1995). OLOs in FA 4 cluster in horizons that

represent depositional settings with high preservation potential and specimen abundance even though their probable lowest occurrences are lower in FA 4, as indicated by the distribution of their ILOs (Fig. 5.10). Few OHOs and no IHOs occur in this interval, and instead, OHOs are smeared downwards from the hiatal surface (Signor and Lipps, 1982) to lower stratigraphic levels in FA 4. The small increase in OLOs above the Skyline Tuff does conform to the expected pattern above a hiatus. Species with OLOs above the Skyline Tuff are well sampled through their ranges, and their confidence intervals are close to their observed ranges (Fig. 5.3). The small cluster of ILOs at ~750 m is only slightly displaced from the spike in OLOs at ~760 m, indicating that these species may have originally first appeared within this interval or during the hiatus.

Above the Skyline Tuff, OLOs decrease and OHOs substantially increase in FA 5 and FA 6. The highest numbers of localities in the formation occur in these facies associations, and several localities produce large numbers of specimens (>100). The floodplain and wetland deposits of FA 5 and FA 6 represent places where animals congregated near water sources, and preservation potential was high in these depositional settings (Chapters 2 and 4). High species richness in FA 5 (Table 5.2) results from the suitable habitats that developed, the favorable preservation of specimens, and the high number of localities (Fig. 5.8). Despite this high richness, *D* is relatively low due to high evenness. In addition to the possible contribution of original species abundance to evenness, increased preservation and sampling in FA 5 resulted in species occurring in similar proportions because they are equally well sampled. Observed turnover is variable in FA 5, as the OHOs of several species are recorded in these rich localities. Few IHOs, however, occur in FA 5, and inferred turnover decreases through this facies association.

The largest number of OHOs occurs well into the stratigraphic span of FA 6 between 900 and 1000 m (Fig. 5.9). High numbers of localities and specimens (Fig. 5.8) from this interval and edge effects at the top of the formation contribute to the pattern of observed turnover (Fig. 5.9). Spikes in OHOs and observed turnover correspond with increases in sampling (Fig. 5.9). Few ILOs are concentrated in these well-sampled horizons, but most occur throughout the upper part of the formation (Fig. 5.10). Inferred turnover increases in FA 6, as the inferred ranges of fairly well-sampled, long-ranging species terminate low in this facies association; inferred turnover is low through the top of the formation but is higher than observed turnover (Fig. 5.10). Richness declines in FA 6 with high observed turnover, and *D* and evenness remain fairly low (Table 5.2) because a few common taxa constitute high proportions of the assemblage. Variability in preservation among taphonomic pathways contributes to the decline in richness. Although some pathways (e.g., channel fill) and localities produce identifiable specimens, most assemblages in FA 6 accumulated through the waterhole pathway, which is dominated by isolated postcrania (Chapter 4, Fig. 4.6) that cannot be referred to genus or species.

The OHOs in FA 5 and FA 6 may be partly an artifact of preservation, as they increase in the uppermost part of the Barstow Formation, which is the top of the section. This is especially the case for long-ranging taxa such as *Aepycamelus*, which has many occurrences interspersed with stratigraphic gaps of varying thicknesses (Fig. 5.3). The top of the formation produces a Signor-Lipps effect (Signor and Lipps, 1982) in the ranges of species in the upper part of FA 6. The OHOs of these taxa are smeared downwards below the unconformable top of the formation, producing the stratigraphic stacking of OHOs toward this boundary. The pattern in IHOs is similar to the observed distribution because many species are well sampled through their ranges, producing well-constrained confidence intervals. Well-sampled species with ILOs in the upper

part of the formation may have left the basin during deposition of FA 5. Long-ranging and poorly sampled species are the most susceptible to edge effects and the stacking of observed and inferred highest occurrences in the upper part of the formation.

In addition to preservation and sampling, the patterns of observed and inferred turnover may reveal the response of faunas to environments or climate. In the upper part of the formation, observed turnover is dominated by OHOs. The numbers of specimens and taxa from this interval are high, but the spikes in OHOs and IHOs are not matched by similar numbers of OLOs or ILOs. The absence of species with lowest occurrences in these well-sampled horizons may indicate that observed turnover in the upper part of the formation is influenced by factors other than sampling and preservation. Across North America, turnover in large mammal faunas corresponds to climate cooling after the MMCO (Figueirido et al., 2012) as middle Miocene faunas went extinct. As the climate cooled after the end of the MMCO, environments in the Barstow Basin became drier (Chapter 3). With this climate shift, mammals increasingly congregated in wetland habitats where their remains were better preserved than in the drier grasslands. Species may also have responded to changing climates by shifting their geographic ranges (Badgley et al., 2015) and leaving the basin.

Faunal composition and faunal units

Changes in faunal composition through the formation have been used to establish various biochronologic schemes (Woodburne et al., 1990; Lindsay, 1972; Pagnac, 2009). Significant observed turnover occurs between the Hemingfordian and Barstovian faunas in the Barstow Formation (between the Rak and Green Hills divisions), as Red Division faunas have their OHOs and species of the Green Hills fauna first occur. The faunal composition and turnover within the

late Hemingfordian of the Barstow Formation are hard to characterize, however, given the low abundance of fossil material in the Red and Rak divisions. Preservation potential was low in FA 1 and the transitional facies of FA 3, and the faunal composition of the Red and Rak divisions probably represents a fraction of the original faunal communities in the basin during this time. ILOs occur throughout the lower portion of the formation, and many more species may have been present than are preserved. It is unlikely that the size distribution of species in the Red and Rak divisions (Fig. 5.7) represents the full range of species present on the landscape, given the preservation bias for medium-size mammals and the small sample size in these faunal units.

The Hemingfordian-Barstovian transition in the Barstow Formation coincides with a change in facies and a significant increase in preservation in FA 3. The pattern of inferred turnover and the distribution of ILOs indicate that turnover between the Hemingfordian and Barstovian faunas in the formation was not as pronounced as indicated by the observed pattern. ILOs are distributed throughout the stratigraphic interval encompassed by FA 3 (Fig. 5.9), and many species of the Barstovian Green Hills fauna may have been present in the basin throughout this time (Figs. 5.3, 5.10). Most species of the Rak Division fauna range into younger parts of the formation, and inferred turnover is not high between the Green Hills and Rak divisions. The median body mass decreased from the Rak to the Barstow divisions, as preservation potential generally increased and smaller mammals became better represented in faunal assemblages. The change in habitats represented by the lake-margin and proximal-channel facies of FA 3 may also have contributed to differences between the Rak and Green Hills faunas. More animals were active in the channel-margin settings of FA 3, and the rich fossil assemblages of the channel-fill pathway captured both common and rare taxa, increasing species richness and diversity (Table 5.2). The Green

Hills fauna encompassed a greater range of body masses than the Rak fauna (Fig. 5.7), and median mass decreased due to an enhanced ability to preserve smaller animals.

The highest observed and inferred turnover occurs within the Green Hills Division in FA 3 (Figs. 5.9, 5.10). This high turnover results from high numbers of OLOs and ILOs at roughly the same stratigraphic interval, and the agreement between observed and inferred turnover patterns may indicate that species entered the basin at this time. If so, the Hemingfordian-Barstovian transition can be distinguished in the Barstow Formation, although the stratigraphic position of this transition is dependent on facies and preservation potential.

Stratigraphic intervals of increased preservation contribute to high specimen abundance and species richness in the Green Hills, Second, and Barstow divisions (Fig. 5.9, Table 5.2). Many of the species with the OLOs and ILOs in the Green Hills Division range through to the Barstow Division but do not occur in the Second Division. The amalgamated sandstone deposits of FA 4 had decreased preservation potential, as indicated by the reduced range of body masses preserved in the Second Division (Fig. 5.7). Leporids and rhinocerotids are absent from this faunal unit, either because these taxa were not present in these environments or they were not preserved in these settings. Species may have left the area with the change in habitats, or they remained and were not preserved in these channel-dominated settings. Increased preservation and sampling in FA 5 and FA 6 also underlies the richness and diversity of the Barstow Division (Table 5.2).

Conclusion

Taphonomic influences on the fossil record of the Barstow Formation operate at the locality scale and facies scale. Changing preservation and sampling significantly affect the diversity in the formation, and facies settings are important to understanding faunal dynamics and turnover.

The channel-margin and wetland settings in FA 3 and FA 5 were especially favorable sites of fossil accumulation and preservation, and these facies associations have the highest species richness and diversity. The majority of fossil material was from medium-size mammals (50-200 kg), and preservation bias for animals in this size range operates in all facies associations and taphonomic pathways. Intervals of observed turnover correspond with stratigraphic intervals with many localities and fossil collections, showing that preservation and sampling control much of the apparent stratigraphic ranges of species. Inferred turnover is variable but occurs throughout the formation without pronounced stratigraphic gaps. The high number of observed lowest occurrences in FA 3 corresponds with the formation of favorable habitats and depositional settings that captured rare and common taxa. Inferred lowest occurrences of many species are distributed throughout the lower part of the formation, spanning several facies transitions. The highest observed and inferred turnover occurs within the channel-margin deposits of FA 3, indicating that faunal composition changed at this time. In the upper part of the formation, many observed and inferred highest occurrences are distributed throughout FA 6. These patterns reflect the edge effects at the top of the section, as well as preservation and sampling on a heterogeneous landscape. Drier conditions in the basin at this time prompted mammals to congregate at ephemeral wetlands where their remains were preserved, serving as the record of their highest occurrence.

As one of the important faunal records of the middle Miocene of western North America, the Barstow Formation represents an opportunity to study the response of mammal diversity to changing climate and tectonics. Environments of the Barstow Formation changed through time with the tectonic evolution of the basin from a closed-drainage setting characterized by alluvial fans and playa lakes to an open-drainage system characterized by stream channels and

floodplains. During the Middle Miocene Climatic Optimum (MMCO), the climate became humid and supported abundant vegetation and a diverse mammalian fauna. Mammal diversity changed through the formation in response to changing environments and the heterogeneity of depositional settings, which had implications for preservation and biostratigraphy. The Hemingfordian-Barstovian transition coincides with changes in facies and depositional environments. Alluvial fans and marginal-lacustrine environments of FA 1 and FA 3 preserve few species in Hemingfordian-age sediments. In contrast, Barstovian-age proximal-channel settings in FA 3 captured common and rare components of the community and the arrivals of new species to the basin. High observed and inferred turnover in this interval indicates that faunal change occurred at this time in the formation, although preservation potential affects the observed stratigraphic position of turnover. Climatic cooling and drying after the end of the MMCO corresponded with progressive loss of species in the basin. The turnover in mammal faunas following the MMCO played out across North America in many basins (Figueirido et al., 2012). In the Barstow Basin, the development of intermittent wetlands and savannas provided a setting for the declining diversity at the end of the Barstovian within the context of changing climate and tectonics.

References

Badgley, C., 1986a, Counting individuals in mammalian fossil assemblages from fluvial environments: PALAIOS, v. 1, no. 3, p. 328-338.

Badgley, C., 1986b, Taphonomy of mammalian fossil remains from Siwalik rocks of Pakistan: Paleobiology, v. 12, no. 2, p. 119-142.

Badgley, C., Smiley, T.M., and Finarelli, J.A., 2014, Great Basin mammal diversity in relation to landscape history: Journal of Mammalogy, v. 95, no. 6, p. 1090-1106.

Badgley, C., Smiley, T.M., and Loughney, K.M., 2015, Miocene mammal diversity of the Mojave region in the context of Great Basin mammal history, *in* Reynolds, R.E., ed., Mojave Miocene: The 2015 Desert Symposium Field Guide and Proceedings: Zzyzx, California, California State University Desert Studies Consortium, p. 34-43.

Baker, C.L., 1911, Notes on the later Cenozoic history of the Mohave Desert region in southeastern California: University of California Publications Bulletin of the Department of Geology, v. 6, no. 15, p. 333-383.

Baskin, J.A., 1998, Mustelidae, *in* Janis, C.M., Scott, K.M., and Jacobs, L.L., eds., Evolution of Tertiary Mammals of North America, Volume 1: Terrestrial Carnivores, Ungulates, and Ungulatelike Mammals: Cambridge, U.K., Cambridge University Press, p. 152-173.

Behrensmeyer, A.K., 1975, The taphonomy and paleoecology of Plio-Pleistocene vertebrate assemblages east of Lake Rudolf, Kenya: Bulletin of the Museum of Comparative Zoology, v. 146, no. 10, p. 473-578.

Behrensmeyer, A.K., 1978, Taphonomic and ecologic information from bone weathering: Paleobiology, v. 4, p. 150-162.

Behrensmeyer, A.K., Western, D., and Dorothy, E.D.B., 1979, New Perspectives in Vertebrate Paleoecology from a Recent Bone Assemblage: Paleobiology, v. 5, no. 1, p. 12-21.

Behrensmeyer, A.K., and Dechant Boaz, D.E., 1980, The recent bones of Amboseli Park, Kenya, in relation to East African paleoecology, *in* Behrensmeyer, A.K., and Hill, A.P., eds., Fossils in the Making: Vertebrate Taphonomy and Paleoecology: Chicago, University of Chicago Press, p. 72-92.

Behrensmeyer, A.K., 1991, Terrestrial vertebrate accumulations, *in* Allison, P.A., and Briggs, D.E.G., eds., Taphonomy: Releasing the Data Locked in the Fossil Record, Volume 9: New York, Plenum Press, p. 291-335.

Browne, I., and Reynolds, R.E., 2015, *Nimravides marshi* (Felidae): An early scimitar-cat from the upper Barstovian section of the Mud Hills, Mojave Desert, California, *in* Reynolds, R.E., ed., Mojave Miocene: The 2015 Desert Symposium Field Guide and Proceedings: Zzyzx, California, California State University Desert Studies Consortium, p. 136-144.

Carrasco, M.A., Kraatz, B.P., Davis, E.B., and Barnosky, A.D., 2005, Miocene Mammal Mapping Project (MIOMAP): Berkeley, California, University of California Museum of Paleontology.

Dickinson, W.R., 2002, The Basin and Range Province as a Composite Extensional Domain: International Geology Review, v. 44, no. 1, p. 1-38.

Figueirido, B., Perez-Claros, J.A., Hunt, R.M., Jr., and Palmqvist, P., 2010, Body mass estimation in amphicyonid carnivoran mammals: A multiple regression approach from the skull and skeleton: Acta Palaeontologica Polonica, v. 56, no. 2, p. 225-246.

Figueirido, B., Janis, C.M., Pérez-Claros, J.A., De Renzi, M., and Palmqvist, P., 2012, Cenozoic climate change influences mammalian evolutionary dynamics: Proceedings of the National Academy of Sciences, v. 109, no. 3, p. 722-727.

Foote, M., and Miller, A.I., 2007, Principles of Paleontology: New York, W.H. Freeman and Company.

Frick, C., 1926, The Hemicyoninae and an American Tertiary bear: Bulletin of the American Museum of Natural History, v. 55, p. 1-119.

Glazner, A.F., Walker, J.D., Bartley, J.M., and Fletcher, J.M., 2002, Cenozoic evolution of the Mojave block of southern California: Geological Society of America Memoirs, v. 195, p. 19-41.

Holland, S.M., 1995, The stratigraphic distribution of fossils: Paleobiology, v. 21, no. 1, p. 92-109.

Honey, J.G., Harrison, J.A., Prothero, D.R., and Stevens, M.S., 1998, Camelidae, *in* Janis, C.M., Scott, K.M., and Jacobs, L.L., eds., Evolution of Tertiary Mammals of North America, Volume 1: Terrestrial carnivores, ungulates, and ungulatelike mammals: Cambridge, U.K., Cambridge University Press, p. 439-462.

Hunt, R.M., Jr., 1998, Amphicyonidae, *in* Janis, C.M., Scott, K.M., and Jacobs, L.L., eds., Evolution of Tertiary Mammals of North America, Volume 1: Terrestrial Carnivores, Ungulates, and Ungulatelike Mammals: Cambridge, U.K., Cambridge University Press, p. 196-227.

Ingersoll, R.V., Devaney, K.A., Geslin, J.K., Cavazza, W., Diamond, D.S., Heins, W.A., Jagiello, K.J., Marsaglia, K.M., Paylor, E.D., II, and Short, P.F., 1996, The Mud Hills, Mojave Desert, California: Structure, stratigraphy, and sedimentology of a rapidly extended terrane, *in* Beratan, K.K., ed., Reconstructing the History of Basin and Range Extension Using Sedimentology and Stratigraphy, Volume 303: Boulder, Colorado, Geological Society of America, p. 61-84.

Janis, C.M., and Manning, E., 1998a, Antilocapridae, *in* Janis, C.M., Scott, K.M., and Jacobs, L.L., eds., Evolution of Tertiary mammals of North America, Volume 1: Terrestrial carnivores, ungulates, and ungulatelike mammals: Cambridge, U.K., Cambridge University Press, p. 491-507.

Janis, C.M., and Manning, E., 1998b, Dromoerycidae, *in* Janis, C.M., Scott, K.M., and Jacobs, L.L., eds., Evolution of Tertiary Mammals of North America, Volume 1: Terrestrial Carnivores, Ungulates, and Ungulatelike Mammals: Cambridge, U.K., Cambridge University Press, p. 477-490.

Janis, C.M., Scott, K.M., and Jacobs, L.L., 1998, Evolution of Tertiary Mammals of North America, Volume 1: Terrestrial Carnivores, Ungulates, and Ungulatelike Mammals, Cambridge, U.K., Cambridge University Press, p. 691.

Lander, B., 1998, Oreodontoidea, *in* Janis, C.M., Scott, K.M., and Jacobs, L.L., eds., Evolution of Tertiary Mammals of North America, Volume 1: Terrestrial Carnivores, Ungulates, and Ungulatelike Mammals: Cambridge, U.K., Cambridge University Press, p. 402-425.

Lindsay, E.H., 1972, Small mammal fossils from the Barstow Formation, California: University of California Publications in Geological Sciences, v. 93, p. 1-104.

Lindsay, E.H., 1995, *Copemys* and the Barstovian/Hemingfordian Boundary: Journal of Vertebrate Paleontology, v. 15, no. 2, p. 357-365.

Lofgren, D.L., and Anand, R.S., 2011, Partial skull of *Zygolophodon* (Mammalia, Proboscidea) from the Barstow Formation of California: Journal of Vertebrate Paleontology, v. 31, no. 6, p. 1392-1396.

Lofgren, D.L., Holliday, A., and Stoddard, R., 2016, Review of small mustelids from the Barstow Formation of California, *in* Reynolds, R.E., ed., Going LOCO: Investigations Along the Lower Colorado River: The 2016 Desert Symposium Field Guide and Proceedings: Zzyzx, California, California State University Desert Studies Consortium, p. 295-302.

Loughney, K.M., and Badgley, C., 2017, Facies, environments, and fossil preservation in the Barstow Formation, Mojave Desert, California: PALAIOS, v. 32, no. 6, p. 396-412.

Lyons, S.K., and Smith, F.A., 2010, Using a macroecological approach to study geographic range, abundance and body size in the fossil record, *in* Alroy, J., and Hunt, G., eds., Quantitative Methods in Paleobiology, The Paleontological Society Papers, vol. 16, p. 117-141.

MacFadden, B.J., Swisher, C.C., III, Opdyke, N.D., and Woodburne, M.O., 1990, Paleomagnetism, geochronology, and possible tectonic rotation of the middle Miocene Barstow Formation, Mojave Desert, southern California: GSA Bulletin, v. 102, no. 4, p. 478-493.

MacFadden, B.J., 1998, Equidae, *in* Janis, C.M., Scott, K.M., and Jacobs, L.L., eds., Evolution of tertiary mammals of North America: Volume 1: Terrestrial carnivores, ungulates, and ungulatelike mammals: Cambridge, U.K., Cambridge University Press, p. 537-559.

Marean, C.W., Spencer, L.M., Blumenschine, R.J., and Capaldo, S.D., 1992, Captive hyaena bone choice and destruction, the Schlepp effect and Olduvai archaeofaunas: Journal of Archaeological Science, v. 19, no. 1, p. 101-121.

Marshall, C.R., 1997, Confidence Intervals on Stratigraphic Ranges with Nonrandom Distributions of Fossil Horizons: Paleobiology, v. 23, no. 2, p. 165-173.

Marshall, C.R., 2010, Using confidence intervals to quantify the uncertainty in the end-points of stratigraphic ranges, *in* Alroy, J., and Hunt, G., eds., Quantitative Methods in Paleobiology, The Paleontological Society Papers, vol. 16, p. 291-316.

Martin, L.D., 1998, Felidae, *in* Janis, C.M., Scott, K.M., and Jacobs, L.L., eds., Evolution of Tertiary Mammals of North America, Volume 1: Terrestrial Carnivores, Ungulates, and Ungulatelike Mammals: Cambridge, U.K., Cambridge University Press, p. 236-242.

Martin, R.E., 1999, Taphonomy: A Process Approach: Cambridge, U.K., Cambridge University Press, 508 p.

McKenna, M.C., and Bell, S.K., 1997, Classification of Mammals Above the Species Level: New York, Columbia University Press, 631 p.

Merriam, J.C., 1919, Tertiary mammalian faunas of the Mohave Desert: University of California Publications Bulletin of the Department of Geological Sciences, v. 11, no. 5, p. 437-585.

Munthe, K., 1998, Canidae, *in* Janis, C.M., Scott, K.M., and Jacobs, L.L., eds., Evolution of Tertiary Mammals of North America, Volume 1: Terrestrial Carnivores, Ungulates, and Ungulatelike Mammals: Cambridge, U.K., Cambridge University Press, p. 124-143.

Pagnac, D., 2005a, A systematic review of the mammalian megafauna of the middle Miocene Barstow Formation, Mojave Desert, California [Ph. D. dissertation]: University of California, Riverside, 384 p.

Pagnac, D., 2005b, New camels (Mammalia: Artiodactyla) from the Barstow Formation (middle Miocene), San Bernardino County, California: PaleoBios, v. 25, no. 2, p. 19-31.

Pagnac, D., 2006, Scaphohippus, A New Genus of Horse (Mammalia: Equidae) from the Barstow Formation of California: Journal of Mammalian Evolution, v. 13, no. 1, p. 37-61.

Pagnac, D., 2009, Revised large mammal biostratigraphy and biochronology of the Barstow Formation (Middle Miocene), California: PaleoBios, v. 29, no. 2, p. 48-59.

Pagnac, D., Browne, I., and Smith, K., Stratigraphy and vertebrate paleontology of the middle Miocene Barstow Formation, San Bernardino County, California, *in* Proceedings 73rd Annual Meeting of the Society of Vertebrate Paleontology, Los Angeles, California, 29 October 2013 2013, p. 1-26.

Pielou, E.C., 1966, Species-diversity and pattern-diversity in the study of ecological succession: Journal of Theoretical Biology, v. 10, p. 370-383.

Rogers, R.R., and Kidwell, S.M., 2000, Associations of vertebrate skeletal concentrations and discontinuity surfaces in terrestrial and shallow marine records: A test in the Cretaceous of Montana: The Journal of Geology, v. 108, no. 2, p. 131-154.

Scott, K.M., 1990, Postcranial dimensions of ungulates as predictors of body mass, *in* Damuth, J., and MacFadden, B.J., eds., Body Size in Mammalian Paleobiology: Estimation and Biololgical Implications: Cambridge, Cambridge University Press, p. 301-335.

Signor, P.W., and Lipps, J.H., 1982, Sampling bias, gradual extinction patterns, and catastrophes in the fossil record: Geological Society of America Special Papers, v. 190, p. 291-296.

Silva, M., and Downing, J.A., 1995, CRC Handbook of Mammalian Body Masses: Boca Raton, Florida, CRC Press.

Sorkin, B., 2006, Ecomorphology of the giant bear-dogs Amphicyon and Ischyrocyon: Historical Biology, v. 18, no. 4, p. 375-388.

Tedford, R.H., Albright, L.B., Barnosky, A.D., Ferrusquía-Villafranca, I., Hunt, R.M., Jr., Storer, J.E., Swisher, C.C., III, Voorhies, M.R., Webb, S.D., and Whistler, D.P., 2004, Mammalian biochronology of the Arikareean through Hemphillian interval (late Oligocene through early Pliocene epochs), *in* Woodburne, M.O., ed., Late Cretaceous and Cenozoic Mammals of North America: Biostratigraphy and Geochronology: New York, Columbia University Press, p. 169-231.

Van Valkenburgh, B., 1990, Skeletal and dental predictors of body mass in carnivores, *in* Damuth, J., and MacFadden, B.J., eds., Body Size in Mammalian Paleobiology: Estimation and Biological Implications: Cambridge, Cambridge University Press, p. 181-205.

Vaughan, T.A., Ryan, J.M., and Czaplewski, N.J., 2015, Mammalogy: Burlington, Mass., Jones & Bartlett Learning, 755 p.

Voorhies, M.R., 1969, Taphonomy and population dynamics of an early Pliocene vertebrate fauna, Knox County, Nebraska: University of Wyoming Contributions to Geology Special Papers, v. 1, p. 1-69.

Wang, B., 2016, Reconstructing the paleoecology and biogeography of rhinoceroses (Mammalia: Rhinocerotidae) in the Great Plains of North America, leading up to their extinction in the early Pliocene [M.S. thesis]: University of Nebraska, 79 p.

Wang, X., 1994, Phylogenetic systematics of the Hesperocyoninae (Carnivora: Canidae): Bulletin of the American Museum of Natural History, v. 221, p. 1-207.

Wang, X., Tedford, R.H., and Taylor, B.E., 1999, Phylogenetic systematics of the Borophaginae (Carnivora: Canidae): Bulletin of the American Museum of Natural History, v. 243, p. 1-391.

White, J.A., 1988, The Archaeolaginae (Mammalia, Lagomorpha) of North America, excluding *Archaeolagus* and *Panolax*: Journal of Vertebrate Paleontology, v. 7, no. 4, p. 425-450.

Woodburne, M.O., Tedford, R.H., and Swisher, C.C., III, 1990, Lithostratigraphy, biostratigraphy, and geochronology of the Barstow Formation, Mojave Desert, southern California: GSA Bulletin, v. 102, p. 459-477.

Zachos, J.C., Pagani, M., Sloan, L.C., Thomas, E., and Billups, K., 2001, Trends, rhythms, and aberrations in global climate 65 Ma to present: Science, v. 292, p. 686-693.

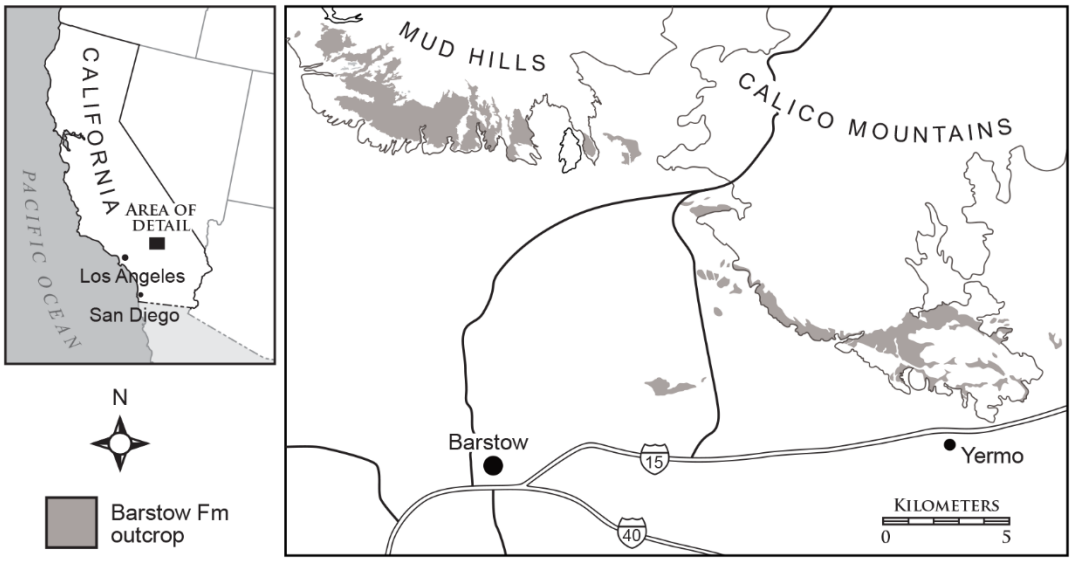

Figure 5.1. Location map of Barstow Formation outcrops.

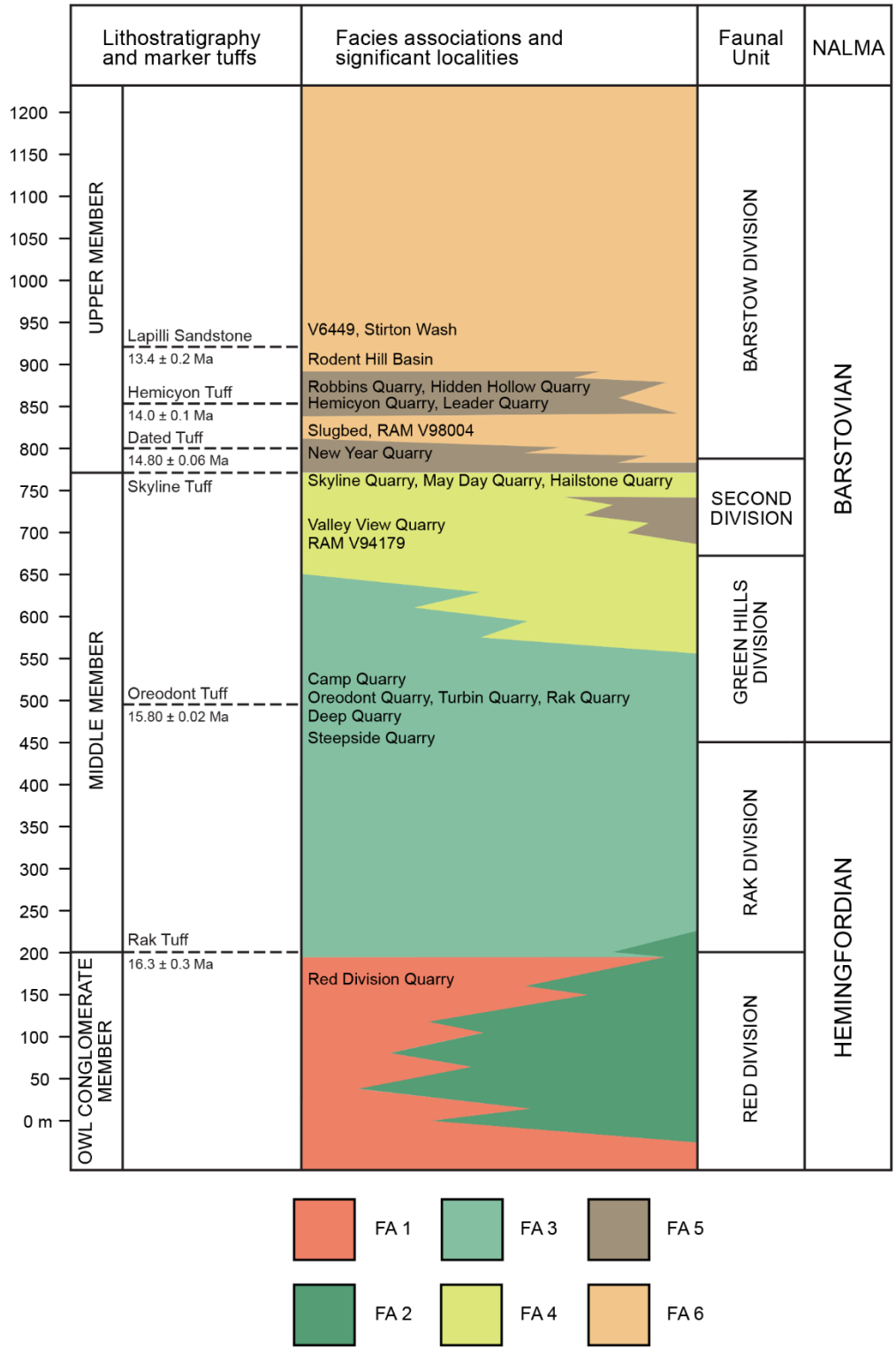

Figure 5.2. Lithostratigraphy and biochronology of the Barstow Formation, showing stratigraphic relationships of facies associations and prominent fossil localities.

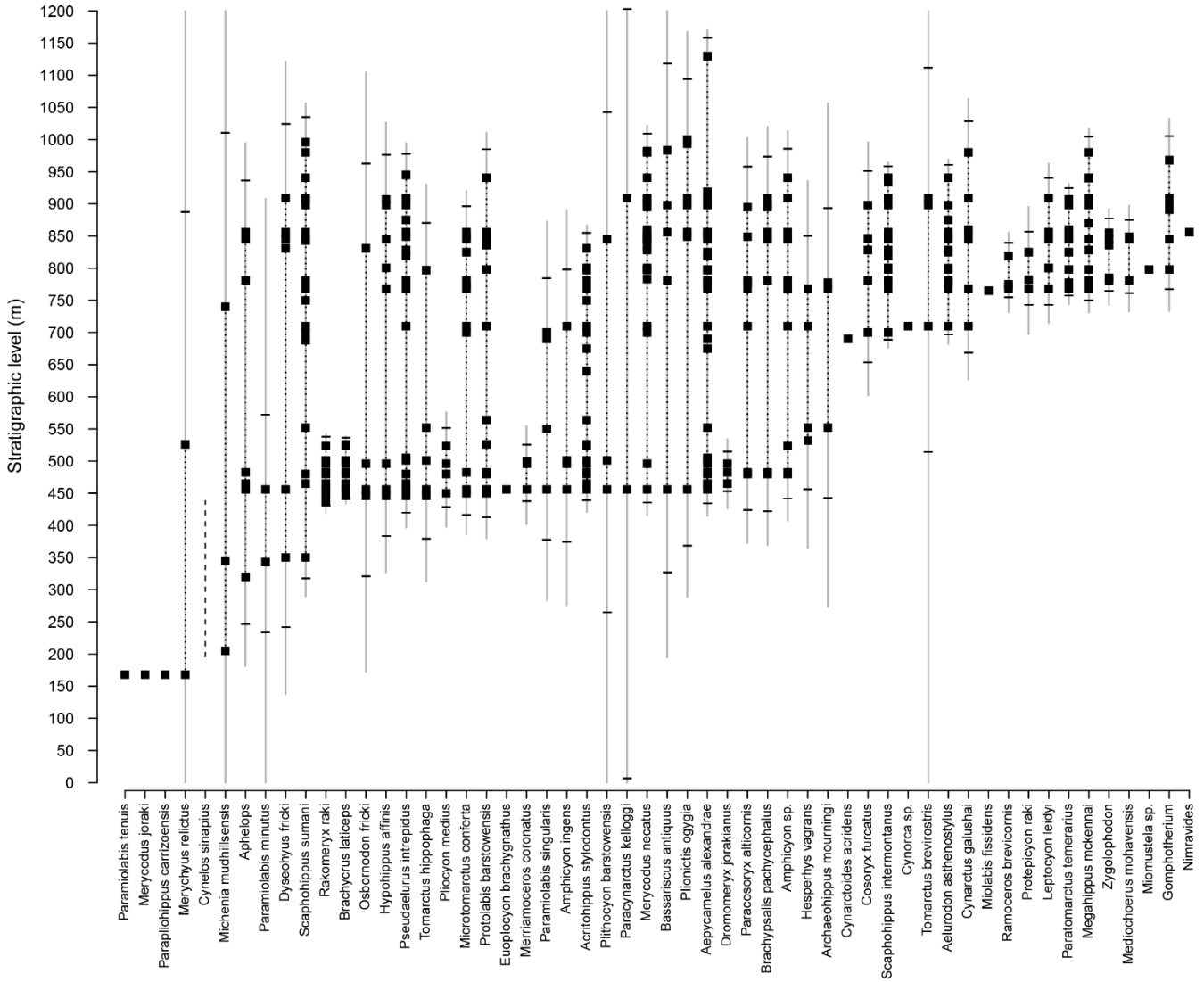

Figure 5.3. Stratigraphic range chart of large-mammal species from the Barstow Formation ordered by observed lowest occurrence datum. Black squares = occurrences; dotted lines = observed ranges; dashed black lines = inferred ranges; gray lines = 80% confidence intervals; dashes = lower and upper point estimates.

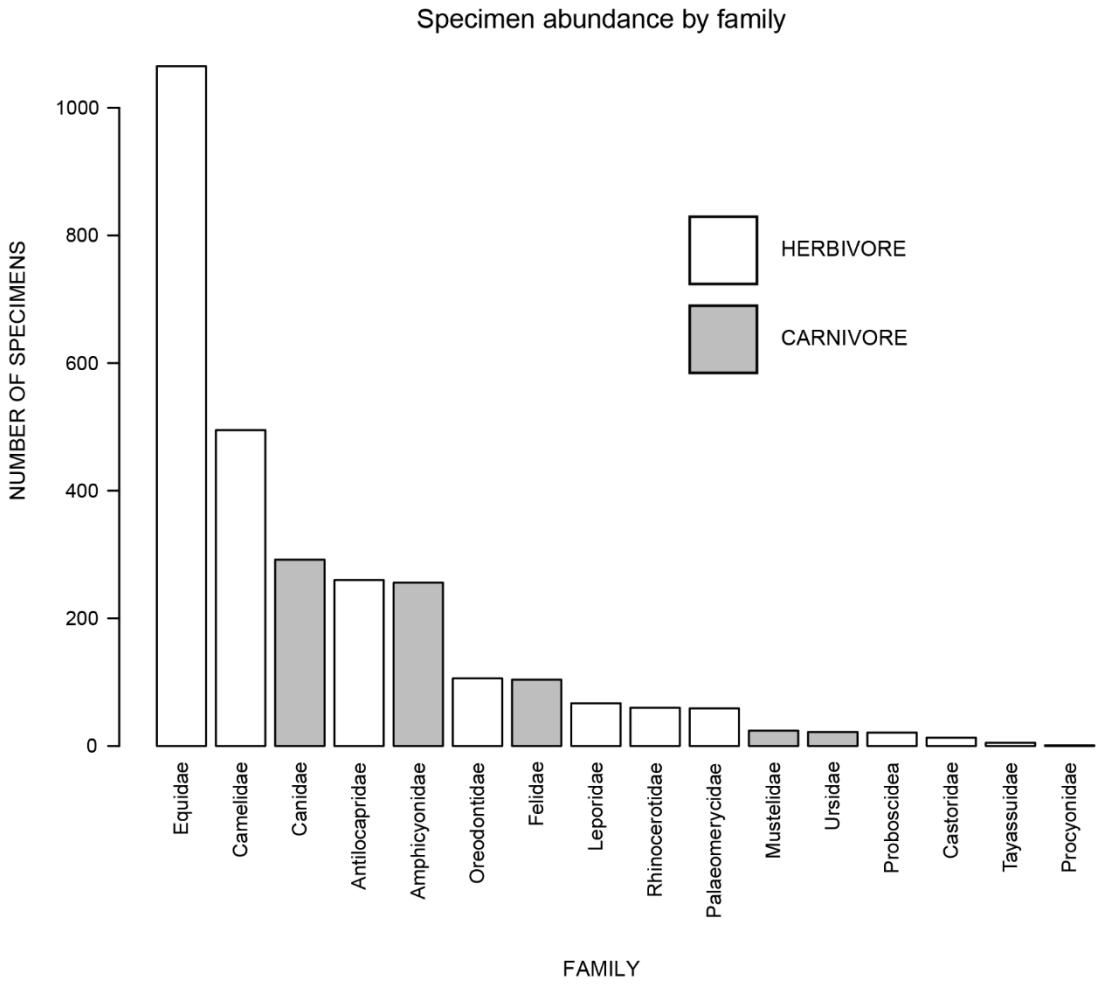

Figure 5.4. Number of specimens by family of material examined in museum collections from 78 localities in the Mud Hills.

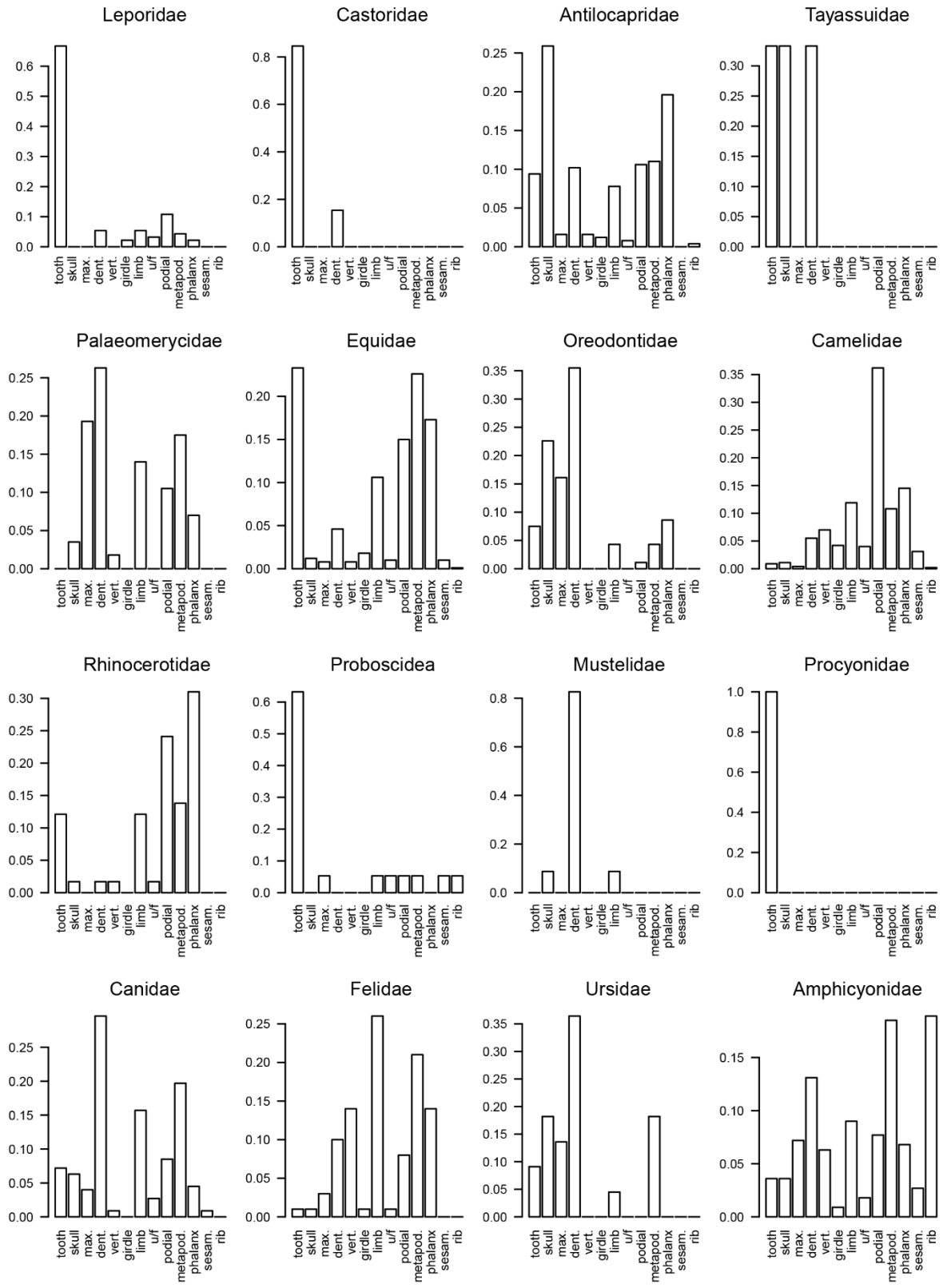

Figure 5.5. Skeletal-element composition of large-mammal families in the Barstow Formation, based on fossil material from 78 localities in museum collections.

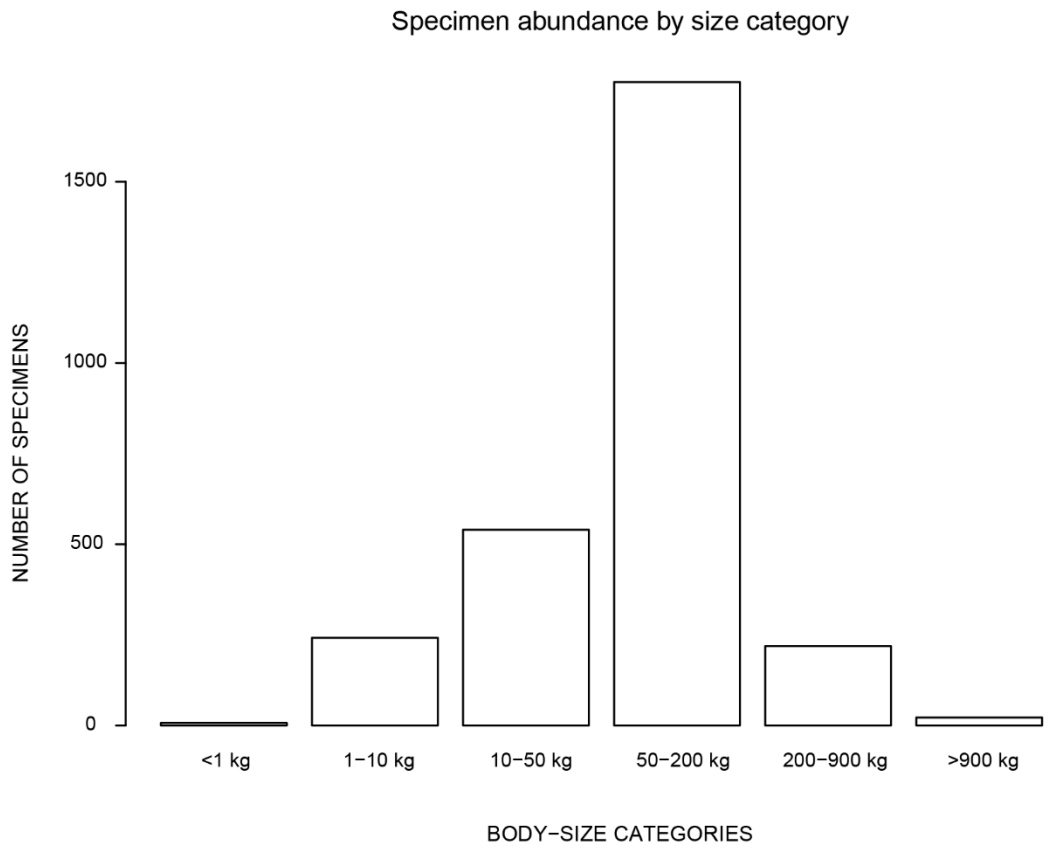

Figure 5.6. Abundance plot by body size of fossil material in museum collections from 78 fossil localities.

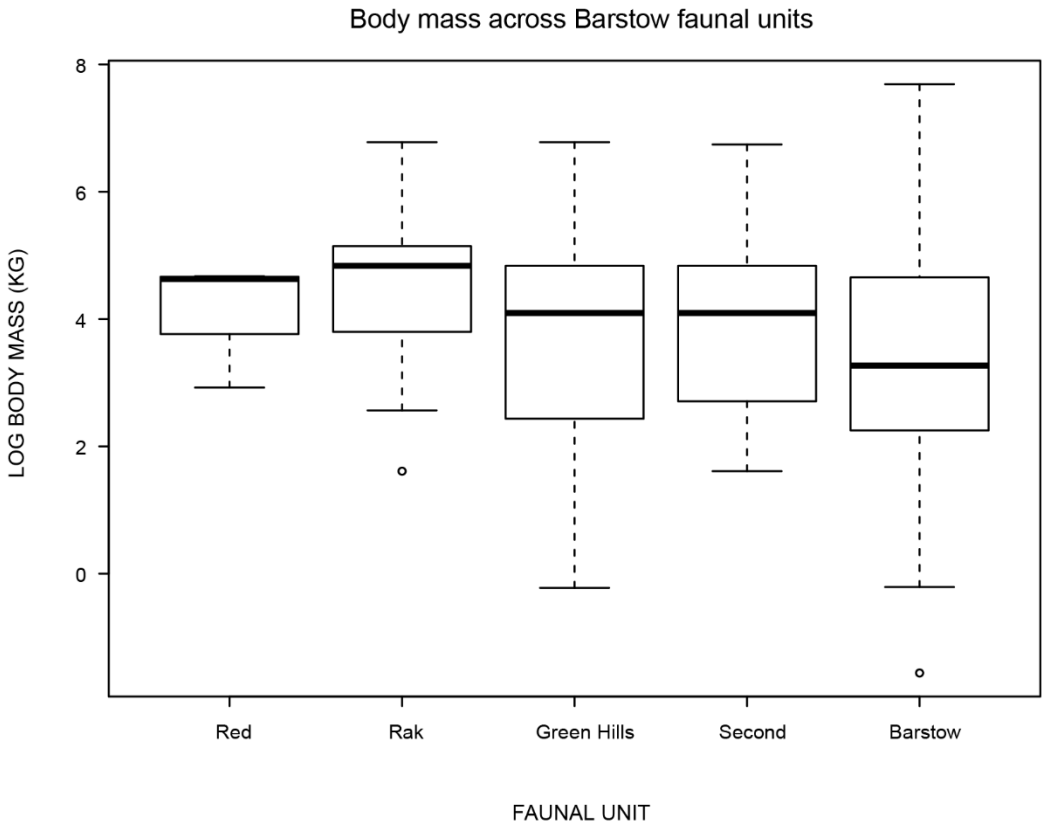

Figure 5.7. Ln-transformed body-mass composition of taxa with occurrences in faunal units of the Barstow Formation, showing minimum, maximum, first and third interquartile, and median ln-body mass.

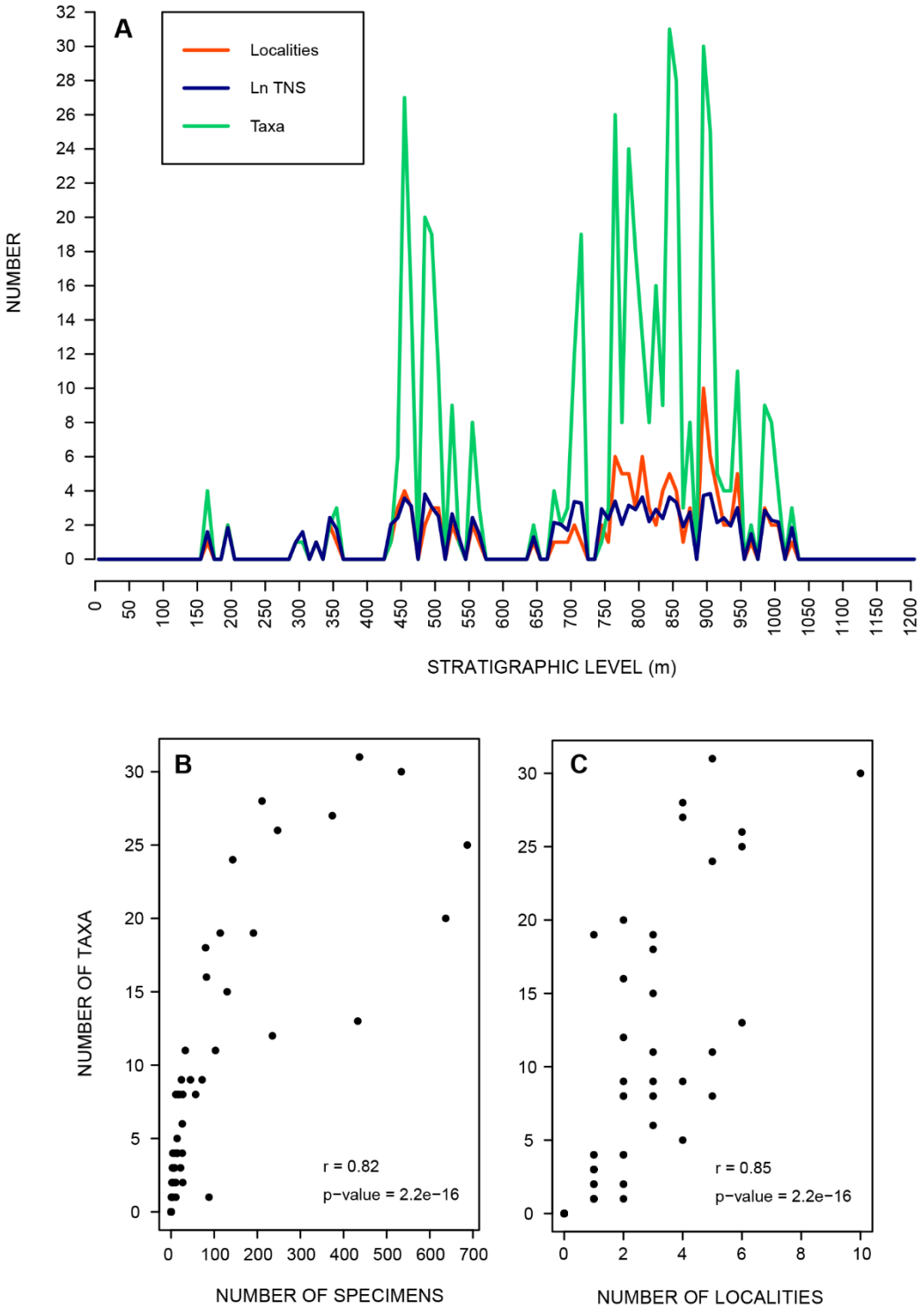

Figure 5.8. Relationship between localities, specimens, and taxa in the Barstow Formation. A) Number of localities, ln total number of specimens (TNS), and number of distinct taxa by stratigraphic level. Scatter plots of number of taxa against number of specimens (B) and number of localities (C), showing value of Pearson's correlation coefficient and p-value.

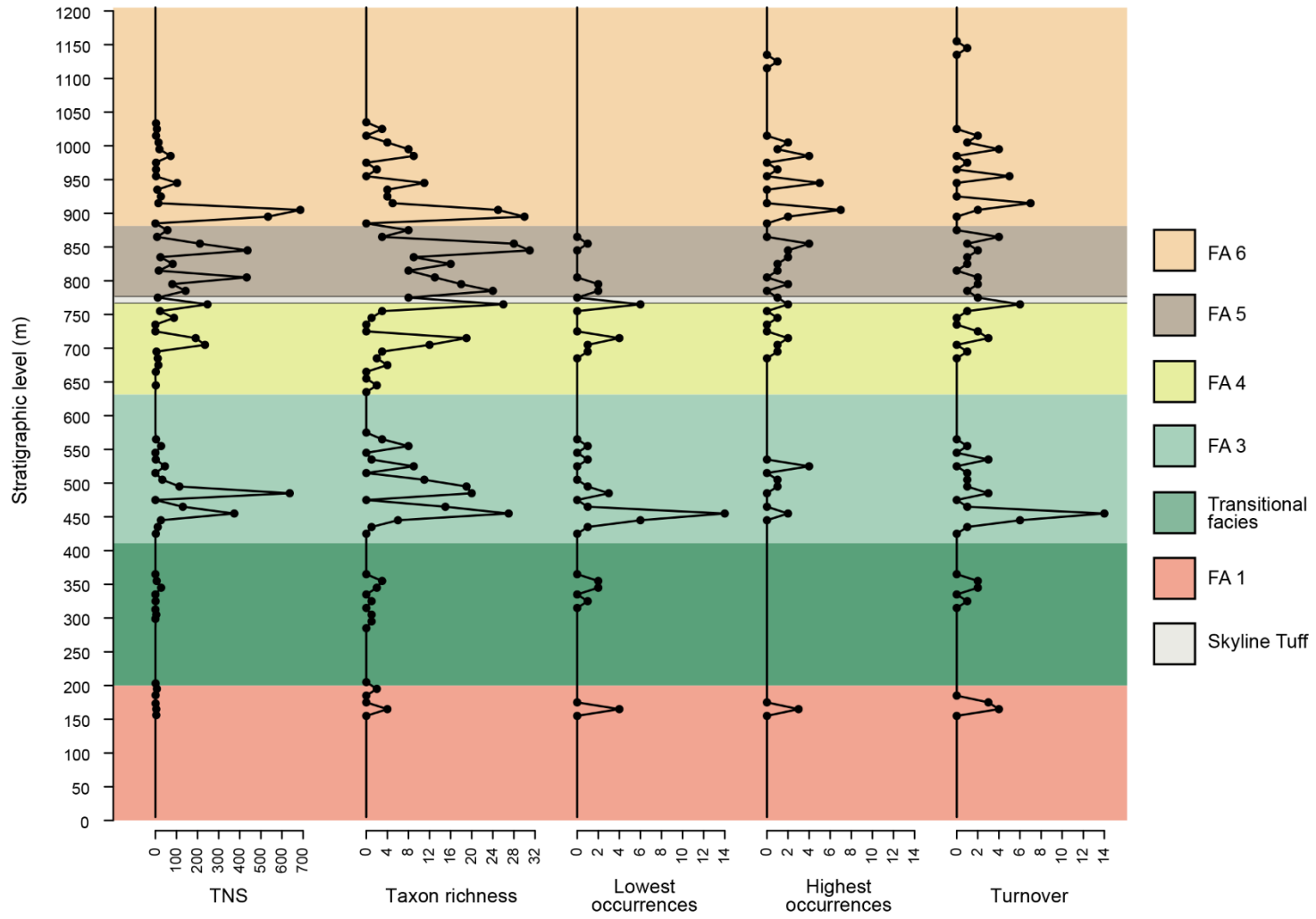

Figure 5.9. Stratigraphic distribution of total number of specimens (TNS), number of distinct taxa, number of observed species lowest occurrences, number of observed species highest occurrences, and turnover of taxa among 10-m bins in the Barstow Formation.

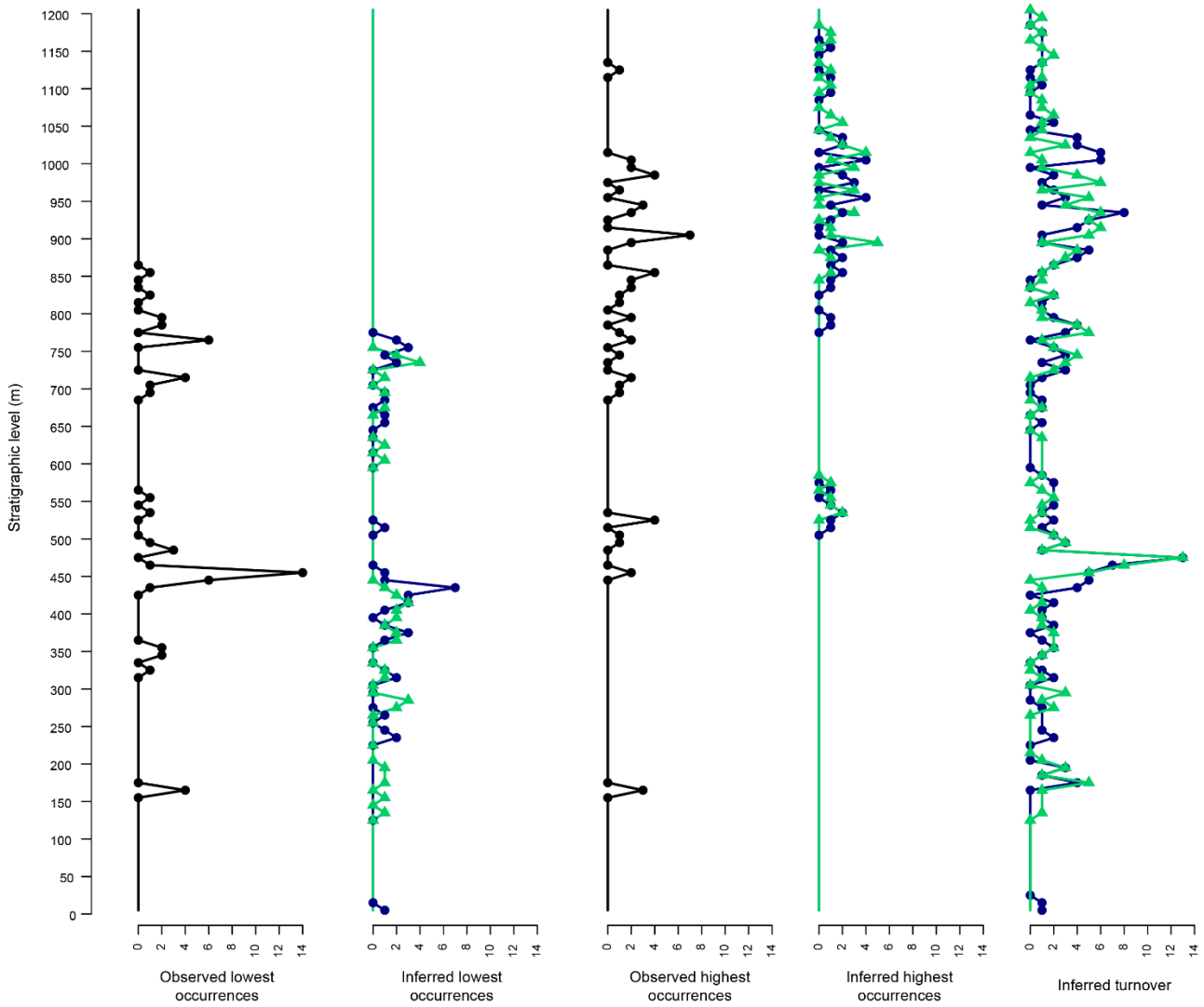

Figure 5.10. Stratigraphic distribution of observed and inferred species lowest and highest occurrences among 10-m bins in the Barstow Formation. Inferred lowest and highest occurrences are based on point estimates (blue circles) and 80% confidence intervals (green triangles) on observed stratigraphic ranges depicted in Fig. 5.3.

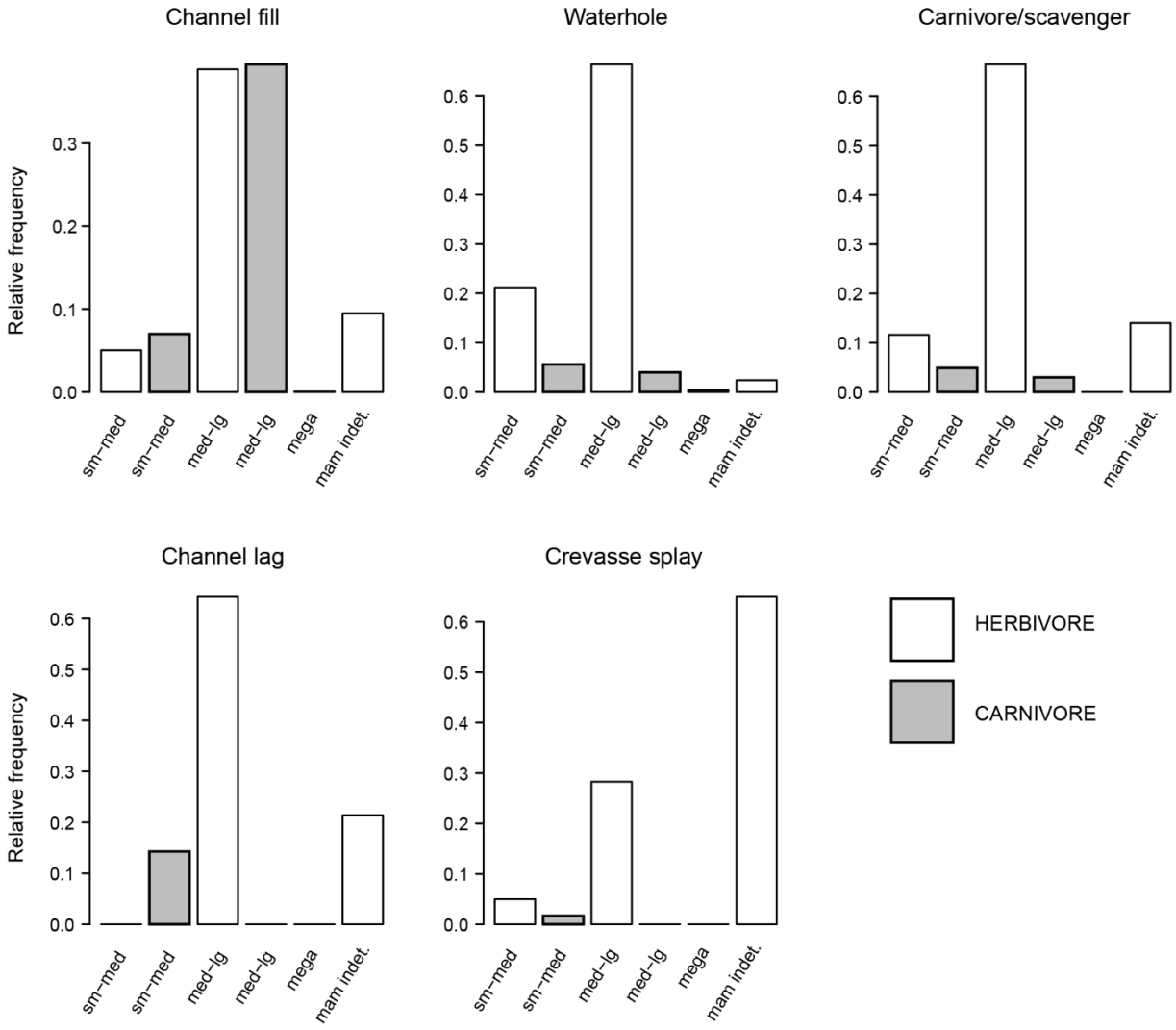

Figure 5.11. Body-size composition of specimens from taphonomic pathways in the Barstow Formation. Small to medium (sm-med) herbivores and carnivores are those <50 kg, medium to large (med-lg) herbivores and carnivores are >50 kg, and mega-mammals (mega) are >900 kg. Fragmentary material (mam indet.) could not be assigned to size category.

Table 5.1. Faunal list of large mammals from the Barstow Formation. After Pagnac (2005) and Pagnac et al. (2013).

Order Lagomorpha
- Family Leporidae
  - Subfamily Archaeolaginae
    - *Hypolagus*

Order Rodentia
- Family Castoridae
  - Subfamily Castoroidinae
    - *Monosaulax pansus*

Order Carnivora
- Family Felidae
  - *Nimravides marshi*
  - *Pseudaelurus intrepidus*
- Family Canidae
  - Subfamily Hespercyoninae
    - *Osbornodon fricki*
  - Subfamily Borophaginae
    - *Cynarctoides acridens*
    - *Paracynarctus kellogi*
    - *Euoplocyon brachygnathus*
    - *Microtomarctus conferta*
    - *Tomarctus hippophaga*
    - *Tomarctus brevirostris*
    - *Protomarctus optatus*
    - *Cynarctus galushai*
    - *Aelurodon asthenostylus*
    - *Paratomarctus temerarius*
    - *Protepicyon raki*
  - Subfamily Caninae
    - *Leptocyon leidyi*
- Family Amphicyonidae
  - Subfamily Amphicyoninae
    - *Cynelos sinapius*
    - *Pliocyon medius*
    - *Amphicyon ingens*
    - *Amphicyon* sp.
- Family Ursidae
  - Subfamily Hemicyoninae
    - *Plithocyon barstowensis*
- Family Mustelidae
  - Subfamily Mustelinae
    - *Brachypsalis pachycephalus*
    - *Plionictis ogygia*
    - *Miomustela* sp.
- Family Procyonidae
  - Subfamily Bassaricinae
    - *Bassariscus antiquus*

Order Artiodactyla
- Family Tayassuidae
  - Subfamily Tayassuinae
    - *Hesperhys vagrans*
    - *Dyseohyus fricki*
    - *Cynorca occidentale*
- Family Oreodontidae
  - Subfamily Ticholeptinae
    - *Merychyus smithi*
    - *Brachycrus laticeps*
    - *Mediochoerus mojavensis*
- Family Camelidae
  - Subfamily Protolabinae
    - *Protolabis barstowensis*
    - *Protolabis* sp.
    - *Michenia mudhillsensis*
    - *Michenia* sp.
  - Subfamily Miolabinae
    - *Paramiolabis tenuis*
    - *Paramiolabis singularis*
    - *Paramiolabis minutus*
    - *Miolabis fissidens*
  - Subfamily Aepycamelinae
    - *Aepycamelus alexandrae*
    - *Aepycamelus* sp.
- Family Antilocapridae
  - Subfamily Cosorycinae
    - *Merycodus joraki*
    - *Merriamoceros coronatus*
    - *Paracosoryx alticornis*
    - *Merycodus necatus*
    - *Ramoceros brevicornis*
    - *Cosoryx furcatus*

Family Palaeomerycidae
Subfamily Dromomerycinae
Rakomeryx raki
Dromomeryx jorakinus

Order Perissodactyla
Family Equidae
Subfamily Anchitheriinae
Hypohippus affinis
Archaeohippus mourningi
Megahippus mckennai
Subfamily Equinae
Parapliohippus carrizoensis
Merychippus isonesus
Scaphohippus intermontanus
Acritohippus stylodontus
Scaphohippus sumani

Family Rhinocerotidae
Subfamily Aceratheriinae
Aphelops sp.

Family Gomphotheriidae
Subfamily Gomphotheriinae
Gomphotherium sp.

Family Mammutidae
Subfamily Mammutinae
Zygolophodon cf. *paravus*
Zygolophodon sp.

Table 5.2. Species richness, diversity (Simpson's *D* and 1 – *D*), and evenness (Pielou's *J*) based on observed occurrences for facies associations and faunal units of the Barstow Formation.

Facies association	Species richness	*D*	1 – *D*	*J*
FA 6	26	0.90	0.10	0.84
FA 5	35	0.93	0.07	0.86
FA 4	26	0.94	0.06	0.91
FA 3	34	0.89	0.11	0.78
FA 1	4	-	-	-

Faunal division	Species richness	*D*	1 – *D*	*J*
Barstow	37	0.93	0.07	0.85
Second	32	0.91	0.09	0.84
Green Hills	35	0.90	0.10	0.78
Rak	15	0.87	0.13	0.88
Red	4	-	-	-

Table 5.3. Weathering stages of fossil specimens from museum collections across body-size categories. Weathering stages follow Behrensmeyer (1978) for bones; teeth were not included. TNS = total number of specimens.

Body-size category	TNS	Number of localities	Weathering stage			
			Incipient	Moderate		Advanced
			0-1	Adv. 1-2	2-3	Adv. 3-5
<1 kg	7	3	6	0	0	0
1-10 kg	242	32	136	25	1	0
10-50 kg	540	49	335	77	2	0
50-200 kg	1775	74	777	314	58	1
200-900 kg	219	29	61	21	90	15
>900 kg	22	13	1	4	2	0

Supplemental Information

Table S5.1. Body-mass estimates of large mammals from the Barstow Formation. Body-size categories (BS): 1 = <1 kg; 2 = 1-10 kg; 3 = 10-50 kg; 4 = 50-200 kg; 5 = 200-900 kg; 6 = >900 kg.

Family	Taxon	BS	Est. weight (kg)	Reference taxon	Common name of reference taxon	Reference
Amphicyonidae	*Amphicyon ingens*	5	550.0	*Amphicyon ingens*		Sorkin (2006), Figuerido et al. (2011)
	Ischyrocyon	5	240.0	*Ischyrocyon gidleyi*		Sorkin (2006), Figuerido et al. (2011)
	Pliocyon	4	150.0	*Pliocyon medius*		Hunt (1998), Figuerido et al. (2011)
	Cynelos	5	200.0	*Cynelos*		Hunt (1998)
	Amphicyon sp.	5	200.0	*Amphicyon*		Hunt (1998), Figuerido et al. (2011)
Antilocapridae	*Merycodus*	3	19.0	*Merycodus*	Extinct pronghorn	Scott (1990)
	Cosoryx	3	15.0	*Merycodus*	Extinct pronghorn	Scott (1990)
	Ramoceros	3	20.0	*Ramoceros*	Extinct pronghorn	Scott (1990)
	Parasocoryx	2	9.0	*Merycodus*	Extinct pronghorn	Janis et al. (1998b), Pagnac (2005a)
	Merriamoceros	3	15.0	*Merycodus*	Extinct pronghorn	Scott (1990)
Camelidae	*Aepycamelus*	5	850.0	*Aepycamelus*	Extinct camel	Scott (1990)
	Paramiolabis singularis	4	130.0	*Michenia*	Extinct camel	Scott (1990), Honey et al. (1998)
	Paramiolabis tenuis	4	110.0	*Paramiolabis*	Extinct camel	Pagnac (2005b)
	Paramiolabis minutus	4	50.0	*Stenomylus*	Extinct camel	Scott (1990)
	Miolabis	4	130.0	*Michenia*	Extinct camel	Scott (1990)
	Protolabis	4	150.0	*Michenia*	Extinct camel	Scott (1990), Honey et al. (1998)
	Michenia	4	130.0	*Michenia*	Extinct camel	Scott (1990)

Table S5.1. Body mass estimates, continued.

Family	Taxon	BS	Est. weight (kg)	Reference taxon	Common name of reference taxon	Reference
Canidae	*Aelurodon*	3	40.0	*Canis lupus*	Gray wolf	Merriam (1919); Van Valkenburgh (1990)
	Microtomarctus	2	10.0	*Vulpes vulpes*	Red fox	Munthe (1998); Wang et al. (1999)
	Tomarctus	3	15.0	*Canis latrans*	Coyote	Munthe (1998)
	Paratomarctus	3	13.0	*Paratomarctus*	Jackal	Munthe (1998); Wang et al. (1999)
	Cynarctoides	2	4.0	*Urocyon cinereoargenteus*	Gray fox	Munthe (1998)
	Leptocyon	2	5.0	*Vulpes vulpes*	Red fox	Munthe (1998)
	Euoplocyon	3	13.0	*Canis mesomelas*	Jackal	Munthe (1998)
	Osbornodon	3	20.0	*Canis lupus*	Gray wolf	Wang (1994)
	Protepicyon	3	40.0	*Canis lupus*	Gray wolf	Munthe (1998); Wang et al. (1999)
	Paracynarctus	2	9.0	*Paracynarctus*		Munthe (1998); Wang et al. (1999)
	Cynarctus	2	5.0	*Cynarctus*		Munthe (1998); Wang et al. (1999)
Castoridae	*Monosaulax*	3	20.0	*Castor canadensis*	North American beaver	Silva and Downing (1995)
Equidae	*Hypohippus*	4	140.0	*Hypohippus*	Browsing horse	Voorhies (1969)
	Scaphohippus	4	105.0	*Equus caballus*	Young adult horse	Pagnac (2005a)
	Archaeohippus	4	60.0	*Equus caballus*	Small pony	Pagnac (2005a)
	Acritohippus	4	105.0	*Equus caballus*	Young adult horse	Pagnac (2005a)
	Parapliohippus	4	105.0	*Pliohippus*	Young adult horse	Pagnac (2005a)
	Megahippus	4	140.0	*Pliohippus*	Young adult horse	MacFadden (1998)
Felidae	*Pseudaelurus*	4	75.0	*Felis concolor*	Mountain lion	Martin (1998)
	Nimravides	4	60.0	*Nimravides marshi*		Browne and Reynolds (2015)

Table S5.1. Body mass estimates, continued.

Family	Taxon	BS	Est. weight (kg)	Reference taxon	Common name of reference taxon	Reference
Leporidae	*Hypolagus*	1	0.8	*Sivilagus audubonii*	Desert cottontail	White (1988)
Mustelidae	*Plionictis*	2	1.0	*Martes foina*	Pine marten	Van Valkenburgh (1990), Baskin (1998)
	Brachypsalis	2	7.0	*Taxidea taxus*	Badger	Silva and Downing (1995), Pagnac (2005a)
	Miomustela	1	0.2	*Mustela erminea*	Ermine	Van Valkenburgh (1990), Baskin (1998)
Oreodontidae	*Brachycrus*	4	140.0	*Tapirus*	Tapir	Silva and Downing (1995), Pagnac (2005a)
	Mediochoerus	4	100.0	*Merycochoerus, Promerycochoerus*	Oreodont	Scott (1990)
	Merychyus	4	100.0	*Ustatochoerus*	Oreodont	Voorhies (1969)
Palaeomerycidae	*Dromomeryx*	4	70.0	*Cranioceras*	Extinct "deer"	Scott (1990)
	Rakomeryx	3	50.0	*Cranioceras*	Extinct "deer"	Voorhies (1969)
Proboscidea	*Gomphotherium*	6	2190.0	*Loxodontia africana*	Small African elephant	Silva and Downing (1995)
	Zygolophodon	6	2190.0	*Loxodontia africana*	Small African elephant	Silva and Downing (1995)
Procyonidae	*Bassariscus*	2	1.0	*Bassariscus*	Ring-tail	Silva and Downing (1995)
Rhinocerotidae	*Aphelops*	5	880.0	*Aphelops*		Wang (2016)
Tayassuidae	*Hesperhys*	4	60.0	*Phacochoerus*	Warthog	Pagnac (2005a)
	Dyseohyus	3	30.0	*Tayassu pecari*	Peccary	Pagnac (2005a)
	Cynorca	3	30.0	*Tayassu pecari*	Peccary	Wright (1998)
Ursidae	*Plithocyon*	4	105.0	*Ursus americanus*	Black bear	Van Valkenburgh (1990), Hunt (1998)

CHAPTER 6

The Barstow Formation and its context within the Great Basin rock and fossil record

Patterns of diversity and fossil preservation are dependent in part on the depositional and environmental contexts under which they formed. In the Barstow Formation, depositional environments changed through time as the basin evolved and climate states changed, and with them, vegetation structure and the preservational settings of fossils changed as well. The fossil record of the Barstow Formation formed during an important interval of climatic and tectonic change, providing the opportunity to evaluate these influences on fossil accumulation and preservation. I have characterized the depositional settings, environmental conditions, and modes of fossil accumulation through the section to provide context for the abundant and diverse fossil record of the Barstow Formation. As environments in the basin changed with changing climatic and tectonic influences, the landscapes that accumulate and preserve fossils changed as well. By characterizing the depositional and taphonomic context of fossil preservation in the formation, I have shown how these factors contribute to reconstructions of faunal diversity and turnover.

History of the Barstow Formation

The oldest sedimentary environments in the Barstow Basin formed between ~17.5 and 16.5 Ma, as the basin rapidly subsided after extension had slowed (Glazner et al., 2002). These early environments were alluvial fans and playa lakes represented by Facies Associations 1 and 2, respectively (Chapter 2; Loughney and Badgley, 2017). The Barstow Basin was dry and warm

during this time, comparable to parts of the modern western interior (Park and Downing, 2001), as indicated by enrichment in carbon isotopes ($\delta^{13}C_{nC27-31}$), hydrogen isotopes (δD), and high average chain length (ACL) of *n*-alkanes and carbon isotopes from soil organic matter ($\delta^{13}C_{SOM}$; Chapter 3). Few fossil localities occur in Facies Association 1, and only four species are recognized from these deposits (Pagnac et al., 2013). Playa-lake environments in the basin supported abundant aquatic macrophytes and were surrounded by wooded grasslands (Park and Downing, 2001). Mammal trackways from Facies Association 2 demonstrate that mammals were present in the basin, but either they did not congregate near these lakes or their remains were not preserved in these environments (Chapter 2). Aridity in the basin prior to 17.0 Ma is reflected in thick gypsum beds towards the top of the playa-lake deposits in the Calico Mountains (Chapter 2) and progressive enrichment of $\delta^{18}O$ of arthropod-bearing concretions (Park, 1995). Relatively dry environments in the basin may have contributed to low mammal richness in Facies Associations 1 and 2. Dry conditions around 17.0 Ma may be related to increasing temperature at the onset of the Middle Miocene Climatic Optimum (MMCO; Zachos et al., 2001).

During the MMCO (17.0–14.0 Ma), environments in the Barstow Basin were wetter and supported more mammals than earlier-forming environments. Rates of subsidence and sediment accumulation decreased, and the basin transitioned from closed to open drainage (Chapter 2). Meandering channels and proximal floodplains of Facies Association 3 developed and supported riparian habitats. Low mean ACL and depletion of δD values between 16.5 and 15.0 Ma indicate wet climatic conditions, perhaps due to increased precipitation during the MMCO. Warm Pacific Ocean surface temperatures were associated with the delivery of summer rainfall to western North America in the middle Miocene, and angiosperm forests existed over the western interior (Lyle et al., 2008). Phytolith assemblages in the Barstow Formation from this interval are

dominated by morphotypes of palms and woody dicots, indicating that riparian environments were present, and diatoms indicate the presence of streams and standing water (Chapter 3). Meandering streams and floodplains of Facies Association 3 supported abundant mammals in the basin at this time. Thirty-four mammal species occur in localities in this facies association, 30 of which have their observed lowest occurrences in this facies association. Inferred lowest occurrences from confidence intervals on species ranges are distributed throughout Facies Association 3 to near its contact with Facies Association 1, indicating that mammals were likely present throughout this time but were only preserved in specific depositional settings (Chapter 5). The presence of so many taxa partly relates to the prevalence of channel-margin environments, especially abandoned channels, which were sites frequented by mammals and that accumulated fossil material over hundreds of years (Chapter 4). The high number of lowest occurrences in Facies Association 3 reflects both the increased preservation potential and abundant specimens from localities in this interval.

Sediment-accumulation rate increased from 266 m/Myr in Facies Association 3 to 357 m/Myr in Facies Association 4, and the development of amalgamated sandstone bodies marks the transition from meandering to braided streams after ~15.5 Ma. The change in fluvial style may be associated with increased erosion of the bounding highlands (Gawthorpe and Leeder, 2000) from increased levels of precipitation during the MMCO and increased sediment delivery to the basin. The change in fluvial style could also be due to changes in regional tectonics, as the Mojave region expanded and moved westward in the middle Miocene (McQuarrie and Wernicke, 2005). Species richness was lower in Facies Association 4 than in Facies Association 3 (Chapter 5), as mammals did not inhabit these environments and fewer localities formed in the amalgamated channel sandstones of this facies association (Chapter 2).

Environments in the Barstow Basin again changed after 15.0 Ma, as sediment-accumulation rates decreased and poorly drained floodplain and wetland environments of Facies Association 5 formed. Facies Association 5 interfingers with Facies Association 6, which represents well-drained floodplain and wetland deposits; the variable drainage in these facies indicates that landscapes were more heterogeneous than earlier (Chapter 2). Many fossil localities occur in these deposits, and fossils accumulated through a variety of taphonomic pathways. Long-term sites of mortality formed in vegetated wetlands and at channel margins, and fossil assemblages also represent the accumulation of remains through carnivore and scavenger activity, as well as through fluvial processes. Thousands of fossil specimens accumulated in these localities, indicating the input and burial of remains over long periods of time (Chapter 4).

After 14.0 Ma, enrichment spikes in $\delta^{13}C_{nC27-31}$, δD, and $\delta^{13}C_{SOM}$ and longer ACL of alkanes show that environments became drier following the end of the MMCO. Phytolith assemblages from this part of the formation are dominated by grass morphotypes or morphotypes of woody dicots, indicating that vegetation ranged from open, wooded grassland to woodland over a heterogeneous landscape. Open-habitat and C_4 grass morphotypes are important components of these assemblages, and enriched $\delta^{13}C_{SOM}$ values from this interval indicate the presence of C_4 biomass in these drier environments following the end of the MMCO. The wetland environments of Facies Association 6 were intermittently wet habitats, as indicated by well-developed pedogenic features (e.g., slickensides) and diatom assemblages indicative of ephemeral water bodies. Mammals congregated in these settings as conditions in the basin continued to dry (Chapter 4). Twenty-four species have observed and inferred highest occurrences in Facies Association 6 (Chapter 5). Truncation at the top of the formation contributes to the number of

highest occurrences (Signor and Lipps, 1982), but some mammal species may have shifted their ranges in response to climatic cooling and drying after the MMCO (Badgley et al., 2015).

The Barstow Formation preserves a record of environmental, faunal, and floral change in the Great Basin through the MMCO. This record provides important clues to the timing of faunal immigration events and the environmental conditions that contributed to dispersal and shifting ranges during a time of climatic and tectonic change. The tectonic evolution of the Barstow Basin was important in determining the development of depositional environments, which contributed to the preservation of fossils in the formation.

The Barstow Formation in the context of Great Basin depositional history

The conditions that control the preservation of the sedimentary record also control the preservation of the fossil record (Holland, 2016). In addition to the effects of climate, tectonics have the ability to influence broad patterns of faunal and floral diversity over time. Through processes of extension and basin creation, tectonics control sediment accumulation and the formation of the rock record on local and regional scales. The timing and amount of sediment delivered to local basins determine the depositional environments that form, which contribute to the preservation of fossil assemblages (Loughney and Badgley, 2017). Over regional scales, sediment thickness may provide a first approximation for assessing the preservation potential of fossiliferous sequences. Rates of extension in the Great Basin were highest during the early and middle Miocene (McQuarrie and Wernicke, 2005), and intervals of high tectonic activity should correspond with basin expansion and the accumulation of thick sediment packages. Thicker sediment accumulation in rapidly forming basins may have increased the likelihood of accumulating and preserving fossil assemblages.

To test whether tectonic activity, sediment thickness, and mammal diversity co-varied in the Great Basin during the middle Miocene, I compiled the average rates of deformation along faults in the northern and southern Great Basin from McQuarrie and Wernicke (2005) for the Miocene. Because the timing of extension was diachronous between the northern and southern Great Basin (McQuarrie and Wernicke, 2005), I compared the deformation rates, sediment thickness, and mammal diversity from these subregions separately (Fig. 6.1). The rates of deformation correspond to rates of horizontal-slip movement along faults (McQuarrie and Wernicke, 2005), and I used them as an approximation for rates of extension and basin formation. I compared these deformation rates to the number of large-mammal genera and the cumulative thickness of fossil-bearing formations in the northern and southern Great Basin through the Miocene (Fig. 6.1). I chose the number of genera to indicate faunal richness in the region because genus was the finest taxonomic resolution for occurrence data grouped by geographic subregion and time bin in Janis et al. (1998). I compiled the number of genera from Janis et al. (1998) for the northern (Mojave region and Nevada) and southern (Arizona, New Mexico, and southeastern Texas) Great Basin (Fig. 6.1). Cumulative formation thicknesses were compiled from the Macrostrat online database (macrostrat.org), USGS data (ngmdb.usgs.gov), and literature sources (Dibblee, 1967; Ladd, 1975; Barghoorn, 1981; Gawne, 1981; Vazzana and Ingersoll, 1981; Schorn et al., 1989; Smith, 2002; May et al., 2014). I binned the number of genera and cumulative sediment thickness by subdivisions of North American Land Mammal Ages (NALMA) following Janis et al. (1998).

Rates of deformation along faults increased markedly in the southern Great Basin at 27 Ma and declined at 15 Ma, whereas rates in the northern Great Basin increased at 24 Ma and declined more gradually between 20 and 10 Ma (Fig. 6.2A). Cumulative thickness of formations

deposited through the Miocene does not closely track deformation rates, but it does correspond to trends in the number of formations and genera (Fig. 6.2B-D). The number of formations, mammal genera, and sediment thickness increased through the Miocene, and the number of genera and sediment thickness significantly increased in three intervals. The number of genera increased for both the northern and southern Great Basin during the Hemingfordian to Barstovian (17.5 to 14.0 Ma), Clarendonian (11.0 to 8.8 Ma), and late Hemphillian (7.0 to 5.2 Ma) NALMAs. Broadly, these peaks coincide with increases in sediment thickness for the entire Great Basin record but do not closely track thickness in either subregion (Fig. 6.2).

The offset between the timing of large-magnitude changes in deformation rates and sediment thickness is likely due to the style of sedimentation in extensional basins. Rapid and significant changes in deformation rates cause rapid changes in rates of accommodation, which is a major control on sedimentation and basin filling (Catuneanu, 2006). The sediments that fill a basin during the early phases of extension are typically coarse conglomerates or breccias shed from the fault scarps and deposited in alluvial fans (Gawthorpe and Leeder, 2000). These settings are not typically favorable for the preservation of vertebrate fossils, and few formations deposited in the Great Basin during the early phases of regional extension have fossil-mammal localities. The cumulative thicknesses of early Miocene formations may then not be represented in these analyses, as only fossiliferous formations are included here.

Extensional basins continue to subside with waning tectonic activity and accumulate sediment under these conditions (Gawthorpe and Leeder, 2000). Subsidence is an important component of accommodation that was not included in the horizontal slip rates calculated by McQuarrie and Wernicke (2005). When subsidence rates are high, rates of accommodation are high, and rapidly subsiding basins are able to accumulate thick packages of sediment

(Catuneanu, 2006). The Barstow Formation accumulated most of its sediments when subsidence rates were high after extension in the basin had ended (Chapter 2). Conditions favoring fossil preservation were higher during these times than during periods of active extension. For extensional basins, the timing of sediment accumulation in relation to tectonic history is important to the preservation of fossils. The regional relationship between deformation rate and sediment thickness (Fig. 6.2A and C) indicates that other fossiliferous formations of the Great Basin may have similar patterns of sediment accumulation and fossil preservation as the Barstow Formation.

Increases in the number of genera during the Hemingfordian, Barstovian, Clarendonian, and Hemphillian NALMAs coincide with increases in cumulative sediment thickness and number of formations during the same time intervals (Fig. 6.2B-D). This relationship is more pronounced in the northern Great Basin than in the southern Great Basin, which has lower cumulative sediment thickness (Fig. 6.2C). The accumulation of sediment and the increasing number of fossil-bearing formations in the Great Basin partly contribute to higher generic diversity during the Miocene, but both regions have similar levels of diversity despite significant differences in sediment thickness. This relationship indicates that other factors besides sediment thickness and deformation rate affected diversity and the preservation of the fossil record in subregions of the Great Basin.

High mammal diversity in North America during the middle Miocene has been proposed to relate to changing climate and environments during the MMCO (Janis et al., 2000; Finarelli and Badgley, 2010). Differences in hydrology and vegetation within the Great Basin, Great Plains, and adjacent regions (Fox and Koch, 2003; Retallack, 2007; Strömberg, 2011; Chen et al., 2015; Bowman et al., 2017; Harris et al., 2017; Smiley et al., 2018) likely affected the distribution of

mammal faunas during and after the MMCO. More paleoenvironmental studies of stratigraphic sequences in the Great Basin are needed to determine the responses of vegetation and fauna to climate and their potential impact on mammal richness. Additionally, the topographic evolution of the Great Basin has been proposed to play an important role in mammal diversification and immigration. Increasingly fragmented topography promoted diversification in localized basins, and significant interchange among faunas did not occur until the MMCO (Badgley et al., 2015). Generic richness is highest in the northern and southern Great Basin during the MMCO (Fig. 6.2B), perhaps due to increased speciation or immigration within or between subregions.

The stratigraphic and fossil records are influenced by climate and tectonics, but the effects of these controls on basin evolution and fossil preservation are hard to disentangle. Comparing fossiliferous stratigraphic sequences forming under different tectonic and climatic regimes provides the basis for identifying patterns of deposition and preservation. Within the Great Basin, regional differences in timing of deposition and changes in mammal diversity also give indications as to how climate and tectonics influenced the fossil record.

Conclusion

Mammal diversity was high overall in North America during the middle Miocene (Figueirido et al., 2012), with the Great Plains and the Great Basin representing two of the most important Miocene fossil records (Janis et al., 1998; Badgley et al., 2014). The mammal fossil records of these regions are often compared in order to understand their similarities, their differences, and the driving factors that underlie their diversity. Quantifying similarities among regional faunas has long been an important method for reconstructing biogeographic relationships and is the basis for biostratigraphic correlation. The different geologic histories of the Great Plains and

Great Basin also make them valuable settings in which to test hypotheses about effects of tectonics and climate on mammal diversity and fossil preservation (Badgley et al., 2014). If tectonics and climate influence depositional controls on the fossil record, patterns of fossil preservation should vary between regions in predictable ways.

Integrating stratigraphy into faunal analyses can provide important insight into the timing and environmental context of biostratigraphic and ecologic transitions. Understanding the timing and style of facies transitions in a basin provides context for constraining first and last occurrences and species turnover, as well as changes in fossil preservation and productivity. Faunal analysis of local and regional Miocene fossil records is strengthened when the environmental, climatic, and tectonic contexts are integrated. The paleontological history of North America is tied to its geological history, and understanding Miocene faunal dynamics and evolution will benefit from continued interest in reconstructing the tectonic, topographic, and drainage history of western North America.

References

Badgley, C., Smiley, T.M., and Finarelli, J.A., 2014, Great Basin mammal diversity in relation to landscape history: Journal of Mammalogy, v. 95, no. 6, p. 1090-1106.

Badgley, C., Smiley, T.M., and Loughney, K.M., 2015, Miocene mammal diversity of the Mojave region in the context of Great Basin mammal history, *in* Reynolds, R.E., ed., Mojave Miocene: The 2015 Desert Symposium Field Guide and Proceedings: Zzyzx, California, California State University Desert Studies Consortium, p. 34-43.

Barghoorn, S., 1981, Magnetic-polarity stratigraphy of the Miocene type Tesuque Formation, Santa Fe Group, in the Española Valley, New Mexico: GSA Bulletin, v. 92, no. 12, p. 1027-1041.

Bowman, C.N., Wang, Y., Wang, X., Takeuchi, G.T., Faull, M., Whistler, D.P., and Kish, S., 2017, Pieces of the puzzle: Lack of significant C_4 in the late Miocene of southern California: Palaeogeography, Palaeoclimatology, Palaeoecology, v. 475, p. 70-79.

Catuneanu, O., 2006, Principles of Sequence Stratigraphy: Amsterdam, Elsevier, 375 p.

Chen, S.T., Smith, S.Y., Sheldon, N.D., and Strömberg, C.A.E., 2015, Regional-scale variability in the spread of grasslands in the late Miocene: Palaeogeography, Palaeoclimatology, Palaeoecology, v. 437, no. Supplement C, p. 42-52.

Dibblee, T.W., Jr., 1967, Areal geology of the western Mojave Desert California, Geological Survey Professional Paper 522: Washington, D.C., 153 p.

Figueirido, B., Janis, C.M., Pérez-Claros, J.A., De Renzi, M., and Palmqvist, P., 2012, Cenozoic climate change influences mammalian evolutionary dynamics: Proceedings of the National Academy of Sciences, v. 109, no. 3, p. 722-727.

Finarelli, J.A., and Badgley, C., 2010, Diversity dynamics of Miocene mammals in relation to the history of tectonism and climate: Proceedings of the Royal Society of London B: Biological Sciences, v. 277, no. 1694, p. 2721-2726.

Fox, D.L., and Koch, P.L., 2003, Tertiary history of C_4 biomass in the Great Plains, USA: Geology, v. 31, no. 9, p. 809-812.

Gawne, C.E., 1981, Sedimentology and stratigraphy of the Miocene Zia Sand of New Mexico: Summary: GSA Bulletin, v. 92, no. 12, p. 999-1007.

Gawthorpe, R.L., and Leeder, M.R., 2000, Tectono-sedimentary evolution of active extensional basins: Basin Research, v. 12, no. 3-4, p. 195-218.

Glazner, A.F., Walker, J.D., Bartley, J.M., and Fletcher, J.M., 2002, Cenozoic evolution of the Mojave block of southern California: Geological Society of America Memoirs, v. 195, p. 19-41.

Harris, E.B., Strömberg, C.A.E., Sheldon, N.D., Smith, S.Y., and Vilhena, D.A., 2017, Vegetation response during the lead-up to the middle Miocene warming event in the Northern Rocky Mountains, USA: Palaeogeography, Palaeoclimatology, Palaeoecology, v. 485, no. Supplement C, p. 401-415.

Holland, S.M., 2016, The non-uniformity of fossil preservation: Philosophical Transactions of the Royal Society B: Biological Sciences, v. 371, no. 1699.

Janis, C.M., Scott, K.M., and Jacobs, L.L., 1998, Evolution of Tertiary Mammals of North America, Volume 1: Terrestrial Carnivores, Ungulates, and Ungulatelike Mammals, Volume 1: Cambridge, U.K., Cambridge University Press, p. 691.

Janis, C.M., Damuth, J., and Theodor, J.M., 2000, Miocene ungulates and terrestrial primary productivity: Where have all the browsers gone?: Proceedings of the National Academy of Sciences, v. 97, no. 14, p. 7899-7904.

Ladd, T.W., 1975, Stratigraphy and petrology of the Quiburis Formation near Mammoth, Pinal County, Arizona [M.S. thesis]: University of Arizona, 103 p.

Loughney, K.M., and Badgley, C., 2017, Facies, environments, and fossil preservation in the Barstow Formation, Mojave Desert, California: PALAIOS, v. 32, no. 6, p. 396-412.

Lyle, M., Barron, J., Bralower, T.J., Huber, M., Olivarez Lyle, A., Ravelo, A.C., Rea, D.K., and Wilson, P.A., 2008, Pacific Ocean and Cenozoic evolution of climate: Reviews of Geophysics, v. 46, no. 2, p. 1-47.

May, S.R., Sarna-Wojcicki, A.M., Lindsay, E.H., Woodburne, M.O., Opdyke, N.D., Wan, E., Wahl, D.B., and Olson, H., 2014, Geochronology of the upper Alturas Formation, northern California: Implications for the Hemphillian-Blancan North American Land Mammal Age boundary: Palaeontologia Electronica, no. 17.3.43A, p. 1-13.

McQuarrie, N., and Wernicke, B.P., 2005, An animated tectonic reconstruction of southwestern North America since 36 Ma: Geosphere, v. 1, no. 3, p. 147-172.

Pagnac, D., Browne, I., and Smith, K., 2013, Stratigraphy and vertebrate paleontology of the middle Miocene Barstow Formation, San Bernardino County, California, *in* Proceedings 73rd Annual Meeting of the Society of Vertebrate Paleontology, Los Angeles, California, 29 October 2013, p. 1-26.

Park, L.E., 1995, Geochemical and paleoenvironmental analysis of lacustrine arthropod-bearing concretions of the Barstow Formation, southern California: PALAIOS, v. 10, no. 1, p. 44-57.

Park, L.E., and Downing, K.F., 2001, Paleoecology of an exceptionally preserved arthropod fauna from lake deposits of the Miocene Barstow Formation, southern California, USA: PALAIOS, v. 16, no. 2, p. 175-184.

Retallack, G.J., 2007, Cenozoic Paleoclimate on Land in North America: The Journal of Geology, v. 115, no. 3, p. 271-294.

Schorn, H.E., Scudder, H.I., Savage, D.E., and Firby, J.R., 1989, General stratigraphy and paleontology of the Miocene continental sequence in Stewart Valley, Mineral County, Nevada, U.S.A., Proceedings of the International Symposium on Pacific Neogene Continental and Marine Events, Volume 246, National Working Group of China for IGCP, p. 157-173.

Signor, P.W., and Lipps, J.H., 1982, Sampling bias, gradual extinction patterns, and catastrophes in the fossil record: Geological Society of America Special Papers, v. 190, p. 291-296.

Smiley, T.M., Hyland, E.G., Cotton, J.M., and Reynolds, R.E., 2018, Evidence of early C_4 grasses, habitat heterogeneity, and faunal response during the Miocene Climatic Optimum in the Mojave Region: Palaeogeography, Palaeoclimatology, Palaeoecology, v. 490, no. Supplement C, p. 415-430.

Smith, K.S., 2002, Mammalian paleontology of the Monarch Mill Formation at Eastgate, Churchill County, Nevada [Ph.D. dissertation]: University of Oklahoma, 710 p.

Strömberg, C.A.E., 2011, Evolution of grasses and grassland ecosystems: Annual Review of Earth and Planetary Sciences, v. 39, p. 517-544.

Vazzana, M.E., and Ingersoll, R.V., 1981, Stratigraphy, sedimentology, petrology, and basin evolution of the Abiquiu Formation (Oligo-Miocene), north-central New Mexico: Summary: GSA Bulletin, v. 92, no. 12, p. 990-992.

Zachos, J.C., Pagani, M., Sloan, L.C., Thomas, E., and Billups, K., 2001, Trends, rhythms, and aberrations in global climate 65 Ma to present: Science, v. 292, p. 686-693.

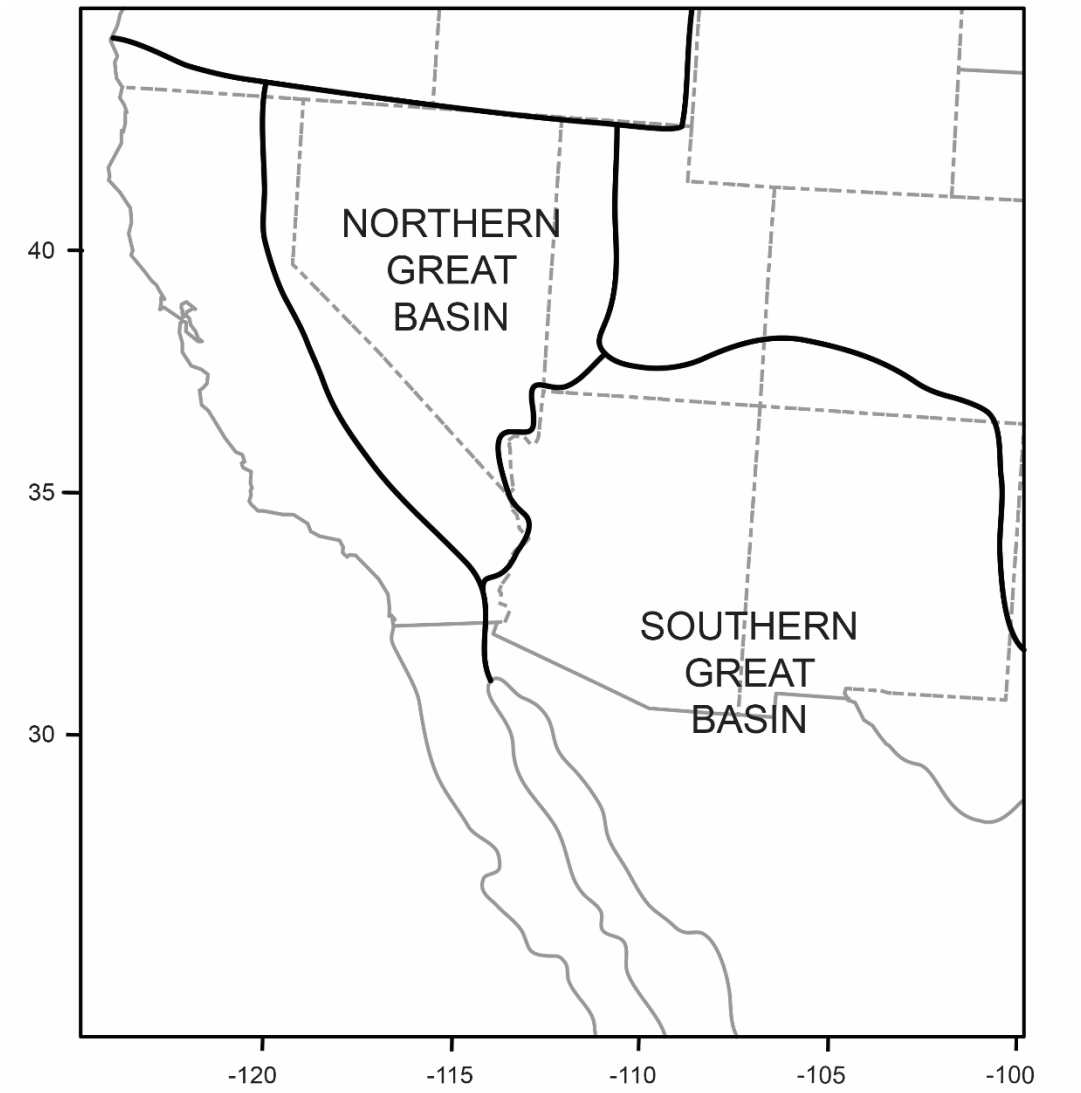

Figure 6.1. Map showing geographic extent of the northern and southern Great Basin subregions of Janis et al. (1998). Modified from Janis et al. (1998).

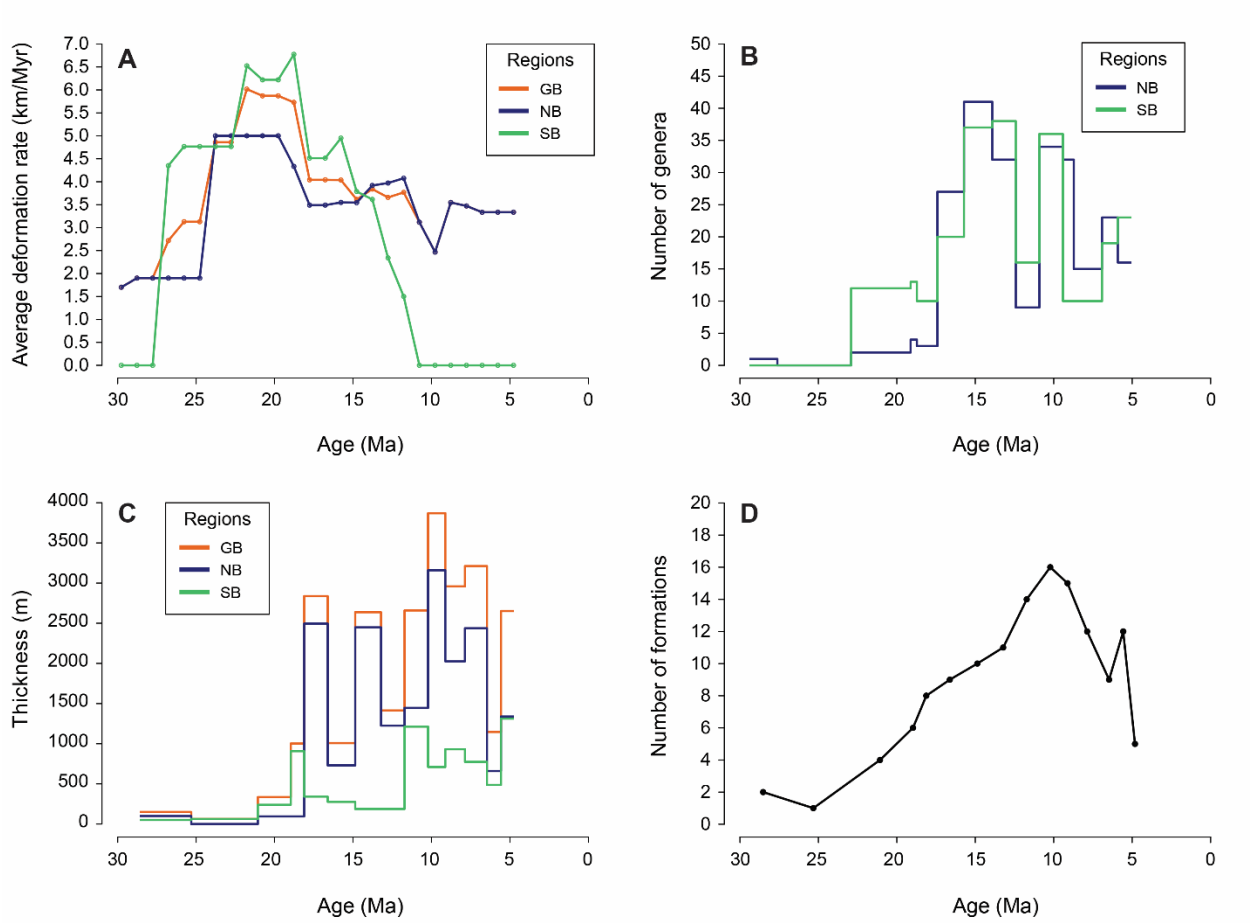

Figure 6.2. Comparison of deformation rate, number of genera, formation thickness, and number of formations in the northern (NB), southern (SB), and entire (GB) Great Basin through the Miocene, following divisions in Janis et al. (1998): NB = Mojave region and Nevada, SB = Arizona, New Mexico, and southwestern Texas. A) Average deformation rates along faults compiled from McQuarrie and Wernicke (2005); B) Number of large-mammal genera with occurrences in the Great Basin, binned by North American Land Mammal Ages (NALMA); C) Cumulative sediment thickness of fossiliferous formations of the Great Basin, binned by NALMA; D) Number of fossiliferous formations of the Great Basin through the Miocene.

APPENDIX

Microstratigraphic sections of fossil localities in the Barstow Formation

Microstratigraphic sections measured at fossil localities in the Barstow Formation. For each locality, the name or locality number is listed; the composite stratigraphic level; the original collecting institution, if known; the taphonomic pathway, if interpreted for the locality; and the facies association. Key to lithologic patterns and symbols applies to all sections. Institution abbreviations: F:AM, American Museum of Natural History; RAM, Raymond Alf Museum of Paleontology; SBCM, San Bernardino County Museum; UCMP, University of California Museum of Paleontology; UCR, University of California, Riverside; UM, University of Michigan.

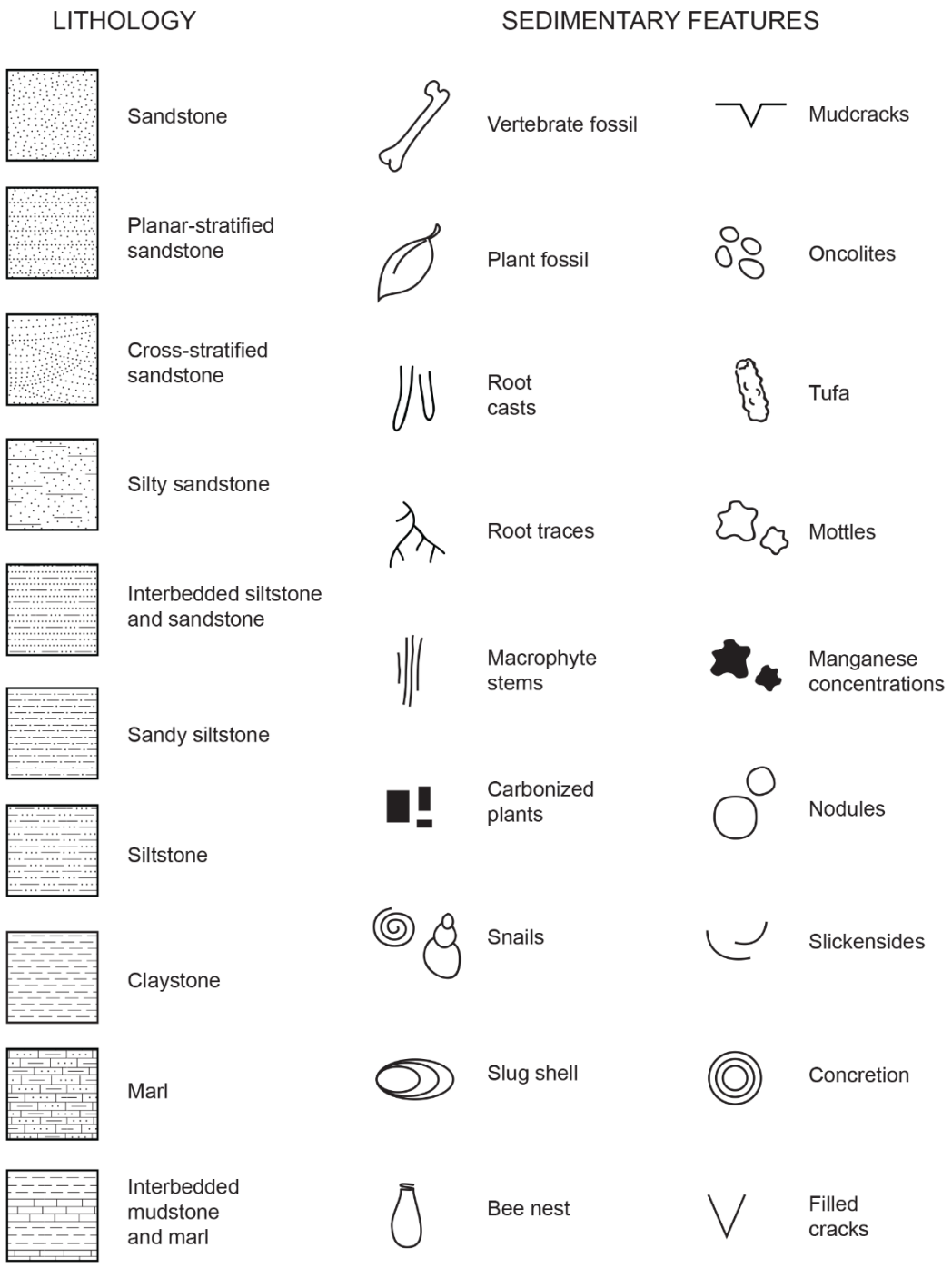

Figure A1. Key to lithologic patterns and symbols for stratigraphic sections.

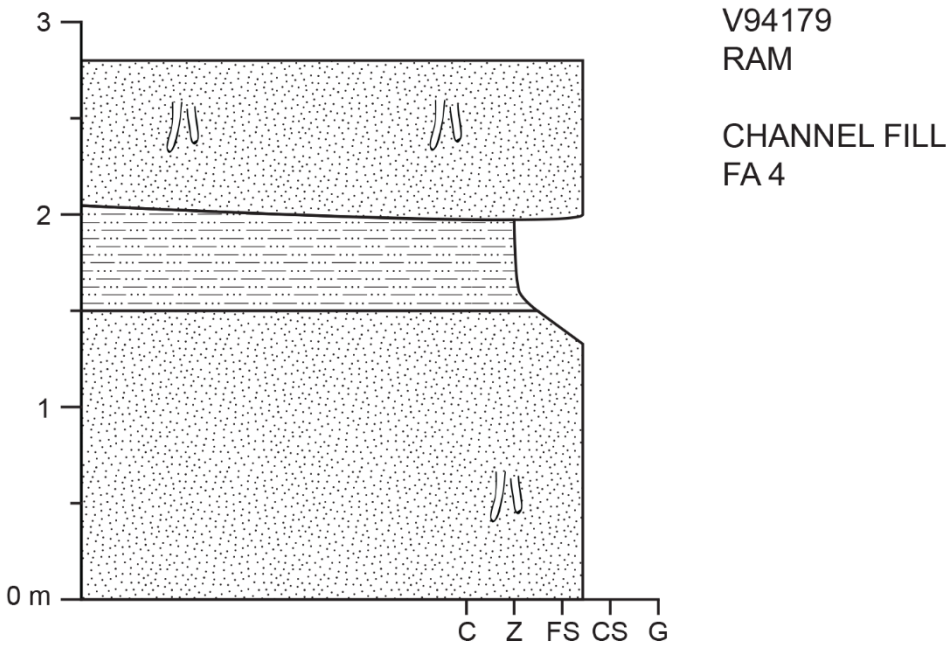

Figure A2. RAM V94179; 700 m.

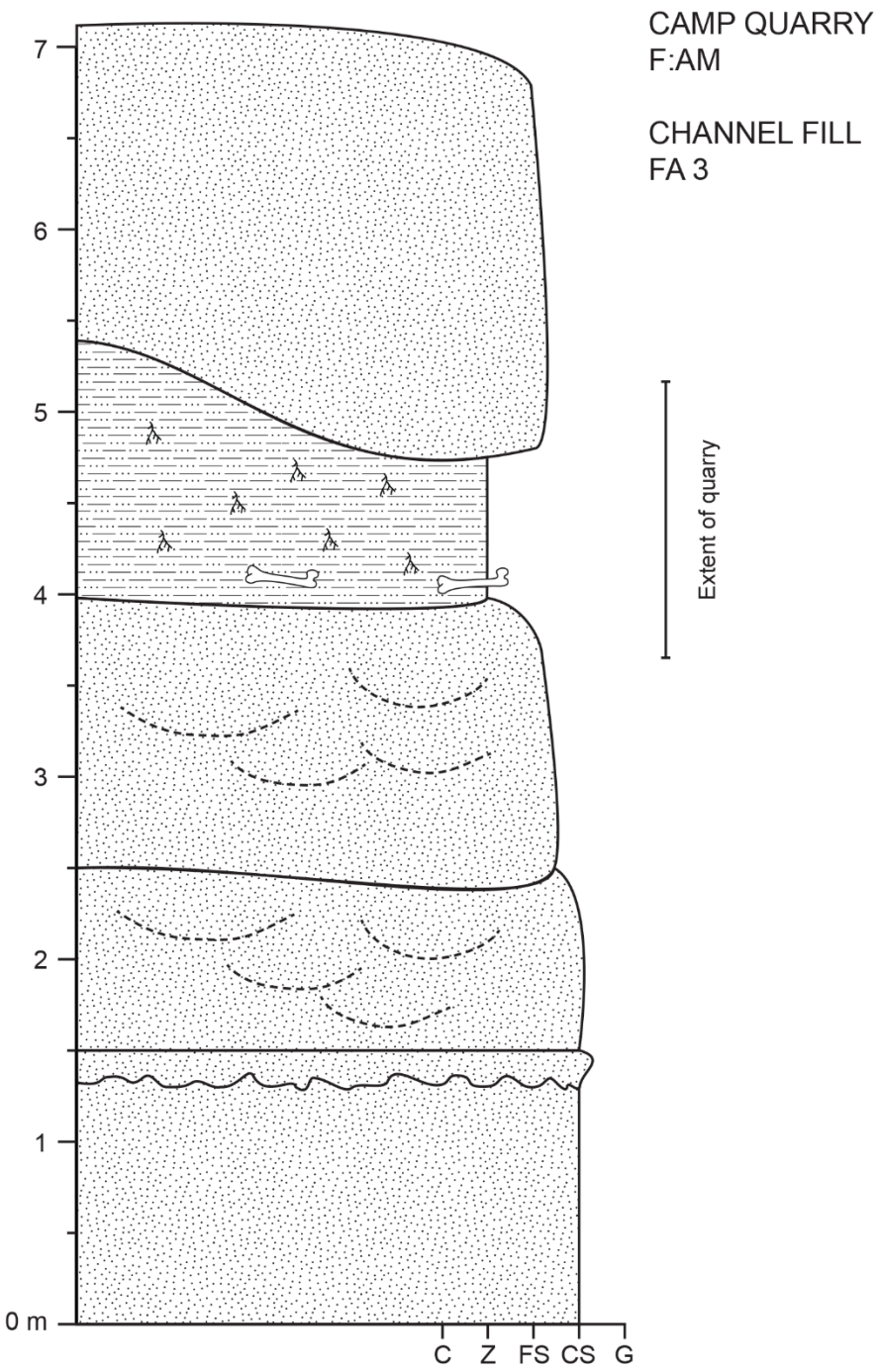

Figure A3. Camp Quarry; 523.5 m.

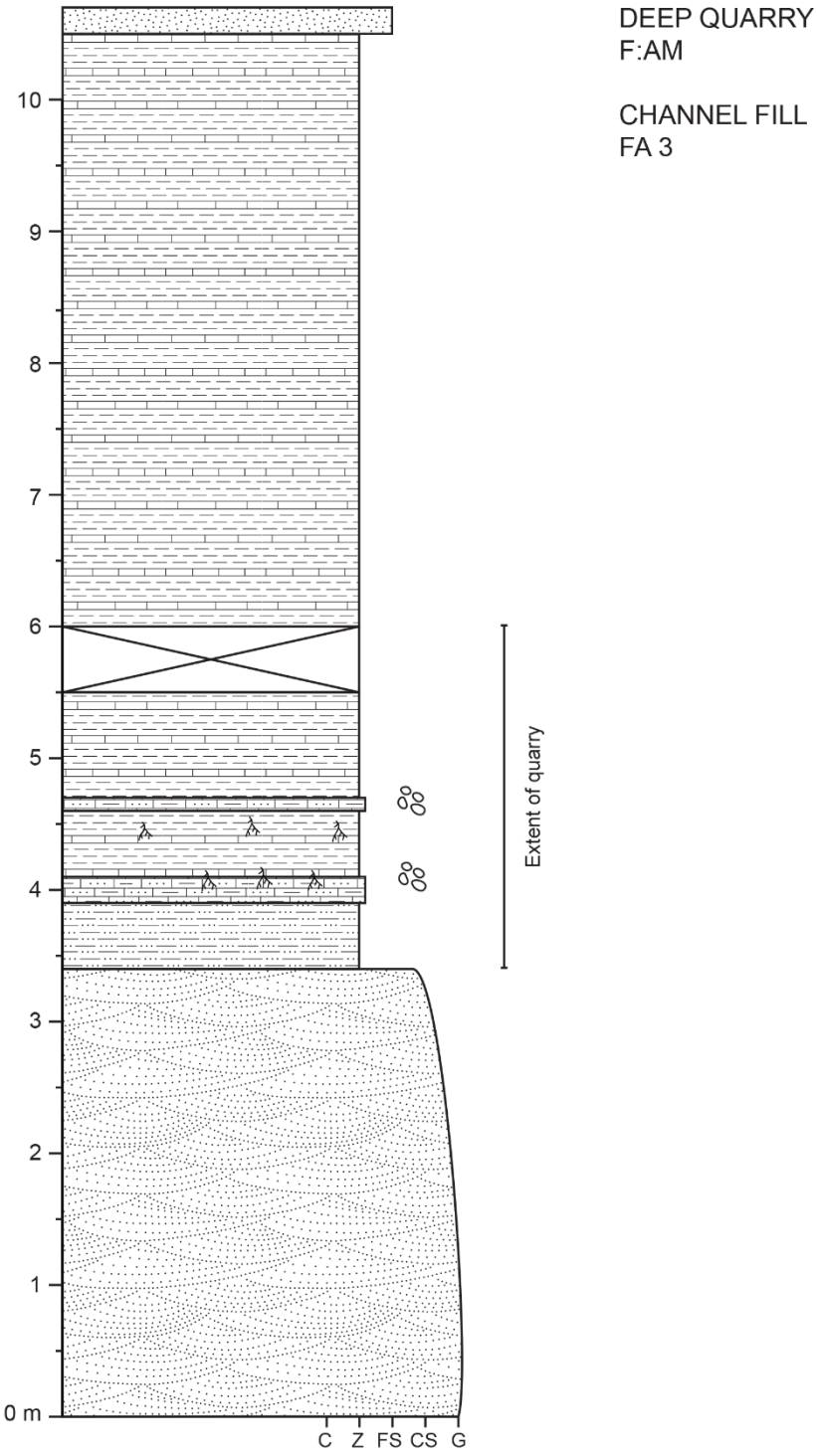

Figure A4. Deep Quarry; 482.5 m.

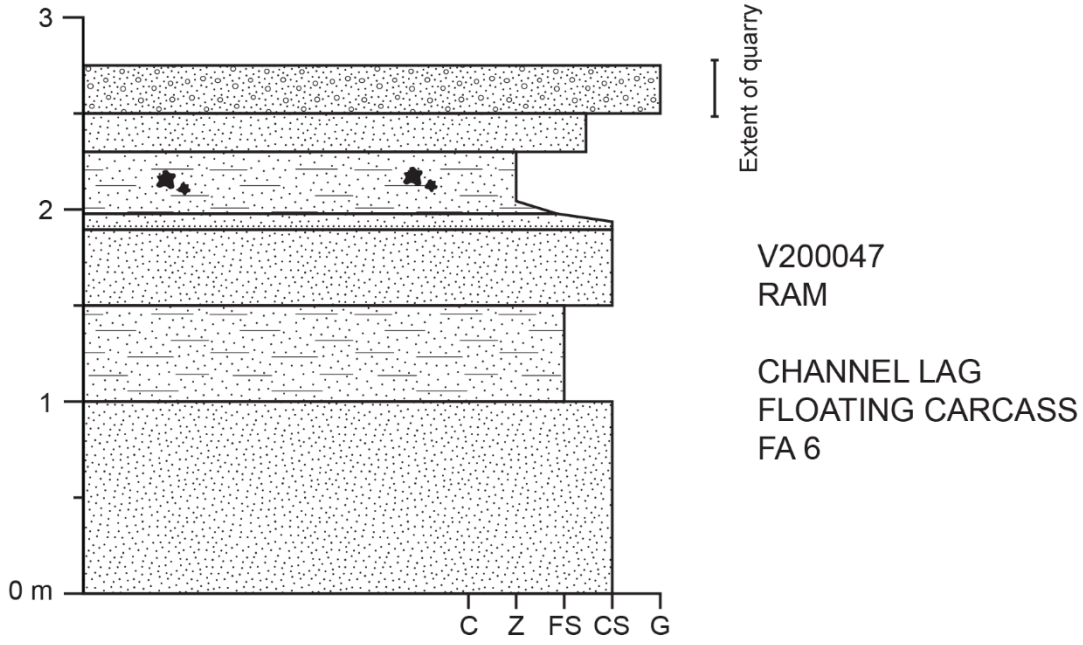

Figure A5. RAM V200047; 836 m.

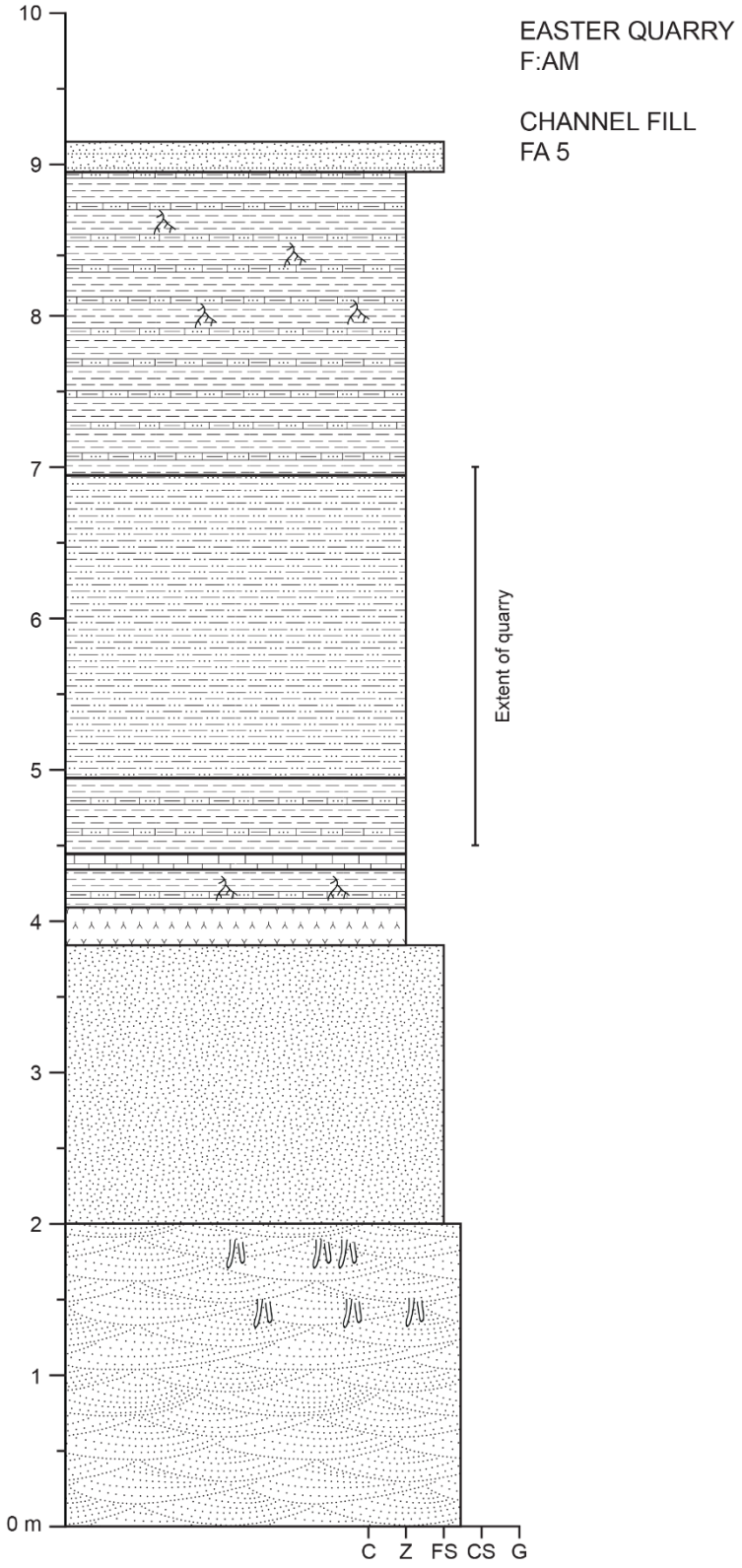

Figure A6. Easter Quarry; 797.3 m.

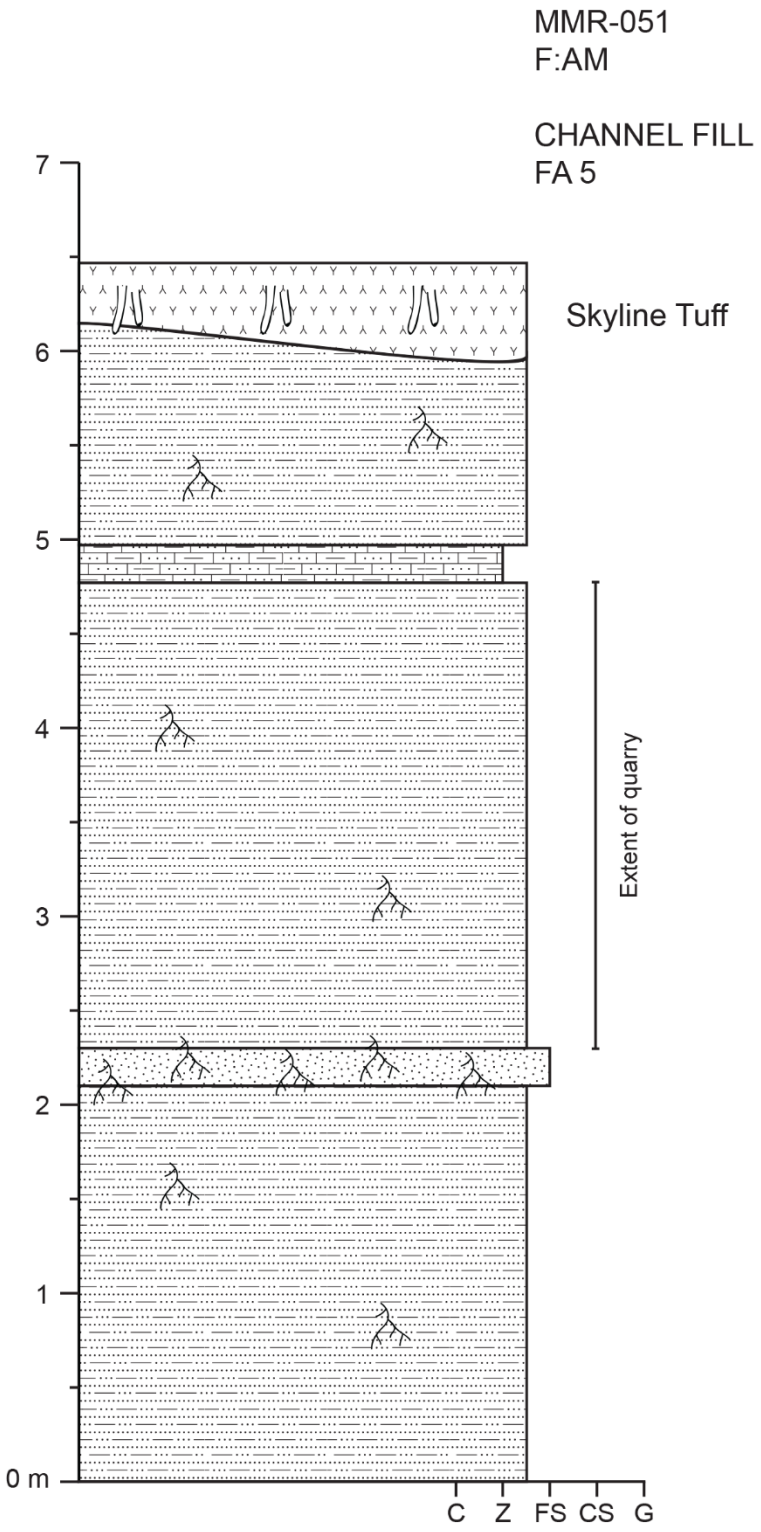

Figure A7. MMR-051; 765.4 m.

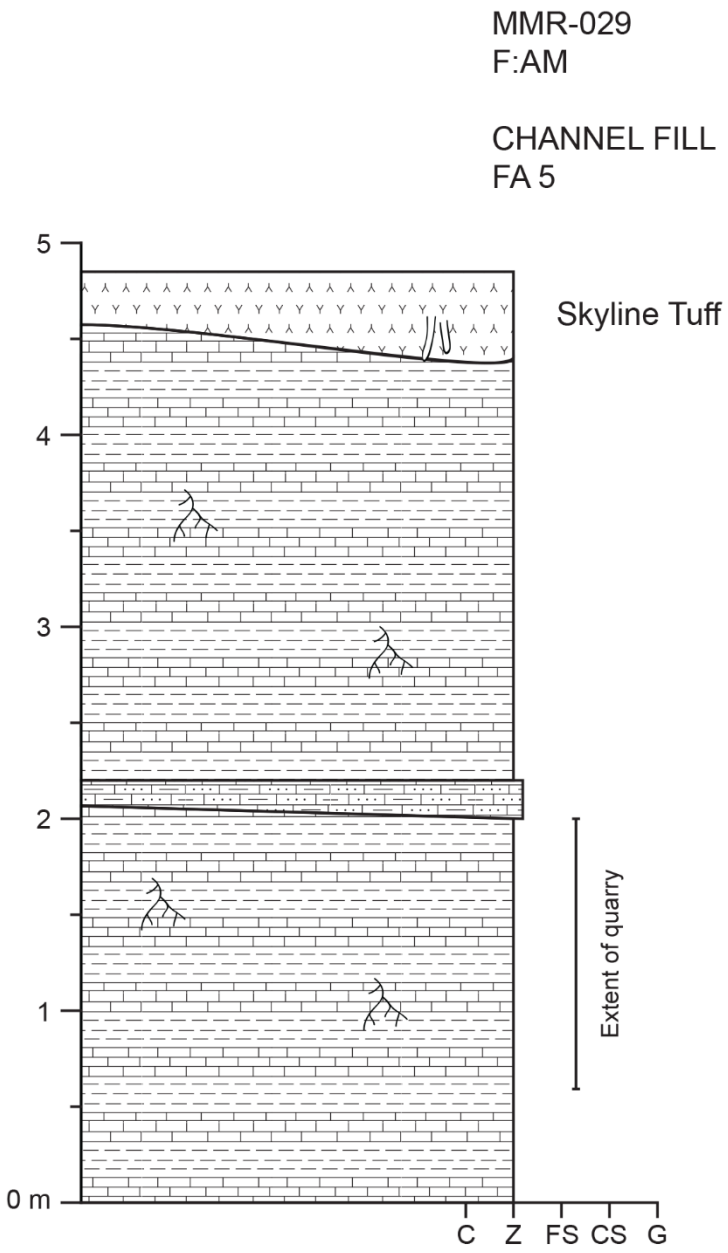

Figure A8. MMR-029; 765.4 m.

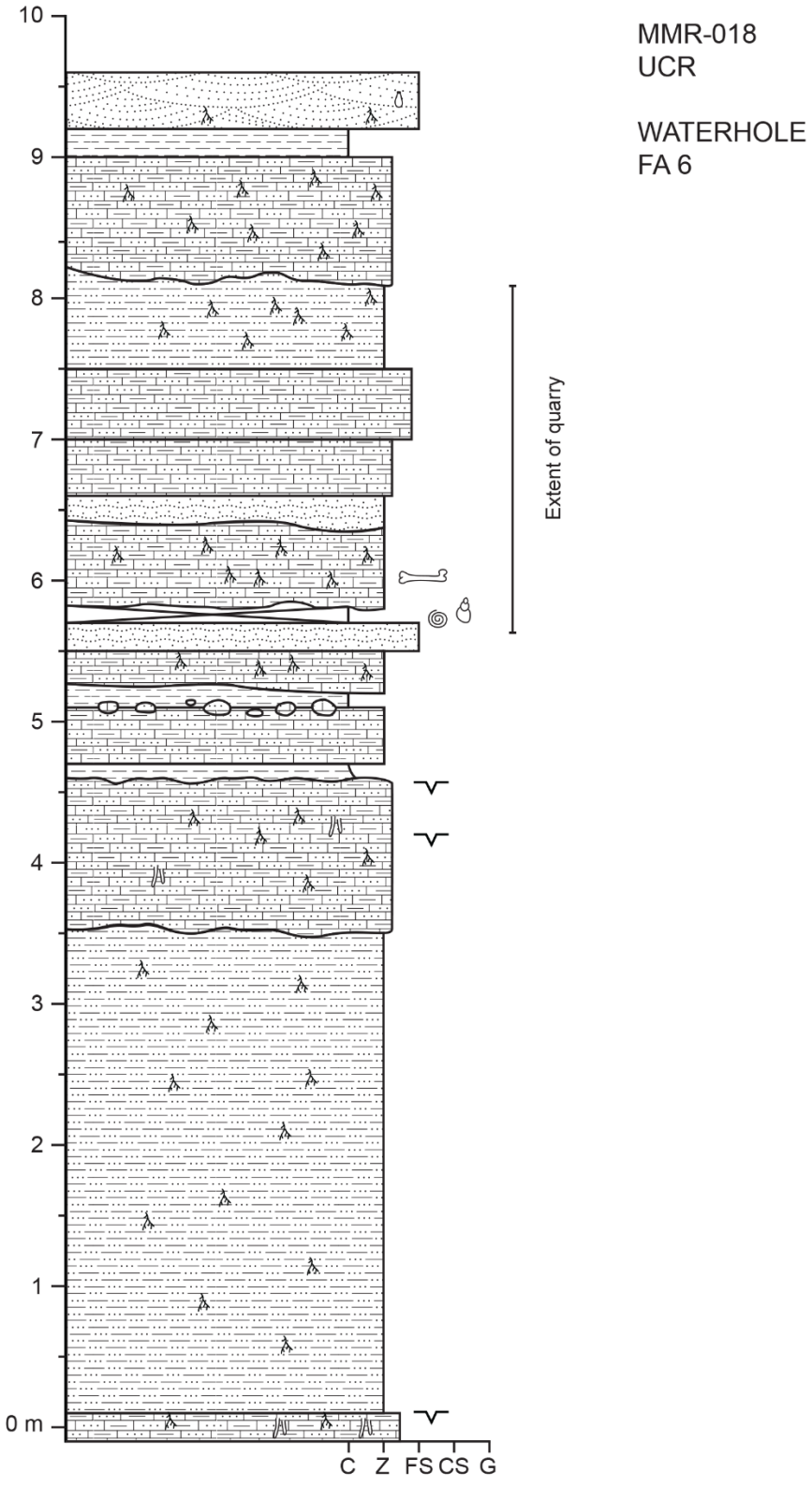

Figure A9. MMR-018; 849 m.

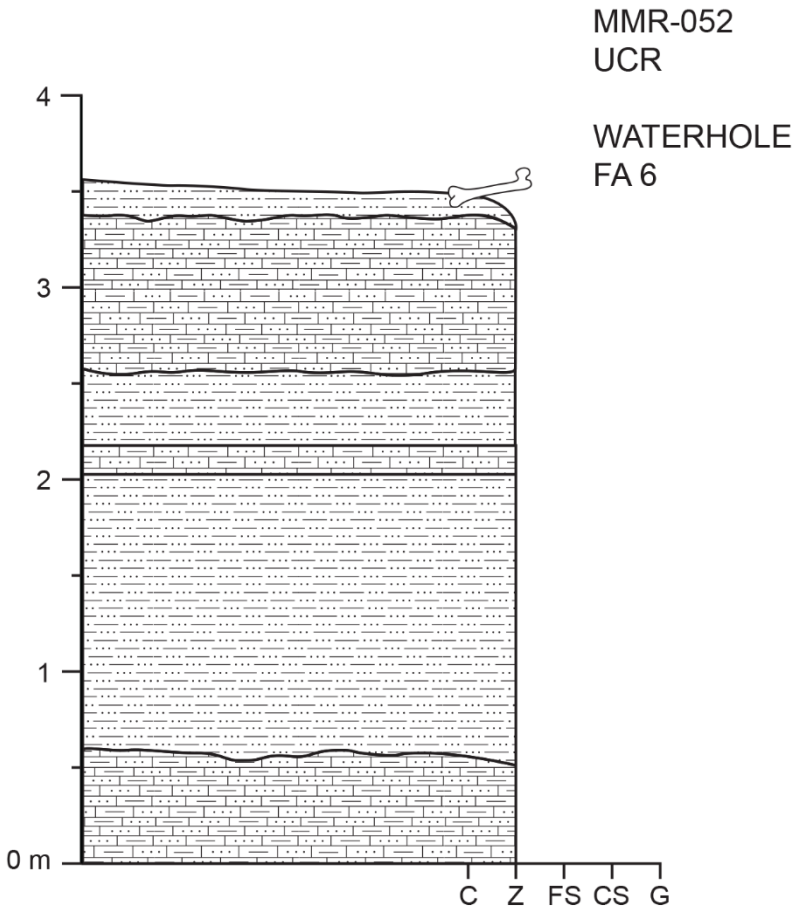

Figure A10. MMR-052; 849 m.

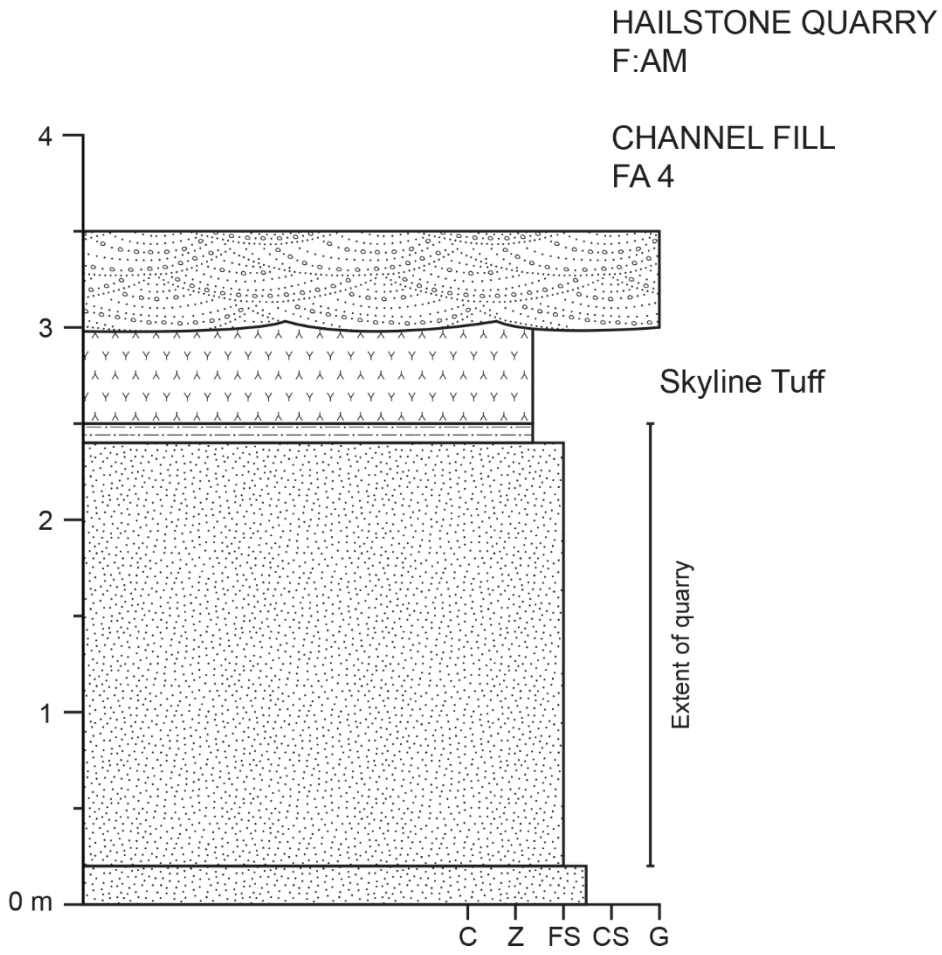

Figure A11. Hailstone Quarry; 767.5 m.

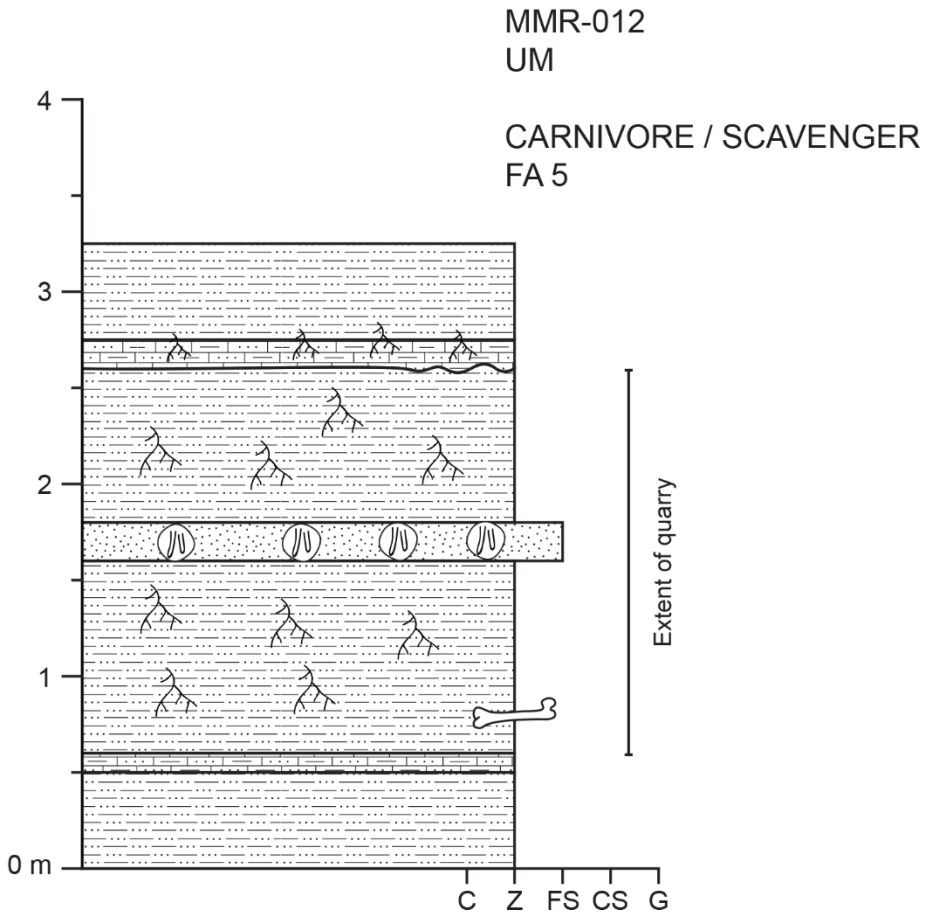

Figure A12. MMR-012; 821 m.

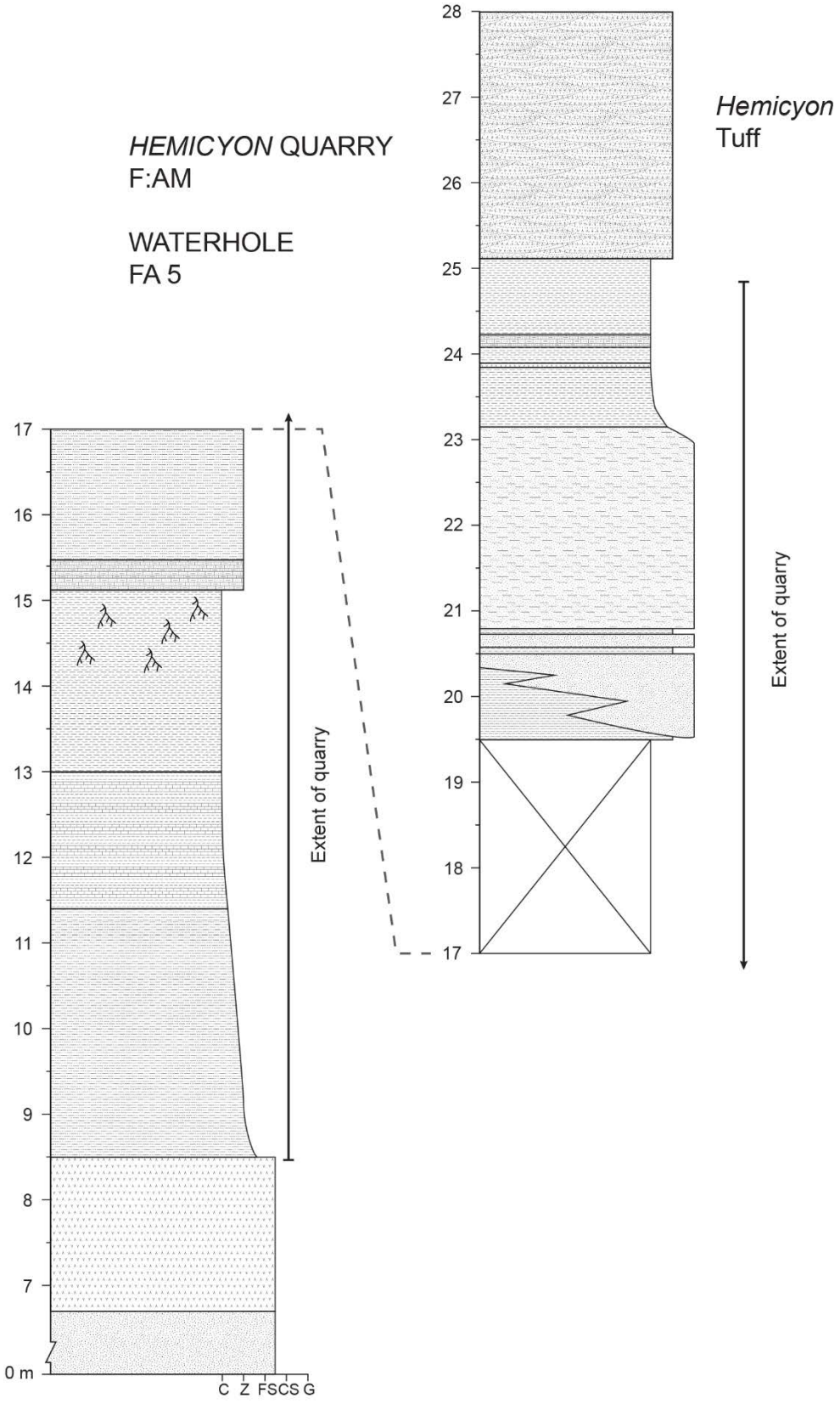

Figure A13. *Hemicyon* Quarry; 845 m.

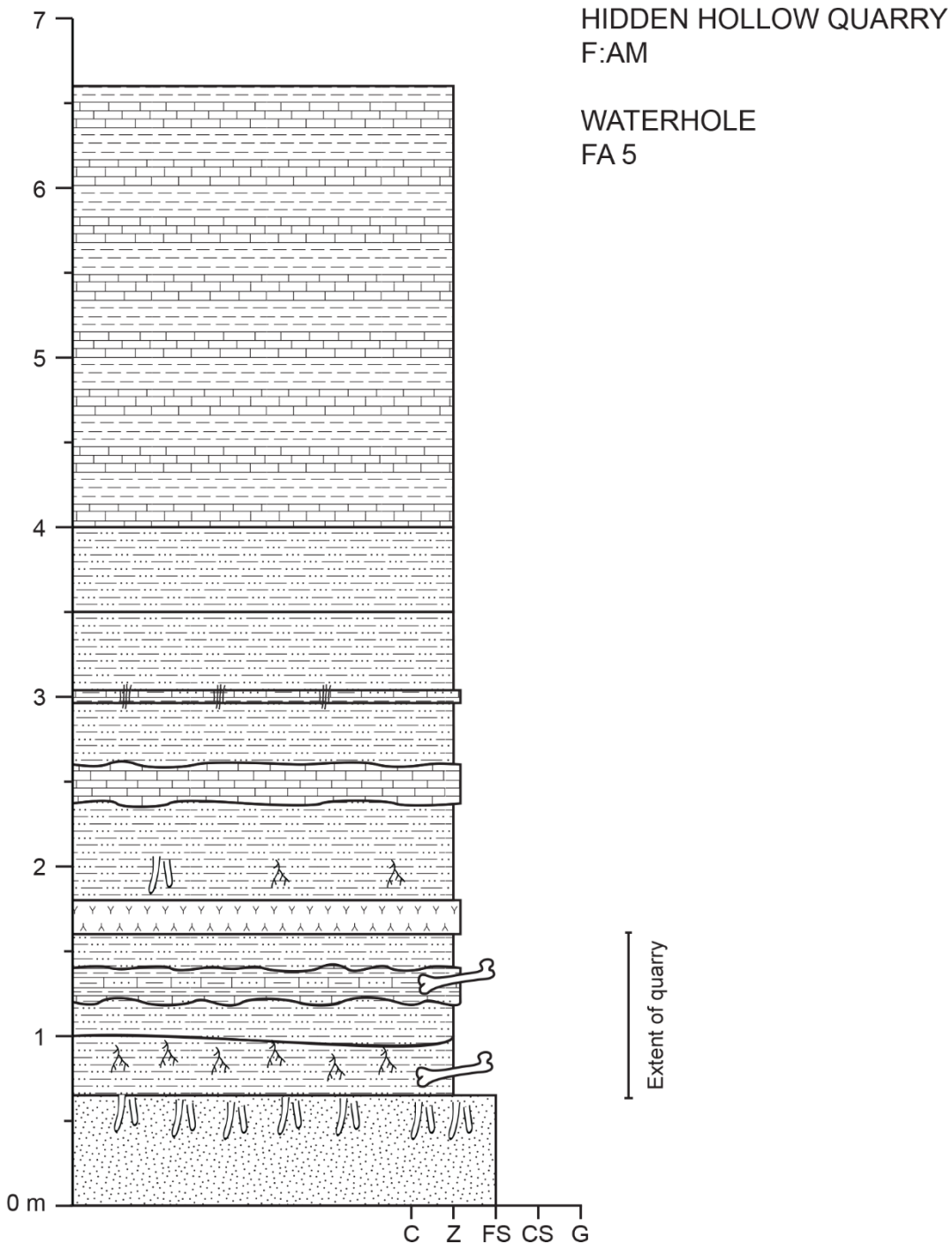

Figure A14. Hidden Hollow Quarry; 856 m.

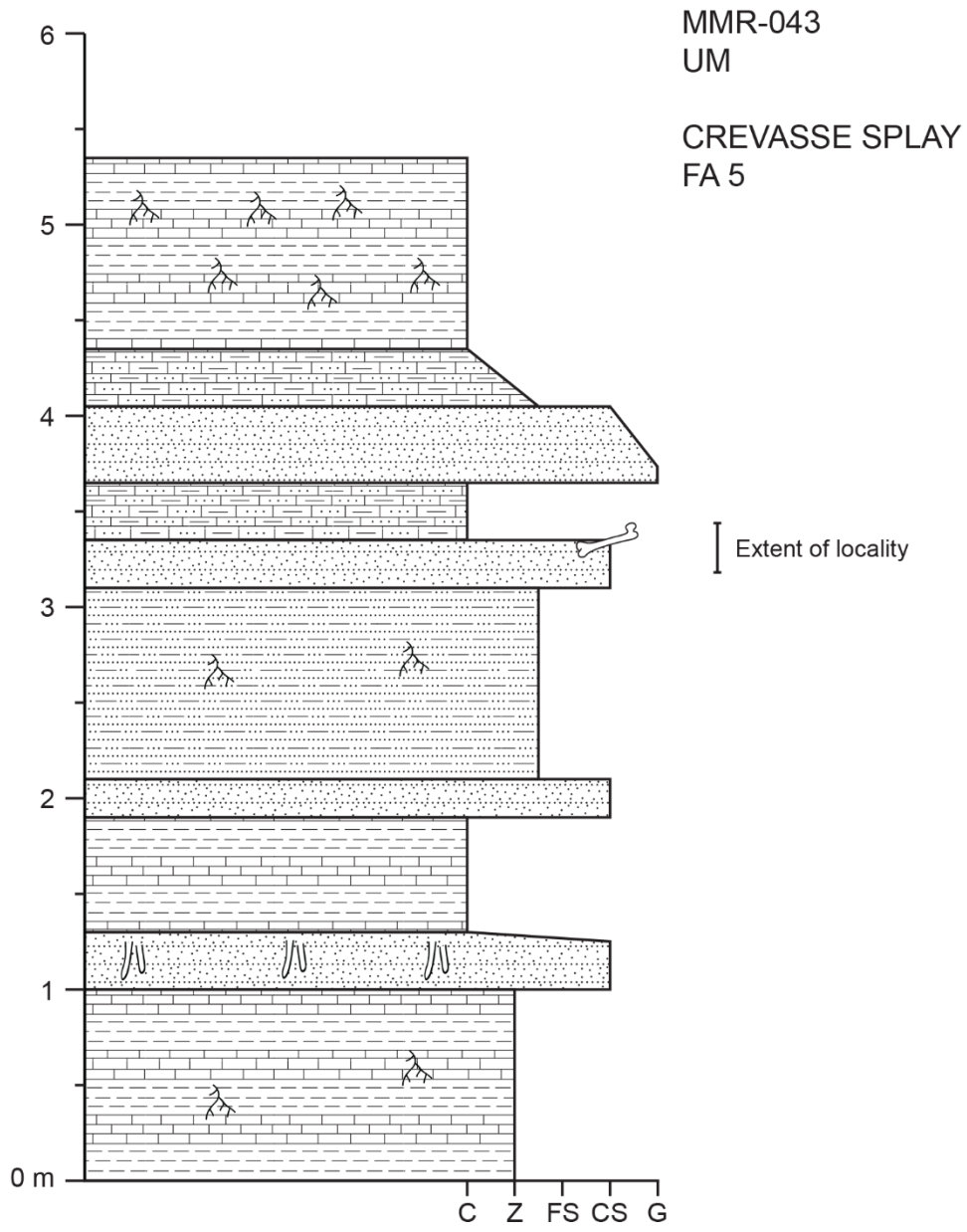

Figure A15. MMR-043; 764 m.

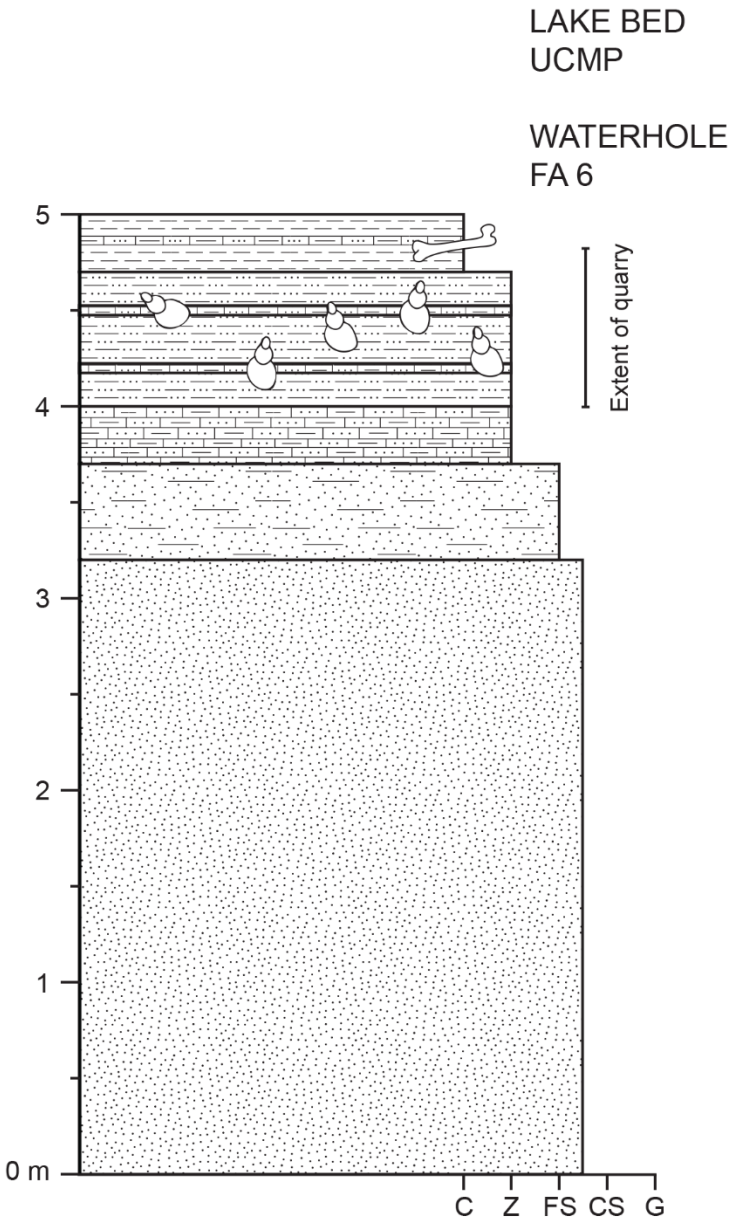

Figure A16. Lake Bed Quarry; 843 m.

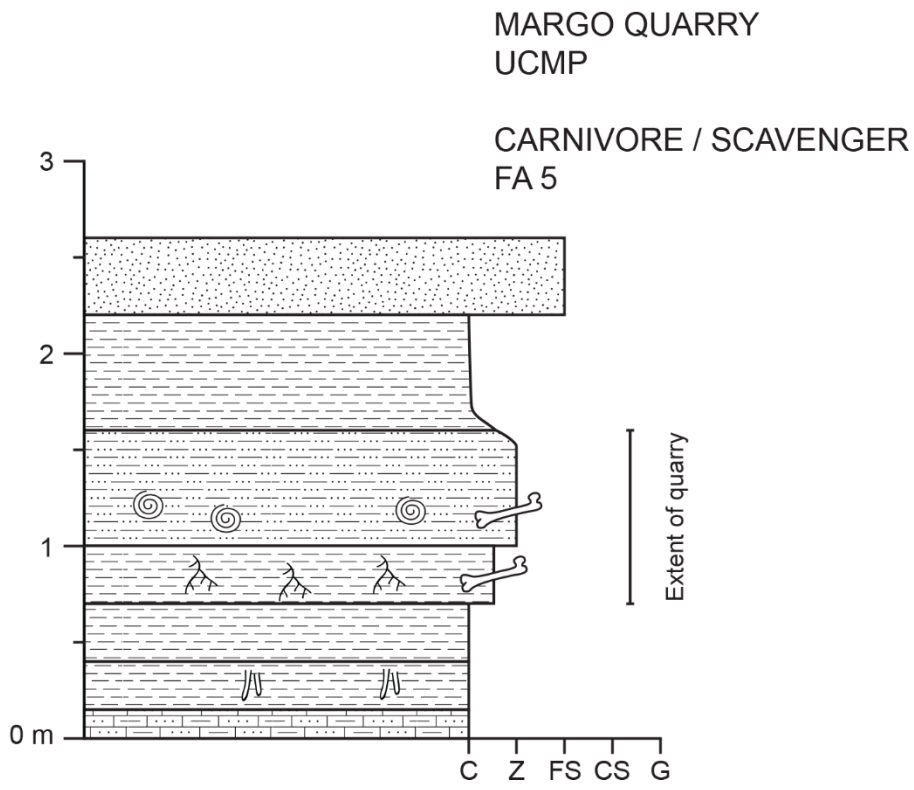

Figure A17. Margo Quarry; 875 m.

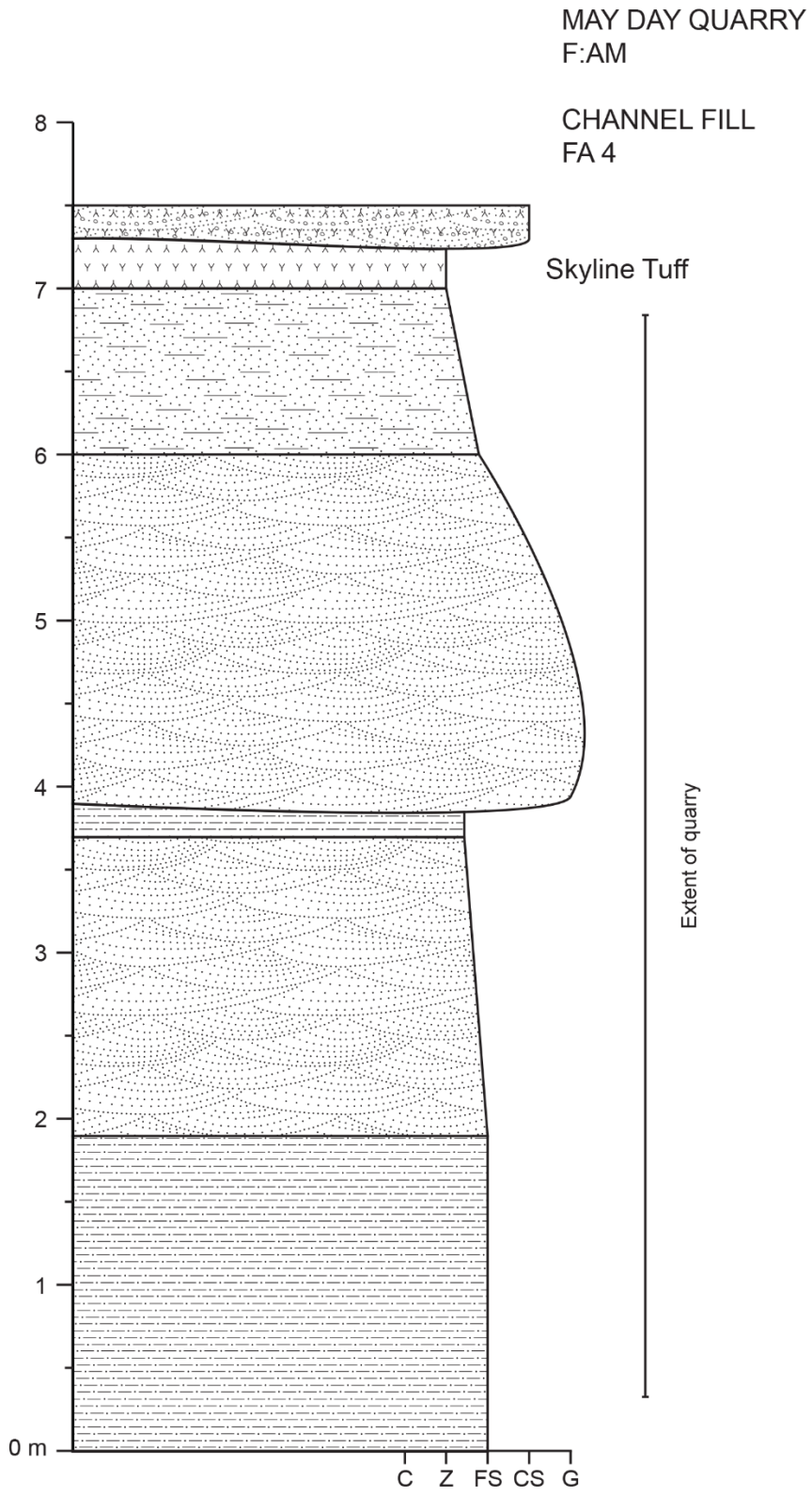

Figure A18. May Day Quarry; 768 m.

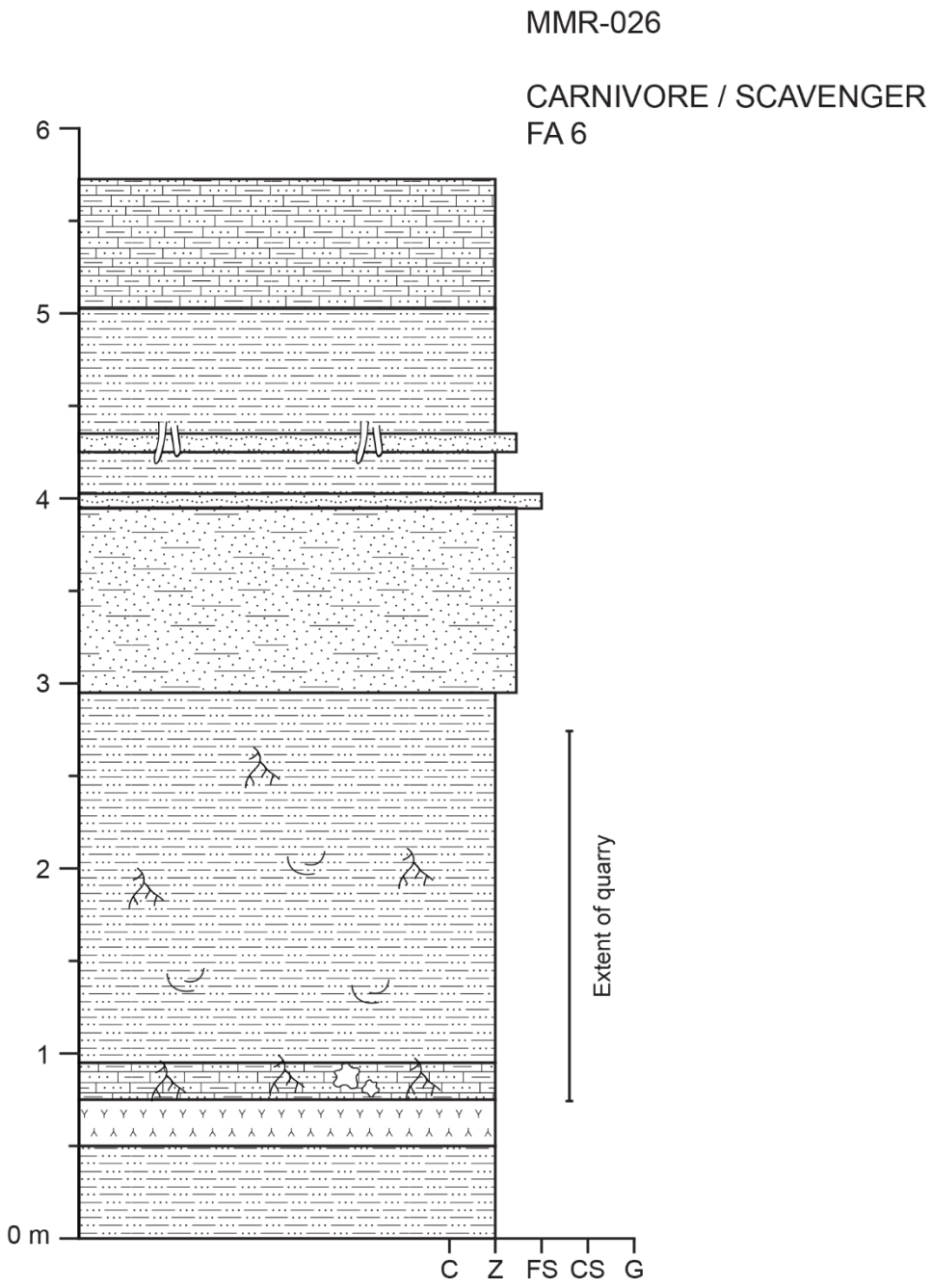

Figure A19. MMR-026; 897 m.

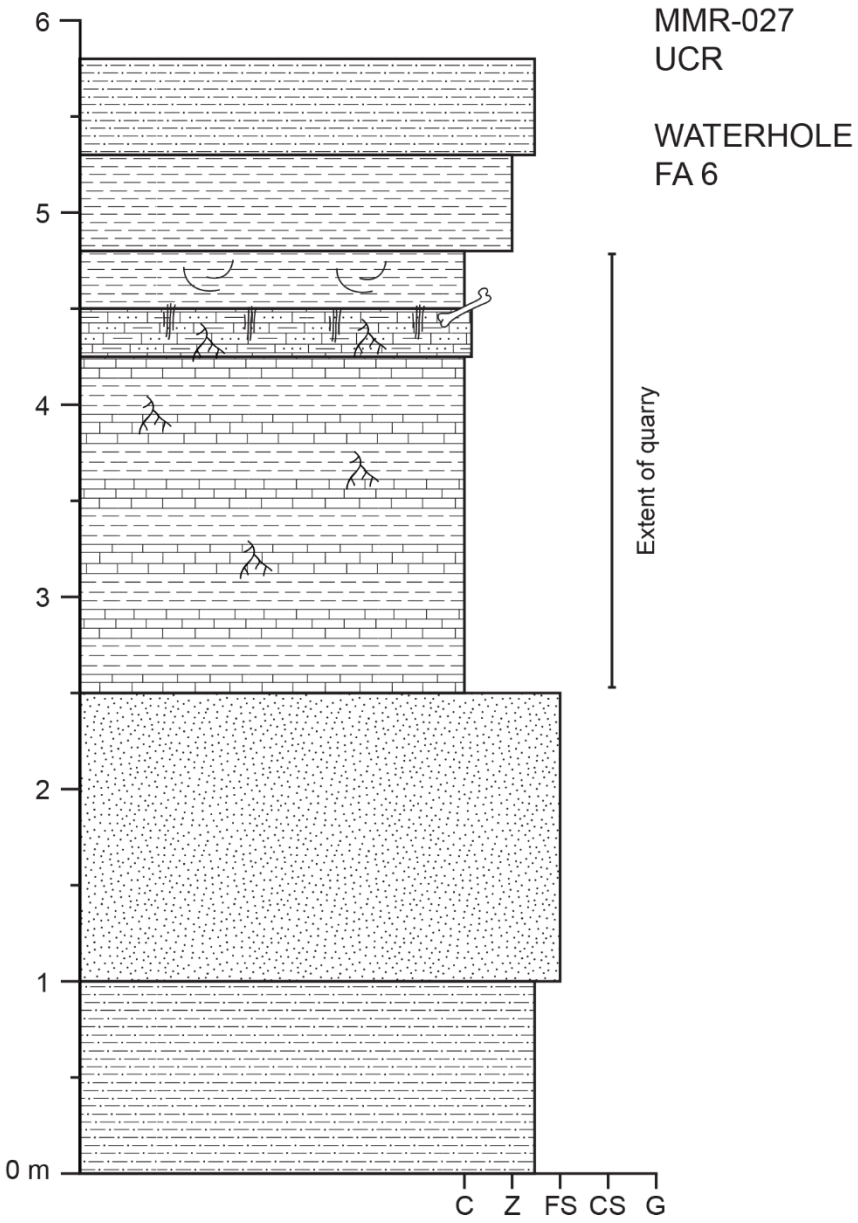

Figure A20. MMR-027; 982 m.

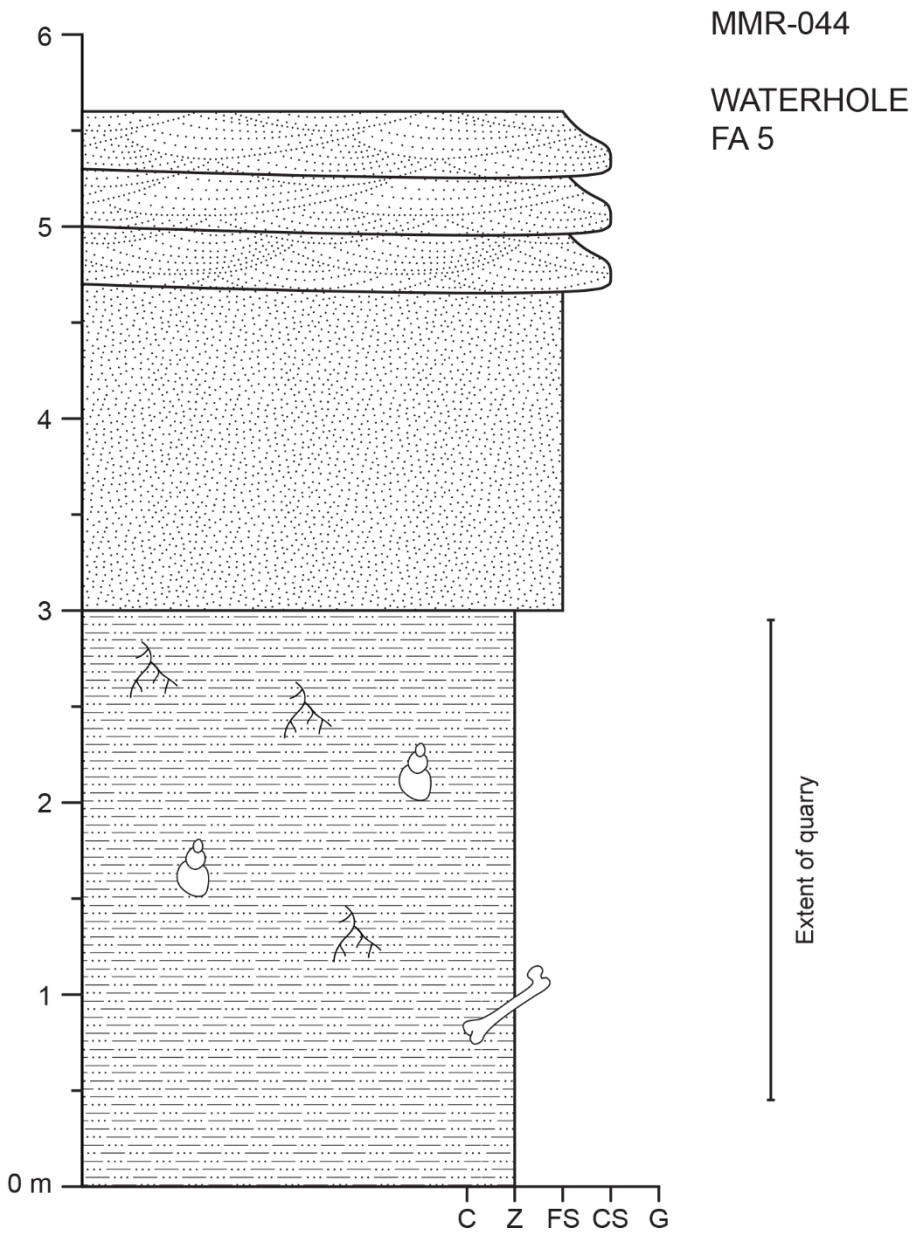

Figure A21. MMR-044; 920 m.

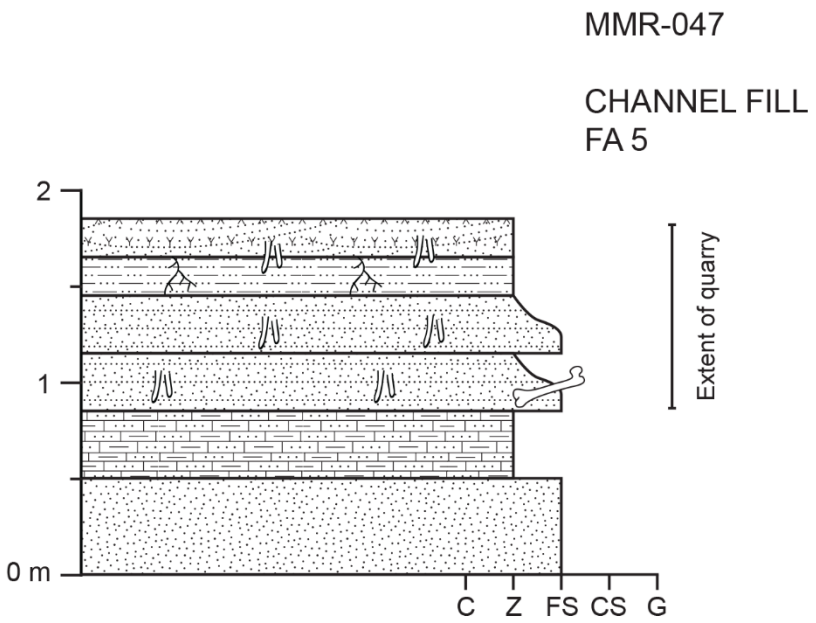

Figure A22. MMR-047; 845 m.

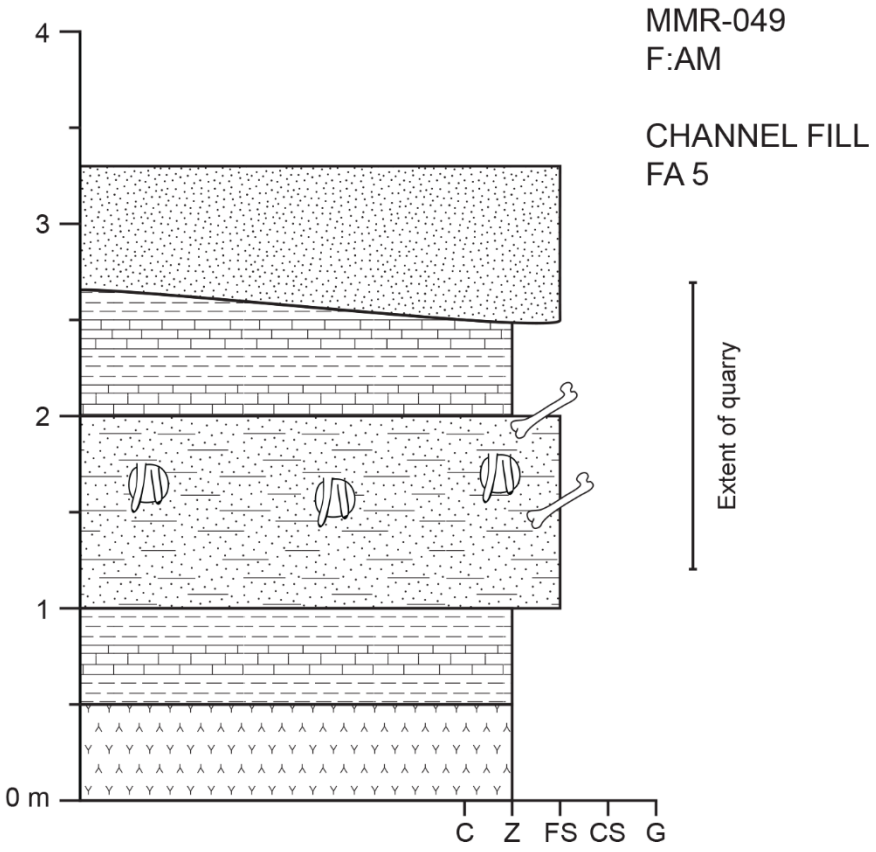

Figure A23. MMR-049; 781 m.

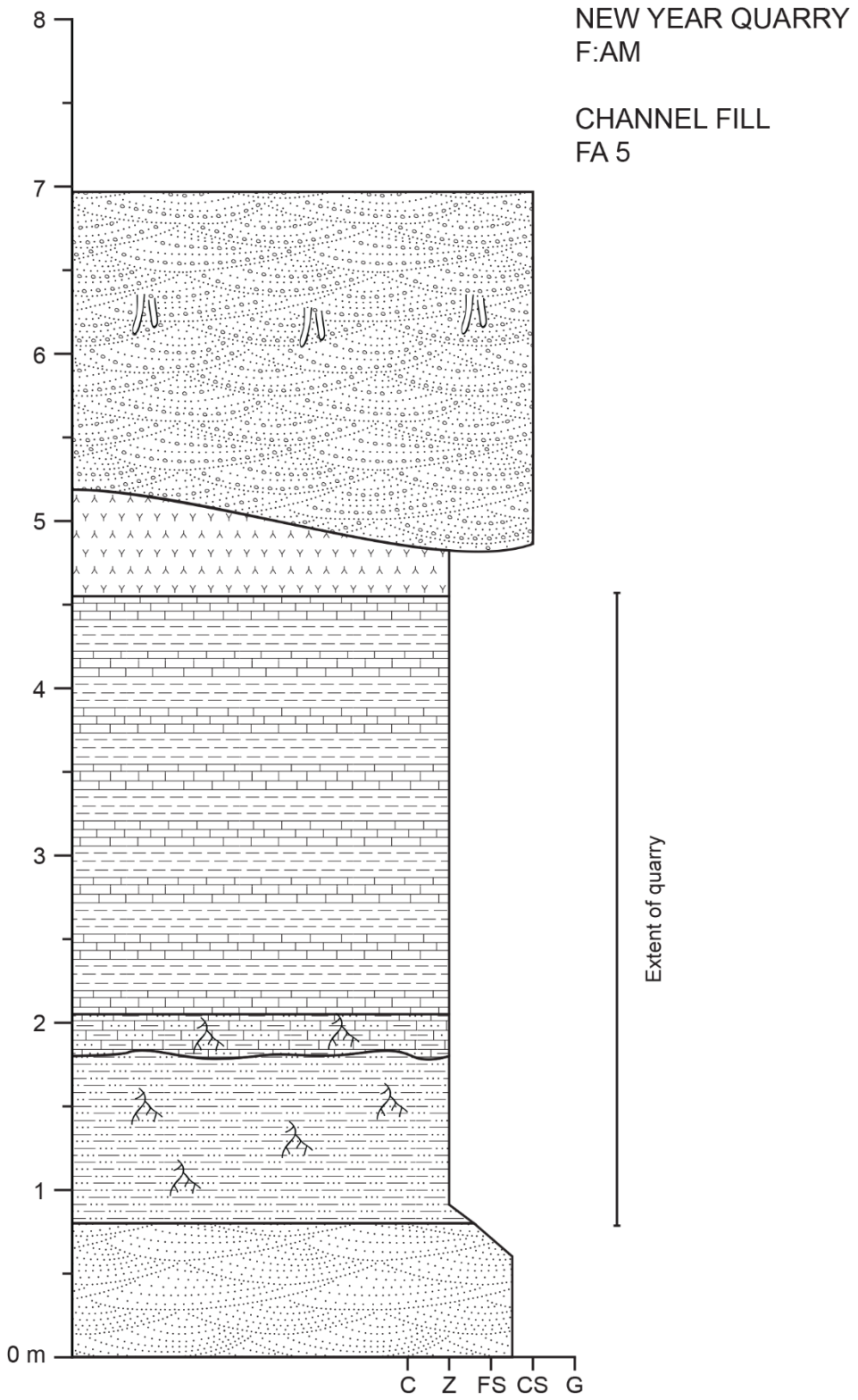

Figure A24. New Year Quarry; 781 m.

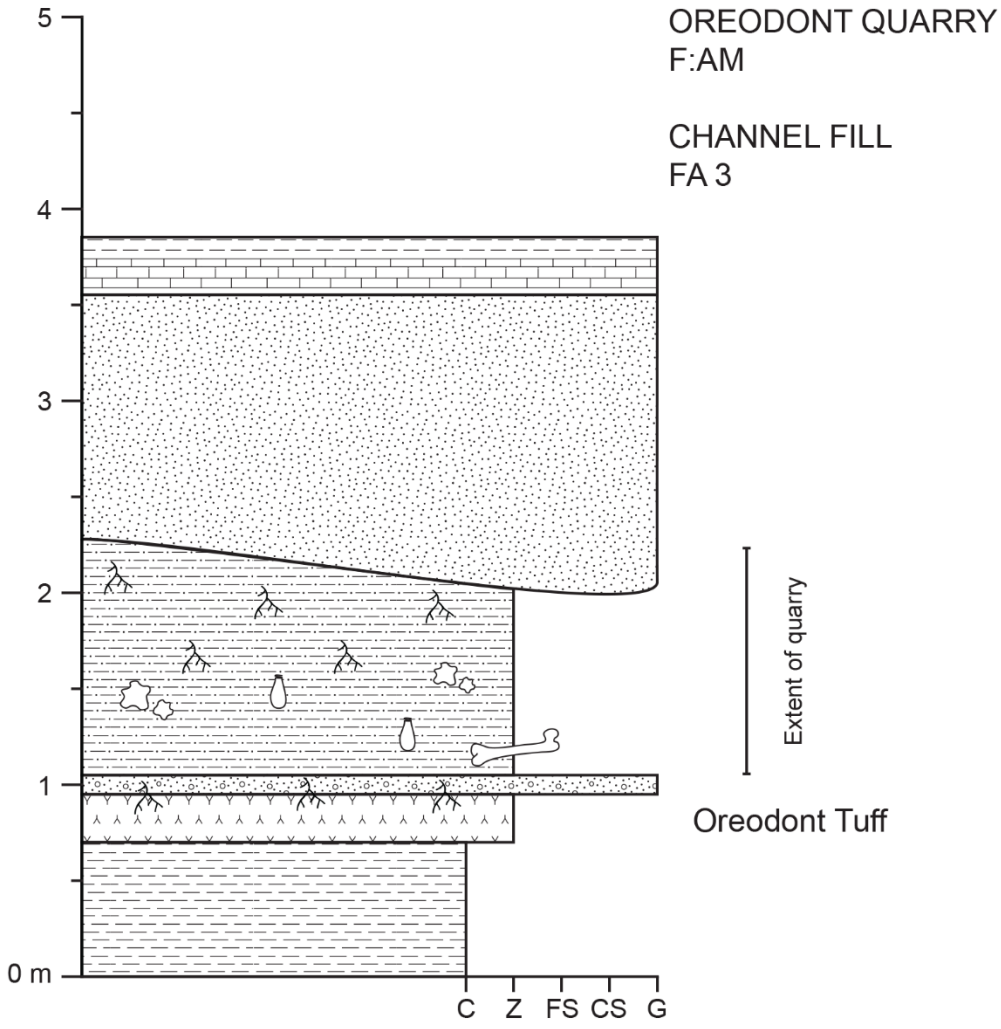

Figure A25. Oreodont Quarry; 496 m.

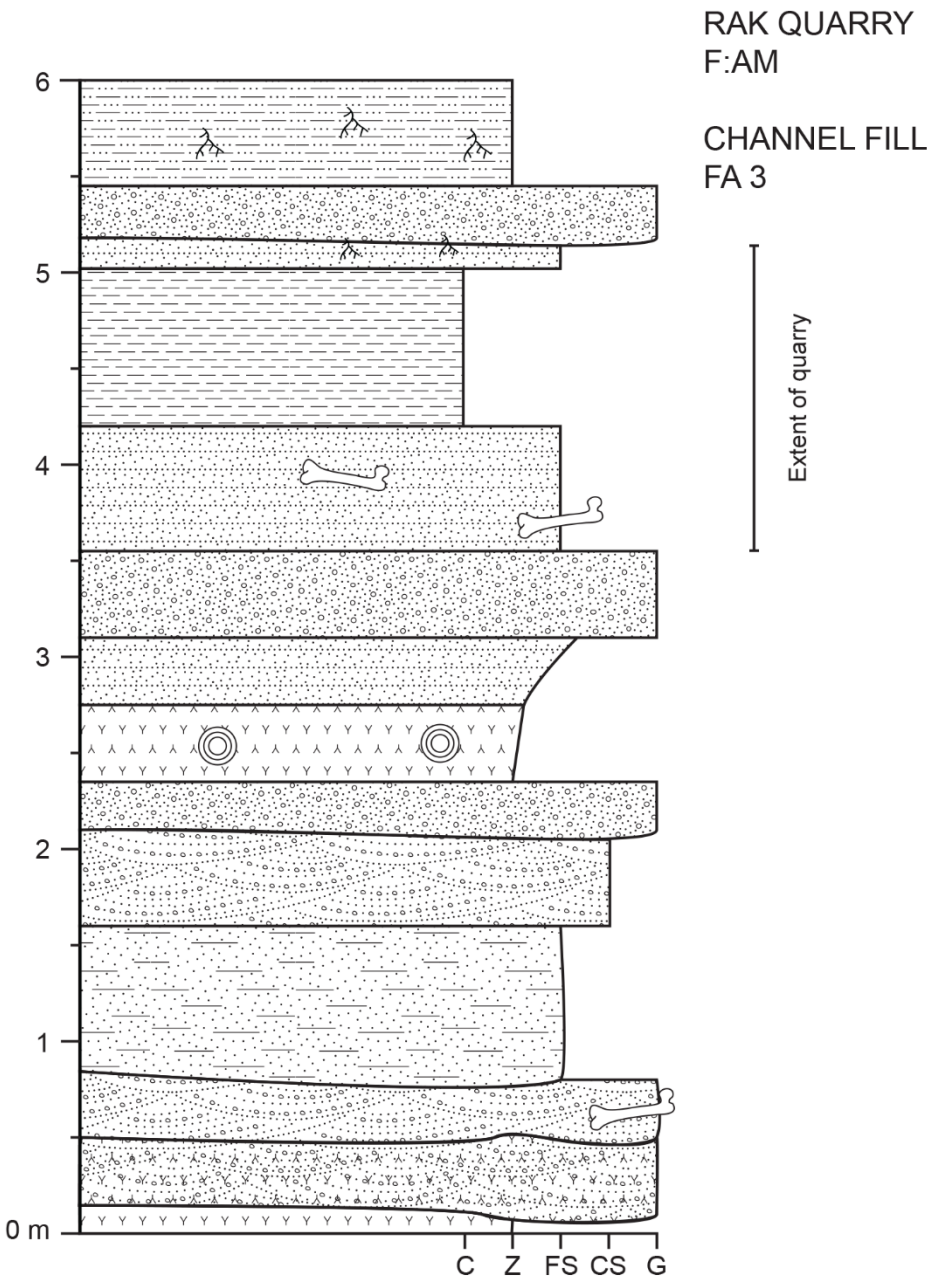

Figure A26. Rak Quarry; 505 m.

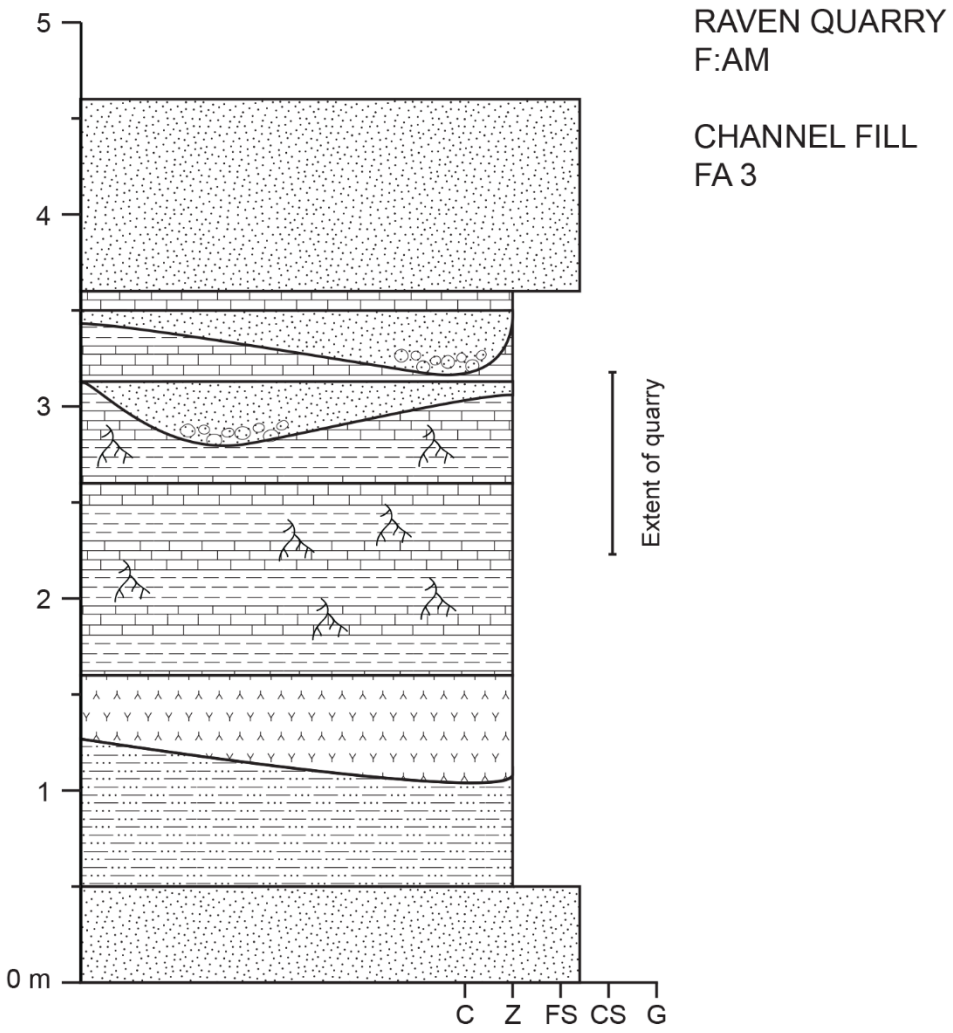

Figure A27. Raven Quarry; 463.5 m.

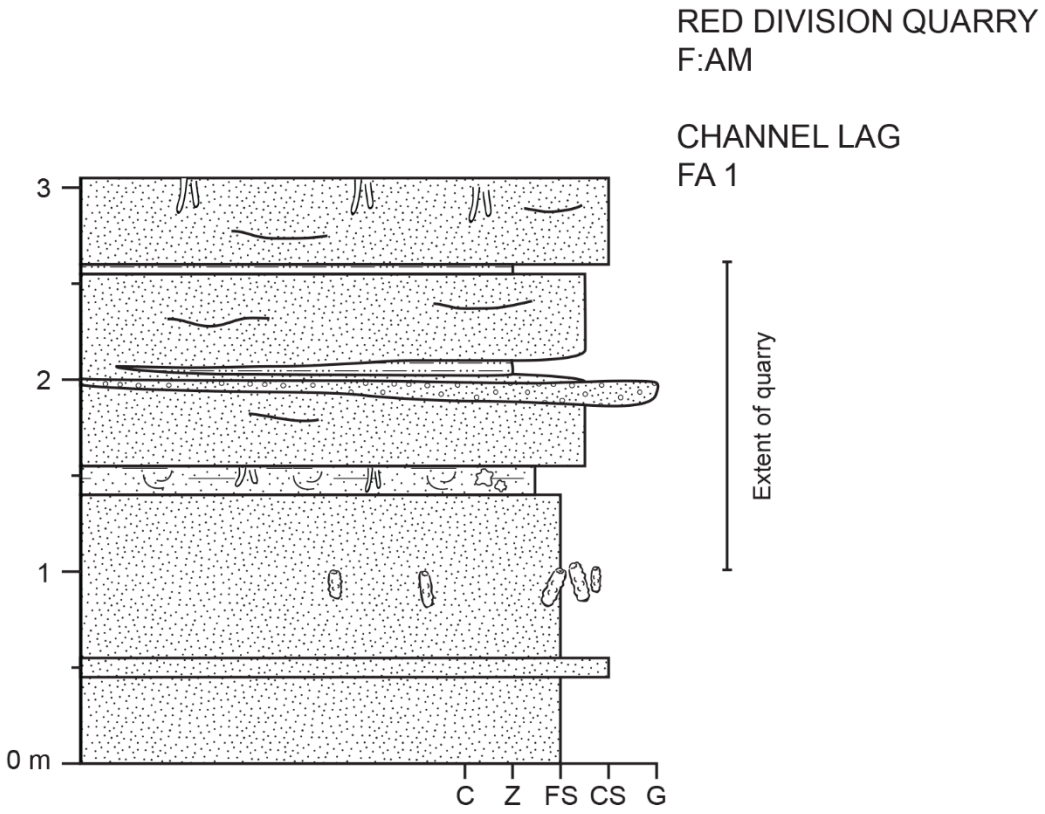

Figure A28. Red Division Quarry; 163 m.

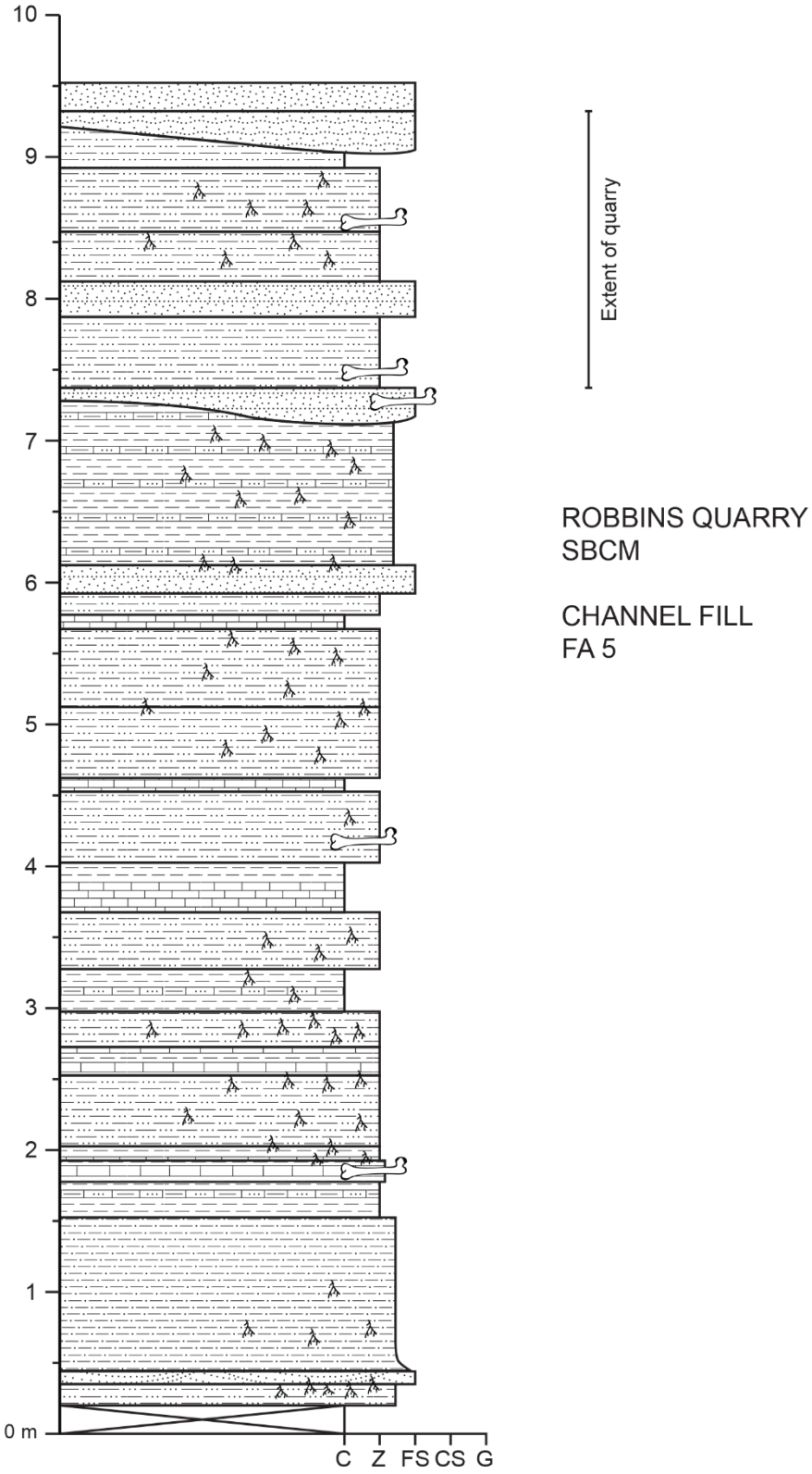

Figure A29. Robbins Quarry; 856 m.

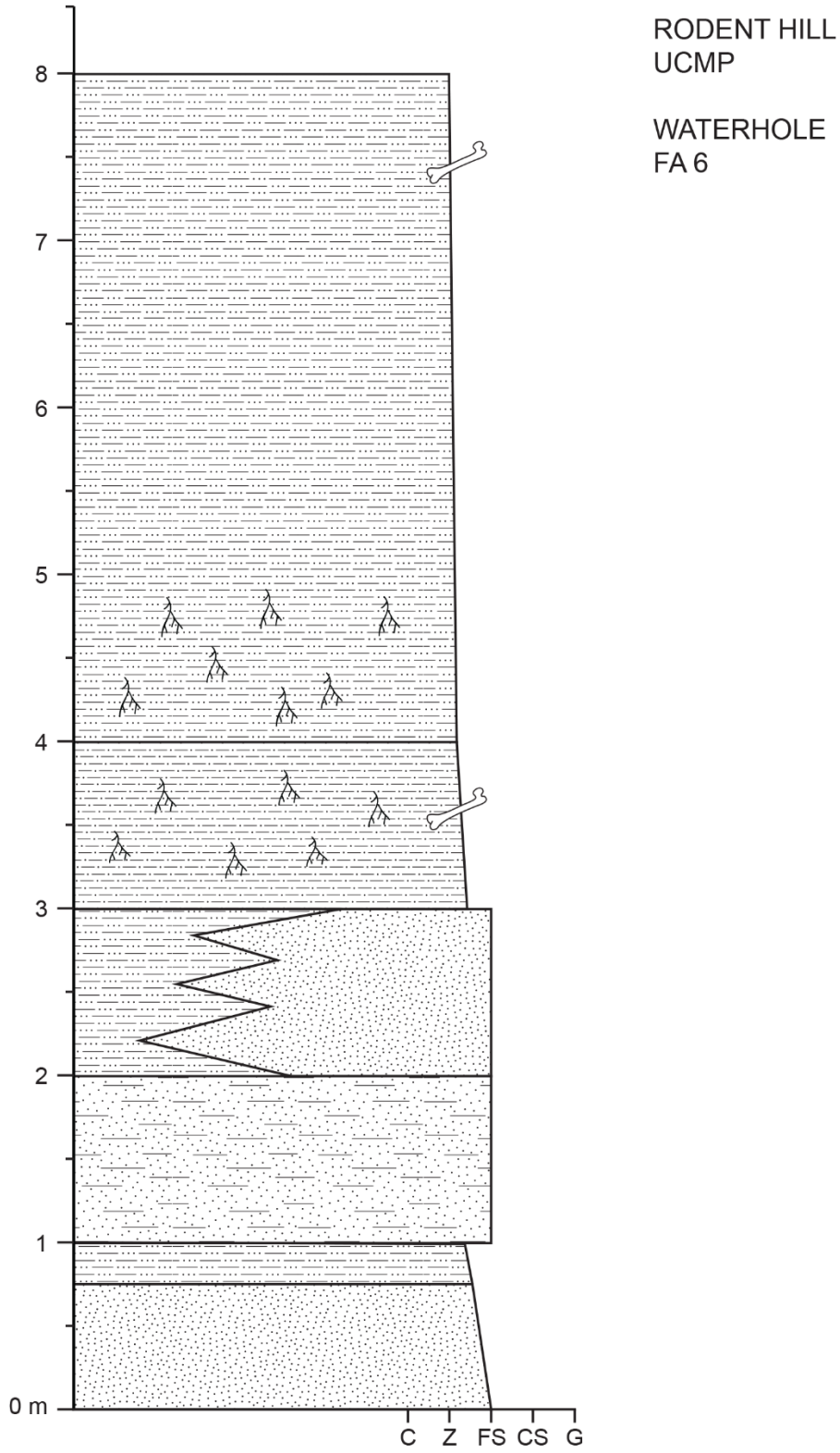

Figure A30. Rodent Hill; 898 m.

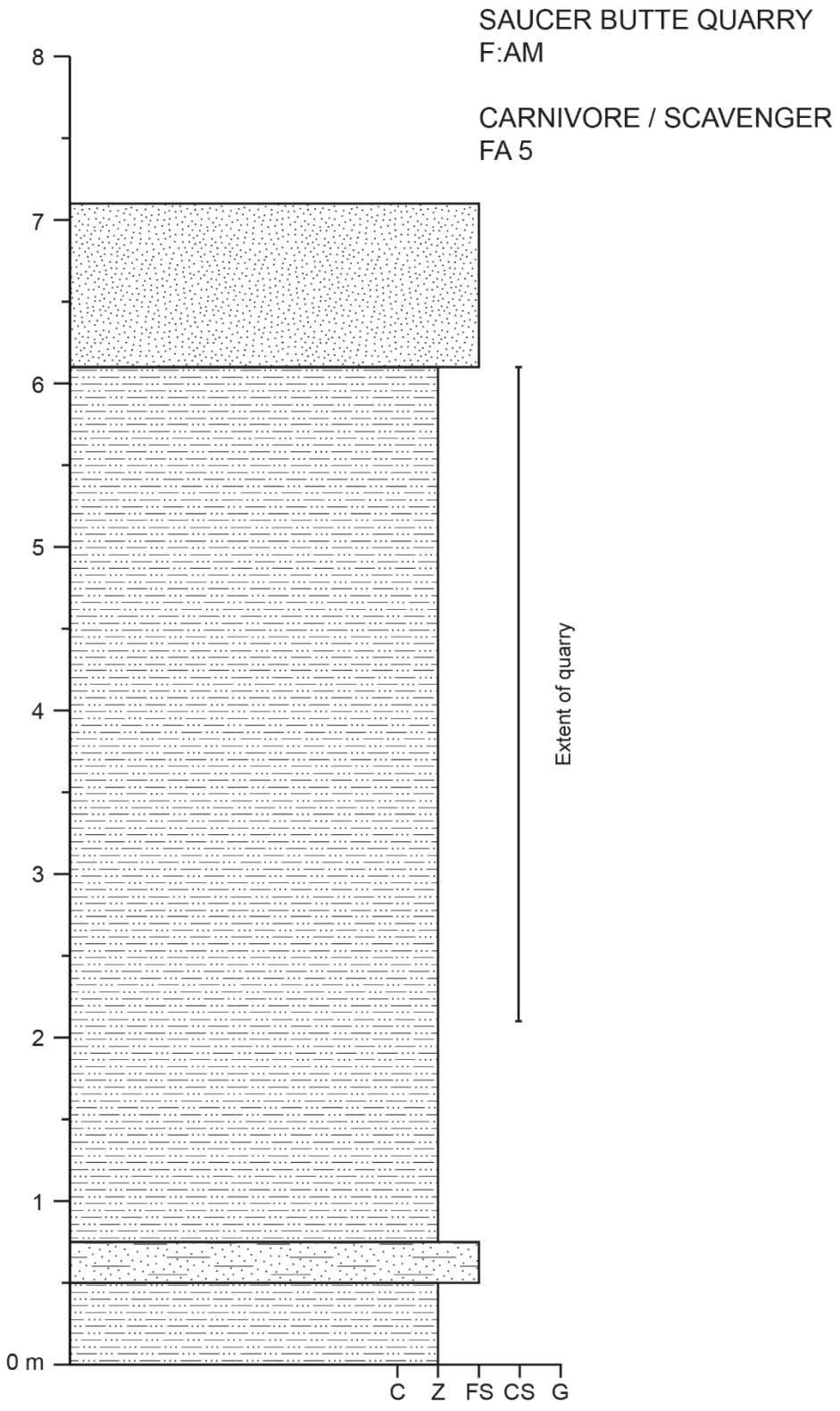

Figure A31. Saucer Butte Quarry; 740 m.

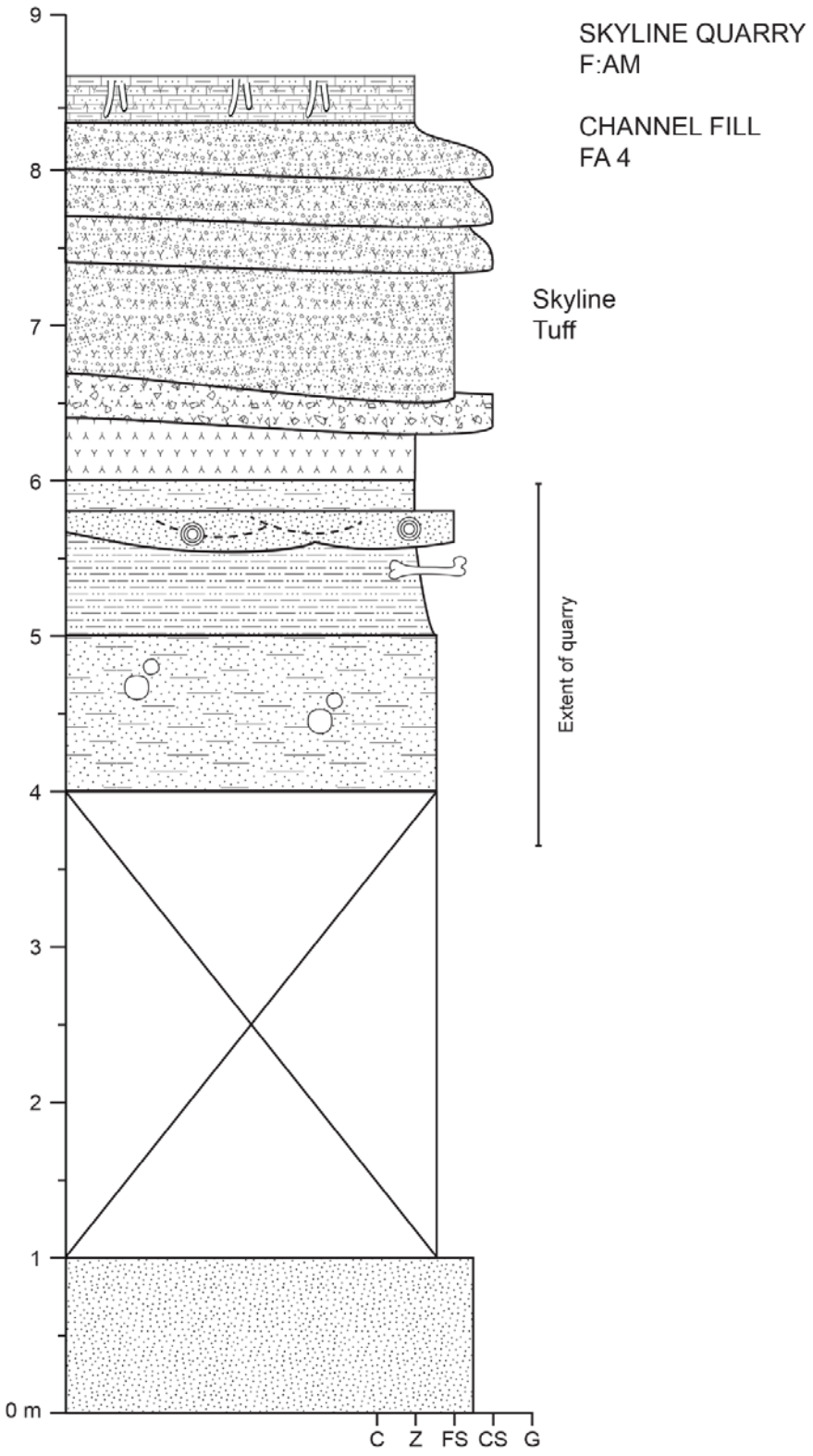

Figure A32. Skyline Quarry; 768 m.

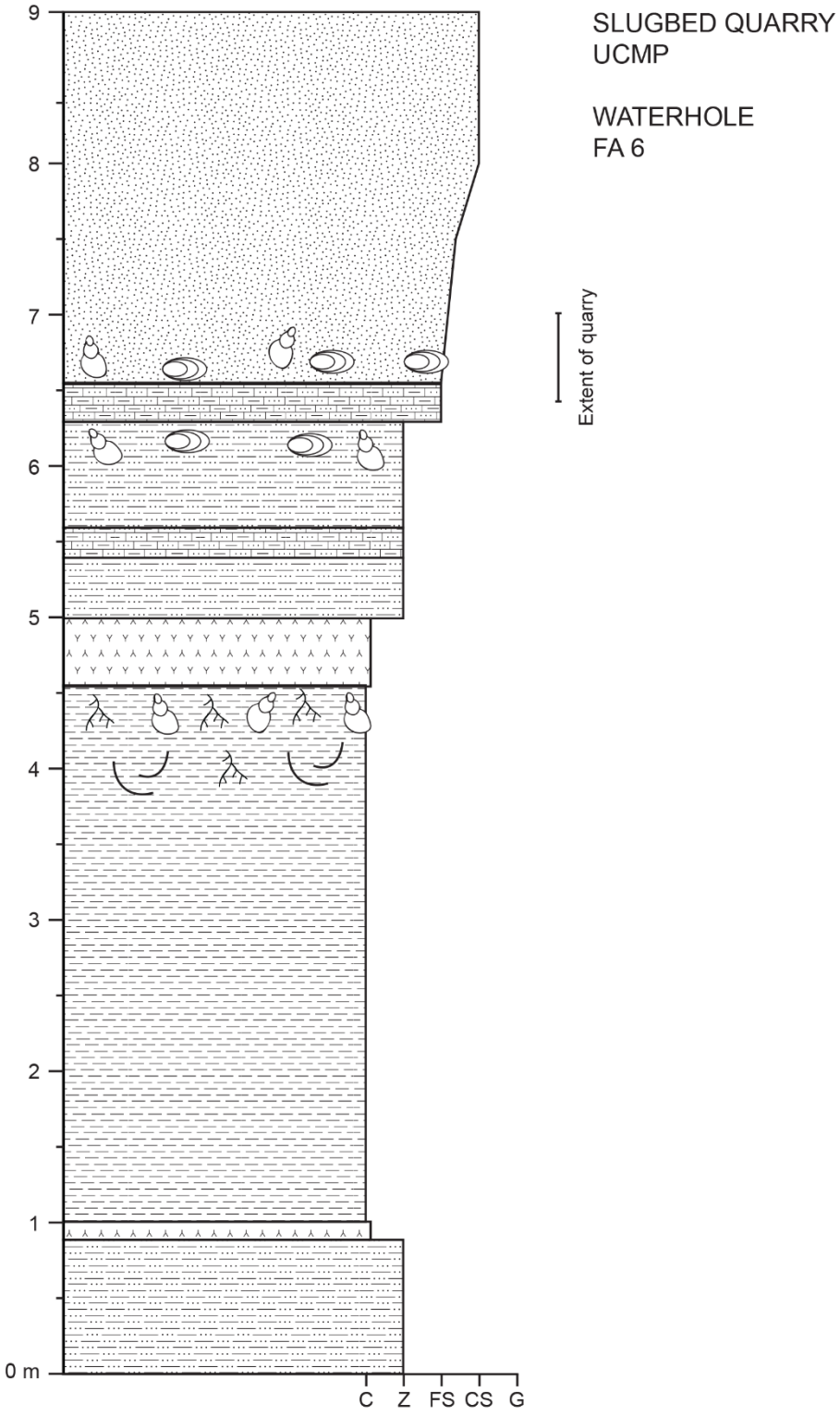

Figure A33. Slugbed Quarry; 828.3 m.

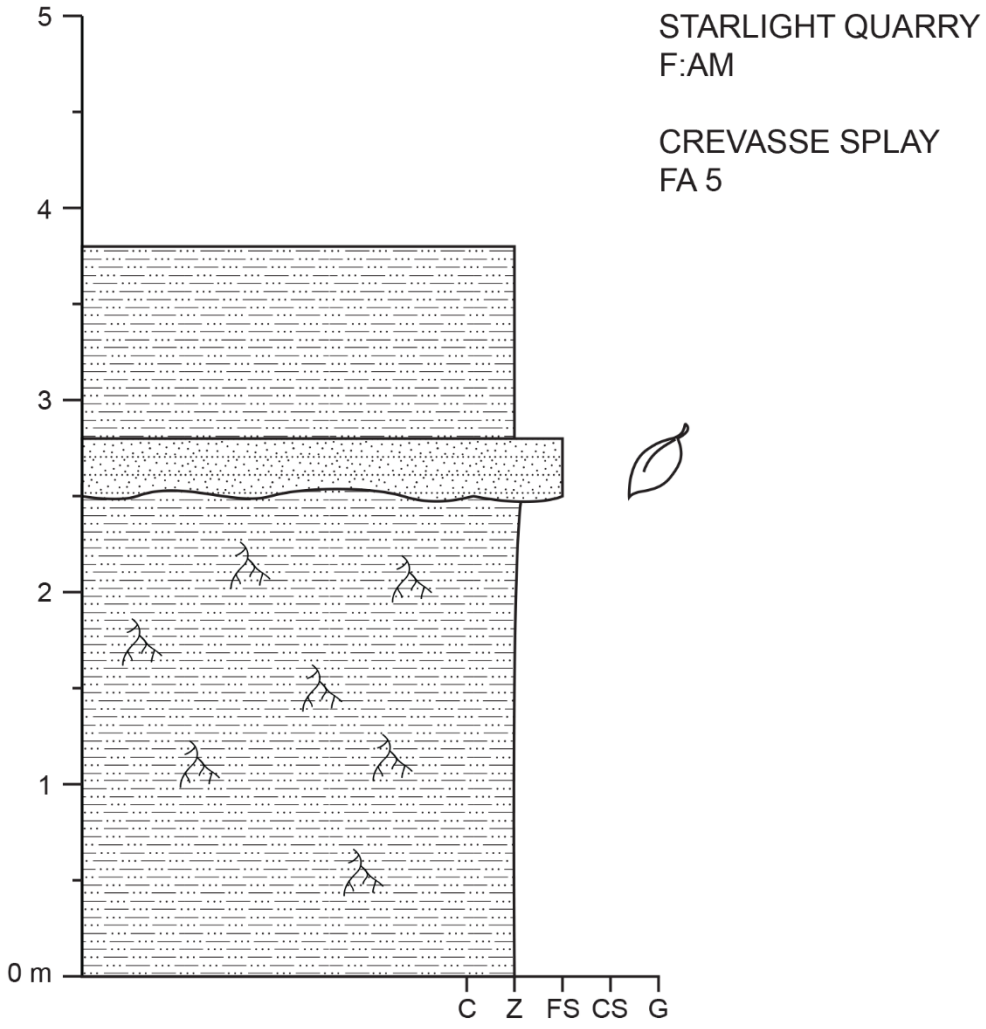

Figure A34. Starlight Quarry; 777.5 m.

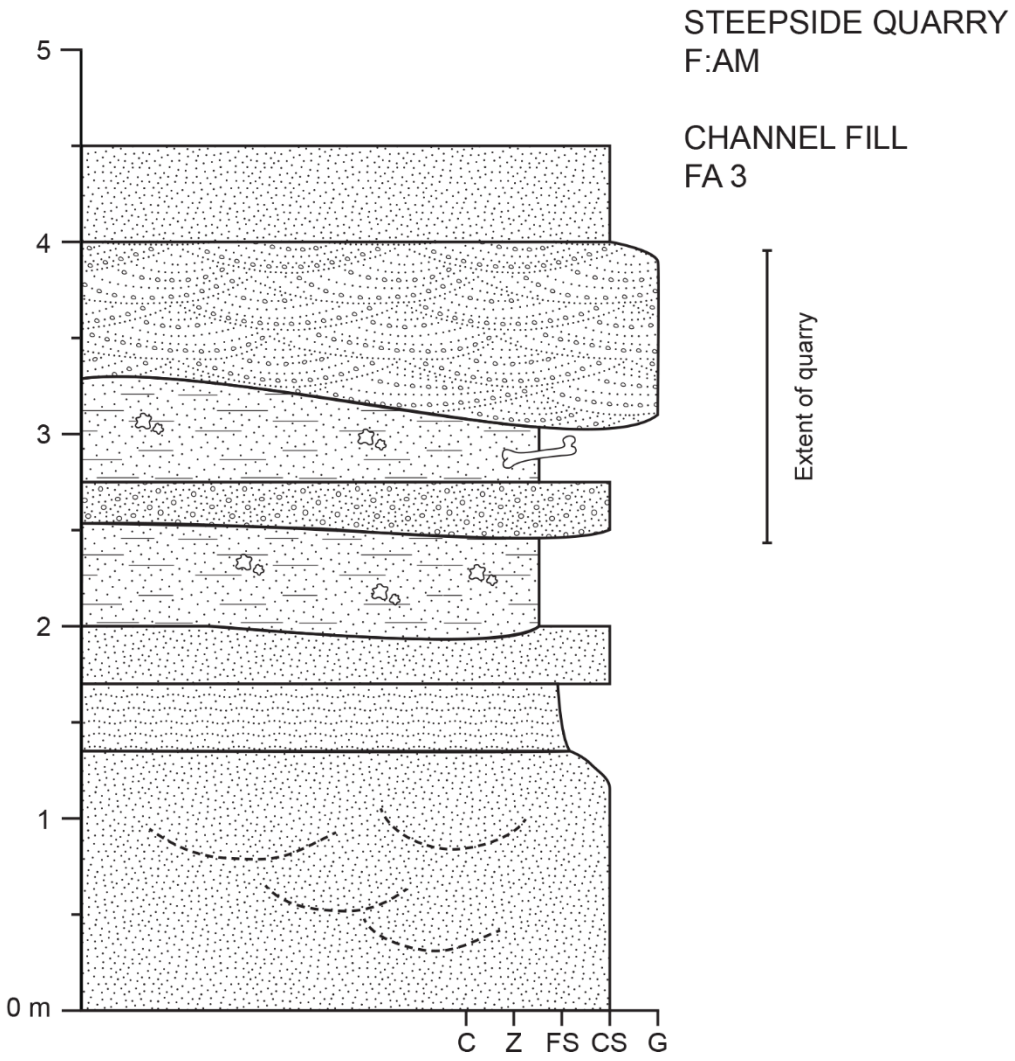

Figure A35. Steepside Quarry; 456 m.

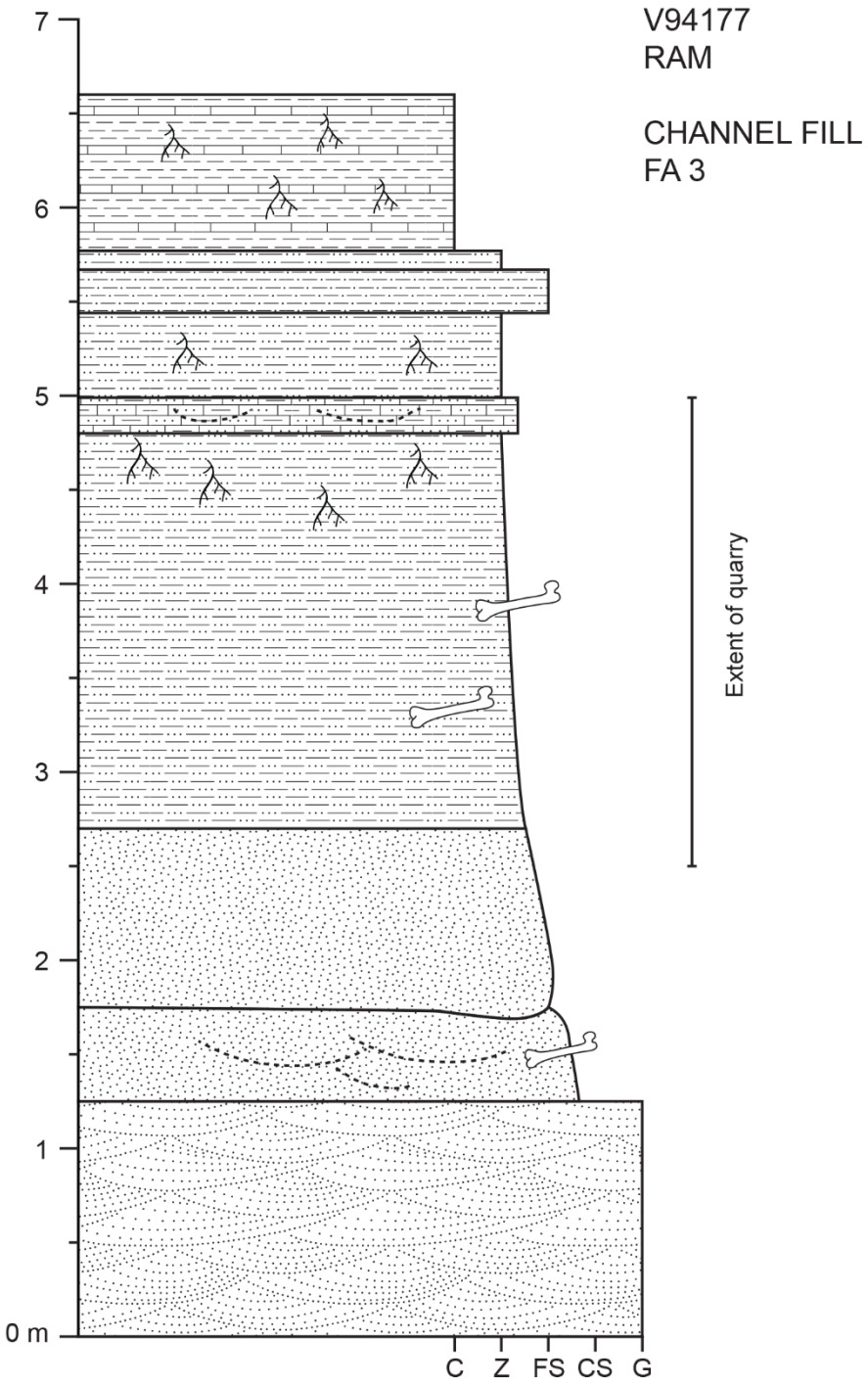

Figure A36. RAM V94177; 552 m.

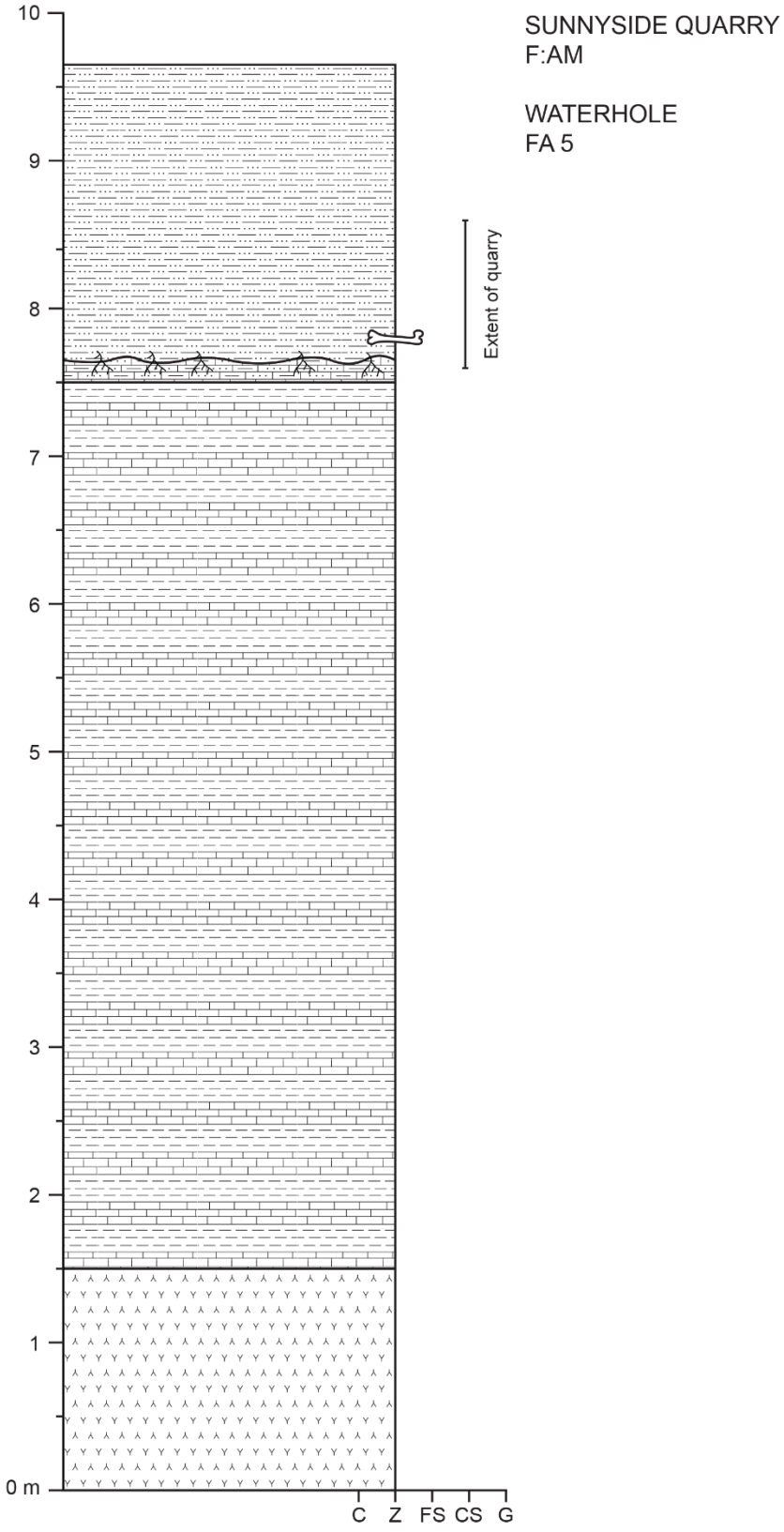

Figure A37. Sunnyside Quarry; 860 m.

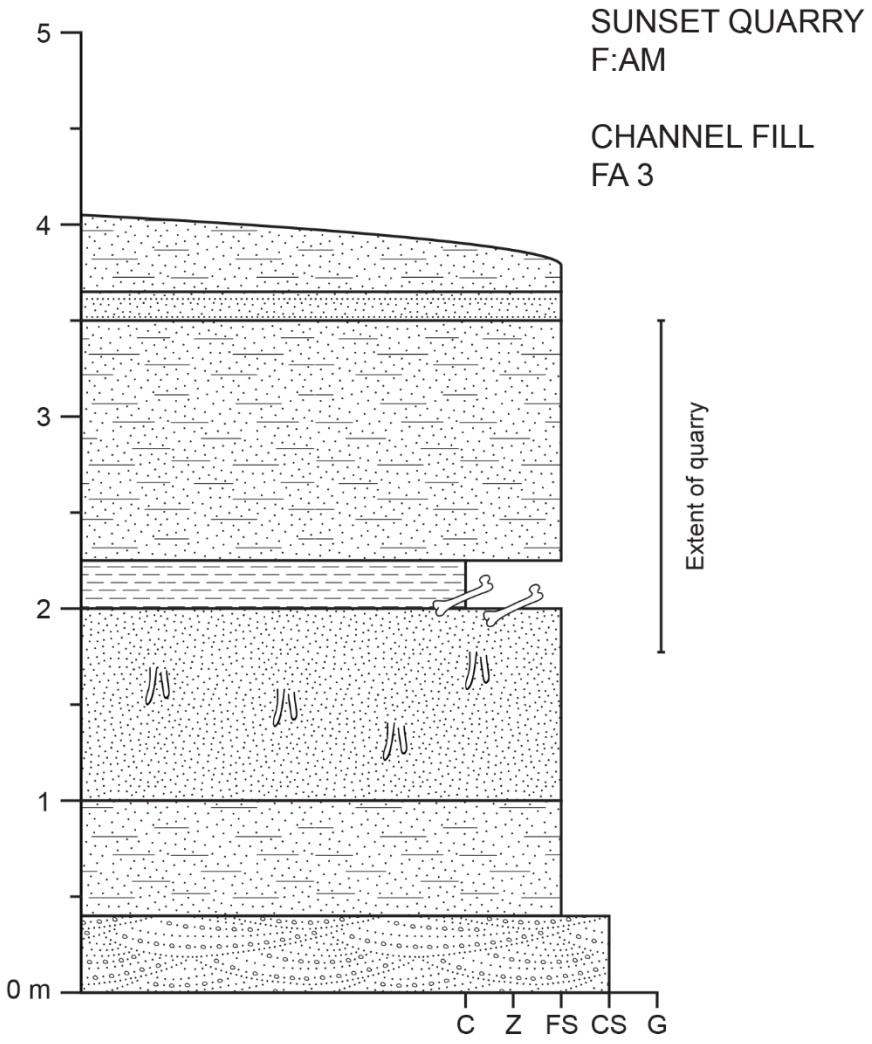

Figure A38. Sunset Quarry; 465 m.

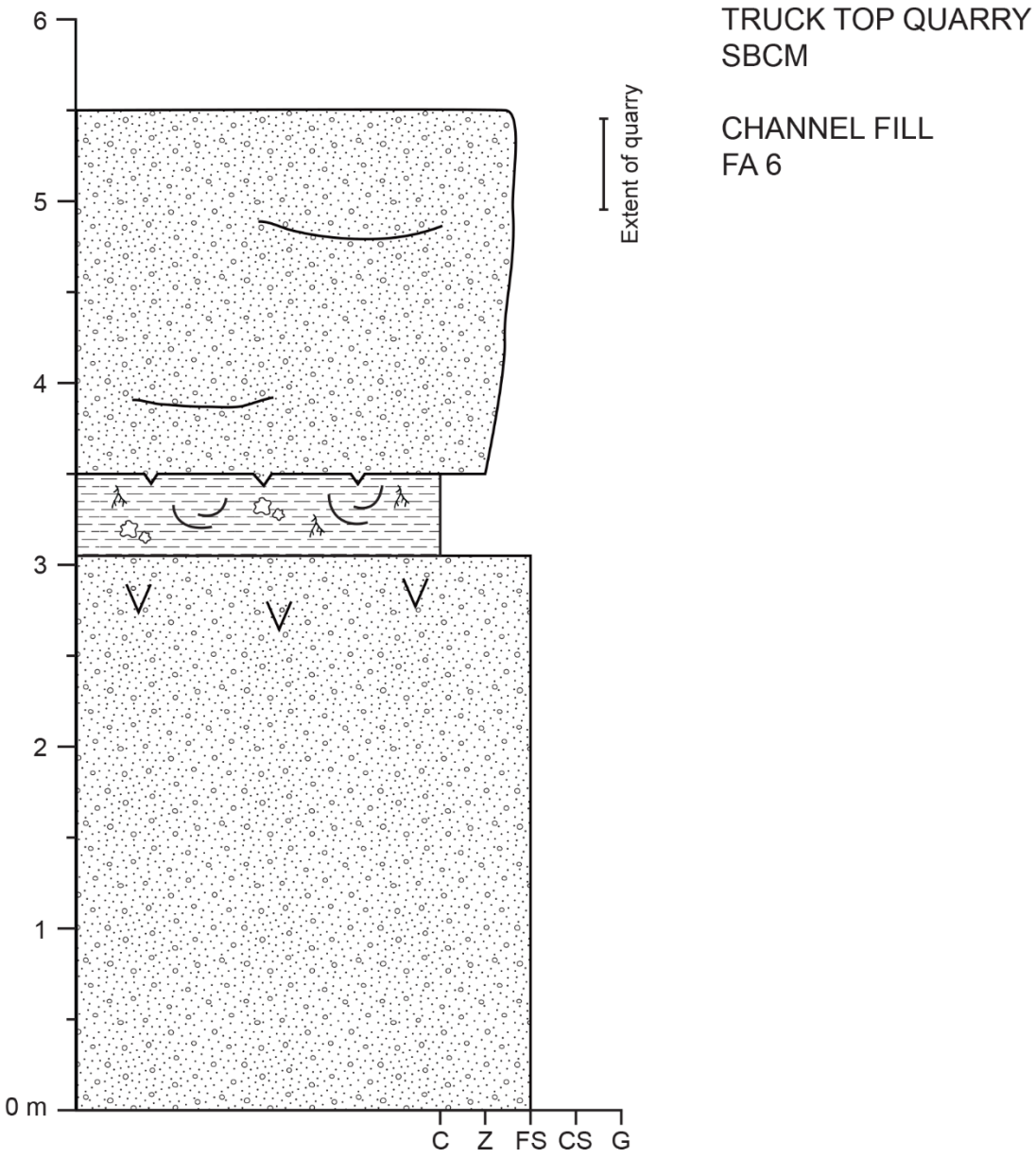

Figure A39. Truck Top Quarry; 1129 m.

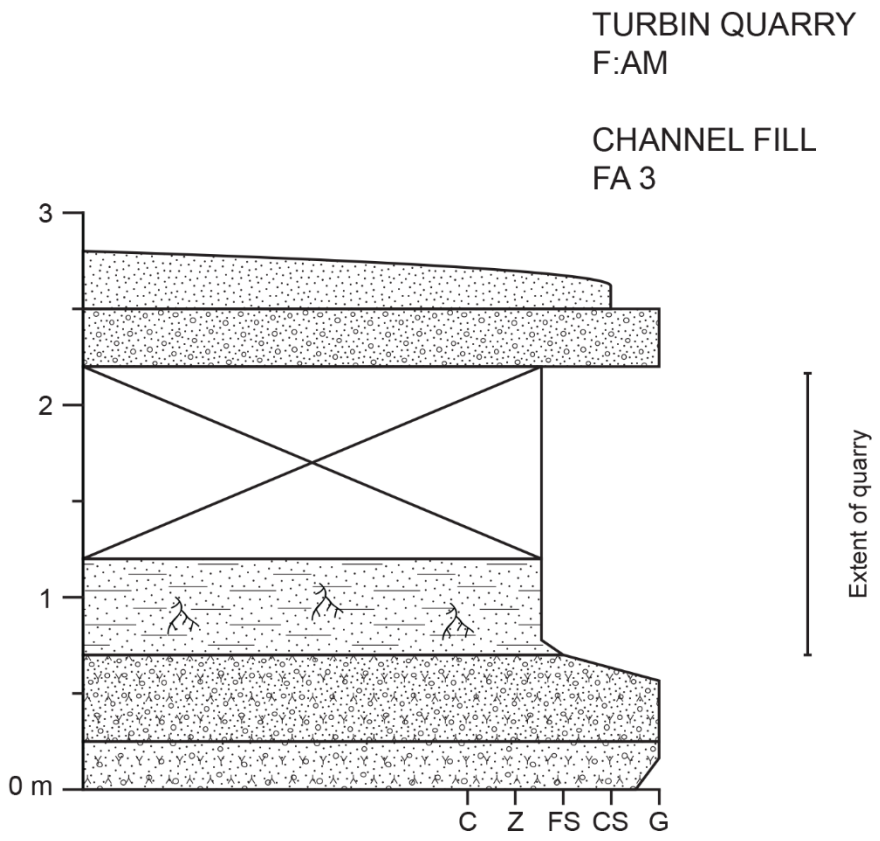

Figure A40. Turbin Quarry; 501 m.

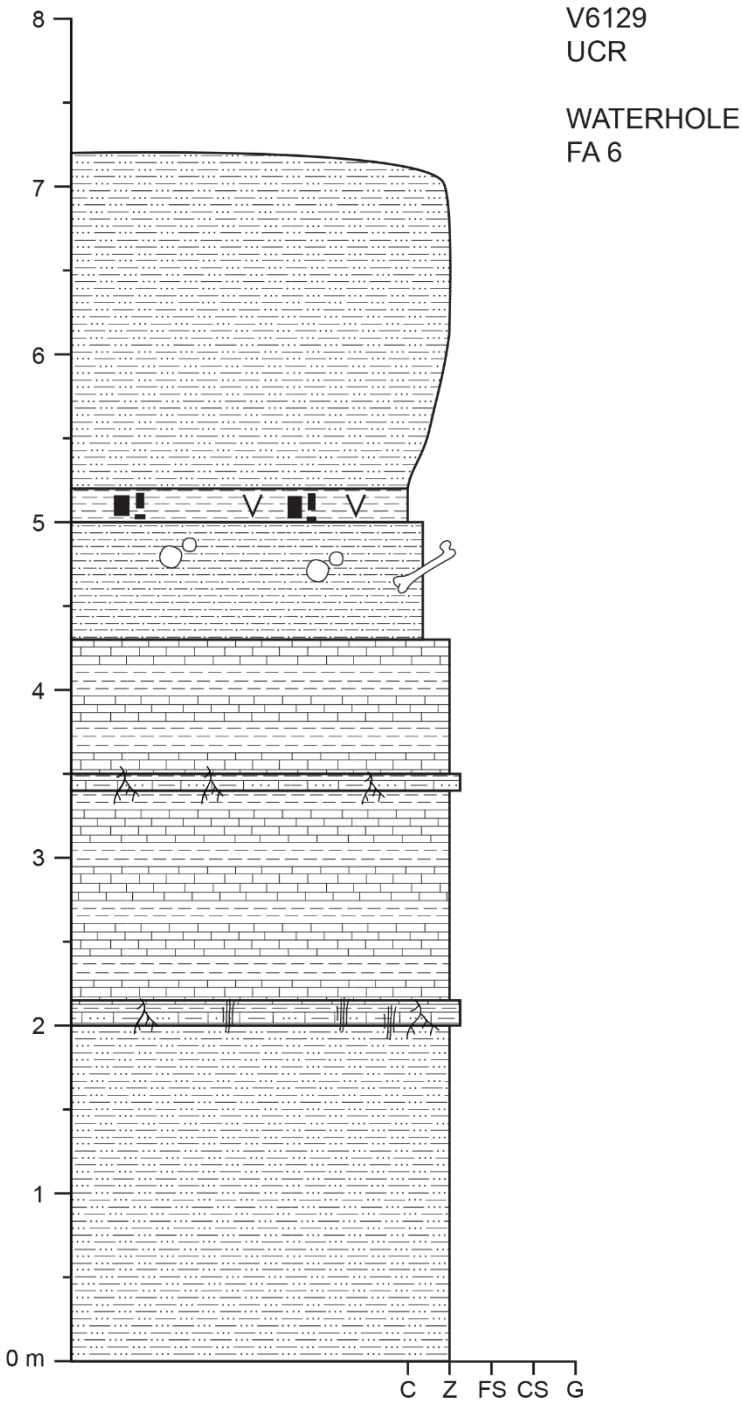

Figure A41. UCR V6129; 934 m.

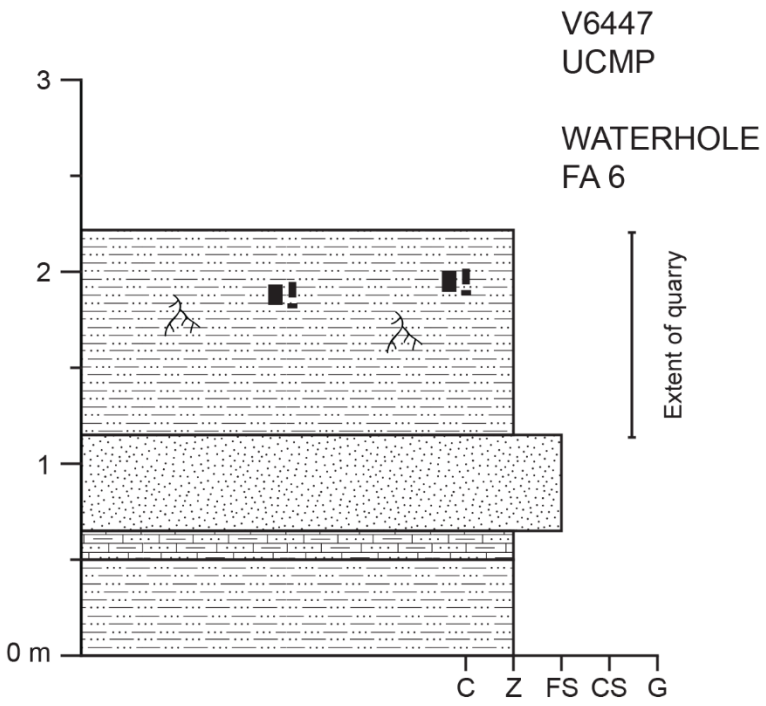

Figure A42. UCMP V6447; 982 m.

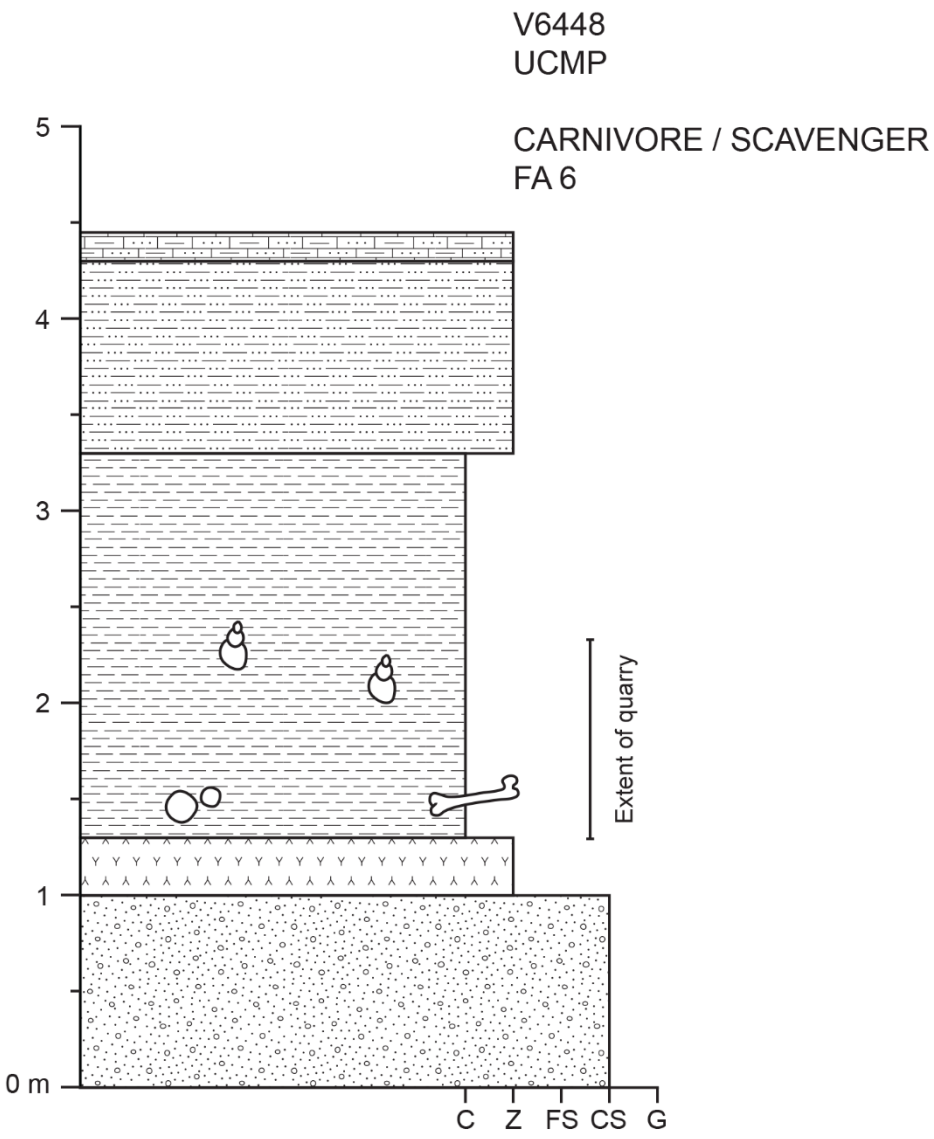

Figure A43. UCMP V6448; 1000 m.

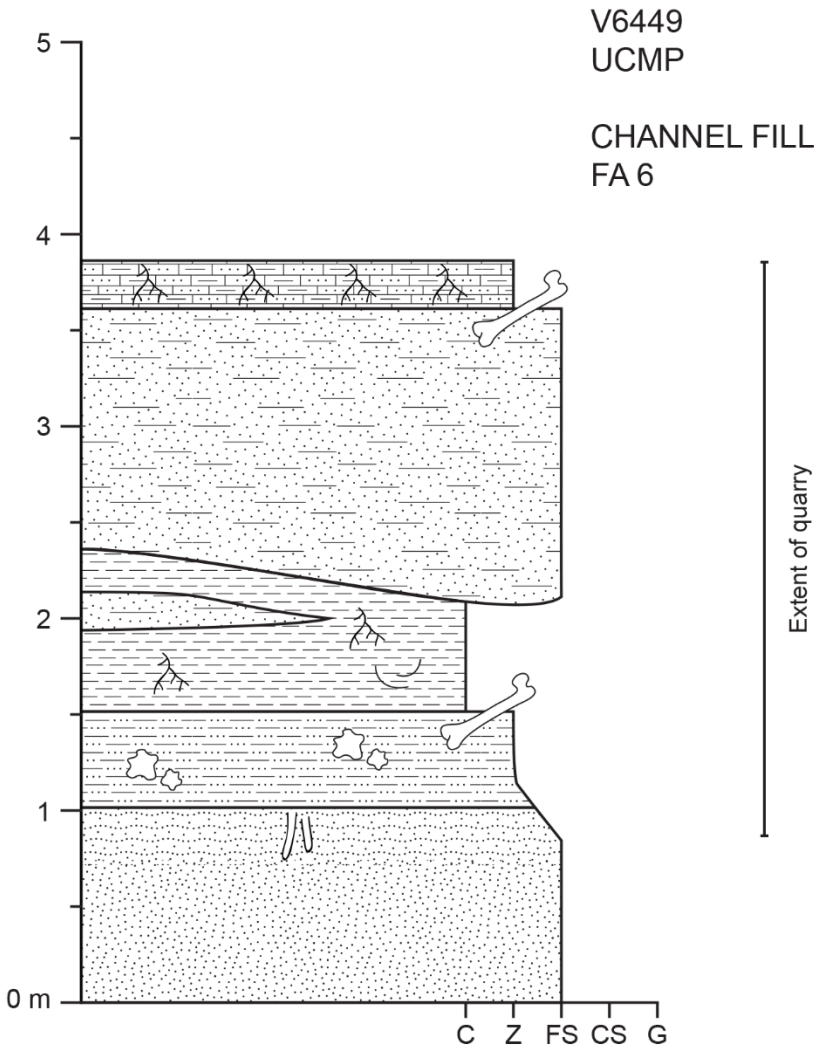

Figure A44. UCMP V6449; 940 m.

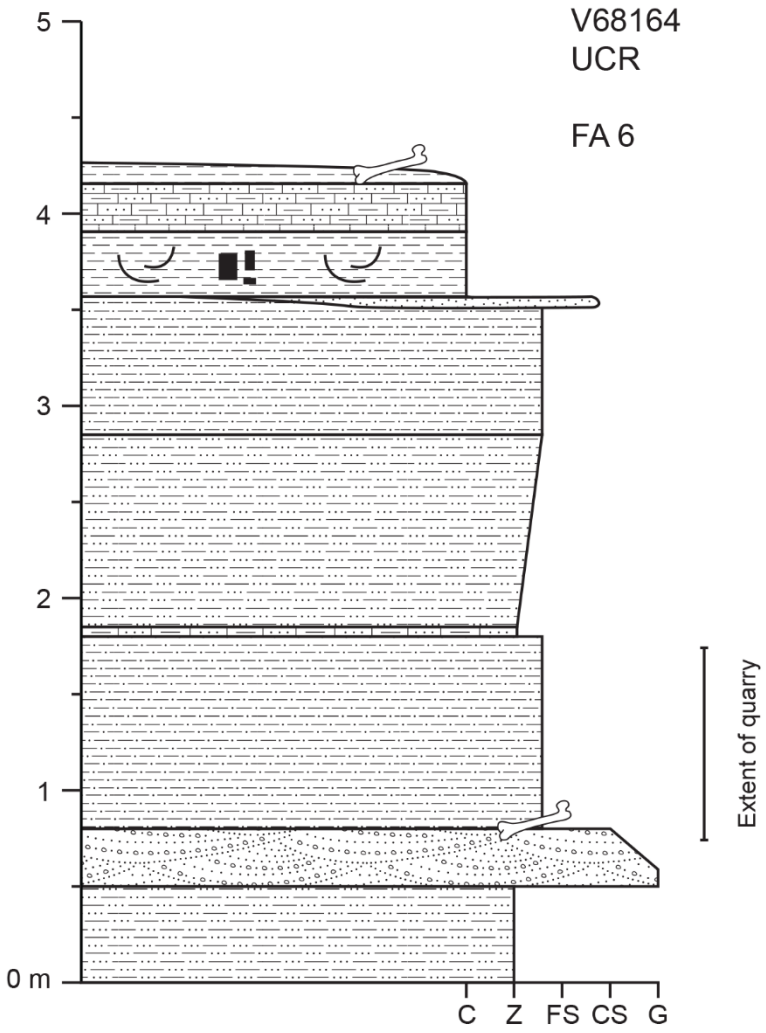

Figure A45. UCR V68164; 920 m.

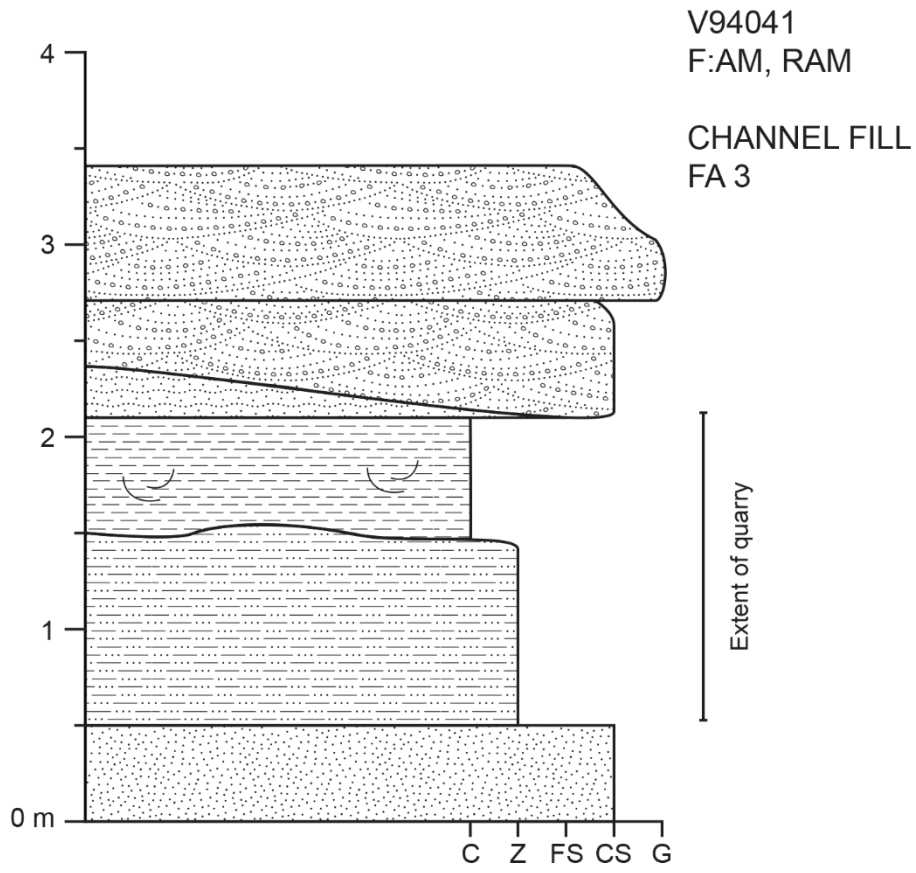

Figure A46. RAM V94041; 463 m.

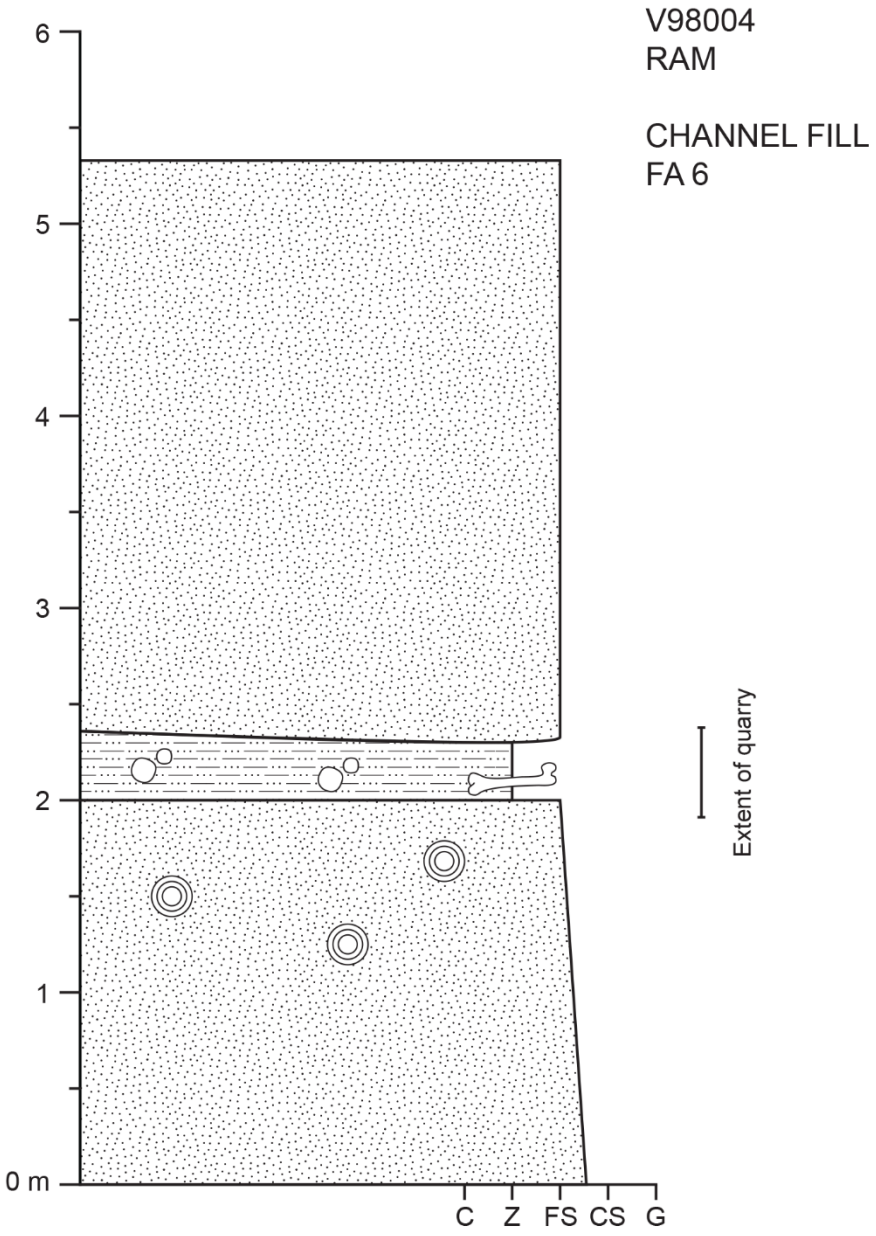

Figure A47. RAM V98004; 798 m.

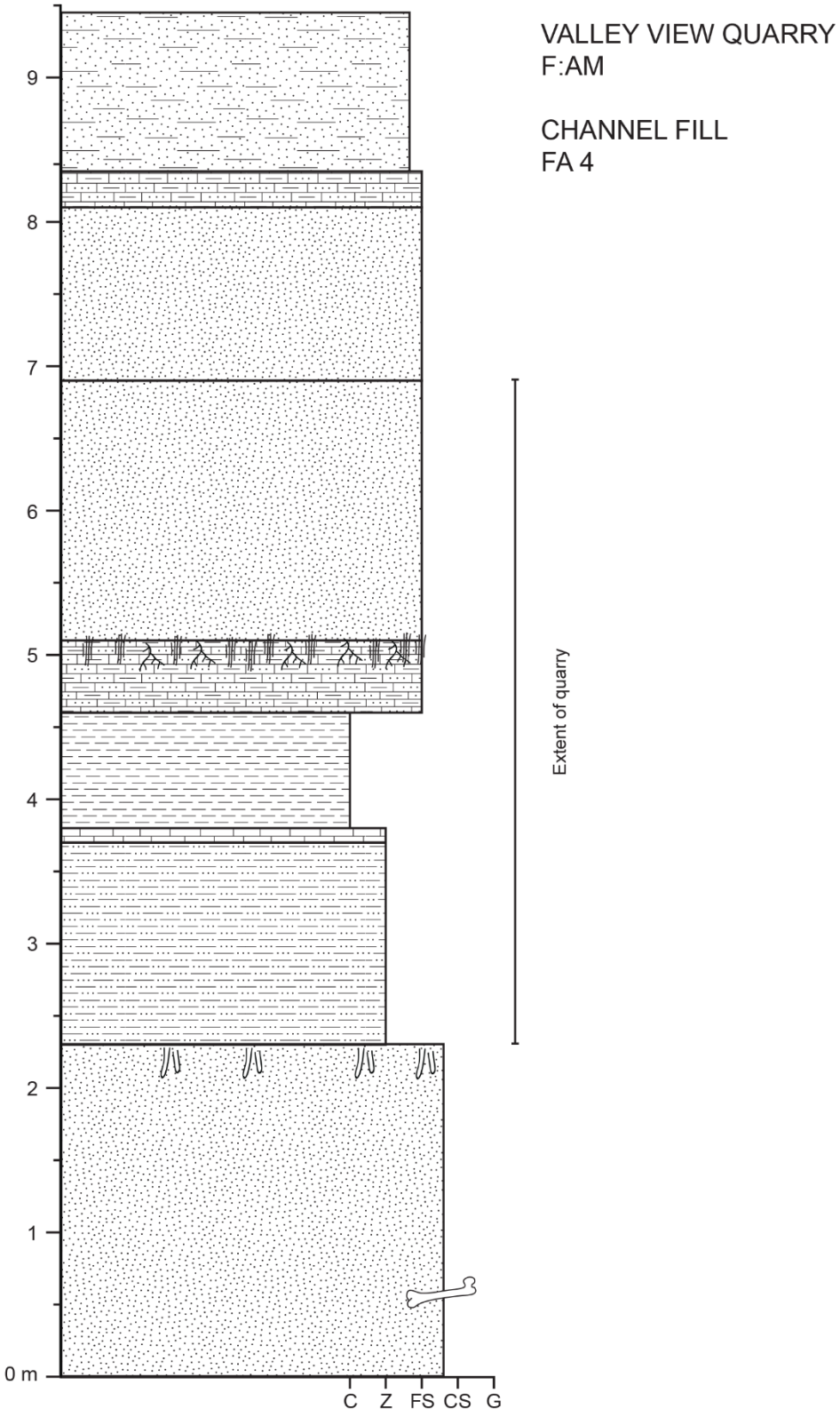

Figure A48. Valley View Quarry; 710 m.